

Sheffield Hallam University

Cytokines regulation of chemokine and chemokine receptor in relation to multiple sclerosis.

FOUILLET, Antoine.

Available from the Sheffield Hallam University Research Archive (SHURA) at:

<http://shura.shu.ac.uk/19675/>

A Sheffield Hallam University thesis

This thesis is protected by copyright which belongs to the author.

The content must not be changed in any way or sold commercially in any format or medium without the formal permission of the author.

When referring to this work, full bibliographic details including the author, title, awarding institution and date of the thesis must be given.

Please visit <http://shura.shu.ac.uk/19675/> and <http://shura.shu.ac.uk/information.html> for further details about copyright and re-use permissions.

Sheffield S1 1WB

25342

101 897 977 8



Sheffield Hallam University
Learning and IT Services
Assets Centre City Campus
Sheffield S1 1WB

REFERENCE

ProQuest Number: 10695715

All rights reserved

INFORMATION TO ALL USERS

The quality of this reproduction is dependent upon the quality of the copy submitted.

In the unlikely event that the author did not send a complete manuscript and there are missing pages, these will be noted. Also, if material had to be removed, a note will indicate the deletion.



ProQuest 10695715

Published by ProQuest LLC (2017). Copyright of the Dissertation is held by the Author.

All rights reserved.

This work is protected against unauthorized copying under Title 17, United States Code
Microform Edition © ProQuest LLC.

ProQuest LLC.
789 East Eisenhower Parkway
P.O. Box 1346
Ann Arbor, MI 48106 – 1346

Cytokines regulation of chemokine and chemokine receptor in relation to multiple sclerosis

Antoine Fouillet

A thesis submitted in partial fulfillment of the requirements of
Sheffield Hallam University for the degree of Doctor of Philosophy

Collaborating organisation: Open University, Milton Keynes, UK

July 1, 2008



I would like to dedicate this work to two special persons: my soon to be wife Amy and our daughter Lily-May,

Abstract

Expression of chemokines CXCL10 and CCL2 is elevated within inflammatory lesions in the central nervous system (CNS) of multiple sclerosis (MS) patients, particularly in astrocytes. These chemokines play a critical role in the recruitment of inflammatory cells into the CNS during inflammation. However, the cerebrospinal fluid of MS patients also shows high levels of CXCL10 at the time of relapse but by contrast CCL2 is decreased. In the present study, the mechanisms controlling the synthesis and release of these two chemokines in MS were assessed in vitro using primary human brain astrocytes isolated from MS and non-MS individuals.

Pro-inflammatory cytokines (interleukin -1β , tumour necrosis factor and interferon γ) increased the expression of both CCL2 and CXCL10 by astrocytes at the mRNA and protein level, as determined by real time PCR and enzyme linked immunosorbent assays (ELISA), respectively. CCL2 binding to astrocytes was then determined to evaluate any autocrine action on astrocytes in a single astrocyte preparation. CCL2 bound constitutively and following cytokine treatment. CCL2-binding was not the result of the interaction with its receptor since astrocytes did not express CCR2 on this astrocyte culture. CCR2-independent binding of CCL2 was confirmed by the absence of intracellular signalling, evidenced by the lack of calcium influx as well as of Erk and Akt phosphorylation, in CCL2-treated astrocytes. Even though astrocytes expressed CXCR3, similar negative results on calcium influx and downstream signalling pathways were observed for CXCL10. D6 chemokine decoy receptor expression was then assessed in vitro and in situ to further investigate the mechanism(s) of chemokine binding to astrocytes. Cultured astrocytes constitutively expressed the D6 decoy receptor at the mRNA and protein level, but levels were unchanged following cytokine treatment. D6 was expressed in situ in MS normal appearing white matter and in control brain tissue, at both the mRNA and protein level. D6 expression was detected on neurons and microglia but not astrocytes using immunohistochemical methods. Incubation of frozen brain sections with biotinylated CCL2 resulted in partial co-localisation with D6 staining.

Altogether, these results suggest a role for astrocytes in regulating inflammation through synthesis and secretion of CCL2 and CXCL10. Subsequently, CCL2 binding to astrocytes, either by binding to D6 decoy receptor or by alternative mechanisms, may establish a chemokine gradient in the CNS, and direct the migration of leukocytes.

Acknowledgments

First, I would like to thank my both supervisors, Nicola and Nacho, for their constant support when I needed them and advices all along the PhD. Thank you for giving me the opportunity to work with you. It has been a great three and half years of my life that I will never forget.

I would like to thank the people in the BMRC especially Helen (as a part of the chemokine team), Martin for great wild moments during conferences and great neighbour in the office, Lindsey for the help with the real time PCR, Robert for the help with statistics, Marie Claude for lending me her laptop when needed and all the others from the BMRC.

I would like to thank Jonty, Laura, Dan, David, Boumi, Michal and the all the others for making my life so much easier when I arrived in England and made me feel like home.

I would like to thank Julie who helped in the past and provided me home while I was homeless in Angers. Thank you Franck for your providing me the scientific papers I could not get here. You have both been really helpful in my life so far and I will be eternally grateful.

I would like to thank my family for the support throughout my studies and help me to achieve what I have accomplished so far, which would not have been possible without their help. I would like to have a special thought for my gran who died in August 2006.

At last and from far the least, I would like to send a special thank you to my partner Amy who has put up with me during the hard time of writing up while she was pregnant and look after me. She has always been here when I felt down and cheered me up with her contagious laugh and positive mind. You made it easier for me and I will be eternally grateful.

Contents

1	Introduction	6
1.1	Central nervous system (CNS) overview	6
1.1.1	Organisation of the CNS	6
1.1.1.1	Neurons	6
1.1.1.2	Oligodendrocytes	6
1.1.1.3	Microglia	7
1.1.1.4	Astrocytes	8
1.2	Multiple Sclerosis (MS)	14
1.2.1	Definition	14
1.2.2	Epidemiology	14
1.2.3	Cause of MS	14
1.2.3.1	Diet	16
1.2.3.2	Viral or bacteria theory	16
1.2.3.3	Genetics and MS	17
1.2.3.4	Migration studies	18
1.2.4	Time course of disease	18
1.2.4.1	Relapsing-remitting MS (RR-MS)	18
1.2.4.2	Secondary progressive MS (SP-MS)	19
1.2.4.3	Primary progressive MS (PP-MS)	19
1.2.5	Diagnosis of MS	19
1.2.5.1	Magnetic resonance imaging (MRI)	19
1.2.5.2	Visual evoked potentials	20
1.2.5.3	CSF analysis	22
1.2.6	Pathophysiology of the disease	22
1.2.6.1	Different type of lesions in MS	22
1.2.6.2	Initial stage of MS: self-reactive lymphocytes	23
1.2.6.3	BBB and cell migration into the CNS	25
1.2.6.4	Inflammation	27
1.2.6.5	Demyelination-axonal damage	30
1.2.6.6	Astrocytes in MS: scar formation	31
1.3	Experimental autoimmune encephalomyelitis (EAE): model for MS	32
1.3.1	Induction of EAE	33
1.3.2	Physiopathology of EAE	33
1.3.3	Advantages and disadvantages of EAE as a model for MS	34
1.4	Chemokines and their receptors	35
1.4.1	Chemokines	35

1.4.2	Chemokine classification	35
1.4.3	Chemokine receptors	36
1.4.4	Chemokine receptor classification	36
1.4.4.1	Silent chemokine receptors	37
1.4.5	Chemokine-chemokine receptor interaction	40
1.4.6	Chemokine-glycosaminoglycan interaction	41
1.4.7	Chemokine receptors intracellular signalling pathways	41
1.4.7.1	Phosphoinositide-specific phospholipase C pathway (PLC)	42
1.4.7.2	Phosphoinositide 3 kinase pathway(PI3K)	42
1.4.8	Function of chemokines	45
1.4.8.1	Leukocyte recruitment	45
1.4.8.2	Differentiation of T lymphocytes	45
1.4.8.3	Activation of dendritic cells	46
1.4.8.4	CNS development	46
1.4.8.5	Control of angiogenesis by chemokines	47
1.4.9	Chemokines and chemokine receptors in MS	47
1.4.9.1	Chemokines in MS	47
1.4.9.2	CCL2 expression in MS	48
1.4.9.3	Function of CCL2 during inflammation in the CNS	50
1.4.9.4	CXCL10 expression in MS	52
1.4.9.5	Function of CXCL10 in the CNS in MS	53
1.4.9.6	Chemokine receptors in MS	54
1.4.10	Chemokines and chemokine receptors in EAE	55
1.4.10.1	Chemokines in EAE	55
1.4.10.2	Chemokine receptors in EAE	55
1.4.11	Chemokines and astrocytes	57
1.5	Aims of this thesis	57

2	Expression of CCL2 and CXCL10 by primary human adult astrocytes	59
2.1	Introduction	59
2.1.1	CCL2 and CXCL10 expression in MS	59
2.1.2	Pro-inflammatory cytokines in CNS inflammation	60
2.1.2.1	Interleukin1- β (IL1- β): effect on CNS resident cells	60
2.1.2.2	Tumor necrosis factor (TNF): effect on CNS resident cells	61
2.1.2.3	Interferon γ (IFN γ): effect on CNS resident cells	62
2.1.3	Aim of the study	63
2.2	Materials and methods	65
2.2.1	Isolation of astrocytes from CNS tissue	65
2.2.2	Characterization of different primary human adult astrocytes by immunocytochemistry using anti-GFAP antibody	66
2.2.2.1	Principle of immunocytochemistry	66

2.2.2.2	Astrocyte characterization by immunocytochemistry for GFAP	67
2.2.3	Visualisation of GFAP staining by astrocytes using confocal microscopy	68
2.2.3.1	Principle of Confocal laser scanning microscopy (CLSM)	68
2.2.4	Detection of mycoplasma in cell cultures by PCR	68
2.2.5	Effect of pro-inflammatory cytokines on the expression of CCL2 and CXCL10 by different astrocyte preparations . .	69
2.2.5.1	Stimulation of astrocytes with pro-inflammatory cytokines	69
2.2.5.2	Comparison of response of three different astrocyte preparations, following pro-inflammatory stimulation	72
2.2.6	Real time PCR to quantitate mRNA isolated from astrocytes stimulated with pro-inflammatory cytokines	72
2.2.6.1	Principle of qRT-PCR	72
2.2.6.2	mRNA extraction	76
2.2.6.3	cDNA synthesis	76
2.2.6.4	Real time PCR optimisation: selection of the most stable housekeeping gene using GeNorm software	76
2.2.6.5	Real time PCR amplification	77
2.2.7	Measurement of CCL2 and CXCL10 secretion by astrocytes following pro-inflammatory stimulation using Enzyme-Linked ImmunoSorbent Assay (ELISA)	78
2.2.8	Statistical analysis	79
2.3	Results	81
2.3.1	Characterization of primary human adult astrocytes using immunocytochemistry	81
2.3.2	Real time PCR: optimisation	84
2.3.2.1	Selection of the housekeeping gene (HK gene) . .	84
2.3.2.2	Determination of primer efficiency	87
2.3.3	Measurement of CCL2 and CXCL10 mRNA expression by stimulated primary human astrocytes using real time PCR	90
2.3.3.1	Determination of CCL2 mRNA expression following cytokine stimulation	90
2.3.3.2	Determination of CXCL10 mRNA following cytokine stimulation	92
2.3.4	ELISA measurement of CCL2 secretion by astrocytes following stimulation with pro-inflammatory cytokines	97
2.3.4.1	Unstimulated cells	97
2.3.4.2	IL- β stimulation	97
2.3.4.3	TNF stimulation	97
2.3.4.4	IFN γ stimulation	98

2.3.5	ELISA measurement of CXCL10 secretion by astrocytes following stimulation with pro-inflammatory cytokines	98
2.4	Discussion	101
2.4.1	Constitutive expression of CCL2 and CXCL10 mRNA by primary human adult astrocytes using qRT-PCR	102
2.4.2	CCL2 mRNA expression by astrocytes following pro-inflammatory cytokine treatment using qRT-PCR	102
2.4.3	CXCL10 mRNA expression by astrocytes following pro-inflammatory cytokine treatment using qRT-PCR	103
2.4.4	CCL2 and CXCL10 secretion by unstimulated astrocytes using ELISA	104
2.4.5	CCL2 secretion by astrocytes following pro-inflammatory cytokine treatment using ELISA	105
2.4.6	Other CCL2 producing cells in the CNS	105
2.4.7	CXCL10 secretion by astrocytes following pro-inflammatory cytokine treatment using ELISA	106
2.4.8	Other CXCL10 producing cells in the CNS	106
2.4.9	Do astrocytes contribute to the differential expression of CCL2 and CXCL10 in the CSF of MS patients at time of relapse?	107
3	Measurement of CCL2 binding to primary human adult astrocytes <i>in vitro</i>	111
3.1	Introduction	111
3.1.1	CCL2 effects on astrocytes	111
3.1.2	CCR2 expression by astrocytes in the CNS in MS	112
3.1.3	CCR2 expression by astrocytes <i>in vitro</i>	112
3.1.4	CCR2 signalling and functional effect of CCL2	112
	3.1.4.1 Calcium flux following CCL2 treatment	113
	3.1.4.2 Erk signalling	113
	3.1.4.3 PKB/Akt signalling	114
3.1.5	Aim of the study	114
3.2	Materials and methods	116
3.2.1	Determination of CCR2 mRNA expression by human adult astrocytes following pro-inflammatory stimulation	116
	3.2.1.1 Sequences of forward and reverse primers for CCR2 gene	116
	3.2.1.2 Sequencing of PCR products to check the specificity of CCR2 primers amplicons	116
	3.2.1.3 Real time PCR on cDNA from stimulated astrocytes	117
3.2.2	Determination of CCR2 expression by primary human adult astrocytes, using flow cytometry	117
	3.2.2.1 Principle of flow cytometry	117
	3.2.2.2 Detection of cell surface expression of CCR2 on unstimulated astrocytes by flow cytometry	123

3.2.2.3	Detection of CCR2 on permeabilised unstimulated astrocytes by flow cytometry	123
3.2.2.4	Measurement of CCR2 expression at the astrocyte cell surface following pro-inflammatory stimulation.	124
3.2.2.5	Acquisition of CCR2 PE-labelled (FL-2) astrocytes using flow cytometry.	124
3.2.2.6	Analysis of CCR2 PE-labelled (FL-2) astrocytes using BD TM CellQuest Pro software.	125
3.2.2.7	CCR2 expression by primary human adult astrocytes by immunocytochemistry	125
3.2.3	Measurement of CCL2 binding to astrocytes using biotinylated CCL2 by flow cytometry	126
3.2.3.1	Optimisation of CCL2 binding to astrocytes: dose response	126
3.2.3.2	Optimisation of binding of biotinylated-CCL2 to astrocytes: time course experiment	126
3.2.3.3	Specificity of CCL2 binding to astrocytes: competition assay	127
3.2.3.4	Detection of CCL2 binding to primary human astrocytes under pro-inflammatory conditions	127
3.2.4	Detection of CCL2 binding to astrocytes using confocal microscopy	127
3.2.5	Measurement of calcium flux following stimulation of astrocytes with CCL2	128
3.2.5.1	Principle of calcium flux measurement	128
3.2.5.2	Procedure for calcium imaging following CCL2 treatment of astrocytes	129
3.2.6	Measurement of Erk and Akt signalling using SDS PAGE and western blotting by detecting phosphorylated forms	131
3.2.6.1	Cell stimulation with CCL2 and fetal calf serum (FCS)	131
3.2.6.2	Sample preparation for the measurement of Erk and Akt phosphorylation following CCL2 treatment by western blotting	131
3.2.6.3	Measurement of Erk and Akt phosphorylation following CCL2 treatment by western blotting	132
3.2.7	Statistical analysis	133
3.3	Results	135
3.3.1	Measurement of CCR2 mRNA expression by astrocytes following cytokine stimulation using qRT-PCR	135
3.3.2	CCR2 expression by astrocytes using flow cytometry	135
3.3.3	Binding of biotinylated CCL2 to the cell surface of human adult astrocytes detected by avidin-FITC and flow cytometry	139
3.3.4	Measurement of calcium flux in astrocytes following CCL2 treatment	146

3.3.4.1	Optimisation of experimental conditions	146
3.3.4.2	Effect of CCL2 treatment on intracellular calcium flux in astrocytes	150
3.3.5	Effect of CCL2 treatment on Erk and Akt signalling pathways in astrocytes	150
3.4	Discussion	153
3.4.1	CCR2 mRNA expression by astrocytes using qRT-PCR	153
3.4.2	CCR2 protein expression by astrocytes using flow cytometry	154
3.4.3	Measurement of signalling pathways induced by CCL2 in astrocytes	155
4	CXCR3 expression by primary human adult astrocytes	160
4.1	Introduction	160
4.1.1	CXCR3: overview	160
4.1.2	CXCR3 expression in the CNS white matter in MS patients	161
4.1.3	Effect of CXCR3 agonists on Erk and Akt signalling	162
4.1.3.1	Aim of the study	163
4.2	Materials and methods	164
4.2.1	Determination of CXCR3 mRNA expression by astrocytes following pro-inflammatory stimulation using qRT-PCR	164
4.2.2	Detection of CXCR3 expression by primary human adult astrocytes using immunocytochemistry	164
4.2.3	Quantitation of CXCR3 chemokine receptor expression by primary human adult astrocytes using flow cytometry	165
4.2.4	Analysis of CXCL10-induced calcium flux in primary human adult astrocytes	165
4.2.5	Erk and Akt phosphorylation analysis following CXCL10 stimulation of primary human adult astrocytes	166
4.2.6	Statistical analysis	166
4.3	Results	167
4.3.1	CXCR3 expression by stimulated primary human adult astrocytes at both mRNA and protein level	167
4.3.1.1	CXCR3 mRNA expression by stimulated astrocytes using qRT-PCR	167
4.3.1.2	CXCR3 protein expression by primary human adult astrocytes following pro-inflammatory cytokine stimulation	167
4.3.2	Effect of CXCL10 treatment on intracellular calcium increase in astrocytes	169
4.3.3	Measurement of phosphorylation of Erk and Akt following CXCL10 stimulation of astrocytes	173
4.4	Discussion	176
4.4.1	CXCR3 mRNA expression by astrocytes following pro-inflammatory cytokine treatment	176

4.4.2	CXCR3 protein expression by astrocytes following pro-inflammatory cytokine treatment	177
4.4.3	Measurement of signalling pathways induced by CXCL10 in astrocytes	178
4.4.4	Effect of CXCL10 on other CNS resident cells	179
5	Expression of decoy chemokine receptor D6	180
5.1	Introduction	180
5.1.1	D6 decoy receptor: characteristics	180
5.1.2	Role of D6 receptor in inflammation	182
5.1.3	D6 in EAE	182
5.1.4	D6 in MS	183
5.2	Aim of the study	183
5.3	Materials and methods	184
5.3.1	Measurement of D6 mRNA expression by astrocytes following pro-inflammatory cytokine stimulation using qRT-PCR	184
5.3.2	Detection of D6 receptor expression by primary human adult astrocytes using western blotting	184
5.3.2.1	Protein extraction	184
5.3.2.2	Protein estimation: bicinchoninic acid (BCA) assay	185
5.3.2.3	Sample preparation for western blotting analysis	185
5.3.2.4	SDS-PAGE and western blotting for D6 expression in primary human adult astrocytes	185
5.3.2.5	Detection of D6 receptor by primary human adult astrocytes using flow cytometry	186
5.3.3	Analysis of D6 expression on human brain tissue	187
5.3.3.1	Tissue characterisation: Oil red O (ORO) staining	187
5.3.3.2	Measurement of D6 mRNA expression in human brain tissue using qRT-PCR	189
5.3.3.3	Detection of D6 in human brain tissue using SDS-PAGE and western blotting	189
5.3.3.4	Detection of D6 on human brain sections by immunohistochemistry: optimisation	189
5.3.3.5	Determination of the cell type expressing D6 by double indirect immunofluorescence staining	190
5.3.4	CCL2 binding to human brain tissue sections by immunofluorescence: optimisation of concentration of biotinylated CCL2 and avidin-FITC	191
5.3.5	Determination of the cell type binding biotinylated CCL2 in human brain sections: dual staining with D6	193
5.3.6	Statistical analysis	193
5.4	Results	194
5.4.1	D6 expression on primary human adult astrocytes	194
5.4.1.1	Measurement of D6 mRNA expression by astrocytes using qRT-PCR	194

5.4.1.2	Measurement of D6 protein expression by astrocytes using SDS-PAGE and western blotting . . .	194
5.4.1.3	Measurement of D6 protein expression by astrocytes using flow cytometry	198
5.4.2	Analysis of D6 expression on human brain tissue sections .	202
5.4.2.1	Characterisation of brain tissue sections using ORO staining	202
5.4.2.2	Measurement of D6 mRNA expression in brain tissue using qRT-PCR.	202
5.4.2.3	Detection of D6 protein expression in brain tissue using SDS-PAGE and western blotting	206
5.4.2.4	Optimisation of D6 staining on human brain sections by immunohistochemistry	206
5.4.2.5	Cell phenotype expressing D6 in brain using immunohistochemistry	210
5.4.3	CCL2 binding to human brain tissue sections	210
5.4.3.1	Optimisation of the binding of biotinylated CCL2 to brain tissue sections	210
5.4.3.2	Determination of the ability of D6 to bind CCL2 in brain tissue sections	215
5.5	Discussion	218
5.5.1	D6 mRNA expression by unstimulated astrocytes using qRT-PCR	218
5.5.2	D6 mRNA expression by astrocytes following pro-inflammatory cytokine treatment using qRT-PCR	219
5.5.3	D6 protein expression by astrocytes using western blotting and flow cytometry	219
5.5.4	D6 mRNA expression <i>in vivo</i> using qRT-PCR	221
5.5.5	D6 protein expression <i>in vivo</i> using western blotting	222
5.5.6	Determination of cell types expressing D6 <i>in vivo</i> using immunohistochemistry	222
5.5.7	Determination of D6 ability to bind CCL2 <i>in vivo</i> using immunohistochemistry	224
6	General discussion	225
6.1	General discussion	225
6.2	Future work	229
	References	234

List of Figures

1.1	The blood brain barrier (BBB)	10
1.2	Geographical distribution of MS	15
1.3	Time course of MS	21
1.4	Proposed molecular mimicry mechanism in MS for the induction of autoimmunity.	28
1.5	A model of the molecular pathogenesis of multiple sclerosis.	29
1.6	Schematic representation of a family A receptor in the cell by crystal structure: G protein coupled receptor (GPCR)	38
1.7	Signalling pathways downstream of chemokine receptor activation.	44
2.1	Principle of immunostaining: direct and indirect labelling	70
2.2	Principle of confocal laser scanning microscope (CLSM)	71
2.3	Characterisation of primary human adult astrocytes using immunostaining for the astrocytic marker, GFAP	82
2.4	Detection of mycoplasma contamination in astrocyte supernatants using PCR amplification	83
2.5	Analysis of the melt-curve to determine the specificity of PCR product	86
2.6	UBC primer efficiency in qRT-PCR: serial cDNA dilutions	88
2.7	Calculation of UBC primer efficiency using the Ct value from qRT-PCR reaction with serial dilutions.	89
2.8	CCL2 and CXCL10 mRNA expression in unstimulated astrocytes.	91
2.9	Effect of pro-inflammatory cytokines on CCL2 mRNA expression by primary human adult astrocytes using qRT-PCR.	93
2.10	Effect of pro-inflammatory cytokines on CCL2 mRNA expression by three different astrocytes preparations using qRT-PCR.	94
2.11	Effect of pro-inflammatory cytokines on CXCL10 mRNA expression by primary human adult astrocytes using qRT-PCR.	95
2.12	Effect of pro-inflammatory cytokines on CXCL10 mRNA expression by three different astrocyte preparations using qRT-PCR.	96
2.13	Effect of pro-inflammatory cytokine stimulation on CCL2 secretion by astrocytes measured by ELISA.	99
2.14	Effect of pro-inflammatory cytokine stimulation on CXCL10 secretion by astrocytes measured by ELISA.	100
3.1	Optical system in a flow cytometer	120
3.2	Two dimension dot plots of PBMCs and astrocyte cells in suspension.	121

3.3	Single dimension histogram determines the level of expression of the protein of interest	122
3.4	Principle of calcium imaging in cells following activation of a receptor.	130
3.5	Detection of CCR2 mRNA expression by astrocytes following pro-inflammatory cytokine stimulation using qRT-PCR.	136
3.6	Comparison of CCR2 mRNA expression between three astrocyte preparations	137
3.7	Histogram representation of cell CCR2 expression using flow cytometry.	138
3.8	Biotinylated CCL2 binding to primary human adult astrocytes detected by avidin-FITC.	141
3.9	CCL2 binding to primary human adult astrocytes (B327/01) using flow cytometry.	142
3.10	Optimisation of CCL2 binding determined by flow cytometry: dose response and time course.	143
3.11	Determination of the specificity of biotinylated CCL2 binding: competition experiments.	144
3.12	Biotinylated CCL2 binding to astrocytes under pro-inflammatory conditions by flow cytometry	145
3.13	Optimisation of the volume of solution injected for detection of calcium flux in astrocytes (1).	147
3.14	Optimisation of the volume of solution injected for detection of calcium flux in astrocytes (2).	148
3.15	Incubation with sulfinpyrazone to prevent dye leakage.	149
3.16	Effect of CCL2 treatment on Erk 1 and 2 phosphorylation in primary human adult astrocytes using SDS PAGE and western blotting.	151
3.17	Effect of CCL2 treatment on Akt phosphorylation in primary human adult astrocytes using SDS PAGE and western blotting.	152
3.18	Hypothetical mechanism for CCL2 binding to primary human adult astrocytes <i>in vitro</i>	159
4.1	Effect of pro-inflammatory cytokines on CXCR3 mRNA expression by primary human adult astrocytes using qRT-PCR.	168
4.2	Detection of astrocyte expression of CXCR3 using immunocytochemistry.	170
4.3	Detection of CXCR3 expression at the cell surface and intracellularly on primary adult astrocytes using flow cytometry.	171
4.4	Effect of pro-inflammatory cytokines on CXCR3 cell surface expression by primary human adult astrocytes using flow cytometry.	172
4.5	Effect of CXCL10 treatment on Erk 1 and 2 phosphorylation by primary human adult astrocytes using SDS PAGE and western blotting.	174
4.6	Effect of CXCL10 treatment on Akt phosphorylation by primary human adult astrocytes using SDS PAGE and western blotting.	175
5.1	Measurement of D6 mRNA expression in astrocytes by qRT-PCR following pro-inflammatory cytokine stimulation.	195

5.2	Detection of D6 receptor on astrocytes using SDS-PAGE and western blotting: optimisation of the protein concentration.	196
5.3	Detection of D6 receptor on astrocytes using SDS-PAGE and western blotting: optimisation of the sample preparation and migration conditions	197
5.4	Histogram representation of D6 expression at the cell surface and intracellularly in primary human adult astrocytes using flow cytometry.	199
5.5	Measurement of D6 expression level at the cell surface and intracellularly on primary human adult astrocytes using flow cytometry.	200
5.6	Effect of pro-inflammatory cytokine stimulation on cell surface D6 expression by primary human adult astrocytes using flow cytometry.	201
5.7	Assessment of demyelination and inflammation in human brain tissue sections: Oil Red O (ORO) staining.	203
5.8	D6 mRNA expression in MS, NAWM and control brain tissue by qRT-PCR.	205
5.9	Detection of D6 receptor in MS, NAWM and control human brain tissue using SDS-PAGE and western blotting.	207
5.10	Quantitative comparison of D6 expression between MS, NAWM and control human brain tissue.	208
5.11	Detection of D6 receptor in human brain tissue sections using immunofluorescence.	209
5.12	Determination of the neuronal expression of D6 in human brain tissue.	211
5.13	Determination of the microglia expression of D6 in human brain tissue.	212
5.14	Determination of the astrocytic expression of D6 in human brain tissue.	213
5.15	Optimisation of binding of biotinylated CCL2 to human brain tissue sections: determination of optimal concentration for biotinylated CCL2.	214
5.16	Optimisation of binding of biotinylated CCL2 to human brain tissue sections: determination of the optimal concentration for avidin-FITC.	216
5.17	Determination of the ability of D6 to bind CCL2 in human brain tissue.	217

List of Tables

1.1	The four classes of chemokine receptor, their main agonists and functions.	39
2.1	Primer sequences of the HK genes tested and target genes used in this study	80
2.2	Ratio and M value determination of the different housekeeping genes analysed using GeNorm software.	85
2.3	Primer efficiency of the housekeeping and target genes.	88
2.4	Summary table for cytokine effects on CCL2 and CXCL10 mRNA expression by astrocytes.	109
2.5	Summary table for the comparison of expression of CCL2 and CXCL10 by CNS resident cells under cytokine stimulations. . . .	110
3.1	Fluorophores compatible with the BD FACScalibur.	119
3.2	Antibodies used to assess phosphorylation of Akt and Erk by western blotting	134
5.1	Case details of donors used to study D6 expression in the CNS . .	188
5.2	Summary table of primary and secondary antibodies used for the detection of the cellular origin of D6 by immunohistochemistry on human brain sections.	192
5.3	Characterisation of eight tissue blocks used in this study by ORO and haematoxylin staining.	204

Abbreviations

AGC: cAMP-dependent, cGMP-dependent, protein kinase C

ANP: atrial natriuretic peptide

ANOVA: analysis of variance

APC: antigen presenting cell

APP: amyloid precursor protein

ATP: adenosine triphosphate

BBB: blood brain barrier

bFGF: basic fibroblast growth factor

BDNF: brain-derived neurotrophic factor

BSA: bovine serum albumin

cDNA: complementary DNA

CNS: central nervous system

CLSM: confocal laser scanning microscopy

CSF: cerebrospinal fluid

DAG: diacylglycerol

DCs: dendritic cells

EAAT1 or 2: excitatory amino acid transporter 1 or 2

EAE: experimental autoimmune encephalomyelitis

EBV: Epstein Barr virus

EC: endothelial cell

EDSS: expanded disability status scale

ELISA: Enzyme linked immunosorbent assay

Erk: extracellular signal-regulated kinase

FCS: foetal calf serum

FITC: fluorescein isothiocyanate

GAG: glycosaminoglycan
GAPDH: glyceraldehyde-3-phosphate dehydrogenase
GFAP: glial fibrillary acid protein
GFP: green fluorescent protein
GLT-1: glucose transporter 1
GM: grey matter
GPCR: G protein coupled receptor
GRKs: GPCR kinases
HEPES: hydroxyethylpiperazine- ethanesulfonate
HEK: human embryonic kidney
HHV-6: human herpes virus
HK: housekeeping gene
HLA: human leukocyte antigen
HPRT: hypoxanthine phosphoribosyl transferase
HUVECs: human umbilical vein endothelial cells
ICAM-1: inter cellular adhesion molecules 1
IgG: immunoglobulin G
IFN γ : interferon-gamma
IL1 β : interleukin 1 β
IP3: inositol 1,4,5 triphosphate
JAM: junctional adhesion molecules
JNK: c-jun kinase
KA: kainic acid
KDa: kilodalton
KO: knock out
LFA-1: leukocyte function-associated-1
LPS: lipopolysaccharide
MAPKs: mitogen-activated-protein-kinases
MBP: myelin basic protein
MCP: monocyte chemoattractant protein

MEM: minimum essential medium
MFI: mean fluorescence intensity
MHC: major histocompatibility complex
MIP: macrophage inflammatory protein
MOG: myelin oligodendrocyte glycoprotein
MMPs: metalloproteinases
MRI: magnetic resonance imaging
mRNA: messenger ribonucleic acid
MRS: magnetic resonance spectroscopy
MS: multiple sclerosis
NAWM: normal appearing white matter
NGF: neuronal growth factor
NK: natural killer cells
NMDA: N-methyl-D-aspartic acid
NO: nitrite oxide
NT: neurotrophin
ORO: oil red O
PBMC: peripheral blood mononuclear cell
PC: pericytes
PCR: polymerase chain reaction
PE: phycoerythrin
PECAM-1: platelet endothelial cell adhesion molecule-1
PLP: proteolipid protein
PLC: phospholipase C
PI3K: phosphoinositide 3 kinase
PKB: Protein kinase B
PKC: protein kinase C
PP MS: primary progressive multiple sclerosis
PTX: pertussis toxin
RANTES: regulated on activation normal T expressed and secreted

RGCs: retinal ganglion cells
ROS: reactive oxygen species
RPL13A: ribosomal protein L 13A
RR MS: relapsing-remitting multiple sclerosis
7 KC: seven ketocholesterol
SFM: serum free media
SP MS: secondary progressive multiple sclerosis
TCR: T cell receptor
TEP: triethyl phosphate
TLRs: Toll-like receptors
T_m: Melting temperature
TMB: 3,3',5,5'-tetramethylbenzidine
TMEV: Theiler's murine encephalomyelitis virus
TNF: tumor necrosis factor
TRAIL: TNF related apoptosis-induced ligand
TPA: 12-O-tetradecanoylphorbol-13-acetate
UBC: ubiquitin C
VEGF: Vascular endothelial growth factor
VEP: visual evoked potential
VCAM-1: vascular cell adhesion molecule-1
VLA-4: very late antigen 4
WM: white matter

CHAPTER 1

Introduction

1.1 Central nervous system (CNS) overview

1.1.1 Organisation of the CNS

The central nervous system (CNS), composed of the brain and spinal cord, controls the human body by interpreting information involved in different functions such as thinking, movement, learning, memory. The CNS is composed of different cell types: neurons, neuroglial cells (oligodendrocytes, microglia, and astrocytes), endothelial cells, pericytes, smooth muscle cells, ependymal cells. [Purves et al., 2001].

1.1.1.1 Neurons

Neurons are both the structural and functional units of the CNS. They enable the transmission of different signals to all parts of the body in response to external stimuli. The ability of neurons to propagate signals all over the body lies on the existence of supporting cells called neuroglia.

1.1.1.2 Oligodendrocytes

Oligodendrocytes are small cells with many processes that produce a myelin sheath which surrounds nerve fibres. This myelin sheath plays an important role

in the transmission of signals along the axon. It acts as an insulating sheath and prevents ion exchange with the outside environment, which is necessary for the propagation of the nerve signal [Simons and Trotter, 2007]. There are gaps between two myelin sheaths known as the Nodes of Ranvier where ion exchange takes place to create depolarization, necessary for nerve signal propagation: the action potential. The action potential at one node is sufficient to excite a response at the next node, so the nerve signal can propagate faster by these discrete jumps rather than the continuous propagation of depolarization/repolarization along the membrane. This enhanced signal transmission is called saltatory conduction [Hartline and Colman, 2007]. The myelin sheath also provides a supportive framework and provides nutrients for the neurons. One oligodendrocyte is able to produce myelin sheaths to several neurons [Purves et al., 2001].

1.1.1.3 Microglia

Microglia, the resident macrophages of the brain, are the smallest neuroglia cells and account for approximately 20% of the glia cells in the brain [Kreutzberg, 1995]. They represent the main cell type that provide immuno-surveillance to the CNS [Kreutzberg, 1996].

Activation of microglia cells following injury is a graded process in response to injury by:

- changing their morphological phenotype
- increasing migratory activity
- proliferating
- secreting chemokines, proteases and others inflammatory mediators
- presenting antigen

These responses are responsible for the clearance of toxic molecules released by damaged and dying neurons and other cell types in the CNS [Bohatschek et al., 2001, Carson et al., 1998, Raivich et al., 1999]. When microglia are activated

in a number of CNS diseases, they express increased levels of MHC II molecules [Minagar et al., 2002] which can, during inflammation, activate lymphocytes and produce pro-inflammatory mediators that could exert a damaging or a protective effect on adjacent axons, myelin and oligodendrocytes [Raivich and Banati, 2004, Carson, 2002].

1.1.1.4 Astrocytes

Astrocytes are the most abundant glial cells within the brain and represent one third of the mass of the brain [Kandel, 1991]. Two different types of astrocytes have been observed depending on their localization in the CNS and their antigenic profile and function [Holley et al., 2003]. Type 1 astrocytes or fibrous astrocytes are localized in the white matter and are in contact with myelinating axons [Karasek et al., 2004]. They have a star-shape with cytoplasmic extensions that surround most of the synapses within the CNS. Astrocytes express glial acidic fibrillary protein (GFAP), an astrocytic marker, which is a component of the cytoskeleton, defining and maintaining the shape of the astrocyte [Eng, 1985]. Astrocytes also express S100 β , a calcium-binding astrocytic protein [Ridet et al., 1997]. Type 2 astrocytes or protoplasmic astrocytes are localized in the grey matter and surround the node of Ranvier. It is characterised by S100 β staining and a variable GFAP staining [Mi and Barres, 1999, Karasek et al., 2004]. For many years, astrocytes have been considered to have limited function within the CNS. However they are involved in the development on the CNS (synapse formation), the formation and maintenance of the blood brain barrier, support of neurons, regulation of neurotransmitters, hormones and homeostasis, and communication with other cells as discussed below.

Development of the CNS:

Astrocytes have been recently shown to have active control of synaptogenesis. It was assumed for a long time that neurons were the only player in synapse formation [Scheiffele, 2003]. However, it has been shown that there is a delay between the arrival of neurons in the CNS and synapse formation which corresponds to the time in which astrocytes develop, suggesting the involvement of astrocytes in synaptogenesis [Pfrieger and Barres, 1997]. Direct evidence was obtained *in vitro*. Using retinal ganglion cells (RGCs) in culture, it was demonstrated that there is a 7 fold increase in synapse formation in the presence of astrocytes, and the synapses were functional [Nagler et al., 2001, Ullian et al., 2001].

Astrocytes are involved in the differentiation of stem cells into neurons [Song et al., 2002]. Enriched cultures of neurons from the hippocampus were prepared and it was shown that adult neural stem cells cultured with astrocytes significantly increased the number of neurons by 10 fold compared to the control (stem cells plated on laminin-coated substrate). Therefore astrocytes are sufficient to induce neurogenesis [Song et al., 2002].

Formation of the blood brain barrier (BBB):

One of the special feature of the CNS is the limitation of immune response to prevent accidental inflammation, which might be deleterious for the whole organism. The CNS is separated from the blood by the blood brain barrier, which is composed of three elements: endothelial cells, pericytes and astrocytes (figure 1.1) [Correale and Villa, 2007]. Endothelial cells form a continuous layer by forming tight junctions and adherens junctions between adjacent endothelial cells (ECs). ECs are thus tightly held together to form a barrier separating the blood from the CNS [Ballabh et al., 2004]. BBB selectively blocks toxic molecules, drugs and infectious agents, to protect the brain [Ballabh et al., 2004]. Paul Erlich in the early 1900s was the first to show the properties of the BBB by intravenous injection of vital dyes leading to the staining of almost the entire body except the

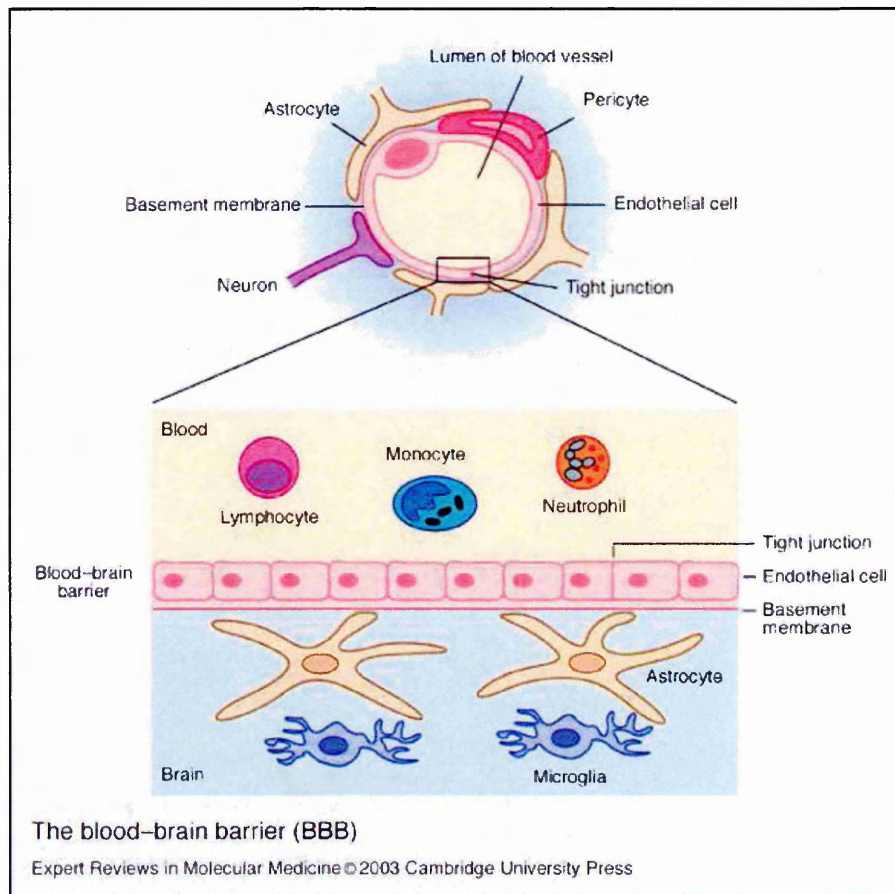


Fig. 1.1: **Schematic representation of the structure of the BBB.** ECs, held together by adherens and tight junctions are wrapped by pericytes and astrocyte end-feet to form a physically impermeable barrier (taken from http://www.medicallook.com/human_anatomy/organs/Blood_brain_barrier.html).

brain. However, the BBB is not fully impermeable and allows the influx or efflux of molecules through transporters for normal brain function. For instance, the BBB allows the transport, from the blood to the CNS of glucose and large amino acids such as leucine via Glut-1 transporter and L-system carrier L1, respectively [Abbott, 2002]. Pericytes (PCs) are cells of microvessels that wrap around the endothelial cells on the CNS side of the BBB [Lai and Kuo, 2005]. They are the least-studied component from the BBB but appear to play a regulatory role in brain angiogenesis, endothelial cell tight junction formation, and blood-brain barrier differentiation [Balabanov and Dore-Duffy, 1998, Dore-Duffy et al., 1993, Lindahl et al., 1997, Ramsauer et al., 2002], as well as contributing to the microvascular vasodynamic capacity and structural stability [Bandopadhyay et al., 2001, Rucker et al., 2000].

Astrocytes form an integral part of the BBB by covering more than 90% of the BBB with end-feet to form a lacework of fine lamellae around the endothelial cells. This close contact is important for the induction and the maintenance of the BBB. *In vivo* experiments have shown that implantation of astrocytes into an area with normally leaky vessels induces tightening of the endothelium, highlighting the role of astrocytes in the induction of the BBB properties [Hayashi et al., 1997, Kuchler-Bopp et al., 1999, Hurwitz et al., 1993].

Regulation of neurotransmitters and hormones:

Astrocytes not only have supportive and structural functions but also act as modulators of function by regulating glutamate concentration at the synapse, to regulate neurotransmission. Glutamate is a strong excitatory amino acid in the brain and is cleared from the synapse by two transporters [Simard and Nedergaard, 2004]. Glutamate transporter 1 (GLT1 also called EAAT2) and the Na⁺-dependent glutamate/aspartate transporter (GLAST also called excitatory amino acid transporter 1 or EAAT1) are highly expressed in the astrocytic processes highlighting the ability of astrocytes to take up glutamate from the extracellular milieu [Rauen et al., 1998, Rothstein et al., 1996, Anderson and Swanson, 2000]. GLAST acts as a water channel and is involved in the regulation of water in the

CNS [MacAulay et al., 2002]. GLT1 appears to limit oedema, resulting from ischemia, within the brain [Namura et al., 2002].

Astrocytes also induce the release of neuropeptides such as atrial natriuretic peptide (ANP) which appears to regulate the fluid and ionic environment in the CNS [Krzan et al., 2003]. Astrocytes have also been shown respond to neuroactive molecules released by neurons such as histamine and acetylcholine [Shelton and McCarthy, 2000]. The fact that astrocytes release these gliotransmitters, modulate the synaptic transmission and respond to neuroactive molecules has led to the concept of the tripartite synapse and highlight the preponderant role of astrocytes as a regulator of neuronal function but also the bi-directional signalling between neurons and astrocytes [Perea and Araque, 2005].

Support of neurons:

Considering the position of astrocytes in the CNS and the metabolism of astrocytes, it is not surprising to see that astrocytes provide support to the axon. As previously said, the transporter EAAT1 and 2 are able to take up glutamate from the synapse, which is converted into glutamine, under the action of glutamine synthase. Glutamine is released into the synaptic compartment where it is used by neurons as a source of energy [Anderson and Swanson, 2000, McKenna, 2007]. Astrocytes, which are in close contact with the capillaries in the brain, possess high numbers of glucose transporters 1 at the end-feet processes and are capable of glycolysis and oxidation of glucose, the main source of energy within the brain. It was thought that glucose was the only source of energy for neurons obtained from the extracellular compartment by the cerebral circulation. However, it has been proposed that neurons can use lactate by oxidation as a source of energy [Bouzier-Sore et al., 2006]. They also showed that neurons preferentially use lactate as their main oxidative substrate. In astrocytes, glucose is converted into lactate by an oxidative pathway before uptake by neurons, via a specific monocarboxylate transporter present on neurons

As well as providing energy for neurons, astrocytes also produce neurotrophic factors including nerve growth factor (NGF) or basic fibroblast growth factor (bFGF) that promote neuronal development, differentiation and survival [Kalehua et al., 2004].

Regulation of homeostasis

Astrocytes are involved in the regulation of ion concentration (including K^+ , Na^+ , Cl^-) in the extracellular compartment in the CNS that enables normal neuronal function.

To control the K^+ concentration in the extracellular compartment, astrocytes take up K^+ by:

- inward rectifying channels
- Na^+/K^+ pump
- $K^+/Na^+/Cl^-$ co transporter [Simard and Nedergaard, 2004].

Astrocytes are able to redistribute intracellular K^+ via gap junctions that connect astrocytes and to regulate intracellular K^+ via outward rectifying channels (Kir 4.1, rSloKCa, Kv 1.5) that expel K^+ into the perivascular space. They are expressed on the end-feet that surround synapses and blood vessels [Higashi et al., 2001, Price et al., 2002, Roy et al., 1996].

Na^+ is taken up by:

- the co transporter $Na^+K^+2Cl^-$
- $2Na^+/Ca^{2+}$ exchanger
- H^+/Na^+ antiport.

Efflux of Na^+ is controlled by Na^+/K^+ pump and the $2Na^+/Ca^{2+}$ exchanger [Simard and Nedergaard, 2004].

The concentration of Cl^- is controlled by influx of Cl^- by inward rectifying channels, co transporter $\text{Na}^+\text{K}^+2\text{Cl}^-$ and $\text{Cl}^-/\text{HCO}_3^-$ exchanger. Cl^- can be extruded by outward rectifying anion currents [Simard and Nedergaard, 2004]. Therefore astrocytes play an important role in the regulation of neuronal activity by regulating ion homeostasis at the synapse.

To conclude on the role of astrocytes, *in vitro* and *in vivo* studies have shown that astrocytes have a more complex role in the CNS than just a structural role. They are also involved in the development, maintenance and function of the CNS.

1.2 Multiple Sclerosis (MS)

1.2.1 Definition

MS is an inflammatory autoimmune disease that mainly affects the white matter of the CNS. It is classified as a putative autoimmune disease due to the accumulation of immunological cells, autoreactive T-lymphocytes and monocytes, in the CNS. These cells specifically attack the myelin sheath resulting in inflammation and demyelination leading to plaque formation and axonal damage. These plaques impair nerve transmission to muscles and other organs, rendering them unable to carry out their normal function [Minagar et al., 2004].

1.2.2 Epidemiology

MS can be diagnosed at any age but is most commonly diagnosed in people between 20 to 40 years old [Sospedra and Martin, 2005]. In the UK, the incidence of MS is 1:1000 and affects more women than men with a ratio of 3:2 [Alonso et al. 2007]. Many studies have shown that MS is not present at the same incidence all over the world [Kurtzke, 1977]. It can be seen on the world map (figure 1.2) that MS is indeed highly prevalent in Northern Europe (UK, Germany and Scandinavia), North America, Australia and New Zealand (between 60-200/100,000)

compared to low risk areas such as Japan (6-20/100,000). This suggests that the disease seems to be preferentially present in the western temperate latitudes. In comparison, Eastern regions and regions below 40° and above 60° latitude are not affected by the disease at the same rate [Kurtzke, 1977].

1.2.3 Cause of MS

This specific distribution of MS in the world has not be fully explained, however various factors including environmental factors e.g. infections, diet and sun exposure levels as well as genetic component or a combination of both have been implicated.

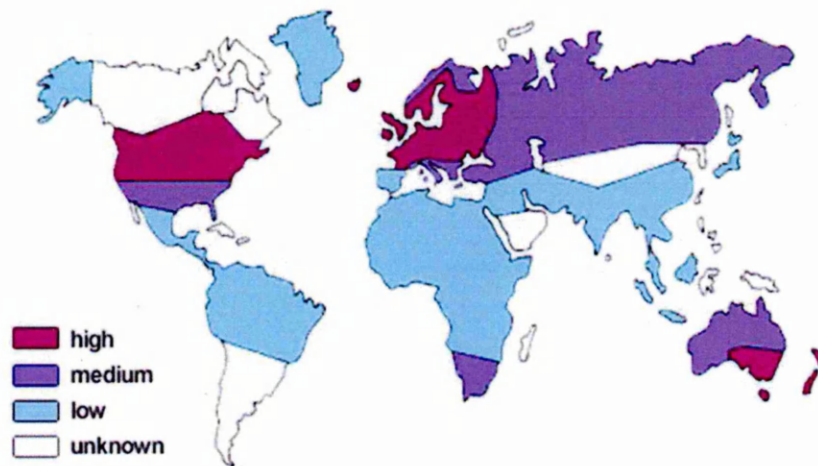


Fig. 1.2: Geographical distribution of MS.

MS is highly prevalent in Northern Europe (UK, Germany and Scandinavia), North America, Australia and New Zealand. The high prevalence is represented by purple colour whereas medium, low and unknown prevalence are represented by violet, blue and white colours respectively. This means that the disease seems to be preferentially present in the western temperate latitudes (obtained from http://www.hendess.net/grf/ms_welt_06_e.gif).

1.2.3.1 Diet

It has been shown that the prevalence of MS is reduced where environmental supplies of vitamin D are higher. It is well known that the active hormonal form of vitamin D (1,25-dihydroxyvitamin D) is a natural immunoregulator with anti-inflammatory effects. Vitamin D seems to reduce the risk of developing MS by about 40% and reduce the exacerbation of the disease [Brown, 2006].

Direct evidence using an animal model of MS, experimental autoimmune encephalomyelitis (EAE) (section 1.3), was obtained by administration of 1,25-dihydroxyvitamin D to rats, which resulted in protection and reduction in the disease activity. Vitamin D deficiency results from insufficient exposure to sunlight and a low vitamin D_3 diet [VanAmerongen et al., 2004].

1.2.3.2 Viral or bacteria theory

Recently, growing evidence has suggested that a viral or bacterial infection could explain the incidence of the disease by activating T cells resulting in so called molecular mimicry (see section 1.2.6.2). It has been shown that almost 100 % of transgenic mice expressing a TCR that is specific for myelin basic protein (MBP), a component of myelin, developed spontaneous EAE when they were housed in a non virus free environment but not in a sterile environment [Goverman et al., 1993].

Among viruses that are pathogenic, the human herpes viruses are good candidates and have been widely studied including, human herpes virus 6 (HHV6) and Epstein-Barr virus (EBV). A study was conducted to determine the frequency of human herpesvirus 6 (HHV-6) on autopsy material from 64 MS lesions, 44 normal appearing white matter in CNS of MS patients (NAWM), 41 healthy brains and 46 brains with other neurological disease [Cermelli et al., 2003]. They found that 15.9% of NAWM samples, 21.7% of patients with non-MS neurologic disorders and 26.8% of control patients were positive for HHV-6 DNA sequences, versus 57.8% of MS plaques ($P \leq 0.0005$). This result was confirmed by a study on NAWM, le-

sional tissue and normal control brain samples [Opsahl and Kennedy, 2005]. They showed that both NAWM and lesional tissues presented higher amounts of HHV6 mRNA and that HHV6 mRNA was present on oligodendrocytes by double mRNA FISH analysis. Therefore these studies show that HHV6 might play a role in the pathogenesis of MS.

Relevance of EBV in MS pathogenesis was obtained by looking at antibody directed against EBV in MS patient sera. In a study of 271 patients (108 MS patients and 163 healthy patients), anti-EBV antibodies were elevated in patients with MS and MS patients reactivate EBV infections more frequently and this correlates with a relapse [Wandinger et al., 2000, Hollsberg et al., 2005].

Among bacteria, *Chlamydia pneumoniae* has been implicated in MS pathogenesis but this issue is still controversial. Collaborative reports from two laboratories (Vanderbilt University Medical center (VMUC) and the University of South Florida (USF)) have shown the presence of *C. pneumoniae* in the CSF of MS patients. Indeed they showed that the prevalence of *C. pneumoniae* was 72 (VMUC) and 61% (USF) in 18 CSF of MS patients, compared to CSF of 11 patients with other neurological disorder patients with a prevalence of 7 (VMUC) and 16 % (USF) [Sriram et al., 2002]. However, other study failed to identify any association of this bacteria with MS using 70 CSF from MS patients and 30 CSF from other neurological disorders [Chatzipanagiotou et al., 2003]. Further work is needed to clearly associate *C. pneumoniae* with MS.

1.2.3.3 Genetics and MS

Genetic involvement in MS is primarily suggested by high risk groups and incidence in specific ethnic populations, regardless of the geographic localization of the population. For instance, observations have shown that MS is mainly a disease of caucasians [Cournu-Rebeix et al., 2001]. Further evidence for a genetic aetiology in MS is illustrated by twin study. Concordance rates in twin study are

higher in monozygotic than dizygotic twins [Dyment et al., 2004].

To date, the human leukocyte antigen (HLA) genes remain the strongest genetic factor influencing MS susceptibility. HLA-DRB1*15 has been found to be consistently expressed in the MS population and confers a 2 to 3 fold increase in the risk of developing MS [Oksenberg and Barcellos, 2005, Lincoln et al., 2005]. The exact mechanism whereby HLA DRB1 affects the susceptibility of MS remains unclear but it seems that it is linked to the binding/presentation of antigen and T cell repertoire determination by negative selection [Stratmann et al., 2003, Wucherpfennig, 2005].

1.2.3.4 Migration studies

Migration studies showed that children born to parents immigrating from South Africa or West Indies (low prevalence of MS) to the UK have high prevalence of MS similar to the general population of England [Elian et al., 1990] highlighting the importance of the environmental factors. It was also shown that populations migrating before the age of 15 from high risk to low risk acquired a low risk status to develop MS but not if there are above 15 [Hammond et al. 2000].

Therefore, whether MS develops in an individual is due to a combination of different factors rather than a unique factor such as genetic predisposition or environmental factor i.e. MS is a multifactorial disease.

1.2.4 Time course of disease

This disease is unusual as people with MS do not follow the same pattern of clinical manifestations. Indeed, MS is characterised by a number of disease courses (figure 1.3):

- Relapsing-remitting
- Secondary progressive
- Primary progressive

1.2.4.1 Relapsing-remitting MS (RR-MS)

This type of disease course is the most common. It is characterised by successions of relapse and remission. Relapse is considered as an aggravation of the disease in terms of symptoms or degree of disability. It is followed by a remission state that corresponds to a complete or partial regression of symptoms. A relapse is considered to be more than 24 hours duration and is separated from the previous relapse by at least 1 month. Usually the patient recovers completely after the first relapse and prolonged symptoms appear after several relapses as the disease progresses [Weinshenker, 1994, Hohol et al., 1995].

1.2.4.2 Secondary progressive MS (SP-MS)

RR-MS is usually followed by secondary progressive MS. This is a progressive evolution of the disease with increasing neurological disability over time [Weinshenker, 1994, Hohol et al., 1995]. It is difficult to determine the exact time when this second form appears but it seems to correlate with the appearance of active inflammatory demyelinating lesions seen on MRI (magnetic resonance imaging) [De Stefano et al., 2000].

1.2.4.3 Primary progressive MS (PP-MS)

20% of patients are affected by this form and this corresponds to a rapid clinical decline. No acute attacks or remissions occur in this form of MS. This course is the most severe form of MS [Kremenchtzky, 2003]. MRI gadolinium scans show that PP-MS has less cerebral lesions and fewer lesions per unit of time, compared to the SP-MS [Thompson et al., 1991] and that in PP-MS the axonal loss is partly independent of demyelination [Bitsch et al., 2000] suggesting different pathological mechanisms compared to other forms of MS.

1.2.5 Diagnosis of MS

When a patient presents with symptoms including fatigue, visual problems and depression, neurologists use a variety of tools to confirm the diagnosis [Poser and Brinar, 2004].

1.2.5.1 Magnetic resonance imaging (MRI)

Imaging technologies such as MRI are used to confirm a diagnosis of MS. The contrast in MRI is due to the different relaxation times of water protons in different environments within the body. Protons with short relaxation times give rise to brighter images. In order to enhance the contrast in a magnetic resonance image it is sometimes necessary to administer a "contrast agent" which will localise in a particular region of the body such as gadolinium (Gd) [Caravan, 2006]. It helps to distinguish new lesions from old lesions on MRI resulting from myelin loss.

1.2.5.2 Visual evoked potentials

Because demyelination of the optical nerve is the most common initial symptom in MS, the visual evoked potential (VEP) which measures the speed of the brain's response to visual, auditory and sensory stimuli can be helpful for the diagnosis of MS, characterised by a delay in the latency of the nerve signal [Weinstock-Guttman et al., 2003].

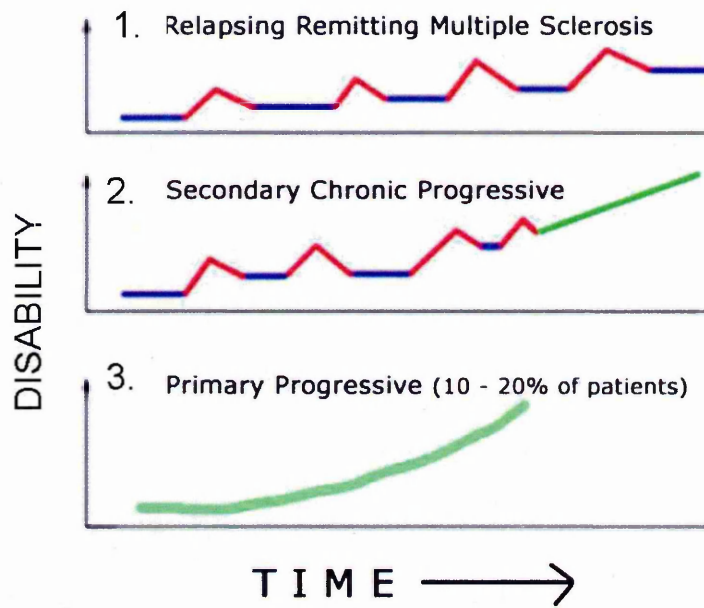


Fig. 1.3: Time course of MS.

Diagram representing the different types of the MS progression modified from http://www.chumsweb.org/pics/ms_class.jpg. There are three type of MS: relapsing remitting, secondary progressive and primary progressive MS

1.2.5.3 CSF analysis

The patient's cerebrospinal fluid is examined for cellular and chemical abnormalities often associated with MS. The rationale underpinning the use of CSF testing is the determination of whether there is clonal synthesis of immunoglobulin G (IgG) in the CNS compartment (intrathecal synthesis) resulting from the disruption of the BBB and the expansion of specific B cells in the CNS resulting in the synthesis of IgG. The screening of CSF against cDNA expression phage display or random peptide libraries did not show any common antigen recognition but showed some reactivity for oligodendrocytes or viruses, although it accounted for a minority of bands [Compston and Coles, 2002].

Using isoelectrofocussing, the presence of a characteristic pattern called oligoclonal bands of immunoglobulin can be identified, which are usually evident in relapsing-remitting MS [Pender, 2005]. Increased CSF cell numbers are also linked to active disease but are not unique to MS.

1.2.6 Pathophysiology of the disease

In MS there are different types of lesion with different levels of axonal damage.

1.2.6.1 Different type of lesions in MS

Acute lesions are the precursors of the MS plaque characterized by perivascular infiltration of inflammatory cells (essentially monocytes and lymphocytes), oedema, myelin swelling and activation of endothelial cells [Trapp et al., 1999, Lassmann, 1998]. These lesions might have variable axonal damage [Lassmann, 1998, 2003].

Chronic active lesions are older plaques with areas of active inflammation and demyelination usually at the margin of these plaques. They are characterized by perivascular lymphocyte infiltration, myelin breakdown leading to decreased numbers of oligodendrocytes, phagocytosis of myelin debris by foamy macrophages

and reactive astrocytosis. Variable axonal damage may be present [Oleszak et al., 2004].

Chronic inactive plaques are old plaques sharply delimited from adjacent normal appearing white matter with reactive gliosis, loss of oligodendrocytes, variable axonal loss and sometimes persistent immunological cells (monocytes, lymphocytes). A thin rim of perivascular collagenous fibrosis might be present in long-standing lesions and there is disruption of the BBB [Oleszak et al., 2004].

Shadow plaques consist of variable size and delimited plaques with demyelination and incomplete remyelination surrounding the principal plaque [Oleszak et al., 2004].

Although the aetiology of MS is still not fully resolved, many studies have focussed on the mechanism of the tissue damage in the disease.

1.2.6.2 Initial stage of MS: self-reactive lymphocytes

The initial stage of the disease is proposed as the activation of self-reactive lymphocytes in the lymph node. Two theories have been proposed [Sospedra and Martin, 2005]:

Existence of myelin autoreactive T lymphocytes

Self tolerance, a fundamental property of the immune system, is a result of the existence of negative selection of self reactive lymphocytes in the thymus called central tolerance and peripheral tolerance, which corresponds to the incapacity of autoreactive T cells to be activated. During negative selection, there is intrathymic expression of many tissue-specific antigens from "ectopic" or "promiscuous" genes, which play a major role in determining the antigen repertoire [Klein et al., 2000]. Indeed, in the thymus, lymphocytes that recognize these antigens, presented by the T cell receptor (TCR) to the MHC class II, are deleted; this is negative se-

lection. This selection is not complete as it has been shown that autoreactive T cells are present in the blood of healthy patients [Ota et al., 1990, Wekerle et al., 1996].

Since both healthy controls and MS patients show the presence of autoreactive T cells which recognised epitopes from MBP (myelin basic protein) and PLP (proteolipid protein), 2 major components of myelin [Bielekova et al., 2000, von Budingen et al., 2001], then the development of MS is not solely due to the presence of autoreactive T cells.

Therefore the question is what is the difference between the autoreactive T cells of healthy controls and MS patients that could explain the incidence of the disease. Studies have shown that the IL-2 receptor (CD25), a hallmark receptor for activated T cells, was more highly expressed on MBP-reactive T cells from MS patients than from normal patients. Therefore T cells in MS patients are in a greater activation state [Zhang et al., 1994, Hellings et al., 2001]. It has been also shown that T cells from peripheral blood in MS patients, but not normal individuals are less dependent on B7 costimulation for their activation [Lovett-Racke et al., 1998, Racke et al., 2000]. B7 is the second costimulatory signal which functions to induce the secretion of IL-2 from activated T-cells. These findings suggest that the explanation for the expansion of self reactive T cells in MS lies in the less stringent requirement of these cells for activation and on their enhanced activation state.

Negative selection is not the only mechanism for inducing self tolerance. A subset of lymphocytes, so called regulatory T cells (Tregs) have been shown to inhibit the activation of autoreactive T cells in the thymus [Sakaguchi et al., 2006]. They are characterised by their cell surface expression of CD4 and CD25 as well as the expression of the transcription factor Foxp3 [Viglietta et al., 2004]. Foxp3 belongs to the forkhead/winged helix family and is responsible for the development of the Tregs [Fontenot et al., 2003].

The role of Tregs in MS pathogenesis has been obtained by comparing the func-

tion of Tregs in MS patients and healthy control. It was shown that Tregs failed to suppress the proliferation of CD25⁻ T cells in MS but not in healthy controls [Viglietta et al., 2004]. This was confirmed by another study where Tregs from healthy or MS patients were co-cultured with CD4⁺CD25⁻T cells. Healthy Tregs induced 80% inhibition of CD25⁻ T cells compared to MS Tregs (20%) [Baecher-Allan and Hafler, 2004]. These results clearly indicate a role for Tregs in the pathogenesis of MS.

Molecular mimicry

The second theory is based on molecular mimicry in which infectious agents mimic epitopes of autoantigen (figure 1.4). Upon infection by bacteria or virus, lymphocytes are activated in the lymph node by APC that present antigenic peptide from the infectious agent [Markovic-Plese et al., 2004, Wucherpfennig, 2001]. As these antigens mimic self antigens (MBP, PLP), the immune response is then directed at self tissue. In MS a number of infectious agents have been proposed but none of them have been directly linked to the initiation of MS (see 1.2.3).

Effect of activated T lymphocytes in the CNS

Activated T cells migrate into the CNS under the influence of chemoattractant molecules called chemokines (see section 1.4). Studies have shown that upon activation, T lymphocytes can induce neuronal death *in vitro* and *in vivo*, independently of their antigen specificity [Giuliani et al., 2003, Newman et al., 2001]. Encephalitogenic CD4⁺ T lymphocytes, using two-photon microscopy, have been shown to possess migratory capacities within the CNS and to interact with the soma and processes of neurons leading to neuronal death. The capacity to induce this neuronal death is due to the expression of TNF related apoptosis-induced ligand (TRAIL) on T lymphocytes [Nitsch et al., 2004, Aktas et al., 2005].

1.2.6.3 BBB and cell migration into the CNS

In MS, immune cells readily cross the BBB and gain access to the CNS, leading to inflammation and demyelination, through the interaction with endothelial cell adhesion molecules at the blood-brain barrier [Engelhardt and Ransohoff, 2005]. This is a critical step in the pathogenesis of inflammatory diseases including MS. Inter cellular adhesion molecules-1 (ICAM-1), vascular cell adhesion molecule-1 (V-CAM1) and E-selectin have been shown to be important molecules in this process [Dore-Duffy et al., 1993, Elovaara et al., 1998, Rieckmann et al., 1997]. ICAM-1 is a 90 KDa surface glycoprotein with 5 extracellular Ig domains that binds to the membrane bound integrin receptors LFA-1 (leukocyte function-associated-1) (CD11a/CD18) on the surface of activated leukocytes [Lee and Benveniste, 1999, Staunton et al., 1988]. V-CAM-1 also belongs to the immunoglobulin superfamily but has 7 extracellular IgG domains. It binds to integrins including VLA-4 (very late antigen 4) that is constitutively expressed by mononuclear cells [Elices et al., 1990, May et al., 2000, Sheremata et al., 2005]. Both I-CAM and V-CAM have been shown to be more highly expressed on endothelial cells from MS brain compared to control brain [Washington et al., 1994]. The selectin family, consisting of L-selectin, E-selectin and P-selectin, are a group of type I transmembrane glycoproteins which have been shown to be expressed by microvascular endothelial cells in MS lesions [Lee and Benveniste, 1999, Washington et al., 1994]. By over-expressing adhesion molecules, activated leukocytes are able to interact with the BBB via E-selectin, this is "rolling" [Ley et al., 1998]. As soon as the interaction between VCAM-1 and LFA-4 occurs, lymphocytes stop rolling and strongly adhere to the BBB. *In vivo*, the involvement of adhesion molecules in leukocyte entry into the CNS parenchyma has been clearly demonstrated by the administration of antibodies against VLA-4 which blocked the transendothelial migration of lymphocytes and monocytes in EAE [Yednock et al., 1992]. These two processes, adhesion and migration, are regulated by molecules that play a major role in the pathogenesis of MS: the chemoattractant cytokines or chemokines (see section 1.4.1).

Lymphocytes are then able to enter into the CNS by diapedesis. Entry is facilitated by the synthesis of MMPs produced by CNS resident cells including endothelial cells and microglia [Zozulya et al., 2007, Cossins et al., 1997]. These enzymes disrupt the BBB and basement membrane thereby facilitating the transmigration of lymphocytes into the CNS [Chavarria and Alcocer-Varela, 2004]. MHC class II⁺ CNS resident cells that present myelin sheath peptides can then reactivate myelin-specific CD4⁺ T lymphocytes, so called epitope spreading [McMahon et al., 2005], which increases the expression of inflammatory mediators such as IL2, TNF and IFN γ resulting in more tissue damage due to increased cell activation and release of secondary antigens [Chitnis, 2007] (figure 1.5).

Evidence for a role of CD8⁺ cells in MS pathogenesis was obtained from the presence of expanded clones of CD8⁺ found in MS lesions as well as blood and CSF from MS patients [Skulina et al., 2004, Babbe et al., 2000]. Moreover, it was shown *in vitro* that CD8⁺ cells interact with neurons resulting in neuronal death through Fas/FasL [Medana et al., 2000]. These activated lymphocytes produce inflammatory mediators which attack the myelin sheath resulting in inflammation, axonal damage and neuronal death [Bar-Or et al., 1999].

1.2.6.4 Inflammation

In the body, direct tissue injury is followed by recruitment of peripheral blood mononuclear cells followed by wound healing and angiogenesis [Lo et al., 1999]. In the CNS, neuroinflammation involves T cells as discussed in section 1.2.6 and glia cells. Microglia cells are also involved in inflammation through antigen presentation and synthesis of pro-inflammatory mediators [Farber and Kettenmann, 2005, Muzio et al., 2007]. Oxidative myelin destruction induced increased levels of 7-ketocholesterol (7KC), a myelin breakdown product, which has been shown to accumulate in the brain in MS patients and correlate with disability and neuronal death in EAE. 7KC does not induce direct neuronal death but has an effect on migration and induces a neurotoxic phenotype in microglia, leading to neuronal death [Diestel et al., 2003].

Inflammation is not solely detrimental and can have some protective effects. A recent study on knock-out (KO) β 2-microglobulin mice lacking mature CD8+ lymphocytes has shown an aggravation of the disease and increased neuronal damage, highlighting the potential anti-inflammatory role of this T lymphocyte subset in MS [Linker et al., 2005].

Secretion of neurotrophins by T-cells such as brain-derived neurotrophic factor (BDNF), neurotrophin-3 (NT-3), NT-4 IL-4 and IL-10, have the potential to induce neuronal recovery and neuronal development *in vitro* and *in vivo* [Chitnis, 2007, Hohlfeld, 2004, Kerschensteiner et al., 1999, Lu et al., 2005].

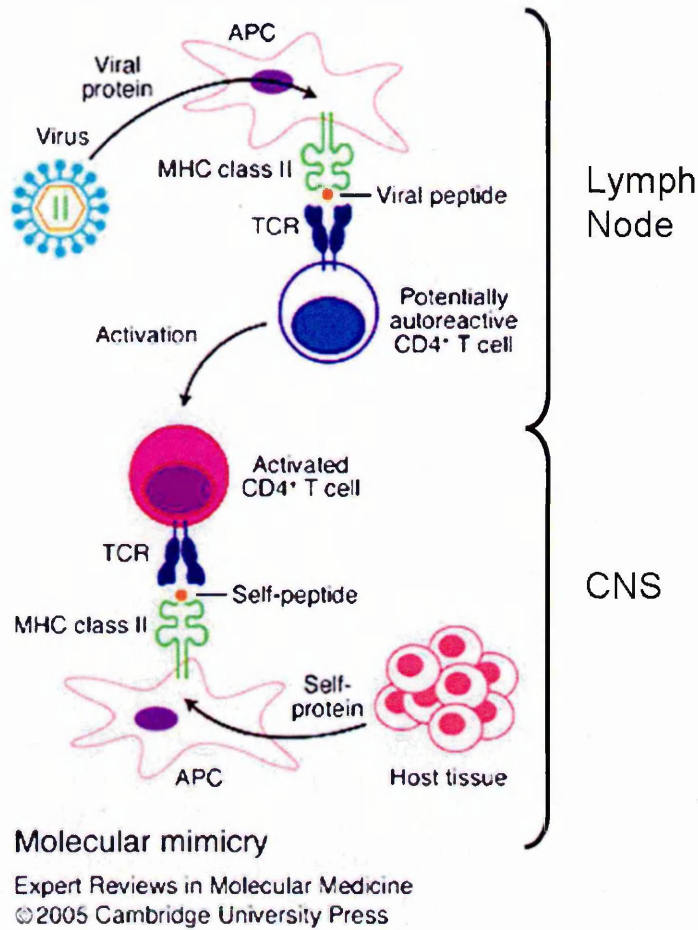


Fig. 1.4: Proposed molecular mimicry mechanism in MS for the induction of autoimmunity.

In the lymph node the potentially autoreactive T cells are activated by antigen presenting cells (APC) which present viral peptide (mimic self antigen) through MHC class II. These activated T cells migrate into the CNS and are reactivated by self peptide leading to the immune response against self tissue. Image obtained and modified from Holmes et al. (2005).

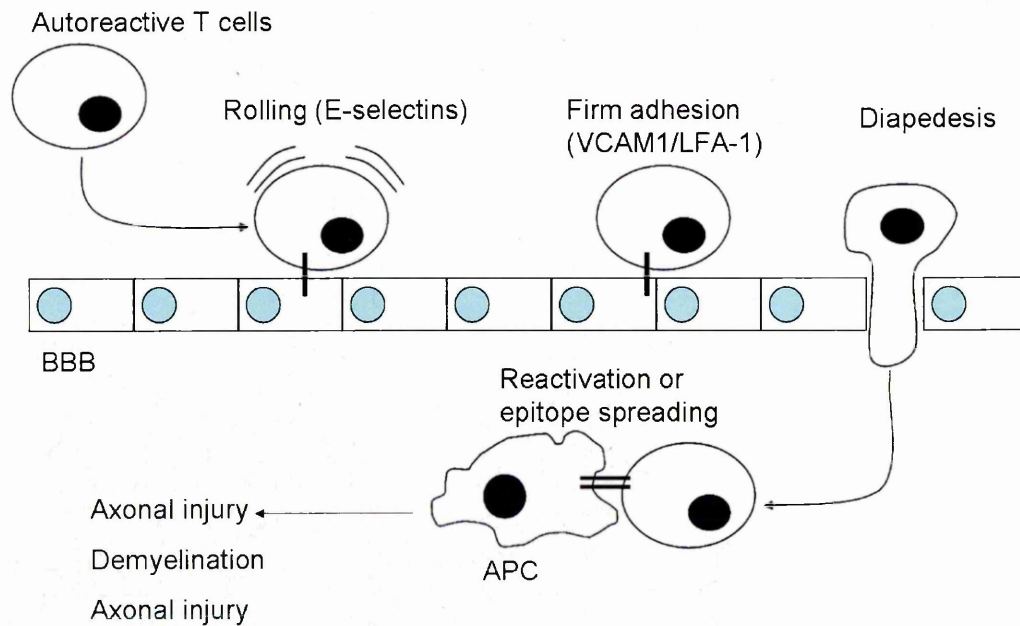


Fig. 1.5: A model of the molecular pathogenesis of multiple sclerosis.

Myelin autoreactive T cells are activated in the periphery and chemoattracted into CNS by chemokine/chemokine receptor interactions. Activated cells adhere to the blood-brain-barrier (BBB) endothelium via E selectin molecules (rolling). Firm adhesion stops the rolling through the interaction between ICAM-1 and LFA-1. Chemokines are involved in this process by acting on firm adhesion, locomotion, diapedesis, and chemotaxis [Savarin et al. 2007]. Activated T cells cross BBB basement membrane and migrate into CNS parenchyma (diapedesis) which is facilitated by matrix metalloproteinases. Auto reactive T cells in the CNS mediate damage to myelin and axonal injury through the synthesis of pro-inflammatory cytokines and activation of glia cells.

1.2.6.5 Demyelination-axonal damage

Demyelination is a characteristic feature of MS plaques. Demyelination occurs with the destruction of both the myelin sheath and oligodendrocytes. Myelin destruction is under the influence of autoreactive activated T-cells that have migrated into the CNS and macrophages (cellular immunity) and plasma cells that secrete antibodies directed against myelin (humoral immunity). There are several mechanisms for myelin destruction [Sospedra and Martin, 2005].

T cells can bind directly to myelin epitopes when presented by the MHC class II molecules expressed by activated microglia that result in the production of Th1 cytokines from T cells leading to the destruction of myelin [Carson, 2002].

One other mechanism is the fixation of myelin specific antibodies from invading B-cells that activate the complement and opsonization by macrophages. As well, release of cytotoxic mediators from immune cells and glial cells create further demyelination [Bruck and Stadelmann, 2003].

Axonal damage can be visualized by accumulation of amyloid precursor protein (APP) in axons at sites of recent axon damage [Kuhlmann et al., 2002]. This accumulation is prominent in early disease and correlates with the extent of accumulation of T cells and macrophages into lesions. Several mechanisms are responsible for the axonal damage. As discussed in section 1.2.6.3, CD8⁺ T cells have been shown to induce neuronal death through the Fas/Fas Ligand pathway but not perforin. Neurons are resistant to perforin secreted by CD8⁺ lymphocytes [Medana et al., 2000]. This finding contradicted a study by Murray (1998) where it was shown that Theiler's virus encephalomyelitis mice model in perforin KO mice showed protection against the axonal damage but not for demyelination [Murray, 2002].

Glutamate has been shown to play a role in neuronal death as discussed in section 1.1.1.4. Indeed, evidence was obtained from a study using of excitatory amino acid receptor antagonist, which resulted in the protection of axons in EAE mouse model [Pitt et al., 2000] (see section 1.3).

Finally, as discussed above in this section, antibodies against myelin from acti-

vated B cells and complement result in axonal damage in the same way described for the demyelination [Mead et al., 2002].

1.2.6.6 Astrocytes in MS: scar formation

Cellular damage in the CNS leads to a response from glia cells and results in the formation of scar tissue also known as reactive gliosis. This scar formation involves different cell types including: astrocytes, microglia, oligodendrocyte precursor cells (OPC) and some meningeal cells [Fawcett and Asher, 1999].

The glial scar produces many signals to block the migration of oligodendrocytes precursor cells (OPC). Astrocytes around the lesion induced secretion of chemokine CXCL1 [Omari et al., 2006], which promotes OPC proliferation but acts as a stop signal for OPC migration [Tsai et al., 2002].

Other evidence was obtained in post-mortem CNS tissue where oligodendrocytes were present with multiple processes for remyelination but failed to interact with viable neurons leading to the absence of demyelination [Chang et al., 2002]. This is supported by the fact that astrocytes produce specific molecules (proteoglycans) that inhibit the growth of neurons [Silver and Miller, 2004].

The structure of the glia scar evolves with time and the cell types involved. In its final form, the glial scar is mainly formed by astrocytes due to enlargement of the astrocyte cell body and processes, called astrogliosis or astrocytic proliferation to replace the damaged tissue [Fawcett and Asher, 1999]. The astrocyte fine processes are tightly apposed one to each other by gap and tight junctions limiting extracellular space. The number of plaques are not directly correlated with the evolution of the disease as they can be located in a region of the brain that has little effect on brain function. In contrast, if the scar is in an region controlling movement for example this leads to disability [Silver and Miller, 2004].

Astrocytes are not only involved in the scar formation in MS. They are also involved in the migration of immune cells into the CNS by increasing the perme-

ability of the BBB [Williams et al., 2007]. Astrocytes have been shown to express matrix metalloproteases (MMPs) that will disrupt the extracellular matrix and the tight junction between endothelial cells, which facilitates extravasation of immune cells into the CNS [Yang et al., 2007]. Once in the CNS, T cells are reactivated by their interaction with local APCs such as microglia or dendritic cells that constitutively express MHC class II molecules [Wu et al., 2007].

Astrocytes have also been shown to be non professional APCs [Williams et al., 2007]. Indeed, IFN- γ have been shown to be the most potent inducer of MHC class II expression and the induction of cell surface co-stimulatory molecules in astrocytes, which convert them into effective antigen presenting cells (APC) [Dong and Benveniste, 2001]. The expression of MHC class II by astrocytes was also observed *in vivo* in post-mortem brain tissue [Zeinstra et al., 2000]. Double labelling immunohistochemistry showed that astrocytes expressed MHC class II molecules in MS lesions but not in control suggesting the potential role for astrocytes to act as APCs. However the ability of astrocytes to act as APCs is controversial. Absence of expression of the co-stimulatory signal B7.1 and 7.2 by astrocytes but not by microglia in MS lesions has shown the incapacity of astrocytes to present antigen to immune cells [De Simone et al., 1995, Aloisi et al., 1995]. These findings are in contradiction with a study where astrocytes have been shown to express both B7.1 and B7.2 molecules in chronic active plaques using double labelling immunofluorescence [Zeinstra et al., 2003].

Therefore astrocytes have a dual role during MS. On the one hand it increases tissue damage by increasing the recruitment of immune cells into the CNS and activation of T cells. On the other hand, they are involved in the scar formation to repair tissue damage following inflammation.

1.3 Experimental autoimmune encephalomyelitis (EAE): model for MS

Experimental autoimmune encephalomyelitis (EAE) is an inflammatory demyelinating disease that is used as a model for the study of MS. It has been extensively used to better understand the pathophysiology of MS and presents the same pathological characteristics as MS (local inflammation and demyelination as a result of activated T cells) [Dogan and Karpus, 2004, Elhofy et al., 2002]. There are three type of EAE depending on the method of induction of EAE (peptide or brain homogenate injection and viral infection).

1.3.1 Induction of EAE

EAE can be induced by immunizing susceptible strains of mice with a mixture of immunodominant peptides from myelin proteins such as myelin basic protein (MBP), myelin oligodendrocyte glycoprotein (MOG) or proteolipid protein (PLP) emulsified with complete Freund's adjuvant [Amor et al., 1996, Tuohy et al., 1992]. It can also be induced by transferring CNS antigen specific reactive CD4+ T cells into animals [Mokhtarian et al., 1984], termed passive transfer of the disease. The disease course in EAE varies depending on the strains of animal injected and the immunogen used. For example, in SJL/J mice injection of PLP or MBP induced the relapsing-remitting form of EAE whereas C57bl/6 mice are resistant to EAE induction by MBP but develop a chronic form of EAE (CREAE) by injecting MOG peptide [Dogan and Karpus, 2004, Elhofy et al., 2002].

Another animal model for MS can be obtained following viral infection. Theiler's murine encephalomyelitis virus (TMEV) is a single strand RNA virus that belongs to the *Picornaviridae* family. Intrathecal TMEV inoculation in susceptible mice strains (SJL) induces a biphasic disease of the CNS, characterized by an early acute disease and a late chronic demyelinating disease [Lipton, 1975, Tsunoda and Fujinami, 1996].

1.3.2 Physiopathology of EAE

As in MS, the initial stage of EAE starts with the activation and differentiation of Th1 cells in the lymph nodes by the injection of the immunodominant peptide from myelin proteins. These cells migrate into the CNS by overexpressing of adhesion molecules such as VLA-4 ($\alpha 4\beta 1$ integrin), LFA-1 and ICAM-1. Treatment of mice with an antibody, anti VLA-4, induced a reduction in binding of T cells to the cerebrovascular endothelium, thereby inhibiting EAE [Kent et al., 1995, Baron et al., 1993]. Similar to anti-VLA-4, treatment of mice with antibodies directed against LFA-1 and ICAM-1 resulted in protection from EAE [Kobayashi et al., 1995]. When T cells re-encounter the peptide (MBP or MOG), they are reactivated and secrete pro-inflammatory molecules including IFN γ and TNF resulting in axonal damage and neuronal death. It has been shown that the expression of IFN γ within the CNS increased during relapse and decreased during remission [Beglka et al., 1998]. Overexpression of IFN γ in myelinating oligodendrocytes of transgenic mice resulted in a progressive demyelinating disease [Renno et al., 1998]. Glabinski et al. (2004) showed that injection of soluble TNF receptor (sTNF):Fc/p80 fusion protein ameliorated relapsing-remitting EAE [Glabinski et al., 2004]. Similar findings were observed with the injection of TNFR-IgG [Korner et al., 1997]. They found that administration of TNFR-IgG prior to onset of disease signs completely prevented the neurological deficit or markedly reduced its severity compared to the untreated EAE model.

1.3.3 Advantages and disadvantages of EAE as a model for MS

There is debate on the validity of the EAE model in increasing understanding of MS pathogenesis.

None of the EAE models truly represent MS therefore the model is an imprecise method for the understanding of MS and for the development and test of new

therapies [Sriram and Steiner, 2005]. Other researchers argue that use of the EAE model is necessary to simplify the questions concerning a highly complex disease such as MS. Once genes and proteins are identified in MS, the EAE model can be used to understand their biological significance. Use of KO EAE animal models or neutralizing antibody injection in EAE models are useful methods to elucidate the role of specific molecules. EAE models have given great input in the understanding of the disease and have led to six medications that received the approval by the US Food and Drug administration (FDA) for MS treatment. Although the animal models are valuable tools to understand the pathology of disease, they are not perfect [Steinman and Zamvil, 2006], hence *in vitro* approach in this study.

The recruitment of immune cells to the CNS is an important feature in both MS and EAE. This cell recruitment is under the control of chemoattractant cytokines called chemokines [Elhogy et al., 2002].

1.4 Chemokines and their receptors

1.4.1 Chemokines

Chemokines are small molecules (8-10 KDa) that belong to the family of pro-inflammatory mediators called cytokines involved in chemoattraction [Rossi and Zlotnik, 2000]. They are produced in various tissues including brain and have additional functions, other than solely chemoattraction. It has been shown that they are involved in the differentiation of T cells [Luther and Cyster, 2001], in leukocyte activation, angiogenesis and anti-microbial functions [Adams and Lloyd, 1997, Coelho et al., 2007]. The importance of the role of chemokines is also highlighted by the fact that they are highly conserved, they show 20 to 70% homology in amino acid sequence [Rossi and Zlotnik, 2000].

1.4.2 Chemokine classification

Chemokines have been subdivided into four classes (α , β , δ and γ) depending on their structure and especially on the relative position of the N-terminal cysteine residues [Murphy, 2002]. In the γ family there is only one cysteine residue whereas in the β , α and δ the first two cysteines are respectively separated by 0, 1 and 3 amino acids respectively. CC (β) and CXC (α) are the largest families. Each class of chemokines acts on different population of cells [Ambrosini and Aloisi, 2004]. CXC chemokines are divided into 2 subclasses depending on the presence or absence of a three amino acid ELR motif (glutamic acid - leucine - arginine) at the N-terminal part. The ELR-CXC chemokines include CXCL8 and CXCL1 that stimulate angiogenesis and act specifically on neutrophils whereas non ELR-chemokines such as CXCL9, CXCL10, CXCL11 stimulate the migration of monocytes and lymphocytes [Laing and Secombes, 2004]. CC chemokines act on cells involved in innate and adaptive immune responses including monocytes, eosinophils, basophils, monocytes and activated T cells [Laing and Secombes, 2004]. XC chemokines or lymphotaxin attract resting T cells and is the only chemokine with this structure identified to date. It binds specifically to the orphan chemokine receptor previously named GPR5/XCR1 and acts on T lymphocytes and NK cells [Laing and Secombes, 2004]. CX₃C chemokine is represented by only one chemokine called fractaline or CX3CL1, which can be found both in a soluble and membrane bound form, where it functions as an adhesion molecule. Produced by neurons and endothelial cells, it acts on T cells, monocytes, immature dendritic cells, microglia and NK cells [Laing and Secombes, 2004].

1.4.3 Chemokine receptors

Chemokines exert their biological function via interaction with chemokine receptors, which are members of the G protein coupled receptor family (GPCRs) (figure 1.6) [Cartier et al., 2005, Rossi and Zlotnik, 2000]. GPCRs are subdivided into three subfamilies but they all share structural features. They are characterized by a polypeptide chain composed of approximately 350 amino acids. They

have seven transmembrane spanning α -helical segments, connected by intracellular (ICL) and extracellular (ECL) loops with a relatively short acidic N terminal domain with glycosylation sites. Cysteine bonds are present in the N terminal domain and in each of the 3 extracellular loops. The DRYLAIVHA motif sequence, which is important for signal transduction, is well-conserved in the second intracellular loop and the intracellular domain contains serine and threonine that act as phosphorylation sites for receptor regulation [Gether, 2000, Murdoch and Finn, 2000]. Chemokine receptors belong to the A family of GPCRs and have been identified in the last 10 years. They possess 50% homology amongst themselves and less than 30% homology with the other G protein coupled receptor families [Kristiansen, 2004].

1.4.4 Chemokine receptor classification

The nomenclature for chemokine receptors follows that used for chemokines by adding "R" for receptor. Four classes of receptor have been identified (XCR, CXCR, CCR and CX₃CR), summarized in Table 1.1 with their respective ligands and functions. The XCR and CX₃CR families contain only one receptor, XCR1 and CX₃CR1. The CXCR family consist of up to 6 receptors (CXCR1-6) and the CCR family is composed of CCR1- CCR10 [Murphy, 2002].

Interaction between chemokines and their receptors are complex and show some redundancy in the system. Each chemokine can bind several receptors and one chemokine can bind to more than one chemokine receptor.

1.4.4.1 Silent chemokine receptors

The chemokine system includes at least three "silent" receptors, DARC, D6 and CCX-CKR, each with distinct specificity and tissue distribution. DARC binds to 11 chemokines belonging to the CXC and CC chemokine family, D6 binds to 9 pro-inflammatory chemokines from the CC family and CCX CKR binds CXC homeostatic chemokines (CCL19, CCL21, CCL25 and CXCL13) [Haraldsen and Rot, 2006]. Although they bind different ligands, they all share the ability to bind

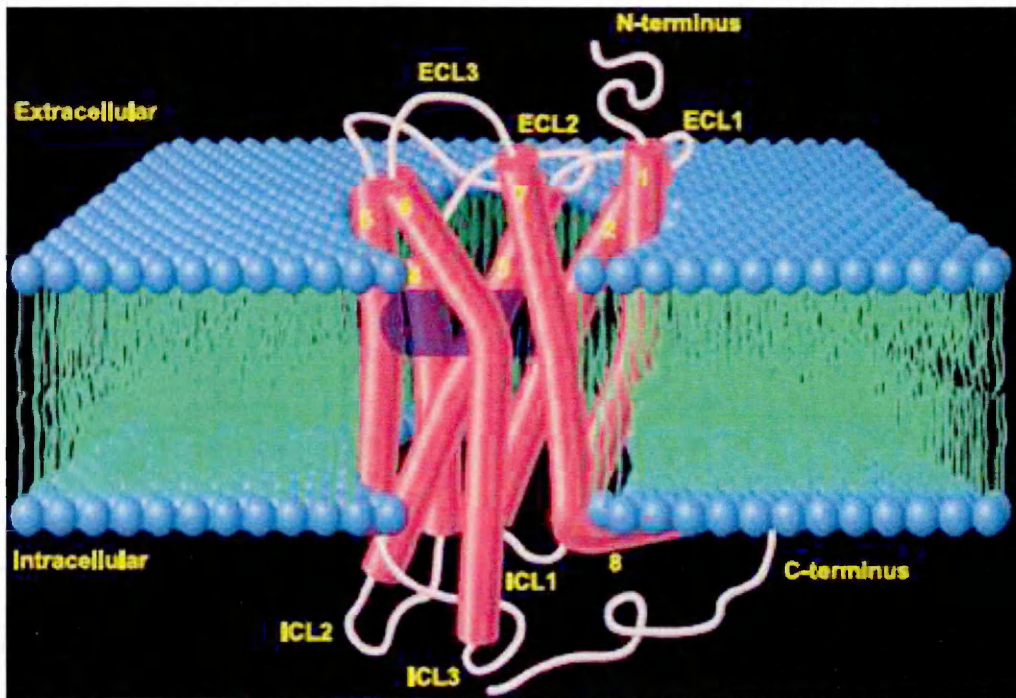


Fig. 1.6: Schematic representation of a family A receptor in the cell by crystal structure: G protein coupled receptor (GPCR).

It is composed of three extracellular loops (ECL) and intracellular loops (ICL) with seven transmembrane domains. The N-terminal domain is required for ligand binding and the C-terminal domain is required for signalling. Obtained from Kristiansen (2004).

Name	Main agonists	Main Functions
CXC subgroup		
CXCR1	CXCL8	Neutrophil migration; innate immunity; acute inflammation
CXCR2	CXCL1-3; CXCL5-8	Neutrophil migration; innate immunity; acute inflammation and angiogenesis
CXCR3	CXCL9-11	T cell migration; adaptive immunity; Th1 inflammation
CXCR4	CXCL12	B cell lymphopoiesis; bone marrow myelopoiesis; central nervous system and vascular development; HIV infection
CXCR5	CXCL13	B cell trafficking; lymphoid development
CXCR6	CXCL16	T cell migration
CC subgroup		
CCR1	CCL3; CCL5; CCL7; CCL8; CCL13-16; CCL23	T cell and monocyte migration; innate and adaptive immunity; inflammation
CCR2	CCL2; CCL7; CCL8; CCL13	T cell and monocyte migration; innate and adaptive immunity; Th1 inflammation
CCR3	CCL5; CCL7; CCL8; CCL11; CCL13; CCL15; CCL24; CCL26	Eosinophil, basophil, and T cell migration; allergic inflammation
CCR4	CCL17, CCL22	T cell and monocyte migration; allergic inflammation
CCR5	CCL3; CCL4; CCL5; CCL8; CCL14	T cell and monocyte migration; innate and adaptive immunity; HIV infection
CCR6	CCL20	Dendritic cell migration
CCR7	CCL19, CCL21	T cell and dendritic cell migration; lymphoid development; primary immune response
CCR8	CCL1; CCL4; CCL17	T cell trafficking
CCR9	CCL25	T cell homing to gut
CCR10	CCL26-28	T cell homing to skin
CX₃C and C subgroups		
CX ₃ CR1	CX ₃ CL1	T cell and NK cell trafficking and adhesion; innate and adaptive immunity; Th1 inflammation
XCR1	XCL1-2	T cell trafficking

Tab. 1.1: The four classes of chemokine receptor, their main agonists and functions.

The nomenclature of the chemokine receptor follows the nomenclature of the chemokines. There are four classes of receptor (CXC, CC, CX₃C and C). This table summarises the different ligands for each receptor as well as their function. Obtained from Murphy et al. (2002). 41

chemokines without inducing any signalling or migratory function. The function of these receptors is to compete with the natural receptor, sequester the ligand and internalise it for targeting to the degradation pathway [Nibbs et al., 2003].

The DARC receptor has been found to be expressed on erythrocytes of Duffy antigen positive subjects but also on endothelial cells. The DARC receptor may have a dual function. It seems to facilitate the transport of chemokines through the vascular endothelium and controls the level of circulating chemokines [Nibbs et al., 2003]. D6 binds most inflammatory CC chemokines and shuttles from the plasma membrane to endocytic compartments where they are targeted for degradation. The receptor is detectable on placenta and on endothelial cells of lymphatic afferent vessels in skin, gut and lung [Weber et al., 2004]. CCX-CKR receptor is expressed on T lymphocytes and immature dendritic cells [Gosling et al., 2000]. As yet, there are no publications on the ability of this receptor to internalize the ligand.

1.4.5 Chemokine-chemokine receptor interaction

Regarding the high affinity chemokine and chemokine receptor interaction, the role of the extracellular loops and N-terminal domain of the receptors has been determined through mutagenesis experiments of the receptor. A report on one isoform of CCR2, CCR2B, has shown that replacement of the first extracellular loop of CCR2B with the corresponding region of CCR1 decreased the binding affinity for CCL2 about 10-fold. It was shown that this segment contains two distinct domains; one involved in the binding of CCL2, whereas the other is involved in receptor activation and signal transduction [Han et al., 1999]. Involvement of the N-terminal domain of chemokine receptors in binding of its ligand has been confirmed by replacing the hexapeptide Thr-Thr-Xaa-Phe-Asp-Tyr in the N-terminal domain of CCR2 by alanine. This segment has been shown to be conserved between CCR1 and CCR2 that binds CCL2 and RANTES. It contains a sulphation site, highlighting the biological importance of this segment [Preobrazhensky et al.,

2000]. CCR5 has also been shown to be post-translationally modified by sulphation of tyrosine and shown to contribute to the binding of CCL3 and CCL4 [Farzan et al., 1999].

In a study on CXCR2, serine or leucine residues were substituted for cysteine in the extracellular domains, and 7 transmembrane domain. These substitutions resulted in the inability of CXCR2 to bind CXCL8, indicating the involvement of the three extracellular domains and transmembrane domains. However, they did not dramatically impair the expression of the receptor at the cell surface and showed minor effects on CXCR2 trafficking [Limatola et al., 2005].

1.4.6 Chemokine-glycosaminoglycan interaction

As well as binding to their cognate receptor and "silent" receptors at high affinity, chemokines bind to cell surface proteoglycans with lower affinity. Proteoglycans consist of glycosaminoglycans (GAGs), long linear polysaccharides and a protein core [Johnson et al., 2005]. Proteoglycans are expressed ubiquitously on cell surfaces and in the extracellular matrix and present high diversity due to the polysaccharide composition, with a length that can vary from 1 to 25, 000 disaccharide units, and the protein core also has diversity. The fact that chemokines bind to the proteoglycan is not surprising because of the highly negative charge, and hence have favorable interaction with chemokines that are primarily basic. However, the interaction between chemokines and proteoglycan seems to show some specificity. For instance, CCL2 has greater affinity for chondroitin sulphate \geq dermatan sulphate \geq heparan sulphate \geq heparin [Kuschert et al., 1999]. These interactions are important for establishment of chemokine gradients, for the recruitment of immunological cells and also for the modulation of the presentation of chemokines to their receptors and their protection from proteolytic cleavage [Johnson et al., 2005].

1.4.7 Chemokine receptors intracellular signalling pathways

When chemokines bind to their receptor, it induces cell migration. Treatment with pertussis toxin (PTX), a specific inhibitor of G proteins, inhibits cell migration, highlighting the importance of G protein signalling in chemokine effects [Cartier et al., 2005]. Upon binding of the ligand to the receptor, conformational changes occur in the receptor. The trimeric G protein composed of an α and $\beta\gamma$ subunit is dissociated due to the replacement of GDP by GTP. Downstream signalling pathways are mostly triggered by the β subunit. Because of the redundancy of the system, a receptor can activate various intracellular pathways, depending on its ligand. It is well known that it is mostly β subunits that activate downstream signalling pathways including the phosphoinositide-specific phospholipase C (PLC) and phosphoinositide 3 kinase (PI3K) (figure 1.7):

1.4.7.1 Phosphoinositide-specific phospholipase C pathway (PLC)

PLC activation leads to the generation of diacylglycerol (DAG) and inositol 1,4,5 triphosphate (IP3) which, upon binding to its receptor on the endoplasmic reticulum, releases intracellular calcium. The increase in intracellular calcium following chemokine binding to its receptor is a well-known feature [Kiselyov et al., 2003]. This calcium release is often monitored to determine the effect of chemokines on their receptor. DAG in conjunction with an increase in intracellular calcium, activates protein kinase C (PKC). PKC activation by chemokines is required for certain responses, such as the respiratory burst of neutrophils [Thelen, 2001].

1.4.7.2 Phosphoinositide 3 kinase pathway (PI3K)

Activation of PI-3K triggers the accumulation of phosphatidylinositol 3,4,5-trisphosphate (PtdIns(3,4,5)P3). Protein Kinase B (PKB) migrates to the mem-

brane and binds to PtdIns(3,4,5)P3 activating the PKB/Akt and Erk pathways.

The PKB/Akt subfamily of the mammalian cAMP-dependent, cGMP-dependent, protein kinase C family of kinases (AGC) consists of three members, PKB α /Akt1, PKB β /Akt2 and PKB γ /Akt3 and are activated by phosphorylation of two residues, Thr³⁰⁸ and Ser⁴⁷³ [Alessi et al., 1996, Walker et al., 1998]. They share strong similarities in a kinase domain and pleckstrin homology (PH) domain, which is a specialized lipid binding domain [Alessi et al., 1996]. They are regulated by the signalling of the phosphatidylinositol phosphate 3 kinase (PI3Kinase), which is activated by growth factors, and GPCR agonists [Hirsch et al., 2007, Radeff-Huang et al., 2004, Vanhaesebroeck and Alessi, 2000]. Akt has many targets including cell polarization, chemotaxis and cell survival [Cartier et al., 2005].

Mitogen-Activated-Protein-Kinases (MAPKs) are serine-threonine protein kinases that are activated by a variety of molecules including cytokines, growth factors, neurotransmitters, hormones, cell adhesion molecules and chemokines [Choi et al., 2001]. The MAPKs are subdivided into three different groups; the extracellular signal-regulated kinase (Erk), c-jun kinase (JNK) and p38 MAPK . Erk is a well characterised signalling kinase, and is activated by phosphorylation on threonine and tyrosine residues by mitogen-activated protein kinase1/2 (MEK1/2) [Chang and Karin, 2001]. Erk has six different isoforms, however the most common are Erk 1 and 2, which share many similarities and have a RMM of 44 and 42 KDa respectively [Chang and Karin, 2001]. Erk activation induces proliferation/differentiation [Cartier et al., 2005].

The intracellular pathways of chemokines are complex as one receptor is able to activate different second messengers depending on its ligand consequently triggering several downstream pathways [Thelen, 2001].

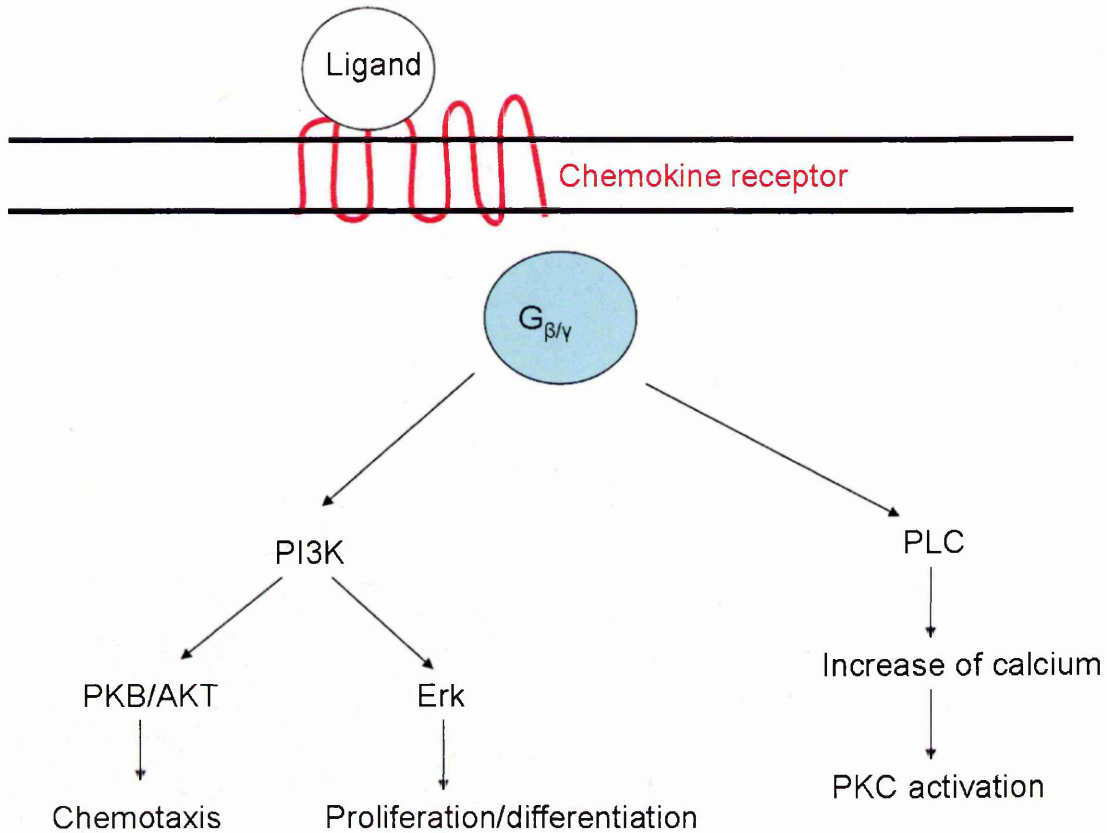


Fig. 1.7: Signalling pathways downstream of chemokine receptor activation.

Following binding, $G_{\beta\gamma}$ dissociates from the GPCR and induces activation of phospholipase C (PLC) resulting in an increase in intracellular calcium and activation of protein kinase C (PKC). It also activates phosphoinositide 3 kinase pathway (PI3K) which activates Erk and PKB/Akt, responsible for cell proliferation/differentiation and chemotaxis respectively.

1.4.8 Function of chemokines

1.4.8.1 Leukocyte recruitment

The most studied action of chemokines is their role in recruitment of leukocytes, which occurs in inflammatory disorders including MS [Baggiolini, 1998]. The recruitment process can be subdivided into three steps, rolling, firm adhesion and diapedesis (section 1.2.6.3). Wan et al. (2003) have shown the involvement of chemokines in the interaction of leukocytes with the endothelium. CCL3 and CCL2 caused a dose-dependent increase in leukocyte rolling, adhesion and recruitment, which was inhibited by an antibody directed against selectin [Wan et al., 2003]. Other evidence was obtained from the EAE model. For example, Huang et al. (2006) showed that EAE mice deficient for CX₃CR1 presented a marked reduction in the migration of NK cells within the CNS compared to WT EAE mice [Huang et al., 2006].

1.4.8.2 Differentiation of T lymphocytes

Studies indicate that chemokines regulate the differentiation of T lymphocytes. Dey et al. (2007) have shown that in *Leishmania donovani*-infected BALB/c mice, CCL2 and CCL3, both induced the expression of the pro-inflammatory cytokine, IL-12, and the suppression of the anti-inflammatory cytokines IL-10 and transforming growth factor-beta (TGF β) in infected macrophages. The chemokine treatment lead also to an increase in IFN γ , TNF and inducible nitric oxide synthase in both liver mononuclear cells as well as in splenocytes, which reflect the switch of CD4⁺ T cells from Th2 to Th1 [Dey et al., 2007].

Chemokines may also affect the differentiation of immune cells by regulating the migration of antigen presenting cells into the lymph node. It was found that mice deficient for CCR2 had a 70% decrease in IFN γ producing cells in the draining lymph nodes compared to WT mice [Peters et al., 2000]. They also showed *in vitro* that both dendritic cells from CCR2^{-/-} and WT mice stimulated with

LPS produced IL12, the cytokine that induces a Th1 phenotype. This suggests an impaired traffic of APC into the lymph node resulting in the decrease in IFN γ producing cells (Th1 cells). Therefore, CCL2 plays an indirect role on the differentiation of naive T cells into a Th1 phenotype by regulating the number of IL12 producing cells (DCs) in the lymph node.

1.4.8.3 Activation of dendritic cells

Dendritic cells are key players in the immune response by activating B cells and T cells. *In vivo* and *in vitro* studies has shown that CCL19, acting on CCR7, directly activates dendritic cells (DCs) that have previously encountered pathogen-associated signals, by increasing co-stimulatory molecules (CD40, B7.1 and B7.2) and pro-inflammatory cytokine production, resulting in the activation of naive T cells into Th1 cells [Marsland et al., 2005]. CCR5, triggered by cyclophilin derived from *T.gondii*, is another example of chemokine effects on DCs. It has been shown that CCR5 activation induced activation of DCs by increasing the production of pro-inflammatory cytokines and particularly IL-12, resulting in activation of a Th1 response and clearance of the pathogen. However this response can induce immunopathology if exaggerated [Marsland et al., 2005].

1.4.8.4 CNS development

Chemokines have a role in neurogenesis. It has been shown recently that CXCL12 and its receptor CXCR4 control the development of distinct brain regions. Inactivation of CXCR4 in mice resulted in loss of motoneurons and dorsal root ganglions and therefore in the reduction of innervation of fore and hindlimbs in the developing mouse [Odemis et al., 2005]. *In vivo* studies on CXCR4 or CXCL12 KO mice showed strong abnormalities of the cerebellar and hippocampal morphology, possibly due to the perturbation of neuronal precursor cell migration [Lu et al., 2002]. These mice also showed defects in B cell development, homing of haematopoietic precursors to the bone marrow and cardiac and vascularization problems and died soon after birth [Ma et al., 1998, Tachibana et al., 1998]. This

example demonstrates the importance of chemokines in CNS development and brain morphogenesis.

1.4.8.5 Control of angiogenesis by chemokines

Angiogenesis is the process of new blood vessel formation and is under the control of various factors including CXC chemokines. The CXC chemokine family has disparate effects on angiogenesis. The ELR⁺ CXC chemokines have angiogenic effects whereas the ELR⁻ CXC chemokines have angiostatic effects on the endothelium. CXCL1, 2, 3, 5, 6, 7 and 8 promote angiogenesis through the binding to their putative receptor, CXCR2 and CXCL4, 9, 10, 11 and 14 exert their inhibitory effect on angiogenesis through CXCR3 [Strieter et al., 2005]. The angiogenic factor in a local environment can exert this effect directly or in a serial manner. The angiogenic effect of VEGF on endothelial cells is an example of a serial manner effect where it activates Bcl2, the anti apoptotic molecule that lead to the up-regulation of CXCL8 by endothelial cell (EC) [Karl et al., 2005], which then acts in a paracrine and autocrine way to maintain the angiogenic phenotype on EC. Therefore the local balance of these chemokines in regulating angiogenesis might be important.

1.4.9 Chemokines and chemokine receptors in MS

The evidence implicating chemokines and their receptors in MS pathology are mainly shown by descriptive and observational analysis using CNS tissue or CSF from MS patients [Kieseier et al., 2002].

1.4.9.1 Chemokines in MS

Distribution of chemokines and chemokines receptors have been assessed in post-mortem brain tissue using immunohistochemistry and *in situ* hybridization. It is not surprising to see that both α - and β -chemokines, the two largest classes of chemokine, are mostly implicated in MS pathology. There is accumulation in the perivascular space of various CC chemokines including CCL3, CCL4, CCL5

and CCL7 [Ambrosini and Aloisi, 2004, Muller et al., 2004]. In acute and chronic lesions, three members of the CC chemokine family (CCL2, CCL7 and CCL8) were highly expressed in the centre of MS lesions with strong staining of astrocytes compared to control brains. In demyelinating lesions, it has been shown that there is a high level of expression of:

- CCL2 associated with astrocytes and macrophages
- CCL3 associated with astrocytes and macrophages
- CCL4 associated with macrophages and microglia
- CCL5 associated with endothelial cells and astrocytes
- CXCL9 and CXCL10 associated with macrophages in the centre of the lesion and reactive astrocytes in the surrounding parenchyma [Balashov et al., 1999, Cartier et al., 2005, Simpson et al., 1998, Tanuma et al., 2006]

This present study focussed on two chemokines: CCL2 and CXCL10, both implicated in MS.

1.4.9.2 CCL2 expression in MS

CCL2 was the first MCP chemokine, belonging to the β -chemokine family, to be identified. It promotes migration of various cell types including: monocytes, activated T-cells, basophils and NK cells. This chemokine exerts its effects by binding to CCR2 [McManus et al., 1998]. The expression level of this chemokine has been extensively studied in brain, CSF and serum in MS.

CCL2 is expressed in MS CNS tissue and especially in acute MS lesions compared to control brain, where no expression is detected [McManus et al., 1998]. Immunohistochemistry and *in situ* hybridization has demonstrated that CCL2 was abundantly expressed by astrocytes within active, chronic-active MS lesions compared to normal appearing white matter (NAWM) tissue [McManus et al., 1998].

CCL2 immunoreactivity in astrocytes correlated with the level of inflammation in the lesion. It has also been shown that reactive and hypertrophic astrocytes in active and chronic-active lesions highly expressed CCL2 showing a strong correlation with inflammation [Simpson et al., 2000a, Van Der Voorn et al., 1999]. Simpson et al. (1998) reported that reactive astrocytes in the adjacent NAWM around lesions were strongly immunoreactive for CCL2. Strong expression of CCL2 by astrocytes at the edge of lesions could be explained by the fact that expression of CCL2 by reactive and hypertrophic astrocytes forms a chemotactic gradient, allowing the recruitment of inflammatory cells to lesions. The correlation with inflammation was confirmed by the absence of expression of CCL2 in the NAWM [Van Der Voorn et al., 1999].

CCL2 levels in CSF have been extensively studied in people with MS. Mahad et al. (2002) showed by ELISA that the concentration of CCL2 in the CSF of MS patients was significantly reduced (around 450pg/ml) compared to people with unexplained headache (850pg/ml), non inflammatory neurological disease (around 900pg/ml) and neurological inflammatory disease controls (around 800pg/ml). The concentration of CCL2 in the CSF correlated significantly and positively with the time of relapse ($n=21$; $p\leq 0.01$, $r=0.58$) highlighting the role for CCL2 in the pathogenesis of MS [Mahad et al., 2002b]. The discrepancy between CCL2 expression in the CNS and reduction in the CSF is not fully resolved as yet. A recent study suggested that CCR2⁺ immune cells would consume CCL2 in the CSF explaining the decrease [Mahad et al., 2006].

The decreased level of CCL2 in the CSF in MS was confirmed by several other studies. Narikawa et al (2004) showed that CCL2 is significantly lower ($p\leq 0.05$) in the CSF of MS patients (125.6 ± 11.3 pg/ml) than controls (174.0 ± 9.2 pg/ml) [Narikawa et al., 2004]. In the Scarpini study (2002), they compared the level of CCL2 in the CSF from active RR-MS, stable RR-MS, SP-MS and PP-MS with patients with no neurological disease (CON), patients with other

neurological disease (OND) and patients with non-inflammatory neurological diseases (NIND). The level of CCL2 in the CSF was significantly reduced in all MS clinical subtypes (active RR-MS: 371 ± 49 pg/ml, stable RR-MS: 495 ± 90 pg/ml and SP-MS: 557 ± 94 pg/ml) compared to control (865 ± 95 pg/ml), OND (887 ± 70 pg/ml) and inflammatory patients (1802 ± 535 pg/ml) [Scarpini et al., 2002].

The level of CCL2 in the serum has also been analysed but gave contradictory evidence. In one study, CCL2 was decreased in active RR-MS (361 ± 35 pg/ml), stable RR-MS (383 ± 69 pg/ml), SP-MS (442 ± 38 pg/ml) and PP-MS (390 ± 110 pg/ml) compared to CON (1038 ± 65 pg/ml) and OND (1374 ± 146 pg/ml) and OIND (1206 ± 269 pg/ml)[Scarpini et al., 2002]. In a second study, no difference between the expression of CCL2 in MS and normal individuals was observed [Kivisakk et al., 1998].

1.4.9.3 Function of CCL2 during inflammation in the CNS

CCL2 has been extensively studied in EAE to understand its role in the pathogenesis of MS. CCL2 expression levels in the spinal cord, using ELISA, correlated with the severity and timing of attacks in relapsing EAE, induced in both rats and mice [Kennedy et al., 1998]. The intrathecal synthesis of CCL2 was assessed by RT-PCR at early time points in mice with and without EAE (PLP induction)[Glabinski et al., 1995]. It was shown that CCL2 synthesis correlated with histological inflammation. *In situ* hybridization, using an antisense probe for CCL2, showed strong staining for astrocytes, but not for inflammatory leukocytes, indicating the cellular source of CCL2 in early evolution of EAE lesions. Thus intrathecal synthesis of CCL2 by astrocytes, was required for leukocyte entry, suggesting a role in amplification of inflammation rather than initiation [Glabinski et al., 1995]. Use of anti-CCL2 treatments using either antibody or DNA vaccination [dos Santos et al., 2005, Youssef et al., 1999], reduced the severity of the disease in relapsing EAE. CCL2 KO mice showed a significant reduction in macrophage recruitment within the CNS [Huang et al., 2001].

Many *in vitro* studies have examined the effect of the interaction between CCL2 and its receptor. *In vitro* studies on foetal and murine astrocytes have shown that similarly to the recruitment of monocytes in inflammation sites, foetal human astrocytes sense and respond to gradients of CCL2 [Andjelkovic et al., 2002]. It was proposed that this chemotactic effect could either promote the recruitment of astrocytes at lesion sites within the brain or affect the position of astrocytes at the BBB [Dorf et al., 2000]. Chemokines released by rat brain endothelial cells [Harkness et al., 2003] may help to guide astrocytes towards microvessels and ensure the development of the BBB [Cancilla, 1993]. In addition to actively responding to chemokines, astrocytes might regulate the chemokine action via internalization of CCL2 via CCR2 as shown by decreased CCL2 binding to human foetal astrocytes with increasing concentrations of CCL2 [Andjelkovic et al., 1999b].

CCL2, via interaction with CCR2, seems to increase the permeability of the BBB by perturbing the tight junctions of endothelial cells, through activation of Rho and Rho kinase pathways facilitating the penetration of inflammatory cells into the CNS [Stamatovic et al., 2003]. Chemokines also act on the extravasion of immune cells by increasing the production of metalloproteinase enzyme (MMPs) by monocytes and macrophages resulting in destabilization of the BBB such as MMP9 [Cossins et al., 1997, Rosenberg, 2002, Sellebjerg and Sorensen, 2003]. Indeed CCL2 has been shown to increase secretion of pro-MMP9 by the monocytic cell line (THP-1 cells) in a dose dependent manner using zymography gels and densitometry [Robinson et al., 2002].

Nevertheless, CCL2 seems to have a more complex role than solely promoting inflammation by recruiting inflammatory cells into the CNS. Kalehua et al. (2004) have shown that CCL2 is involved in neuronal recovery in the hippocampus in mice. Immunohistochemical analysis has shown that intrahippocampal injection

of kainic acid results in a late and unexpected increase in CCL2 expression by reactive astrocytes after 21-45 days. Microarray experiments on cDNA of rodent astrocytic cell line (CTX TNA2 cell line) showed that stimulation by CCL2 leads to secretion of bFGF, that would facilitate neuronal cell differentiation and promote survival of neurons *in vitro* [Kalehua et al., 2004]. Further evidence on the protective effect of CCL2 on neuronal apoptosis, induced by N-methyl-D-aspartic acid (NMDA), was obtained by an *in vitro* study where mixed culture of human neurons and astrocytes induced a reduction in neuronal apoptosis following treatment with CCL2 but not for CXCL10 [Eugenin et al., 2003]. The co-treatment of NMDA with CCL2 on mixed cultures of neurons and astrocytes induced a reduction in glutamate release compared to NMDA only [Eugenin et al., 2003]. Therefore astrocytes seem to protect neurons from glutamate excitotoxicity by regulating the level of glutamate through transporters (GLT1 and GLAST) [MacAulay et al., 2002].

Despite the contradictory evidence, CCL2 seems to play an active role in MS. The reason why CCL2 is highly expressed in active demyelination lesions and the level of CCL2 decreased in the CSF of MS patients at the time of relapse remains unclear.

1.4.9.4 CXCL10 expression in MS

CXCL10 belongs to the α -chemokine family and promotes the recruitment of T lymphocytes through binding to its receptor, CXCR3. The role of CXCL10 in the pathogenesis of MS has been elucidated by studying the level of expression of this chemokine in the CSF and serum of MS patients.

Studies on brain tissue of control individuals and in NAWM of MS patients showed that no reactivity was observed [Balashov et al., 1999]. In active MS lesions, expression of CXCL10 has been reported by several groups [Balashov

et al., 1999, Simpson et al., 2000b, Sorensen et al., 1999]. CXCL10 was highly expressed on macrophages and lymphocytes but not in silent and silent/inactive lesions [Simpson et al., 2000b]. CXCL10 is not only expressed by macrophages and lymphocytes, studies have reproducibly localized CXCL10 immunoreactivity to reactive astrocytes within active demyelinating MS lesions, suggesting astrocytes as a potential cellular source of CXCL10 in the CNS [Sorensen et al., 1999, Simpson et al., 2000b].

In the CSF, CXCL10 has been shown to be present in significantly higher levels in patients with relapsing remitting MS (RR-MS), secondary progressive MS (SP-MS) and primary progressive MS (PP-MS) compared to controls (CON), other neurological disorders (OND) and other inflammatory neurological disorders (OIND). Scarpini et al. (2002) showed that CXCL10 was more highly expressed in active RR-MS ($453 \pm 63\text{pg/ml}$), stable RR-MS ($293 \pm 43\text{pg/ml}$) SP-MS ($424 \pm 130\text{pg/ml}$) and OIND ($1734 \pm 674\text{pg/ml}$) compared to PP-MS ($78 \pm 15\text{pg/ml}$), CON ($79 \pm 27\text{pg/ml}$) and OND ($79 \pm 42\text{pg/ml}$). These findings were confirmed by another study that reported an increase in CXCL10 level in the CSF in MS patients compared to normal individuals [Mahad et al., 2002b]. The same pattern was observed with CXCL10 expression in the serum with lower expression of CXCL10 in CON, OND and PP-MS (between $59 \pm 29\text{pg/ml}$ and $78 \pm 15\text{pg/ml}$) than active RR-MS, stable RR-MS, SP-MS and OIND (between 221 ± 52 and $635 \pm 175\text{pg/ml}$). Similar findings were observed by Narikawa et al. (2004) using CSF of 13 relapsing neuromyelitis optica (RNMO), 17 MS and 15 control. CSF CXCL10 levels in RMNO ($2147.9 \pm 560.5\text{pg/ml}$) and in MS ($2308.1 \pm 857.4\text{pg/ml}$) were significantly higher than control ($755.5 \pm 366.2\text{pg/ml}$). However, the CXCL10 level in the serum did not shown any difference between the three patient groups.

The fact that CXCL10 increases in CSF and possibly in the serum of all the subtypes of MS, but not PP-MS compared to controls, suggests that CXCL10 is involved in inflammation but not demyelination. Additionally, CXCL10 levels in

the CSF correlated with the CSF leukocyte count, suggesting *in vivo* chemoattractant activity of CXCL10 on these cells [Sorensen et al., 1999].

1.4.9.5 Function of CXCL10 in the CNS in MS

The role of CXCL10 has been extensively studied using EAE animal models. CXCL10, measured by ELISA, was increased before the clinical symptoms of the disease in SJL mice with EAE. The production of CXCL10 was also maintained at high levels during the peak of the disease [Fife et al., 2001]. Injection of an antibody against CXCL10 in the adoptive transfer model of EAE showed an amelioration of the disease and a reduction in the accumulation of pathogenic T cells [Fife et al., 2001, Liu et al., 2001]. This evidence highlights the role of CXCL10 in the recruitment of pathogenic cells at the lesion site into the CNS.

1.4.9.6 Chemokine receptors in MS

Expression of CCR1, CCR2, CCR3 and CCR5 on CNS post-mortem tissue from MS patients have been detected on foamy macrophages and activated microglia in chronic active lesions, which correlated with the level of expression of their ligands [Balashov et al., 1999, Simpson et al., 1998, 2000a].

Other evidence for chemokine receptor involvement in MS was obtained in a study by Trebst et al. (2003). CCR8 expression was found in MS white matter and localized on phagocytic macrophages and activated microglia which showed correlation with the degree of demyelination [Trebst et al., 2003].

The importance of chemokine receptor expression on PBMCs has been obtained using blood and CSF from MS patients and healthy controls. CCR2 and CCR5 expression on CD4⁺ cells was shown to be significantly higher in MS patients at relapse compared to control, whereas CCR3 and CCR4 expression on CD4⁺ T cells was significantly lower [Misu et al., 2001]. Chemokine receptors are also modulated on CD8⁺ T cells. CCR5 expression was shown to be significantly up-regulated in MS patients compared to control, whereas CCR4 was shown to

be down-regulated [Misu et al., 2001].

CXCR3 expression was also observed on CSF cells as well as lymphocytes in the perivascular cuffs in inflammation lesions. It was found that peripheral T lymphocytes have up-regulated CXCR3 expression in MS patients compared to controls [Nakajima et al., 2004]. Another study has implicated CXCR3 in the pathogenesis of MS [Mahad et al., 2003]. CXCR3 expression was shown to be up-regulated on peripheral blood CD4⁺ T cells in MS patients blood compared to controls which correlate with relapses.

All these *in vivo* findings on the expression of chemokine receptors suggest that they play an important role in the pathogenesis of MS. Other evidence for the involvement of chemokine receptors in MS are further discussed in the chapters 3 and 4.

1.4.10 Chemokines and chemokine receptors in EAE

1.4.10.1 Chemokines in EAE

Many studies have described an increase in chemokine expression in the CNS of animals with EAE. In acute EAE, CCL4, CCL5, CCL3, CXCL10 were up-regulated at the initiation of the active stage of the disease [Godiska et al., 1995]. During disease relapse, the same chemokines and CXCL1 was up-regulated [Glabinski et al., 1997]. The importance of these chemokines in the pathogenesis of the disease was supported by other studies. For instance, the use of anti-CCL3 neutralizing antibodies ameliorates clinical signs in acute EAE [Kennedy et al., 1998]. The importance of chemokines has been also highlighted using specific antagonists. Use of Met-RANTES, a peptide that blocks both CCR1 and CCR5, has been shown to ameliorate the course of EAE disease [Matsui et al., 2002]. The time course of expression of chemokines follows the clinical and histological stages of the disease. For instance CXCL10 mRNA expression level has been linked to the extent of histological inflammation [Ransohoff et al., 1993]. Indeed, CCL2 and CXCL10 expression was never detected in the absence of leukocyte infiltrates

[Glabinski et al., 1995]. In a recent study using CXCL13-deficient mice, it was shown that mice develop a less severe form of the disease indicating that CXCL13 plays an important role in the development of EAE [Bagaeva et al., 2006].

1.4.10.2 Chemokine receptors in EAE

Because the recruitment of inflammatory cells occurs via establishment of chemotactic gradients of chemokines, together with chemokine receptor expression on the responding cell surface, receptor expression has been extensively studied. A number of recent studies using knock-out mice for different chemokine receptors have been reported. The use of mice deficient for CCR1 and CCR2, revealed that they play an important role in the development of acute EAE [Fife et al., 2000, Rottman et al., 2000]. In CCR1 deficient mice, there is a 50% decrease in the clinical disease severity. This could be explained by a study that looked at the expression pattern of CCR1 mRNA in chronic-relapsing EAE [Glabinski et al., 2002]. They showed that the mRNA pattern of CCR1 increased and correlated with the number of Th1 T cells in the spinal cord at relapse.

Studies using CCR2^{-/-} mice have shown that these mice were resistant to EAE and had no CNS histopathology [Izikson et al., 2000, Fife et al., 2000]. CCR2^{-/-} mice had reduced mononuclear cell migration both into and within the CNS. Similarly, CCL2 deficient mice showed a failure in peripheral macrophage recruitment [Huang et al., 2001]. In EAE CCR2^{-/-} mice, induced by injection of encephalitogenic MOG₃₅₋₅₅ emulsified in incomplete Freund's adjuvant, showed a delayed onset and attenuated disease, with a greatly reduced clinical severity of relapse [Gaupp et al., 2003].

These findings support a significant functional role for CCR2 in the pathogenesis of the disease.

Inactivation of the CXCR3 gene in EAE mice, would be expected to ameliorate the disease due to decreased T cell recruitment to the CNS. Surprisingly, CXCR3

gene inactivation in MOG-induced EAE, resulted in an increase in the severity score of the disease by almost 50% compared to the WT, at day 12 post induction [Liu et al., 2006b]. Similarly, injection of antibody directed against CXCR3 in PLP₁₃₉₋₁₅₁ adoptive transfer EAE at days 9, 13 and 16 post-induction induced an increase in the EAE score up to 3.5 at the day 30 compared to the control antibody which had an EAE score of 1 [Liu et al., 2006b]. There was no alteration in the migration of T lymphocytes into the CNS, which confirmed a previous study where CXCR3 has been shown not to be required for transendothelial migration [Callahan et al., 2004]. No difference was observed in the relative CNS population of CD4⁺, CD8⁺ T cells and TCR $\alpha\beta$ and TCR $\gamma\delta$ cells between CXCR3^{-/-} and WT mice at the peak and the recovery of EAE [Liu et al., 2006b]. It was shown that isolated lymphocytes from the lymph node had an increase in proliferation and decrease in IFN γ production when the CXCR3 gene was inactivated, which was confirmed *in vivo*. They also showed that the BBB was disrupted and there was an increase in angiogenesis, shown by an increase in expression of Von Willebrand factor, in CXCR3^{-/-} mice [Liu et al., 2006b].

These findings suggest that CXCR3 exerts its effect on EAE at the effector phase by increasing the synthesis of IFN γ by T cells rather than by controlling the migration and retention of immunological cells at the inflammation site.

1.4.11 Chemokines and astrocytes

As previously discussed, astrocytes have been shown to be actively involved in MS pathogenesis by producing a wide range of chemokines including CCL2 and CXCL10. It was shown that astrocytes also secrete CCL5, CCL7, CCL8, CXCL12 which result in the recruitment of activated T cells, monocytes and B cells as discussed in table 1.1 [Kim et al., 2004, Krumbholz et al., 2006, Trebst and Ransohoff, 2001]. Thus, astrocytes contribute to the orchestration of the inflammatory response in the CNS by producing chemokines to recruit immune cells.

1.5 Aims of this thesis

The overall aim of this thesis is to elucidate the involvement of astrocytes in control of chemokine expression in the CNS. Indeed, astrocytes are the most abundant cells within the brain and are located at the vicinity of the BBB, they are in a perfect location to regulate the level of chemokines and hence cell recruitment. This aim will be addressed by the following objectives:

1. Determine whether there is a differential expression of chemokines, CCL2 and CXCL10, by astrocytes under pro-inflammatory conditions.
2. Determine whether astrocytes can sequester CCL2 in the CNS, either under basal and pro-inflammatory conditions.
3. Determine the expression of CXCR3 under basal and pro-inflammatory conditions and the effects of CXCL10 on astrocytes.
4. Determine the expression of chemokine decoy receptor, D6, by astrocytes *in vitro* and *in vivo* and its involvement in the regulation of CC chemokine levels under pro-inflammatory conditions.

CHAPTER 2

Expression of CCL2 and CXCL10 by primary human adult astrocytes

2.1 Introduction

2.1.1 CCL2 and CXCL10 expression in MS

Reports on CCL2 and CXCL10 expression in the CNS white matter in MS pathogenesis have found that both CCL2 and CXCL10 are strongly expressed at the lesion site compared to control [McManus et al., 1998, Simpson et al., 2000a]. However, it was also shown that CCL2 expression was decreased in the CSF of MS patients at the time of relapse whereas CXCL10 expression was increased [Scarpini et al., 2002, Narikawa et al., 2004]. Reports on serum levels of CCL2 are contradictory. Scarpini et al. (2002) showed a decrease of CCL2 in MS compared to control [Scarpini et al., 2002] whereas Kivisakk et al. (1998) showed no difference between the expression of CCL2 in serum of MS patients and normal controls [Kivisakk et al., 1998].

2.1.2 Pro-inflammatory cytokines in CNS inflammation

Cytokines are soluble proteins that are involved in many pathological processes in the CNS such as oligodendrocyte death, axonal degeneration and neuronal dysfunction [Bjartmar et al., 2003, Owens, 2002, Lucchinetti et al., 1998]. Modulation of cytokine expression levels in MS indicate a key role for cytokines in the pathogenesis of MS. Mycko et al. (2004) analysed gene expression in chronic active and chronic inactive lesions in MS by cDNA microarray analysis. IL6 and TNF showed significant increases of 15.2 and 8.1 fold between chronic active and chronic inactive lesion [Mycko et al., 2004]. Similar findings were seen for IL-17 which was increased in MS brain compared to control [Lock et al., 2002]. Another study showed that PBMC secretion of IL6 and TNF was significantly increased in MS patients compared to control but no difference was observed with IL-10 and IFN γ [Ozenci et al., 2000].

During MS pathogenesis, astrocytes become reactive and increase expression of cytokines and growth factors [Meeuwssen et al., 2003]. Three cytokines, expressed at CNS inflammatory sites [Link, 1998, Pan et al., 1997, Rothwell and Luheshi, 2000], are commonly used in *in vitro* studies: IL-1 β , TNF and IFN γ .

2.1.2.1 Interleukin1- β (IL1- β): effect on CNS resident cells

IL1- β is a 17KDa protein expressed by numerous cells within the CNS including astrocytes, neurons and oligodendrocytes as well as microglia and invading macrophages, during inflammation [Vitkovic et al., 2000, Davies et al., 1999, Blasi et al., 1999]. IL1- β exerts its biological effect through the binding to a 68KDa cell surface receptor which requires an accessory protein for induction of signalling events [Rothwell and Luheshi, 2000].

IL1- β has been shown to induce oligodendrocyte cell death when co-cultured with astrocytes and microglia but not in pure cultures of oligodendrocytes. The mechanism responsible for the cell death seems to be related to the impairment of glutamate uptake by astrocytes [Takahashi et al., 2003]. Glutamate has been

shown to be taken up by five transporters, including GLT-1 and GLAST, principally expressed by astrocytes, which are down regulated by IL-1 β [Hu et al., 2000, MacAulay et al., 2002, Rothstein et al., 1996]. Thus, IL-1 β can regulate the level of glutamate which results in an increase in extracellular glutamate level inducing excitotoxic neurodegeneration.

Further evidence for a detrimental role for IL-1 β in MS was obtained by a genetic study which discovered that MS patients who were carriers of the IL1RN2 allele and non-carriers of the IL1B2 allele had a higher rate of progression than the patients with other allelic combinations [Schrijver et al., 2003].

However, the role of IL-1 β is not only detrimental but has also been reported to mediate neuroprotection. *In vitro* studies have shown that incubation of neurons with NMDA resulted in cell death which was partly inhibited by co-incubation with IL-1 β (at 25 and 50ng/ml). The IL-1 β neuroprotective effect was inhibited when IL1RA (IL1 receptor antagonist) was added thus confirming the *in vitro* neuroprotective effect of IL-1 β on neurons [Carlson et al., 1999]. The mechanism underlying the neuroprotection has been partly elucidated in studies using IL1 KO mice, in which IL-1 β might promote oligodendrocyte repair via induction of insulin growth factor I (IGF-I) by astrocytes and macrophages/microglia [Mason et al., 2001].

2.1.2.2 Tumor necrosis factor (TNF): effect on CNS resident cells

TNF is a 17 KDa protein that is expressed by many immune cells including T and B lymphocytes, NK cells, eosinophils and monocytic cells. In the CNS, activated microglia are the main producers of TNF, although astrocytes also produce TNF but to a much lesser extent [Sawada et al., 1989, Kuno et al., 2006]. TNF exerts its biological effect through binding to two different receptors, TNFR1 (p55) and TNFR2 (p75). Following CNS injury, TNF expression is dramatically increased and leads to the activation of mononuclear phagocytic cells,

endothelial cells and gliosis and eventually to initiation of apoptosis of oligodendrocytes. Takeushi et al. (2006) showed that TNF induced activation of microglia cells resulting in the release of glutamate leading to neuronal excitotoxicity and death. TNF has been shown to enhance expression of Fas, TNFR1 and MHC class I molecules resulting in oligodendrocyte apoptosis by direct cytotoxic effect [Buntinx et al., 2004].

TNF has been shown to induce demyelination and neuronal degeneration either directly or indirectly via the production of toxic mediators such as NO and reactive oxygen species (ROS) [Tanaka et al., 1994].

However, there is also evidence to suggest beneficial effect of TNF on remyelination. For example, TNF deficient animals display a significant delay in remyelination associated with a reduction in the pool of proliferating oligodendrocytes and a reduction in the number of mature oligodendrocytes [Arnett et al., 2001]. TNF not only acts on oligodendrocytes but also on astrocytes and especially in induction of the secretion of growth factors such as NGF (nerve growth factor).

2.1.2.3 Interferon γ (IFN γ): effect on CNS resident cells

IFN γ is a pleotropic cytokine that plays an important role in the regulation of the immune response. It has been shown to activate mononuclear cells, differentiate T cells into Th1 phenotype, increase cell expression of MHC class I and II molecules and induce apoptosis of T cells and other cell types [Imitola et al., 2005]. The exact role of IFN γ in MS pathogenesis is not clear. It has been shown to have a detrimental effect on oligodendrocyte function and survival. In presence the of IFN γ , oligodendrocytes have been shown to up-regulate the expression of surface receptors that mediate cell-cytotoxicity such as MHC class I or the death receptor Fas [Agresti et al., 1998, Pouly et al., 2000]. Other evidence has been obtained by over-expressing IFN γ in the CNS which results in oligodendrocyte apoptosis and inhibition of myelination [Balabanov et al., 2006, Horwitz et al., 1997, Lin et al., 2006]. Therefore IFN γ play an active role in demyelination.

Paradoxically, a low level of IFN γ provides protection to mature oligodendrocytes against demyelination in MBP/IFN γ transgenic mice [Gao et al., 2000]. It was shown that these mice presented with higher levels of expression of IGF-1 which protects oligodendrocytes *in vitro* [Ye and D'Ercole, 1999]. Similarly, IFN γ KO mice were more susceptible to EAE and showed a more severe invasion of CNS by immune cells [Ferber et al., 1996]. This surprising finding might be explained by the anti-proliferative effect and the pro-apoptotic effect of IFN γ on T cells therefore preventing the accumulation of activated T cells in the CNS [Chu et al., 2000].

IFN γ has been shown to be involved in the immune response by increasing the expression of MHC class II molecules on astrocytes, which allows them to act as APCs as discussed in section 1.2.6.6 [Dong and Benveniste, 2001]. A recent study reported that, following IFN γ treatment of murine astrocytes, the upregulation of genes involved in the immune response, including chemokines, cytokines and most predominantly MHC class I and II antigen presentation pathway genes. In addition to MHC class II molecules, IFN γ treatment induced upregulation of B7.1, B7.2 and HLA-DM expression by murine astrocytes indicating that astrocytes are able to present antigen and activate naive T cells [Carpentier et al., 2005, Halonen et al., 2006].

2.1.3 Aim of the study

To elucidate why there is differential expression of CCL2 and CXCL10 in the CSF and the possible contribution of astrocytes to this process, the rate of synthesis and secretion of these two chemokines under pro-inflammatory conditions was investigated. Indeed, chemokine expression by astrocytes is affected by the cytokine milieu within the CNS during active inflammation, as evidenced by studies on post-mortem tissues.

This aim will be addressed by the following objectives:

1. To determine whether human adult astrocytes express CCL2 and CXCL10 mRNA and protein.

2. To assess whether pro-inflammatory cytokines are able to modulate the expression of CCL2 and CXCL10 mRNA and protein.

3. To determine any difference between the levels of expression of CCL2 and CXCL10 in between control and cytokine stimulated astrocytes.

2.2 Materials and methods

2.2.1 Isolation of astrocytes from CNS tissue

Primary adult human astrocytes were isolated from CNS normal appearing white matter tissue obtained from the UK MS Society Tissue Bank (UKMSTB; donor labelled SMS262) following Open University, Kings College Hospital (KCH) and UKMSTB ethics guidelines. Seven other primary human adult astrocytes were used in this thesis and were isolated from CNS normal appearing white matter tissue (SMS-12), MS lesions (donor labelled MS16 and MS21) from the UK MS Society Tissue Bank or from temporal lobectomy resections at KCH (B327/01, B668/01, B1029, B79/01 and Ep15). These astrocyte preparations were provided by Dr. Ignacio Romero from the Open University.

Astrocytes were isolated as described by Flynn et al. (2003). Approximately 1 g of brain tissue per preparation was used. Meninges and visible blood vessels were removed with forceps to avoid contamination with fibroblasts. Samples were minced with scalpel and the tissue fragments were transferred to 10 ml of Hank's balanced salts solution containing 10 mM HEPES, 50 U/ml penicillin and 50 $\mu\text{g}/\text{ml}$ streptomycin, and 2.5 $\mu\text{g}/\text{ml}$ fungizone (Invitrogen, UK) and centrifuged for 5 min at 600 g in a Sorvall legend RT (Thermo Scientific, UK). The pellet was resuspended by trituration in 15 ml of 1 mg/ml collagenase dispase solution containing 10 mg/l DNase I and 0.147 mg/l N-p-tosyl-L-lysine chloromethyl ketone (TLCK), an irreversible inhibitor of trypsin, and incubated for 1 h at 37°C with shaking every 10 min. After digestion, the astrocytes were separated from microvessel fragments and other material by density-gradient centrifugation for 30 min at 1000 g with 20 ml of 25% bovine serum albumin (BSA). 75-cm² flasks were coated with poly-L-ornithine diluted in PBS (1.5 g/l; Sigma, UK) for 1 hour at (RT). The floating myelin layer was removed and plated onto coated 75-cm² flasks in astrocyte media composed of 1:1 nutrient mixture F-10 and MEM alpha medium, supplemented with 10% heat-inactivated foetal calf serum, 1% human serum, 50 U/ml penicillin and 50 $\mu\text{g}/\text{ml}$ streptomycin (Invitrogen, UK) in a humid

atmosphere at 37°C in 95% air/5% CO₂. After 48 h, the medium was changed to remove unattached cells and myelin debris. Cells resembling astrocytes grew to confluence within 2-3 weeks. 1x10⁶ astrocytes were resuspended in 1 ml freezing media (1ml DMSO (Sigma Aldrich, UK), 1ml FCS and 9ml media) and kept overnight at -80°C before being stored in liquid nitrogen.

Astrocytes were used up to passage 8 to have optimal viability and avoid senescence of astrocytes [Flynn et al., 2003].

2.2.2 Characterization of different primary human adult astrocytes by immunocytochemistry using anti-GFAP antibody

To assess the purity of the astrocyte preparations, immunostaining with antibody directed against GFAP was performed. Astrocytoma cell line (U373-MG) was used as a positive control.

2.2.2.1 Principle of immunocytochemistry

The technique of immunofluorescence was first described by Coons et al. in 1941 using on tissue sections [Coons, 1941]. It is now commonly used to identify the expression and distribution of proteins in cells or tissues by specific antigen/antibody interaction. The immunofluorescence technique is based on the binding of antibodies, often IgG class, to a specific antigen.

Two types of antibodies can be used: polyclonal or monoclonal antibody. Polyclonal antibodies can be produced in number of animal species, particularly rabbit, horse, goat, and chicken by injecting an immunogen (peptide) which results in antibody production specific to the immunogen. Monoclonal antibodies are mostly produced in mice. Polyclonal antibodies have higher affinity and wide reactivity but lower specificity when compared with monoclonal antibodies.

Detection of bound antibody is revealed either by direct or indirect labelling (secondary antibody) with fluorescent probes, enzymes or radioactive elements (figure 2.1). In this chapter, indirect immunostaining using fluorescent probes has been used. In chapter 3, direct labelling of antibody is used for flow cytometry detection of antigen. Indirect immunofluorescence is more sensitive due to the amplification of the signal with the secondary antibody [Myers, 1989].

2.2.2.2 Astrocyte characterization by immunocytochemistry for GFAP

Seven astrocyte preparations were tested for GFAP staining: B327/01, Ep15, MS16, MS21, B668/01, B79/01, B1029. Glioblastoma-astrocytoma cell line (U373-MG), from a human Caucasian (ECACC 89081403), was used as a positive control. The cells were grown in 75 cm² in astrocyte media at 37°C in 95% air/5% CO₂. After several days in culture, astrocytes were washed once with PBS (Gibco, UK) and 3 ml of trypsin-EDTA (Gibco, UK) was added to the cells for 5 min to detach them from the flask. Cells were resuspended in astrocyte media and 0.4ml of 1x10⁵/ml cell suspension were plated in each well of an 8 well chamber slide (Nalge Nunc International, UK) and incubated overnight at 37°C in 95% air/5% CO₂. Cells were washed twice in PBS and 0.4ml of 4% paraformaldehyde in PBS, pH 7.2 (Appendix) was added to cells for 15 minutes at RT. Cells were then washed 3 times (5 min each) with PBS. 100 µl of polyclonal rabbit anti-GFAP antibody (Abcam, UK) at a dilution of 1:1000 in PBS with 0.5% Triton X100 (for permeabilization of the cell membrane) was added to cells and incubated overnight at 4°C. Cells were washed 3 times with PBS and then 100 µl of goat anti-rabbit IgG-Alexa 488 (Molecular Probes, UK) was added at 1:500 in PBS. Cells were incubated for 1.5h in the dark in a humid chamber. Antibody was washed away as described above, the chambers were gently removed and the slides were washed 3 times in PBS. The seal from the chamber was gently removed and one drop of mounting medium with DAPI (Vector Laboratories Inc., UK) was added to mount the coverslip. Slides were incubated for 1h at in the dark to allow the DAPI to stain the nuclei. Coverslips were sealed with nail varnish to avoid drying out. La-

bellung of cells was observed with an Axiovert 200 M (Zeiss) confocal microscope with an LSM 510 laser module (see below).

2.2.3 Visualisation of GFAP staining by astrocytes using confocal microscopy

2.2.3.1 Principle of Confocal laser scanning microscopy (CLSM)

CLSM is a technique that is able to produce high resolution optical images. A laser emits a light source, which passes through a pinhole aperture, reflected by a dichromatic mirror and light is collected in an objective to be scanned across the sample on the focal plan. The sample is also scanned in depth by fixed increments (Z-stack) that can be reconstructed into three dimensions. The light is then refracted and collected again in the lens. There is therefore a mixture of refracted and emitted light. The dichromatic mirror directs the reflected fluorescence through a detector pinhole aperture. This pinhole allows light from the focal plane to reach the detector but rejects the out-of-focus photons that contribute to background in the image. The light is collected in the photon multiplier tube to be converted into an electronic signal, which is then digitalized by an analogue-digitalized converter and a digital image processor that create an image. This image can be further processed by the computer [Lucitti and Dickinson, 2006, Paddock, 2000].

An Axiovert 200M microscope (Zeiss) with an LSM 510 laser module (Zeiss) was used to assess cell staining in this thesis. The LSM 510 program was used and the laser (488 nm) was switched on and warmed up for 30 min prior to use. The current and the output of the laser were respectively 6.3A and 50%.

2.2.4 Detection of mycoplasma in cell cultures by PCR

It is vital to ensure that cells maintained in continuous culture are not infected with mycoplasma. Mycoplasma is a bacteria contamination that perturbs the nor-

mal metabolism of cells and interferes with biological processes and could mask the normal response of astrocytes to cytokine stimulation [Rottem et al. 1993]. Detection of mycoplasma was assessed using PCR amplification following the manufacturer's instruction (GeneFlow Ltd, UK). Briefly, supernatant from astrocyte cultures was spun for 5 min at 250g in a Mini Spin Plus centrifuge (Eppendorf, UK) to remove cellular debris. This supernatant was further centrifuged for 10 min at 12,000g. The supernatant was discarded and 50 μ l of buffer solution provided in the kit was added to the pellet and heated at 95°C for 3 min. PCR was undertaken using the following conditions: hold 94°C 30 s; 35 cycles of 94°C 30s, 60°C 120s, 72°C 60s and 1 cycle 94°C 30s; 60°C 120 s and 72°C 5 min. PCR products were loaded on a 50 ml 2% agarose gel with 5 μ l ethidium bromide (Sigma, UK). A positive control, giving a band at 270bp, was run alongside the samples and gels were visualized using a UVP Bioimaging system (Bio-Rad, UK).

2.2.5 Effect of pro-inflammatory cytokines on the expression of CCL2 and CXCL10 by different astrocyte preparations

2.2.5.1 Stimulation of astrocytes with pro-inflammatory cytokines

Astrocytes (SMS-12) were seeded into 24 well plates at a density of 1×10^5 cells/ml/well in astrocyte media and then allowed to adhere for 24 hours. Media was removed and cells were rinsed with PBS. The cytokines diluted in the same medium without serum were applied to the cells. The cells were stimulated in triplicate wells with the cytokines IL-1 β , TNF or IFN γ at 0, 1, 10 and 100ng/ml (Peprotech, UK) and incubated for 2 to 48 hours in a humid atmosphere at 37°C in 95% air/5% CO₂. Supernatants were removed and spun for 5 min at 300g to pellet the cellular debris and collected for CCL2 and CXCL10 quantification by ELISA (performed by Dr. Omer Suliman) and stored at -20°C. Stimulations were performed in triplicate. The cells were harvested with Tri reagent (Sigma, UK) for RNA extraction and real time PCR as described in section 2.2.6.2.

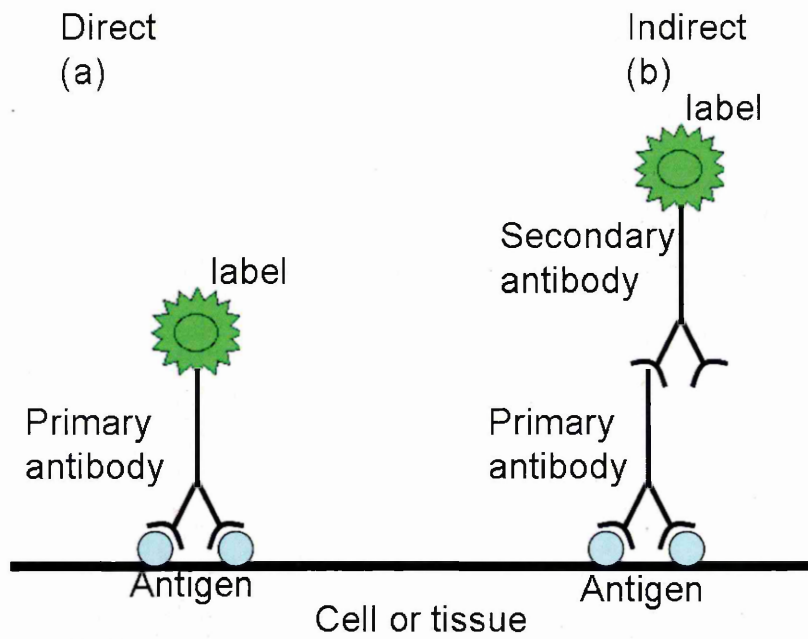


Fig. 2.1: **Principle of immunostaining: direct and indirect labelling.**

Immunofluorescence is based on the properties of an antibody to specifically bind to a protein (antigen) enabling the detection and localization of a protein on cells or tissue. There are two type of immunofluorescence. Direct immunofluorescence is performed with the antibody directly labelled with a probe (fluorescent, enzyme or radioactive) (a). Indirect immunofluorescence requires two steps (b): the first step is the interaction of the antigen with an antibody and the second step is the detection of the interaction using a secondary antibody directed against the immunoglobulin species of the primary antibody coupled with a probe. For example if the primary antibody is a mouse antibody, the secondary antibody is rabbit or goat anti mouse.

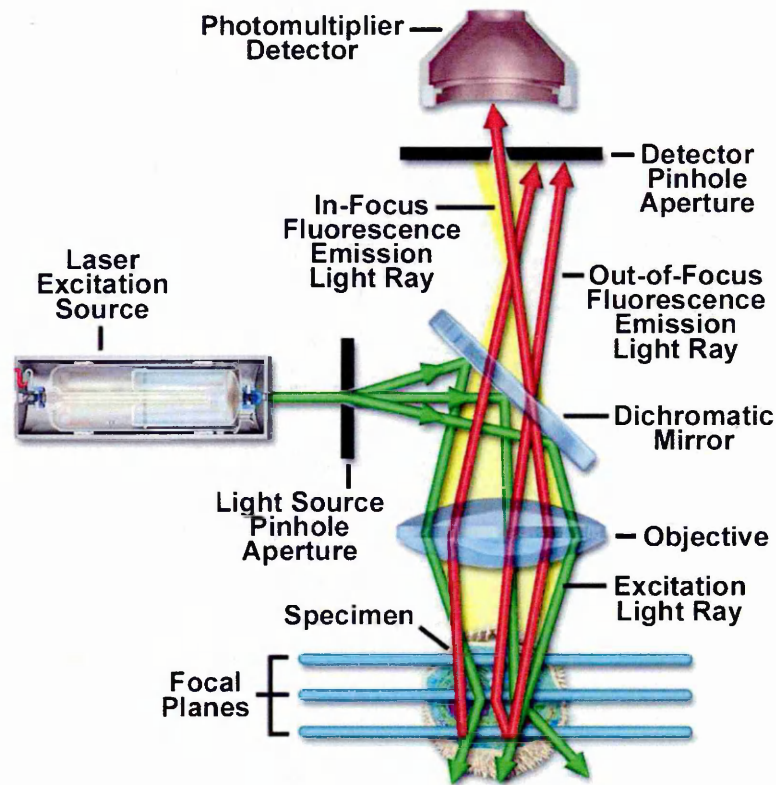


Fig. 2.2: Principle of confocal laser scanning confocal microscope (CLSM).

Schematic diagram of the optical pathway and principal components in a laser scanning confocal microscope. The laser passes through the light source pinhole aperture to be collected by a lens. The light is scanned on the sample and reflected to the dichromatic mirror. The light is then collected by a detector pinhole aperture but not the non-focused light. The photons are then converted into a digital signal by the computer that generates an image of the sample. Taken from www.olympusconfocal.com/theory/LSCMIntro.pdf

2.2.5.2 Comparison of response of three different astrocyte preparations, following pro-inflammatory stimulation

Comparison of the response of three different normal human adult primary astrocyte cell preparations (SMS-12, B327/01 and Ep15) was performed following stimulation with IL-1 β , TNF and IFN γ (10ng/ml) for 24 hours, as described above. RNA was extracted to perform qRT-PCR.

2.2.6 Real time PCR to quantitate mRNA isolated from astrocytes stimulated with pro-inflammatory cytokines

2.2.6.1 Principle of qRT-PCR

The technique of real time PCR (qRT-PCR) is based on the RT-PCR reaction [Heid et al., 1996, Wilhelm and Pingoud, 2003]. As with RT-PCR, qRT-PCR consists of two steps. The first step translates mRNA into cDNA, followed by a classical PCR reaction. In the classical PCR reaction, 2 primers (forward and reverse) match and anneal to sequences that are on each side of the sequence to be amplified. The polymerase enzyme can therefore amplify the desired DNA sequence. The product is double-stranded DNA characterized by a length corresponding to the length of DNA between the two primers, determined when the primers are designed. At the end of the amplification, a graph is produced that shows the amount of DNA amplified for each cycle.

In this thesis, SybrGreen DNA binding dye is used to detect the amplification products because of its simplicity. It produces a fluorescent signal only when bound to double stranded DNA upon light stimulation. In contrast with other probes, SybrGreen is not specific and cannot differentiate amplified gene target and non specific PCR products formed like primer-dimer in the reaction (Wittwer et al., 1997). Therefore, it is important to run a melt curve following qRT-PCR by increasing the temperature by 1°C and recording the fluorescence. By viewing a melt curve, you ensure that the desired amplicon was detected.

Amplification and detection during qRT-PCR are directly visualized and correspond to the quantity of fluorescence in each cycle of the PCR reaction. Quantification is based on the increase in fluorescence directly linked to the increasing amount of double-stranded DNA [Heid et al., 1996]. Thus the amount of fluorescence is correlated to the amount of mRNA of the target gene that is present.

qRT-PCR is composed of 3 steps:

- Denaturation: 95°C.
- Annealing: dependent on the characteristics of the primers and especially the quantity of bases cytosine (C) and guanine (G) in the primer sequence.
- Elongation: 62°C.

Before using qRT-PCR on different samples, the selection of the most appropriate housekeeping gene must be performed to use as an internal control for normalisation.

Housekeeping genes

A housekeeping gene (HK) is a class of gene that has a basal cellular function in organisms and is constitutively expressed in all cells. In molecular biology, the comparison of the rate of synthesis of a protein is fundamental for the understanding of cellular mechanisms. Before carrying out such experiments, an internal control, which should not vary amongst the various cells or under different experimental conditions, must be selected: this is the HK gene [Thellin et al., 1999]. However, since the expression rate of HK genes may be modulated under different experimental conditions, tests must be performed to select the best set of housekeeping genes for use in the experimental conditions under study. In this study, five HK genes commonly used were assessed; glyceraldehyde-3-phosphate dehydrogenase

(GAPDH), β -actin, hypoxanthine phosphoribosyl transferase 1 (HPRT1), Ubiquitin C (UBC) and ribosomal protein L 13A (RPL13A) [Vandesompele et al., 2002].

Primer design using primer3 software

There are some requirements for the design of efficient primers [Innis MA, 1990]:

- the length should be between 17 and 28 bp
- the composition should be 50-60% of (G+C)
- 3' primer end should be G and/or C
- Melting temperature (T_m) should be between 55 and 80°C

The primers, used in this thesis, were designed using Primer3 software [Rozen and Skaletsky, 2000] which considers many factors including the melting temperature, the length, the GC composition and the primer-dimer formation between two copies of the same primer.

Quantification of PCR products: comparative Ct method

In the amplification curve, the fluorescence is very low and corresponds to the baseline. As soon as fluorescence increases and is above the baseline, which is evidence of the accumulation of PCR products, a fixed fluorescence threshold can be established above the baseline. The Ct (Cycle threshold) value is defined as the fractional cycle at which the fluorescence crosses the fixed threshold [Bustin, 2000, 2002]. The early cycles of qRT-PCR are characterized by an exponential increase in DNA product. When the components of the reaction become limiting, the amplification is strongly decreased corresponding to the plateau. Since slight variations in the reaction components can induce large differences in the amount of PCR product at the end of the reaction, the Ct value is used for quantitation of RNA in the sample. Indeed, during the exponential phase of the reaction, none of the components are in a limiting state so that the Ct value is reproducible and

accurate. It gives therefore a more reliable measure of starting copy number than the end point of the PCR product [Bustin, 2002].

This method compares the Ct value of a reference (HK) and the test sample. The Ct value method is also known as the $2e^{-(\Delta \Delta Ct)}$ method where $\Delta \Delta Ct$ corresponds to $\Delta Ct_{control} - \Delta Ct_{stimulation}$ [Livak and Schmittgen, 2001]. Here ΔCt corresponds to the $Ct_{sample} - Ct_{HK}$. This method does not account for primer efficiency. Thus if the primer efficiencies between the sample and the HK are very different, the determination of the ratio of expression between the HK gene and the target gene will not be accurate. Calculation of the primer efficiency is therefore vital for the quantification of the PCR product and will allow use of the formula to calculate the fold increase or decrease. To obtain the primer efficiency, the slope (a) is calculated from the graph $Ct \text{ value} = ax[\log \text{ of dilution}] + b$. Then the efficiency is calculated by the formula; $\text{Efficiency} = 10^{-(1/\text{slope})} - 1$.

Ideally the efficiency of the primers should be 100%, meaning that templates double after each cycle during the exponential phase. But some factors can affect the efficiency of the primer, e.g. the length of primer, secondary structure and the use of non optimal reagent concentration [Bustin, 2004]. Such factors can therefore decrease the efficiency of the primer below 90%. A good primer efficiency is between 90 and 110%.

Quantification of PCR products: Pfaffl method

If the efficiency of the primers are different, the Pfaffl method, which considers the primer efficiency of the target and HK gene, has to be used [Pfaffl, 2001] following the formula:

$$\text{Efficiency} = (E_{target})^{Ct_{control} - Ct_{sample}} / (E_{HK})^{Ct_{control} - Ct_{sample}}$$

Determination of the primer efficiency is therefore important for the quantification of the PCR product, which will determine the formula to use to calculate

the fold increase or decrease of the target gene.

2.2.6.2 mRNA extraction

RNA was extracted from stimulated primary human adult astrocytes using Tri reagent (Sigma, UK) according to the manufacturer's instructions. Briefly, 2 wells of cells from 24 well plates at a density of 1×10^5 cells/well (2×10^5) were resuspended in 1ml of Tri reagent, transferred into an eppendorf tube and 0.2ml of chloroform (Sigma,UK) added to samples, mixed and incubated for 10 min at RT. Samples were centrifuged in a Mini Spin Plus centrifuge (Eppendorf, UK) for 15 min at 12 000 g at 4°C and the aqueous phase was collected for RNA precipitation with 1.5 ml of isopropanol (Sigma, UK). Samples were centrifuged at 12,000 g for 10 min at 4°C. Pellets were washed with 1ml of ethanol (75%) and resuspended in autoclaved water, usually $20 \mu\text{l}$ to $30 \mu\text{l}$, depending on the size of the pellet. The integrity of RNA (double bands corresponding to the two different subunit of RNA) was confirmed by running $1 \mu\text{l}$ of mRNA with $5 \mu\text{l}$ of RNA loading buffer (Appendix) on 1% agarose gel electrophoresis.

2.2.6.3 cDNA synthesis

The mRNA was transcribed into cDNA using the iScript cDNA synthesis kit (Biorad,UK). Two to four μl of mRNA, depending on the amount of mRNA visualized on the 1% agarose gel, was mixed with $4 \mu\text{l}$ of 5X iScript Reaction mix, $1 \mu\text{l}$ iScript reverse transcriptase and nuclease free water to a final volume of $20 \mu\text{l}$. Samples were incubated for 5 min at 25°C, 30 min at 42°C and 5 min at 85°C using a QBD2 heating block (Grant Instruments, UK). Samples were stored at -20°C until required.

2.2.6.4 Real time PCR optimisation: selection of the most stable housekeeping gene using GeNorm software

GeNorm software is an excel based software which was used to select the most stable housekeeping gene between UBC, GAPDH, HPRT, RLP13A and β -actin.

The GeNorm program, which has been cited in over 600 papers, is based on the $\Delta\Delta Ct$ value method. It determines the gene expression stability measure (M) and the average pairwise variation (V) of the tested gene under IL1- β , TNF and IFN γ (100ng/ml) treatment, by calculating the ratio:

Ratio = $2^{(Ct_{sample}-Ct_{control})}$, where control corresponds to the unstimulated astrocytes.

Stepwise exclusion of the gene with the highest M value allows ranking of the tested genes according to their stability leading to the selection of the most stable HK gene [Vandesompele et al., 2002].

2.2.6.5 Real time PCR amplification

CCL2 primers were provided by Dr. Alison Cross who designed them using Primer Express software (Applied Biosystems). CXCL10 primers were obtained from published sequences [Grassi et al., 2003]. The sequences of primers used in this study are summarized in table 2.1. The fold increase in the target gene was determined using the formula $2e^{-(\Delta \Delta Ct)}$ (for CCL2 and CXCL10).

Each cDNA from the cell stimulations experiments (section 2.2.5.1) (n=3) was amplified twice. The real time PCR reactions were conducted with Absolute SybrGreen (Abgene,UK). 2.5 μ l of cDNA was combined with 0.5 μ M of each primer, 3 or 4mM MgCl₂ (for CCL2 and CXCL10 respectively) and 1X absolute SybrGreen. The real time PCR conditions were as follows: hold 95°C 15 min; 40 cycles of 95°C 15s, 60°C 15s, 72°C 30s; 1 cycle 95°C 30s; 1 cycle 50°C 30s and the melt ramp from 50°C to 95°C at 1°C/10s to determine the product specificity. All samples were run on the iCycler (Biorad).

2.2.7 Measurement of CCL2 and CXCL10 secretion by astrocytes following pro-inflammatory stimulation using Enzyme-Linked ImmunoSorbent Assay (ELISA)

Supernatants from cell stimulation experiments (section 2.2.5.1) were spun down for 5 min at 300g to pellet the cellular debris. Supernatants were transferred into clean eppendorf tubes and stored at -70°C. ELISAs were performed by Dr. Omer Suliman. Briefly, 100 μ l of capture antibody CCL2 and CXCL10 (R&D Systems, UK) were loaded into wells at 4 μ g/ml and incubated overnight at 4°C. Wells were washed three times with 400 μ l of PBS and then 300 μ l PBS containing 1% BSA, 5% sucrose, 0.05% NaN₃ was added to the wells and incubated for 1 hour at RT to prevent non specific binding. Wells were washed three times with PBS. Standard curve were performed in duplicate with recombinant human CCL2 or CXCL10 (Peprotech, UK) using the following concentrations: 2000, 1000, 500, 250, 62.5 and 37.25 pg/ml. 100 μ l of standard dilutions or 100 μ l of supernatants were loaded into wells and incubated for two hours at RT. Following washing as described above, biotinylated primary antibody was applied to wells (50ng/ml for CCL2 and 100ng/ml for CXCL10, R&D Systems, UK) and incubated for 2 hours at RT. Wells were washed three times with PBS and 100 μ l of streptavidin HRP (R&D Systems, UK) at a dilution of 1/200 was added and incubated for 20 min at RT. Wells were washed as previously and 100 μ l of substrate (3,3',5,5'-tetramethylbenzidine (TMB) Liquid Substrate System, Sigma UK) was added per well and incubated for 30 min at RT in the dark. 100 μ l of stop solution (sulphuric acid, 1M) was added per well. Absorbance was read using a plate reader (Wallac Victor²) at 450 nm. Secreted CCL2 and CXCL10 was determined by using the equation from the standard curve, $y=ax + b$ where a is the slope of the standard curve. Chemokine secretion under pro-inflammatory stimulations was performed in triplicate and expressed as fold increase compared to the baseline (unstimulated cells).

2.2.8 Statistical analysis

Real time PCR and ELISA data are shown as mean \pm SEM. For experiments on mRNA level expression and protein expression, level of significance for comparison between samples was determined using the ANOVA parametric test, which allows comparison between three or more groups. Dunnett's test was used to determine if there was any difference in the mean value of the stimulated astrocytes compared to the reference (unstimulated astrocytes). In all cases, $P \leq 0.05$ was considered significant.

Primers	Sequences	T _m (°C)
GAPDH forward	ACCCAGAAGACTGTGGATGG	59.4
GAPDH reverse	CACATTGGGGGTAGGAACAC	59.4
β -Actin forward	TGTTACCAACTGGGACGACA	57.3
β -Actin reverse	GGGGTGTTGAAGGTCTCAA	57.3
RPL13A forward	CCTGAAGAAGAGGAAAGAGA	62.4
RPL13A reverse	TTGAGGACCTCTGTGTATTTGTCAA	59.7
HPRT forward	TGACACTGGCAAAACAATGCA	55.9
HPRT reverse	GGTCCTTTTCACCAGCAAGCT	55.9
UBC-forward	ATTTGGGTCCCGGTTCTT	53.7
UBC-reverse	TGCCTTGACATTCTCGATGGT	57.9
CCL2-forward	CTGTGCCTGCTGCTCATAGC	61.4
CCL2-reverse	GCACTGAGATCTTCCTATTGGTGAA	61.3
CXCL10-forward	TGAGCCTACAGCAGAGGAA	57.6
CXCL10-reverse	TACTCCTTGAATGCCACTTAGA	56.5

Tab. 2.1: Primer sequences used in this study.

Commonly used housekeeping genes were tested in this study to determine which was the most stable gene. GAPDH, β -actin, RPL13A, HPRT and UBC were tested using GeNorm software. The primers for the two target genes, CCL2 and CXCL10 were either designed by Dr. Alison Cross using primer express software (Applied Biosystems) or obtained from published sequences.

2.3 Results

2.3.1 Characterization of primary human adult astrocytes using immunocytochemistry

Seven different human primary astrocyte preparations (SMS-12, B37/01, 668/01, B1029, B79/01, MS16, MS21) and an astrocytoma cell line (U373-MG) were tested by immunocytochemistry using an antibody against GFAP, a specific marker of astrocytes. All the primary adult astrocytes were positive for GFAP (figure 2.3 c-i). However, a non-fibrillary staining pattern was observed as seen for B327/01, Ep15, MS 21 and MS16 (figure 2.3c,d, e and f respectively). This was not due to technical issues as U373-MG, an astrogloma cell line, showed the characteristic fibrillary staining for GFAP. Despite positive staining for GFAP, several astrocyte preparations showed an uncharacteristic phenotype e.g. B668/01 (figure 2.3g), B79/01 (figure 2.3h) and B1029 (figure 2.3i) with a small rounded cell morphology, not characteristic of astrocytes, whereas other astrocytes showed the characteristic star-shaped cell phenotype. No difference in the phenotype was observed between normal astrocytes and astrocytes from MS lesions.

SMS-12, B327/01, Ep15, MS21 and MS16 preparations were tested for contamination with mycoplasma using a PCR mycoplasma test kit. Mycoplasma is an intracellular bacteria that perturbs the normal metabolism of cells and interferes with biological processes (Rottem et al 1993). This PCR based kit for detection of mycoplasma amplified a conserved and mycoplasma-specific 16 S ribosomal RNA gene region (positive control). The absence of a band at 270 bp in astrocyte supernatants demonstrated that the astrocyte preparations were not contaminated by mycoplasma (figure 2.4).

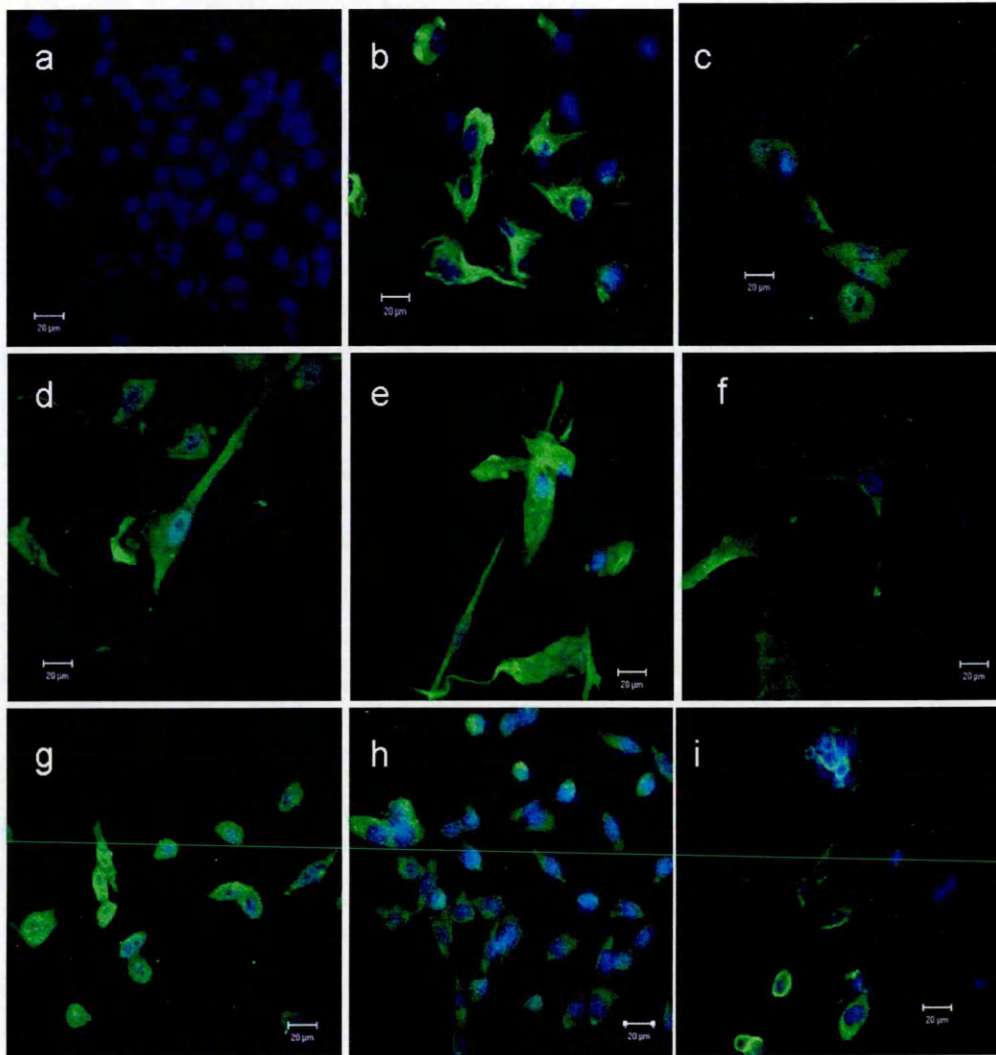


Fig. 2.3: Characterisation of primary human adult astrocytes using immunostaining for the astrocytic marker, GFAP.

Cells were stained with rabbit anti-GFAP antibody and mouse anti-rabbit antibody labelled with alexa fluor 488. Staining was visualized by confocal microscopy. (a) the negative control corresponds to the omission of the primary antibody. (b) Astrocytoma, U373-MG, was used as a positive control. Seven astrocyte preparations were tested for GFAP staining (c)B327/01, (d)Ep15, (e)MS16, (f)MS21, (g)B668/01, (h)B79/01 and (i)B1029). No difference in the phenotype was observed between astrocytes from MS lesion and from NAWM.

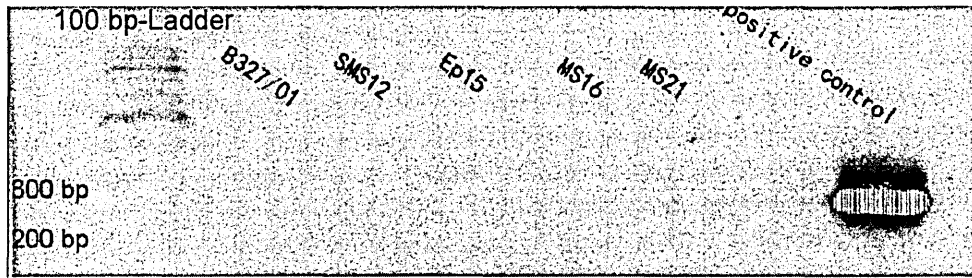


Fig. 2.4: Detection for mycoplasma contamination in astrocyte supernatants using PCR amplification.

Mycoplasma contamination of cells was tested by PCR on the supernatant of cultured astrocytes, using primers specific for conserved-mycoplasma ribosomal RNA subunit. Supernatant of five astrocyte preparations, which had a normal astrocytic phenotype were tested (B327/01, SMS-12, Ep15, MS16 and MS21). The positive control, which corresponds to the mycoplasma-specific 16S rRNA gene region, was used and gave a band at 270bp, following amplification by PCR. 100bp ladder was used to determine the size of the PCR products. Absence of bands at 270bp in astrocyte preparations indicates they were free of mycoplasma.

2.3.2 Real time PCR: optimisation

2.3.2.1 Selection of the housekeeping gene (HK gene)

In this pilot project, five HK genes commonly used with GeNorm software were tested to determine the most stable housekeeping gene [Vandesompele et al., 2002].

- β -actin
- GAPDH
- UBC
- RPL13A
- HPRT

To assess the selection of the best HK gene, astrocytes were stimulated with IL1- β , TNF and IFN γ (100ng/ml), mRNA was extracted and transcribed into cDNA. Samples were run on qRT-PCR and ratios were calculated following the formula: $\text{Ratio} = 2^{(Ct_{\text{sample}} - Ct_{\text{control}})}$ where control corresponds to the unstimulated astrocytes and sample corresponds to the stimulated astrocytes (table 2.2). The ratios for the different set of primers were analysed with geNorm program. Table 2.2 shows the result of the calculation of the M value by GeNorm software. The highest M value was obtained with GAPDH gene, whereas the lowest M value was obtained with the HPRT gene. This means that GAPDH was the least stable HK gene between the five HK genes tested. Because the M value of GAPDH was above the cut off value of 1.5 (not stable enough) and β -actin, RPL13A, UBC and HPRT were lower than 1.5, the primer efficiency of these four HK genes was determined. By stepwise exclusion of the gene with the highest M value, UBC and RPL13A were the most stable genes.

HK gene Treatment	Actin	RLP13A	HPRT	UBC	GAPDH
0	1	1	1	1	1
IFN-100	2.549121	2.549121	4	3.605002	0.7579
TNF-100	3.24901	2.549121	5.098242509	3.363589	48.503
IL-1 β -100	1.681793	2.297397	3.732131966	3.482202	5.6569
M value	0.926	0.886	0.870	0.884	2.447

Tab. 2.2: Ratio and M value determination of the different housekeeping gene analysed using GeNorm software.

Real time PCR was performed in duplicate on cDNA of unstimulated and stimulated astrocytes (SMS-12). Ratios were determined following the formula $2^{(Ct_{sample}-Ct_{control})}$. This ratio was used with GeNorm software to determine the most stable housekeeping gene by calculating the gene expression stability value or M value (Vandesompele et al., 2002). Genes that have an M value below the cut-off value (1.5) are considered stable and can be used as reference gene for the real-time PCR.

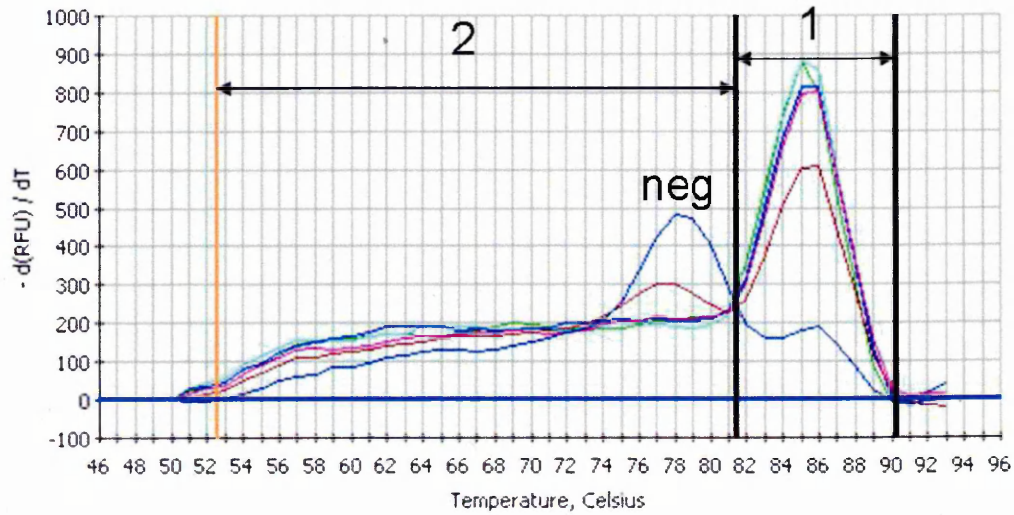


Fig. 2.5: Analysis of the melt-curve to determine the specificity of PCR product.

Melt curve analysis is used to determine whether the amplification is specific. The Y-axis is the change of fluorescence (dF) / change of temperature (dT) which is plotted against X-axis (temperature) The negative control has an increase in fluorescence in region 2 (lower temperature) corresponding to the primer dimer formation and in region 1, which corresponds to the melting temperature of specific products. RPL13A was not selected for further experiments due to the non specific amplification seen in the negative control (dark blue curve). Other HK genes did not show amplification in the region 1 (light blue (UBC), blue (β -actin), brown (HPRT) and green (GAPDH) curves) under the same conditions.

2.3.2.2 Determination of primer efficiency

As previously stated, determination of the primer efficiency is essential for quantitative determination of the fold increase in the product. To assess the primer efficiency of the housekeeping gene, different dilutions of cDNA were prepared: neat, 1/5, 1/50, 1/500 and 1/5000, in duplicate. Figure 2.6 is an example of an amplification curve with the UBC set of primers, with diluted cDNA. Theoretically, a 10 fold dilution should give a shift in the appearance of the fluorescence of 3.3 cycles. The primer efficiency was calculated using the Ct value of the diluted cDNA using the formula:

Efficiency = $(10^{-(1/\text{slope})}) - 1$ where the slope is obtained from the graph Ct value = slope[log of cDNA dilution] + b (figure 2.7).

Efficiencies of the four HK genes are summarized in table 2.3. RPL13A and the UBC primers were the two best candidates for further experiments. But the melt-curve analysis for RPL13A showed an amplification of fluorescence at the specific melting temperature of specific products for the negative control (blue curve, figure 2.5, region 1). The melt curve analysis also showed the formation of primer-dimer for the negative control at the lower temperature (figure 2.5, region 2). Therefore, RPL13A was not selected for the further experiments. UBC was the best candidate for the internal control, with an efficiency of 102% and no specific amplification for the negative control. For the two target genes CCL2 and CXCL10, efficiency was determined with five different dilutions (neat, 1/5, 1/25, 1/50, 1/500 and 1/2500). The efficiencies summarized in table 2.3 were close to 100% ($2e^{-\Delta \Delta Ct}$ method). The dilution used for the qRT-PCR reaction for CCL2 and CXCL10 was 1/25 and neat respectively. Different cDNA dilutions were used for the two chemokines in order to obtain the optimal signal for real-time PCR analysis. The same dilution was used for the HK gene depending on the target gene amplified.

	Actin	RLP13A	UBC	HPRT	CCL2	CXCL10
Slope	-2.78	-3.383	-3.2684	-2.448	-3.51	-3.01
1/Slope	-0.3679	-0.2956	-0.3096	-0.4084	-0.28	-0.32
Efficiency (%)	133	97.5	102	156	93	109

Tab. 2.3: **Primer efficiency of the housekeeping and target genes.**

The primer efficiency was determined following the formula: Efficiency = $(10^{-1/\text{slope}}) - 1$ where the slope is obtained from the graph Ct value = slope[log of cDNA dilution] + b. The best candidate for the internal control was UBC with an efficiency of 102%. Experiments were done in duplicate.

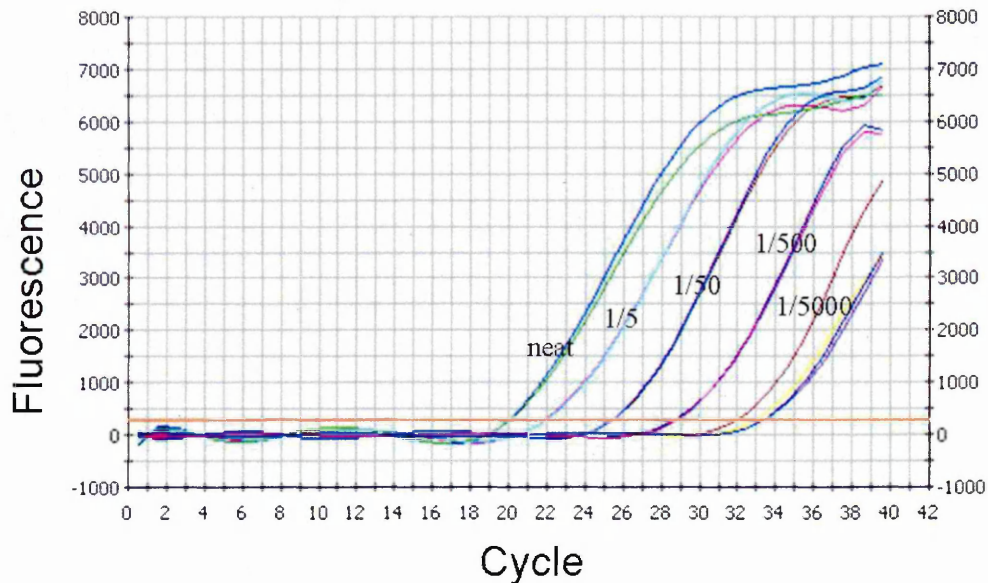


Fig. 2.6: **UBC primer efficiency in qRT-PCR: serial cDNA dilutions.**

The efficiency of the set of primers for the UBC gene was determined using different dilutions of cDNA (neat, 1/5, 1/50, 1/500 and 1/5000). Theoretically, a 10 fold dilution should give a shift in the appearance of the fluorescence of 3.3 cycles. The shift obtained between 1/5 and 1/50 dilution was 3.5.

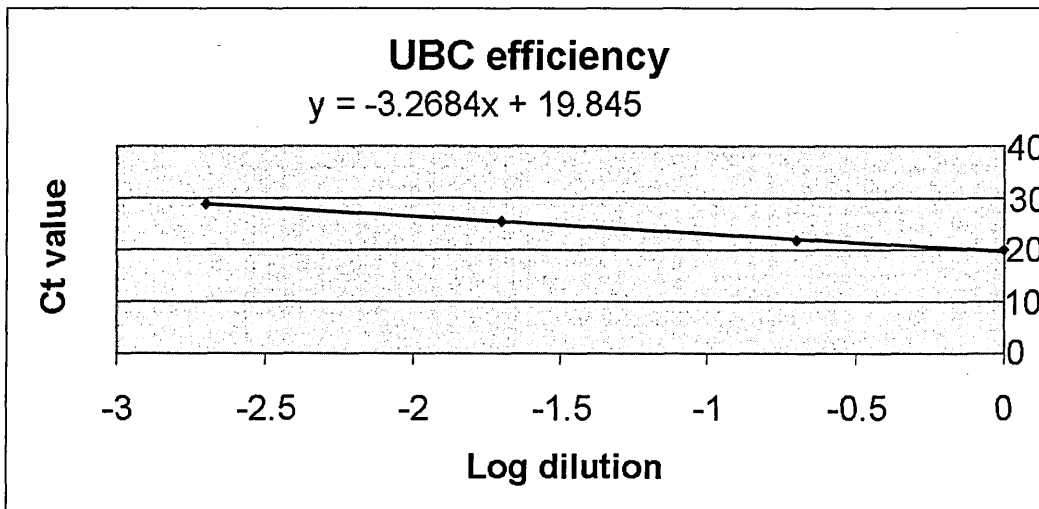


Fig. 2.7: Calculation of UBC primer efficiency using the Ct value from qRT-PCR reaction with serial dilutions.
 This graph demonstrates the Ct value obtained from the diluted cDNA using the specific set of primers, in this case UBC, against the log of dilution of the cDNA. The slope of the curve is used further to determine the primer efficiency of the gene of interest.

2.3.3 Measurement of CCL2 and CXCL10 mRNA expression by stimulated primary human astrocytes using real time PCR

At baseline, in unstimulated cells, CCL2 mRNA was more highly expressed than CXCL10 mRNA (figure 2.8).

2.3.3.1 Determination of CCL2 mRNA expression following cytokine stimulation

CCL2 mRNA expression was upregulated following 24 and 48 h stimulation in primary human adult astrocytes (SMS-12) with all three pro-inflammatory cytokines (IL1- β , TNF and IFN γ) (figure 2.9a-b). IL1- β induced the greatest increase in CCL2 mRNA expression at 1 ng/ml for 24 h (29.6 ± 5.4 fold increase, $P \leq 0.01$) (figure 2.9a). TNF induced a significant increase in CCL2 mRNA expression, which peaked at 48 h following stimulation with 100ng/ml (26.2 ± 7 fold increase, $P \leq 0.01$) (figure 2.9b). IFN γ had a maximal effect at 100ng/ml for 24 h (7.9 ± 0.5 fold increase, $P \leq 0.01$) but to a lesser extent compared to IL1- β and TNF.

These results were confirmed by stimulating primary astrocytes isolated from three different preparations (SMS-12, B327/01 and Ep15) for 24 h with IL1- β , TNF and IFN γ at 10ng/ml (n=6). All three astrocyte preparations had a significant increase in CCL2 mRNA expression following IL1- β and TNF treatment but not with IFN γ using ANOVA followed by Dunnett's test. (figure 2.10).

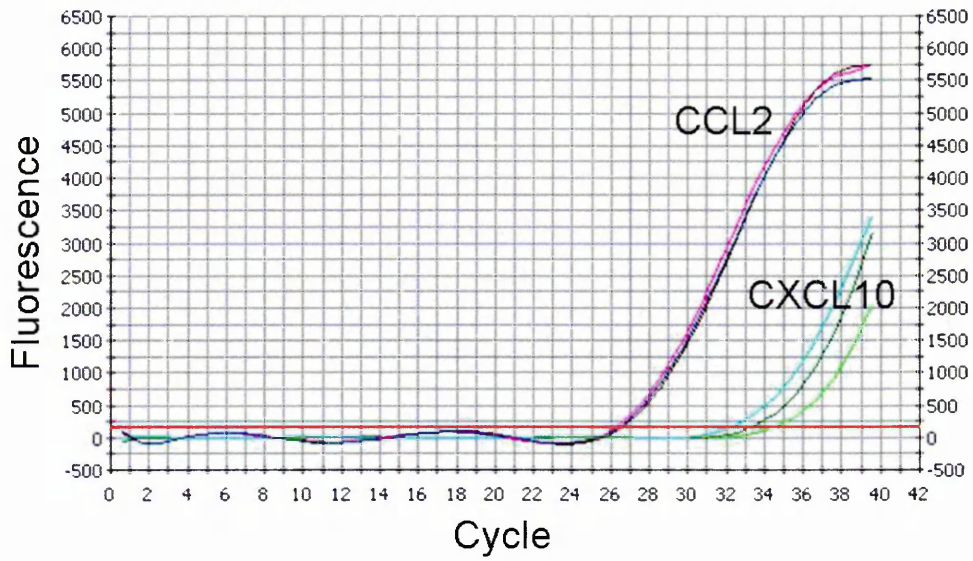


Fig. 2.8: CCL2 and CXCL10 mRNA expression in unstimulated astrocytes.

The Ct value for CCL2 and CXCL10 mRNA expression is 26 and 33 respectively. Since the efficiency for CCL2 and CXCL10 were close to 100%, then CCL2 was more highly expressed than CXCL10 at the baseline.

2.3.3.2 Determination of CXCL10 mRNA following cytokine stimulation

CXCL10 mRNA increased in expression following 24 and 48 h stimulation with the three pro-inflammatory cytokines IL-1 β , TNF and IFN γ . IFN γ induced a dose dependant increase, with a maximum effect observed at 100ng/ml reaching a 479.0 ± 139.6 fold increase ($P \leq 0.05$) and 2903.0 ± 848.5 fold increase ($P \leq 0.05$), following 24 and 48 h stimulation respectively. TNF (10ng/ml) and IL-1- β (100ng/ml) showed an slight increase in expression of CXCL10 with a maximum effect reaching 4.4 ± 2.9 fold increase and 4.1 ± 0.4 fold increase at 24 and 48 h respectively.

Comparison of the mRNA from three astrocyte preparations showed that in two preparations out of three, IFN γ was the most potent inducer of CXCL10 at 201.9 ± 32.1 fold and 613.7 ± 324.4 fold increase for SMS-12 and Ep15 using ANOVA followed by Dunnett's test. However, in the third preparation (B327/01), TNF and IFN γ were the most potent inducer of CXCL10 with 483.4 ± 120.2 fold increase and 284.5 ± 59.8 fold increase. IL1 β did not induced any significant effect on CXCL10 synthesis in all three cell preparations assessed.

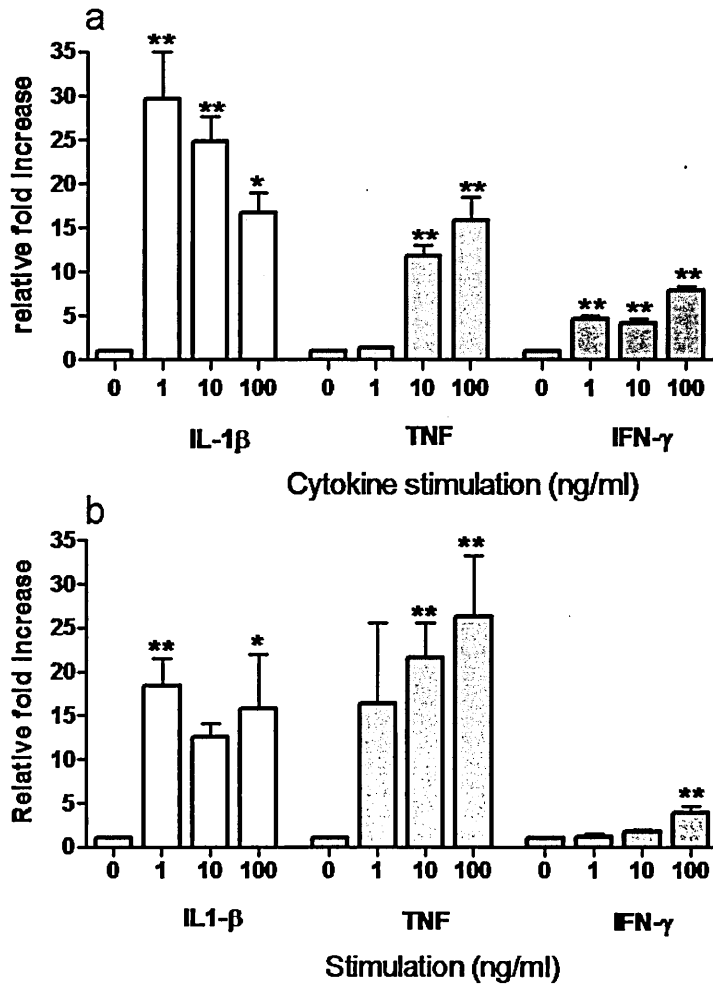


Fig. 2.9: Effect of pro-inflammatory cytokines on CCL2 mRNA expression by primary human adult astrocytes using qRT-PCR.

Cells (SMS-12) were stimulated with IL1- β (white), TNF (grey) and IFN γ (dark grey) at 0 to 100ng/ml for 24h (a) and 48h (b) (n=3) performed in duplicate. UBC was used as internal control. ANOVA followed by Dunnett's test was applied. *p \leq 0.05, **p \leq 0.01

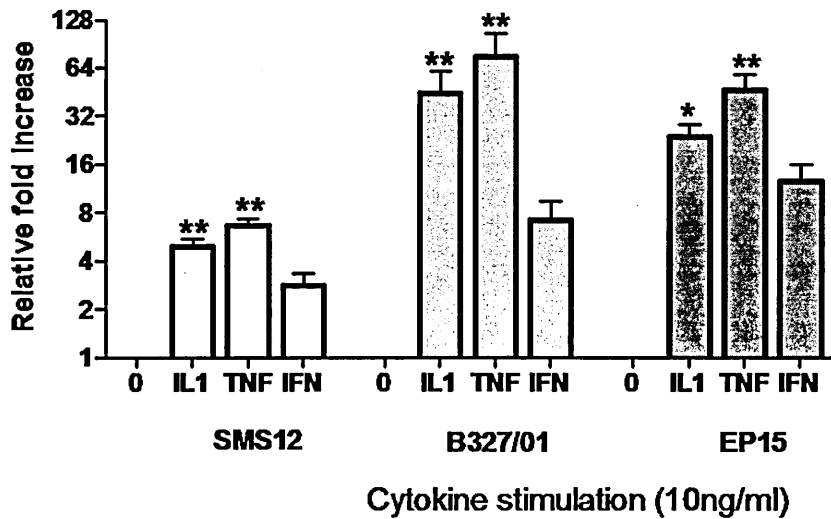


Fig. 2.10: Effect of pro-inflammatory cytokines on CCL2 mRNA expression by three different astrocytes preparations using qRT-PCR. CCL2 mRNA expression by astrocytes from three different donors (SMS-12, B327/01 and Ep15) were measured by qRT-PCR using SybrGreen (n=3) performed in duplicate. ANOVA followed by Dunnett's was used to assess the significance. * $p \leq 0.05$, ** $p \leq 0.01$

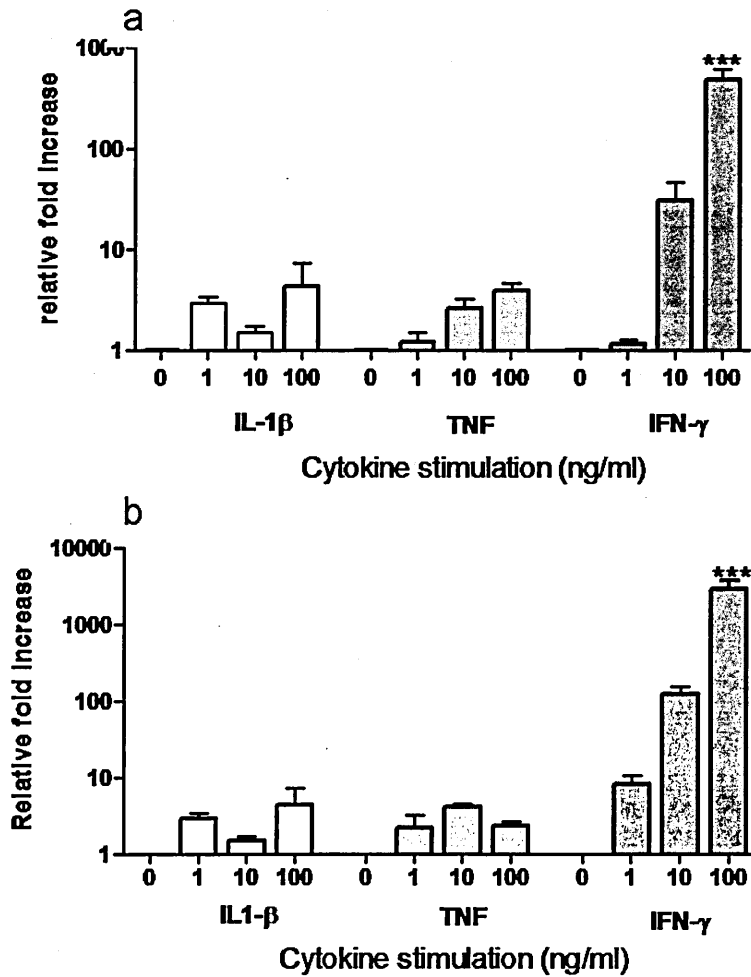


Fig. 2.11: Effect of pro-inflammatory cytokines on CXCL10 mRNA expression by primary human adult astrocytes using qRT-PCR. CXCL10 mRNA expression by primary human adult astrocytes was assessed following pro-inflammatory stimulation, using real time PCR with SybrGreen. Cells (SMS-12) were stimulated with IL1- β (white), TNF (grey) and IFN γ (dark grey) at 0 to 100ng/ml for 24h (a) and 48h (b) (n=3) performed in duplicate. UBC was used as internal control. ANOVA followed by Dunnett's test was assessed and *, ** and *** indicates $p \leq 0.05$, $p \leq 0.01$, $p \leq 0.001$.

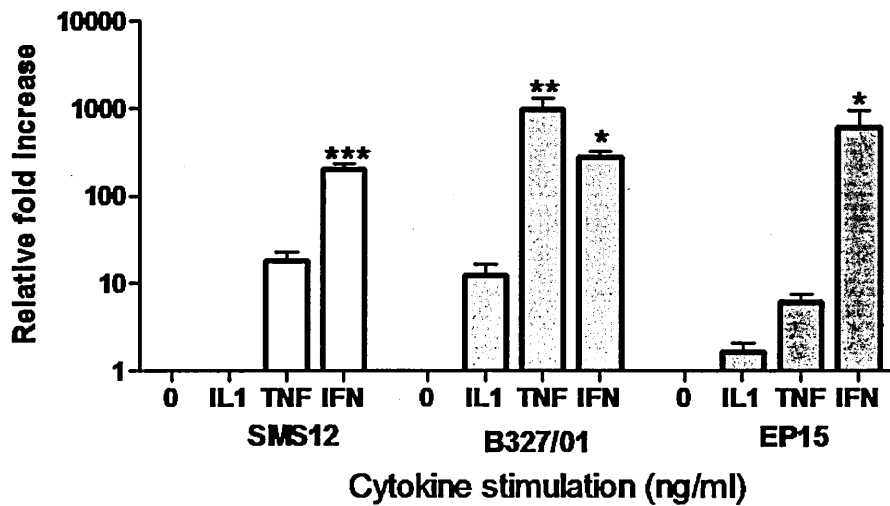


Fig. 2.12: Effect of pro-inflammatory cytokines on CXCL10 mRNA expression by three different astrocyte preparations using qRT-PCR. CXCL10 mRNA expression by astrocytes prepared from three different donors (SMS-12, B327/01 and Ep15) was assessed following 24 h cytokine stimulation by real time PCR using SybrGreen (n=3) performed in duplicate. ANOVA followed by Dunnett's was assessed. * $p \leq 0.05$, ** $p \leq 0.01$, *** $p \leq 0.001$

2.3.4 ELISA measurement of CCL2 secretion by astrocytes following stimulation with pro-inflammatory cytokines

Secretion of CCL2 was assessed under IL1- β , TNF, IFN γ and serum free media using ELISA.

2.3.4.1 Unstimulated cells

Unstimulated cells were found to produce and secrete CCL2 constitutively at 24 h (352.9 ± 8.56 pg/ml) and 48 h (1820 ± 201.8 pg/ml). As expected, the expression of CCL2 at baseline increased following 48 hours stimulation due to accumulation of secreted CCL2 in the supernatant. To determine the relative secretion of CCL2 following cytokine stimulation compared to the unstimulated control, the baseline level of CCL2 was normalized to 1.

2.3.4.2 IL- β stimulation

Following 24 h stimulation, the most potent effect on CCL2 secretion was observed with IL1- β at 1, 10 and 100ng/ml (4.2 ± 0.5 fold increase, 4.0 ± 0.4 fold increase, 3.2 ± 0.2 fold increase respectively, $p \leq 0.01$)(figure 2.13a).

Following 48 h stimulation, the most potent effect was observed at 1ng/ml (5.6 ± 0.1 , $p \leq 0.01$) compared to 10 and 100 ng/ml with respectively 5.2 ± 0.1 fold increase and 4.3 ± 0.4 fold increase, $p \leq 0.01$)(figure 2.13b). However, no significant difference was observed between the three cytokine concentrations at 24 and 48 h using ANOVA followed by Bonferroni test.

2.3.4.3 TNF stimulation

Following 24 h stimulation, TNF significantly increased CCL2 secretion, with the maximum effect observed at 1ng/ml (4 ± 0.9 , $p \leq 0.01$) compared to 10 ng/ml

(3.8 ± 0.9 , $p \leq 0.01$) and 100ng/ml (3.1 ± 0.4 , $p \leq 0.05$) (figure 2.13a).

Following 48 h stimulation (figure 2.13b), the level of CCL2 did not show significant difference compared to non stimulated astrocytes with 4.2 ± 0.9 fold increase (1ng/ml, $p \leq 0.01$), 5.2 ± 0.4 (10ng/ml, $p \leq 0.01$) and 4.0 ± 0.5 (100ng/ml, $p \leq 0.01$). No significant difference in CCL2 secretion was observed between the three concentrations of TNF (Dunnett test).

2.3.4.4 IFN γ stimulation

IFN γ had a modest effect on CCL2 secretion at 24 h compared to that induced by IL-1 β but a similar effect compared to TNF stimulation (figure 2.13a). The maximum effect on CCL2 secretion was observed at 10 and 100 ng/ml (3.7 fold increase ± 0.8 , 3.5 fold increase ± 0.1 , $p \leq 0.01$) compared to 1ng/ml (2.6 ± 0.1 , $p \geq 0.05$). Following 48 h stimulation the only significant increase in CCL2 secretion was observed at 100ng/ml (3.3 ± 0.1 , $p \leq 0.01$) (figure 2.13b).

2.3.5 ELISA measurement of CXCL10 secretion by astrocytes following stimulation with pro-inflammatory cytokines

Unstimulated astrocytes (SMS-12) secreted CXCL10 constitutively at 24 h (82.22 ± 4.235 pg/ml) and 48 h (993 ± 22.86 pg/ml) (data not shown). Similarly to the changes observed at the mRNA level, CXCL10 secretion was increased only by IFN γ stimulation in a dose dependent manner (figure 2.14a). However only IFN γ at 10 and 100ng/ml reached statistical significance with respectively 1.8 \pm 0.1 fold increase, $n=6$, $p \leq 0.001$) and 2.4 fold increase ± 0.2 ($p \leq 0.001$). IL1 β and TNF did not have any effect on the secretion of CXCL10 compared to the baseline from 0 upto 100ng/ml cytokine treatment.

The same pattern of expression for the secretion of CXCL10 was observed following 48 h cytokine treatment (figure 2.14b). Only IFN γ at 100ng/ml induced a

significant increase in CXCL10 secretion (1.9 fold increase ± 0.4 , $p \leq 0.01$).

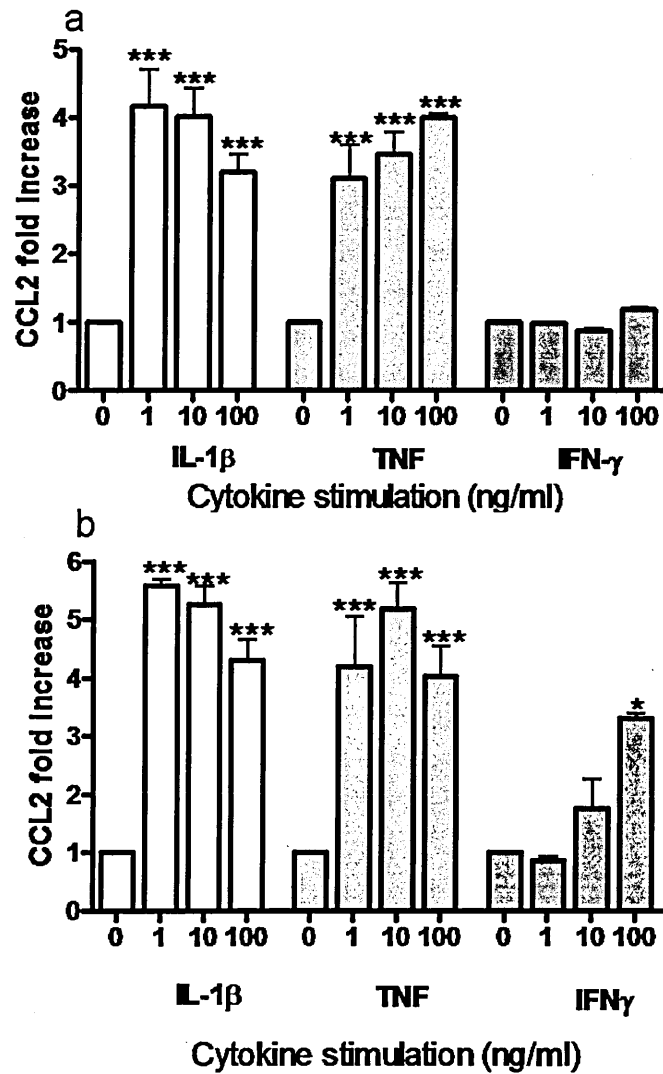


Fig. 2.13: Effect of pro-inflammatory cytokine stimulation on CCL2 secretion by astrocytes measured by ELISA.

CCL2 expression was assessed on astrocytes (SMS-12) following pro-inflammatory stimulation. SMS-12 were stimulated with IL1- β (white), TNF (grey) and IFN γ (dark grey) at 0 to 100ng/ml for 24h (a) and 48h (b) (n=3) performed in duplicate. CCL2 secretion was measured by ELISA. CCL2 expression in the supernatant of stimulated astrocytes was expressed as a fold increase compared to the baseline (unstimulated cells). ANOVA followed by Dunnett's test was assessed. *** $p \leq 0.001$

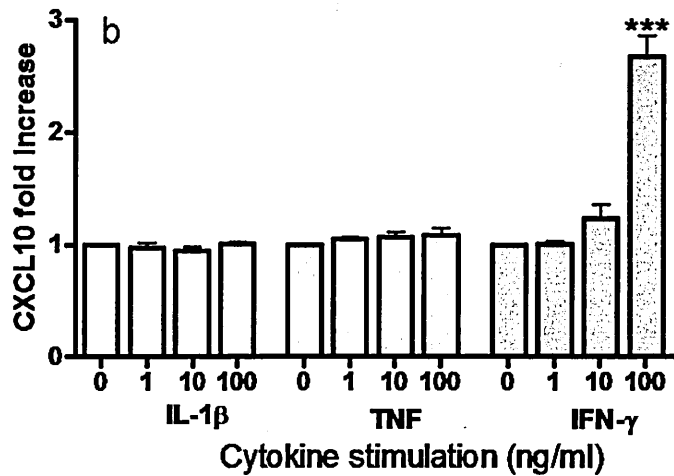
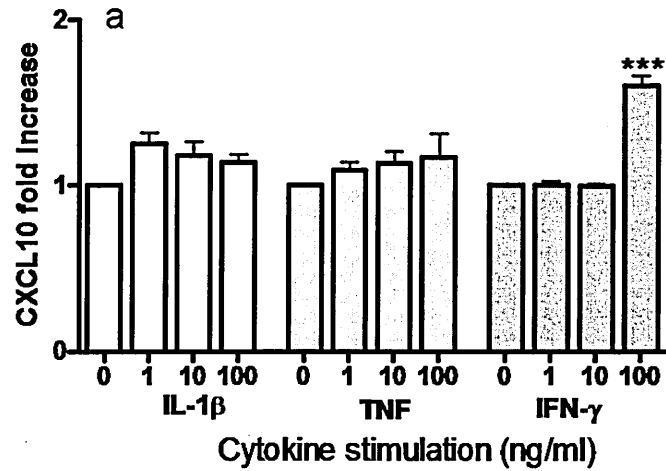


Fig. 2.14: Effect of pro-inflammatory cytokine stimulation on CXCL10 secretion by astrocytes measured by ELISA.

CXCL10 expression was assessed on astrocytes (SMS-12) following pro-inflammatory stimulation. SMS-12 were stimulated with IL1- β (white), TNF (grey) and IFN γ (dark grey) at 0 to 100ng/ml for 24h (a) and 48h (b) (n=3) performed in duplicate. CXCL10 expression in the supernatant of stimulated astrocytes was expressed as a fold increase compared to the baseline (unstimulated cells). ANOVA followed by Dunnett's test was assessed. ***p \leq 0.001

2.4 Discussion

Chemokines are low relative molecular mass proteins from 8 to 10 KDa and have a variety of functions including: cell migration, differentiation of T-cells [Luther and Cyster, 2001], leukocyte activation, angiogenesis and antimicrobial function [Adams and Lloyd, 1997]. The evidence implicating a role for chemokines in MS pathology are mainly shown by descriptive and observational analysis of post-mortem tissue and studies on CSF and serum from MS patients [Kieseier et al., 2002, Scarpini et al., 2002].

Histological examination of autopsy MS brain tissue has demonstrated CXCL9, CXCL10, CCL2, CCL3, CCL5, CCL7 and CCL8 immunoreactivity localised to reactive astrocytes in demyelinating lesions and in the surrounding parenchyma [Banisor et al., 2005, Sospedra and Martin, 2005]. There are many reports of CCL2 and CXCL10 expression in CNS white matter in MS pathogenesis. It has been shown that CCL2 and CXCL10 are strongly expressed at the lesion site by astrocytes compared to control [McManus et al., 1998, Simpson et al., 2000a]. However, it has been reported that CCL2 expression is decreased in the CSF of MS patients at times of relapse, whereas CXCL10 expression is increased [Narikawa et al., 2004, Scarpini et al., 2002]. Contradictory findings are reported for the serum level of CCL2. Scarpini et al. (2002) showed a decrease in CCL2 in MS compared to control [Scarpini et al., 2002] whereas Kivisakk et al. (1998) showed no difference between the expression of CCL2 in serum of MS and normal individuals.

Because astrocytes, the most abundant cell type in the CNS, are located at the BBB and have been reported to express chemokines in the CNS using immunohistochemistry on post-mortem tissue, the rate of synthesis and secretion of CCL2 and CXCL10 by primary human adult astrocytes, following pro-inflammatory stimulation was examined to assess whether there are differences in the rate of synthesis and/or secretion of CCL2 and CXCL10, which could explain this differ-

ence in chemokine levels, reported within the CSF. It has to be mentioned that other cells can produce CCL2 such as microglia, endothelial cells and neurons [Coughlan et al., 2000, Hua and Lee, 2000, Harkness et al., 2003]. Therefore, other CNS resident cells might also be involved in the regulation of CCL2 in the CNS.

2.4.1 Constitutive expression of CCL2 and CXCL10 mRNA by primary human adult astrocytes using qRT-PCR

In this study, astrocytes (SMS-12) expressed CCL2 and CXCL10 mRNA constitutively. However, CCL2 mRNA was much more highly expressed at baseline and under pro-inflammatory conditions than CXCL10. The difference in gene expression cannot be explained by lower primer efficiencies for CXCL10 compared to CCL2, since the primer efficiencies, which were determined during real time PCR optimisation, were both close to 100%. Previous studies on primary human foetal astrocytes and primary human adult astrocytes showed that CCL2 mRNA was highly expressed whereas CXCL10 mRNA was not detected by ribonuclease protection assay [Hua and Lee, 2000, Oh et al., 1999]. The absence of expression of CXCL10 mRNA by astrocytes reported by Hua et al. (2000) and Oh et al. (1999) studies could be explained by the fact that they used a ribonuclease protection assay which is less sensitive than real time PCR.

2.4.2 CCL2 mRNA expression by astrocytes following pro-inflammatory cytokine treatment using qRT-PCR

Following 24 and 48 h stimulation with the three pro-inflammatory cytokines tested, CCL2 mRNA was upregulated. All of the three cytokines induced an increase in expression of CCL2 mRNA, however IL1 β and TNF were the most potent inducers of CCL2 mRNA. These results are in agreement with previous studies on human foetal and simian astrocytes [Croitoru-Lamoury et al., 2003, Oh et al., 1999]. Croitoru Lamoury et al. (2003) showed that IL1- β and TNF

induced a 3 to 3.5 fold increase in CCL2 mRNA compared to IFN γ , which did not affect the expression of CCL2 mRNA following 72 h stimulation. Oh et al. (1999) showed that IL1- β and TNF induced an 8 fold increase compared to IFN γ , which induced a 5 fold increase in CCL2 mRNA. Although IL1 β and TNF were the most potent inducers for CCL2 mRNA expression in astrocytes in the work reported here, differences in CCL2 mRNA expression were found, compared to published literature, which could be explained by the different methodologies used. Indeed, Croitoru-Lamoury et al. (2003) and Oh et al. (1999) stimulated astrocytes for 72 h and 10 h respectively and assessed mRNA by semi quantitative RT-PCR and ribonuclease protection assay whereas, in the current study, astrocytes were stimulated for 24 and 48 h and CCL2 mRNA expression was assessed by real time PCR.

The response obtained with the astrocyte preparation, SMS-12, was reproduced in two other preparations of primary adult human astrocytes from normal appearing white matter. CCL2 mRNA expression did not show any significant difference between the three astrocyte preparations following corresponding cytokine stimulations, using ANOVA followed by Dunnett's test. This comparison of three astrocyte preparations confirms the potent effect of IL1 β and TNF but not IFN γ on CCL2 mRNA synthesis and that it was not specific to one astrocyte preparation. Analysis of the expression of CCL2 mRNA by astrocytes from MS lesion (MS16) did not show any difference with normal astrocytes (data not shown).

2.4.3 CXCL10 mRNA expression by astrocytes following pro-inflammatory cytokine treatment using qRT-PCR

For CXCL10, although the three cytokines induced an increase in mRNA synthesis, IFN γ was the most potent inducer of CXCL10 synthesis, in a dose dependent manner. These results are in agreement with a previous study [Hua and Lee, 2000] using foetal human astrocytes stimulated for 5 h with IL1 β , TNF and IFN γ at 10ng/ml. Both IL1 β and TNF induced CXCL10 mRNA expression but to a lower extent compared to IFN γ .

Two out of three astrocyte preparations showed the same pattern of expression (SMS-12 and Ep15), whereas B327/01 astrocyte preparation showed that both IFN γ and TNF induced a strong increase on CXCL10 mRNA synthesis. Since the same cDNA was used for the mRNA comparison between astrocyte preparations for both CCL2 and CXCL10, then the difference might be dependent on the astrocyte preparations. Despite this difference for B327/01, IFN γ was the most potent inducer for CXCL10 mRNA.

2.4.4 CCL2 and CXCL10 secretion by unstimulated astrocytes using ELISA

Similar to mRNA expression, CCL2 protein was more highly expressed at baseline than CXCL10 with almost 4 and 2 times more CCL2 than CXCL10 following 24 and 48 h respectively. The differential expression between CCL2 and CXCL10 decreased following 48 h incubation possibly due to an increase in constitutive expression of CXCL10. Therefore, the ability of astrocyte to express CXCL10 at the baseline increases with time. Croitoru-Lamoury et al. (2003) showed that CXCL10 was not constitutively expressed by astrocytes whereas CCL2 was (20ng/ml, following 24 h incubation in serum free media). Although the qualitative response of astrocytes to stimulation by cytokines is similar for CCL2 and CXCL10, their level of expression is not the same. In our study, the constitutive expression of CCL2 and CXCL10 (following 24 h incubation) was 352.9 ± 8.56 pg/ml and 82.22 ± 4.235 pg/ml respectively. It was not possible to compare the level of expression of CCL2 in foetal and human astrocytes in this thesis, however from the current study adult astrocytes expressed almost 60 times less CCL2 than human foetal astrocytes, based on published levels reported for foetal astrocytes [Croitoru-Lamoury et al., 2003]. Although the same ELISA kit was used, different experimental conditions could explained this differences. Developmental stage of astrocytes might also be one explanation for the difference in CCL2 levels. Since chemokines are involved in embryogenesis by regulating the migration of progenitor cells into the post natal brain [Tran et al., 2007, Lazarini et al., 2003], it is

then not surprising to observed differences in the level of expression of chemokines between foetal and adult astrocytes.

2.4.5 CCL2 secretion by astrocytes following pro-inflammatory cytokine treatment using ELISA

Following 24 h and 48 h stimulation IL1 β and TNF were the most potent inducers of CCL2 (5.2 fold increase, 9464 \pm 180 pg/ml) whereas IFN γ had a limited effect on CCL2 secretion especially following 48 h stimulation. These results are in agreement with a previous study Croitoru-Lamoury et al (2003) where they found that CCL2 was mainly secreted following IL-1 β and TNF stimulation (around 150 and 180 ng/ml respectively, Table 2.4) compared to IFN γ (around 60ng/ml) and unstimulated cells (around 50ng/ml). In this study they found a difference in the amount of released chemokines between simian adult and foetal human astrocytes. Human foetal astrocytes clearly secreted more chemokine than the simian adult astrocytes (between 2 and 5 fold higher). Although no comparison between human adult and other astrocytes have been assessed in our study, the difference in the basal level of expression of the secreted chemokine between human adult (352.9 pg/ml) and foetal astrocytes (around 25ng/ml) might reflect the different developmental stage of the astrocytes as discussed above.

2.4.6 Other CCL2 producing cells in the CNS

Astrocytes are not the only cells in the CNS to produce CCL2 (Table 2.5). Endothelial cells have also been shown to secrete CCL2 following IL1- β , TNF and IFN γ . It was shown that CCL2 secretion, following TNF stimulation at 10 ng/ml, was maximal effect in brain endothelium cells (5.2 \pm 0.22 ng/ml) [Harkness et al., 2003]. This finding was confirmed by another study which analysed the expression of CCL2 on cytokine-activated human microvascular endothelial cells. They reported that TNF was the most potent inducer (14.8 \pm 0.4 ng/ml) compared to IFN- γ (7.3 \pm 0.1 ng/ml) [Brown et al., 1994]. Although no direct comparison in

CCL2 secretion between astrocytes and ECs was assessed, it seems that ECs had a higher capacity to secrete CCL2. Therefore, they are another active player in the recruitment of immune cells into the CNS.

CCL2 expression by macrophages is contradictory. Microglia have been found to express CCL2 mRNA *in vitro* and CCL2 protein *in vivo* [Calvo et al., 1996, Hua and Lee, 2000]. However, CCL2 secretion was not detected in the supernatant of microglia cells following stimulation with pro-inflammatory cytokines [Hayashi et al., 1995]. Neurons have also been shown to express CCL2 *in vivo* [Meng et al., 1999]. However, it was shown that CCL2 secretion was lower compared to levels secreted by human foetal astrocytes [Coughlan et al., 2000].

2.4.7 CXCL10 secretion by astrocytes following pro-inflammatory cytokine treatment using ELISA

Changes observed for CXCL10 secretion mirrored changes observed for CXCL10 mRNA. Indeed, CXCL10 was mainly increased by IFN γ with the maximum effect at 100ng/ml at both 24 and 48 h (276.3 pg/ml and 1972 pg/ml) respectively. These findings are in agreement with Croitoru-Lamoury et al. (2003) where they showed that CXCL10 was mainly increased with IFN γ at 50ng/ml following 24 and 72 h stimulation on primary human fetal astrocytes (almost 50 and 100 ng/ml respectively, Table 2.4)). However, the changes observed for the mRNA are much more important compared to the changes observed for the protein. This might be explained by regulatory mechanisms that control the mRNA level expression before being translated into protein such as nonsense-mediated mRNA decay or RNA surveillance mechanism [Shyu et al., 2008].

2.4.8 Other CXCL10 producing cells in the CNS

CXCL10 production is not solely due to astrocytes (Table 2.5). It was shown that microglia are also involved in the synthesis of CXCL10 [Hua and Lee, 2000]. *In vitro* stimulation of microglia cells resulted in the increase in secretion of CXCL10 (around 2500 pg/ml) compared to the control (1000 pg/ml). This increase in CXCL10 secretion was abrogated by co-incubating microglia with TNF and antibody directed against TNF [Seguin et al., 2003]. Endothelial cells have also been shown to secrete CXCL10 under IFN γ stimulation to reach 102 ± 18 ng/ml [Marx et al., 2000]. Another study demonstrated the ability for aortic ECs to secrete CXCL10 [Raju et al., 2003]. CXCL10 was increased from 13.4 ± 10.8 pg/ml to 299.5 ± 13.4 pg/ml following incubation of ECs with PBMCs, which was inhibited by an antibody directed against IFN γ (33.8 ± 17.8 pg/ml). Although the other CNS resident cells produce CXCL10, levels of CXCL10 expression is difficult to compare with the current study because of the different experimental conditions.

2.4.9 Do astrocytes contribute to the differential expression of CCL2 and CXCL10 in the CSF of MS patients at time of relapse?

In the brain, CSF, produced by the plexus choroid, has many functions such as in mechanical support, but also acting as a drainage pathway for the brain, where products from metabolism or inflammatory mediators are diluted and eliminated. Thus the CSF composition reflects the state of the CNS at a specific time when sample is taken [Segal, 1993, Brown et al., 2004].

The reason why CCL2 is decreased in the CSF at the time of relapse in MS patients is unclear. One explanation for the differential expression of CCL2 and CXCL10 in the CSF at the time of relapse might be the reflection of the cytokine milieu in the brain at the time of relapse. Indeed higher concentration of IFN- γ compared to IL1 β or TNF would result in stronger CXCL10 expression compared

to CCL2 although no published evidences are available in human. It was shown in EAE study that there was a differential expression of TNF and IFN- γ in EAE mice [Tanuma et al., 1999]. TNF was shown to be associated with the first attack in chronic relapsing EAE whereas IFN- γ was closely related to the latter attacks. This could explain the differential expression of chemokines during the pathogenesis of the disease. The question addressed in this chapter was the possible contribution to this finding by a differential expression of CCL2 and CXCL10 by primary human adult astrocytes in the CNS under control and inflammatory conditions. Our study showed that the synthesis of these two chemokines were increased under pro-inflammatory conditions but also that CCL2 was more highly expressed than CXCL10 both at the mRNA and protein level. Thus, the decrease in levels of CCL2 in the CSF, during relapse in MS patients cannot be explained by a differential expression of CCL2 and CXCL10, either by an impairment in the synthesis or secretion of CCL2 by astrocytes, during relapse in MS patients.

With the caveat that *in vivo* astrocytes may behave differently, several hypotheses could explain the decrease in the CSF of CCL2, based on the *in vitro* findings reported here:

- sequestration of CCL2 by CNS resident cells. CCL2 has been shown to bind to various CNS resident cells including endothelial cells and astrocytes [Andjelkovic et al., 1999a, Stamatovic et al., 2003]
- consumption of CCL2 in the CNS by invading immune cells. A recent study *in vitro* showed that CCL2 was removed from the extracellular fluid by CCR2-positive migrating cells as they cross the BBB, which was proposed to explain the decrease in CCL2 level in the CSF in MS patients [Mahad et al., 2006].

Cell type	CCL2	CXCL10	Reference
Human adult astrocytes	IL1 β , TNF	IFN γ TNF, IFN γ	Current study (qRT-PCR) Oh et al. (1999) (RPA)
Fetal human astrocytes	IL1 β , TNF	IFN γ	Hua et al. (2000) (RPA) Croitoru-Lamoury et al. (2003)(RT-PCR)

Tab. 2.4: Summary table for cytokine effects on CCL2 and CXCL10 mRNA expression by astrocytes.

In this table, the main inducers for CCL2 and CXCL10 are given. IL1 β was the most potent inducer for CCL2 whereas IFN γ was main inducer for CXCL10. Different methodologies were used in the different study. Real time PCR (qRT-PCR), semi quantitative reverse transcription PCR (RT PCR) and ribonuclease protection assay (RPA) were used respectively in the current study, Croitoru-Lamoury et al. (2003); Oh et al. (1999) and Hua et al. (2000).

Cell type	CCL2 (ng/ml)	CXCL10 (ng/ml)	Reference
Human adult astrocytes	9.5 (IL1 β , TNF)	1.9 (IFN γ)	Current study
Human foetal astrocytes	150 (IL1 β) 180 (TNF)	50-100 (IFN γ)	Croituru-Lamoury et al. (2003)
Brain endothelial cells	5.2-14.8 (TNF)	0.3-102 (IFN γ)	Brown et al. (1994) Harkness et al. (2003) Marx et al. (2000)
microglia	ND	2.5 (TNF)	Seguin et al. (2003)

Tab. 2.5: Summary table for the comparison of expression of CCL2 and CXCL10 by CNS resident cells under cytokine stimulations.

Data from the current and published studies showed that CCL2 is mainly induced by IL1 β and TNF whereas CXCL10 was mainly induced by TNF and IFN γ . Data shown in the table correspond to the maximal secretion of CCL2 and CXCL10 following cytokine stimulation. Although the comparison of chemokine secretion was not performed in the current study, human adult astrocytes seems to produce less chemokine than human foetal astrocytes.

CHAPTER 3

Measurement of CCL2 binding to primary human adult astrocytes *in vitro*

3.1 Introduction

CCL2 exerts its biological effect through binding to CCR2, a G protein coupled receptor (GPCR). CCR2 has two isoforms: CCR2-A and CCR2-B, which differ in the C terminal cytoplasmic domain of the receptor [Sozzani et al., 1997].

3.1.1 CCL2 effects on astrocytes

Astrocytes have been shown to sense and respond to gradients of CCL2 in an *in vitro* chemotactic assay [Andjelkovic et al., 2002]. It was proposed that this chemotactic effect could either promote the recruitment of astrocytes at lesion sites within the brain or affect the position of astrocytes at the BBB [Dorf et al., 2000]. It was also shown *in vitro* that astrocyte treatment with CCL2 leads to secretion of bFGF, which would facilitate neuronal cell differentiation and promote

survival of neurons *in vitro* [Kalehua et al., 2004]. Thus astrocyte gene expression is altered in response to CCL2, indicating that they express receptors for CCL2.

3.1.2 CCR2 expression by astrocytes in the CNS in MS

A recent immunohistochemical study on CNS tissue from secondary progressive MS patients (SPMS) has reported that CCR2 expression was strong at the rim of the lesion with ongoing demyelination but not in the centre. Double staining with anti-GFAP and CCL2 or CCR2 antibodies demonstrated that reactive astrocytes stain strongly for both CCL2 and express CCR2 [Tanuma et al., 2006]. However the expression of CCR2 by astrocytes is controversial. Simpson et al (2000) have shown that CCR2 reactivity was associated with foamy macrophages and activated microglia in chronic active lesions. Another study reports a low immunoreactivity for CCR2 in the CNS, mainly associated with T cells and rare activated monocytes [Mahad et al., 2006].

3.1.3 CCR2 expression by astrocytes *in vitro*

Expression of CCR2 on astrocytes has been assessed *in vitro*. However contradicting data was obtained. Expression of CCR2 was reported in foetal human astrocytes using immunocytochemistry [Andjelkovic et al., 2002, Rezaie et al., 2002]. These findings are in contradiction with Heesen et al. (1996) and Flynn et al. (2003) studies, which failed to detect CCR2 using post-natal murine mouse and human adult astrocytes by RT-PCR and flow cytometry respectively. Further work has to be performed to confirm the expression of CCR2 by astrocytes *in vitro*.

3.1.4 CCR2 signalling and functional effect of CCL2

Chemokines have been shown to interact with their cognate receptor to induce various functional effects including chemotaxis, cell adhesion molecule expression,

such as integrins, through activation of downstream signalling pathways [Wain et al., 2002, Ashida et al., 2001, Datta et al., 2006]. CCR2 has been shown to increase integrin expression in monocytes as well as increase their migration following MAPK activation following CCL2 stimulation [Ashida et al., 2001]. It was demonstrated that CCL2 induces Erk and PKB signalling pathways following binding to CCR2 [Ashida et al., 2001].

3.1.4.1 Calcium flux following CCL2 treatment

As discussed in section 1.4.7.1, binding of chemokines to their receptors induces activation of PLC resulting in an increase in intracellular calcium. There is much evidence on the effect of CCL2 on levels of intracellular calcium. It was shown in a study by Salentin et al. (2003) that CCL2 treatment of monocytes transfected with CCR2, induced a strong increase in intracellular calcium. Astrocytes have also been shown to increase intracellular calcium following CCL2 treatment, although the expression of CCR2 in astrocytes is controversial [Andjelkovic et al., 2002].

The level of expression of GPCRs at the cell surface is an important factor in induction of increased in the intracellular calcium. Indeed, It was shown in a dendritic cell line (D1 cells) treated for 2-3 h with LPS (10 μ g/ml) that the decrease in CCR1 expression mirrored the changes observed for the level of intracellular calcium when stimulated with CCL3 [Foti et al., 1999]. Therefore calcium flux is an accurate indicator to monitor the downstream effect of chemokines on cells when bound to their receptors.

3.1.4.2 Erk signalling

Erk is a well characterised signalling kinase, and is activated by phosphorylation on threonine and tyrosine residues by MAPK/Erk kinase 1/2 (MEK1/2) as discussed in section 1.4.7.2 [Chang and Karin, 2001].

CCL2, 7, 8 and 13 have been shown to rapidly and transiently activate the

MAPK in peripheral blood mononuclear cells and in HEK-293 cells expressing CCR2. U0126, an inhibitor of MAPK-kinase activation, not only prevented Erk 1/2 activation but also significantly inhibited CC chemokine-mediated chemotaxis [Wain et al., 2002]. In another study, it was shown that family members of the MAPKs have different effects on the monocytic cell line (THP-1 cells) when activated by CCL2 [Ashida et al., 2001]. They showed that CCL2 induced an increase in integrin expression by THP1 cells, which was inhibited by a MEK inhibitor but not by the p38-MAPKs inhibitors. CCL2 also induced chemotaxis of THP1 cells but it was mediated by p38 MAPK, not Erk.

3.1.4.3 PKB/Akt signalling

The PKB/Akt subfamily consists of three members, PKB α /Akt1, PKB β /Akt2 and PKB γ /Akt3 which are activated by phosphorylation of two residues; Thr³⁰⁸ and Ser⁴⁷³ [Alessi et al., 1996, Walker et al., 1998] as discussed in section 1.4.7.2.

Much evidence has confirmed the involvement of PKB/Akt signalling in the process of chemotaxis. Wain et al. (2001) showed that inhibition of the PI3 Kinase by Wortmannin (0.1 μ M) and LY294002 (100 μ M) partly inhibited THP-1 cell chemotaxis. Similarly, Datta et al. (2006) have shown that incubation of CD4⁺ T cells with cyclosporin A, a common immunosuppressant, selectively inhibits PKB/Akt but not the Erk 1 and 2 pathway, resulting in a decrease in transendothelial migration *in vitro*, following CXCL12 stimulation.

PKB/Akt have also been shown to be involved in CCL2 synthesis by vascular endothelial cells. When cells were incubated with Wortmannin, an inhibition of TNF-dependent CCL2 secretion was seen in a dose dependent manner. Human umbilical vein endothelial cells (HUVECs) transfected with a dominant negative PKB/Akt resulted in the suppression of activation of the promoter of CCL2 under TNF stimulation [Murao et al., 2000].

3.1.5 Aim of the study

In chapter 2, it was found that primary human adult astrocytes express CCL2 at much higher levels than CXCL10. Thus decreased CCL2 expression by astrocytes does not appear to explain the decreased expression of CCL2 reported in the CSF in people with MS. CCL2 may bind in an autocrine manner to astrocytes leading to sequestration preventing it from reaching the CSF compartment.

This aim will be addressed by the following objectives:

1. Investigate the synthesis and expression of CCR2 under pro-inflammatory conditions using qRT-PCR and flow cytometry.
2. Determine the effect of pro-inflammatory cytokine treatment on binding of CCL2 to astrocytes using biotinylated CCL2 assessed by flow cytometry and immunocytochemistry.
3. Determine the functional effect of CCL2 binding to astrocytes by measuring calcium flux and phosphorylation of Erk1 and 2 and Akt, following CCL2 stimulation.

3.2 Materials and methods

3.2.1 Determination of CCR2 mRNA expression by human adult astrocytes following pro-inflammatory stimulation

3.2.1.1 Sequences of forward and reverse primers for CCR2 gene

The same procedure was followed as described in section 2.2.6. The primer sequences used for the amplification of the CCR2 cDNA were designed using Primer3 software as described in section 2.2.6.1

- forward primer: 5'-TTGGCGGAATCTTCTTCATC-3' (T_m, 55.3°C)
- reverse primer: 5'-CGTGGACAGAAGCAAACACA-3' (T_m, 57.3°C)

3.2.1.2 Sequencing of PCR products to check the specificity of CCR2 primers amplicons

PCR products were cleaned using Sigmaspin post reaction purification columns (Sigma, UK) prior to sequencing, according to the manufacturer's instructions. Briefly columns were spun at 300 g for 2 min in the mini spin plus centrifuge (Eppendorf, UK). 30 μ l of PCR product was loaded on the top of the column and centrifuged for 5 min at 300g. Columns were washed once using washing buffer and centrifuged again for 2 min at 300g. Samples were collected in a new eppendorf tube by applying elution buffer and centrifugation for 2 min at 300g. Samples were sequenced at the Core Genetics Service, Sheffield University.

3.2.1.3 Real time PCR on cDNA from stimulated astrocytes

Real time PCR was performed in duplicate on cDNA from astrocytes (SMS-12) stimulated three times for 24 and 48 h with IL1- β , TNF and IFN γ from 0 to 100ng/ml as previously described in section 2.2.6.5. Comparison of three different human adult primary astrocyte preparations (SMS-12, B327/01 and Ep15) for CCR2 mRNA expression was performed by stimulation with IL-1 β , TNF and IFN γ (10ng/ml) for 24 hours.

3.2.2 Determination of CCR2 expression by primary human adult astrocytes, using flow cytometry

3.2.2.1 Principle of flow cytometry

Flow cytometry is a technique used for counting and examining cell suspensions in a stream of fluid. It allows simultaneous multiparametric analysis of the physical and/or chemical characteristics of a single cell through the excitation of a bound fluorescent marker. The flow cytometer is composed of three main systems: fluidics, optics, and electronics [Givan, 2001]. The fluidics system transports the samples to the laser beam to be analysed and quantifies the intensity of fluorophore upon laser excitation. The optics system consists of lasers to illuminate the cells and optical filters to direct the signal to the appropriate detectors. There are three optical filters (figure 3.1) which are summarized in the table (3.1). The electronics system converts the detected light signals into electronic signals that can be processed by the computer. One cell excited by the laser beam will produce data composed of at least three values: the size of the cells (FSC), the complexity of the cells (SSC) and the intensity of the fluorophore depending on the laser used (FL1-3) (figure 3.1). The light from the laser beam is defracted and reflected at 90° and is collected by a lens and then directed to the detector by the beam splitter. The FSC measures the size of the particles or cells by measuring mostly diffracted light from the laser beam. The light is collected off the axis of

the laser beam in the forward direction by the FSC photodiode (figure 3.1). The combination of the two parameters allows the analysis and differentiation of different cell types. For instance, the analysis of peripheral blood mononuclear cells (PBMC) isolated from whole blood using histopaqueTM (Sigma Aldrich), kindly provided by H. Denney (BMRC, Sheffield Hallam University) with these two parameters (FSC and SSC) allows differentiation of the lymphocyte and monocyte populations (figure 3.2a). When a cell line is subjected to flow cytometry, the analysis of the FSC and SSC parameters should give a single, uniform population in the two dimension dot plot (figure 3.2b).

When examining the expression of a specific protein in cells, antibodies specific for that protein labelled with a fluorophore are used. The different fluorophores compatible with the FACSalibur are summarized in table 3.1. Only fluorescein isothiocyanate (FITC) and phycoerythrin (PE) were used in this study.

The data generated by a flow cytometer is presented in two windows. The first window is a two-dimension dot plot with FSC (X-axis) plotted against the SSC (Y-axis) to determine the physical characteristics of the cells in the cell suspension. The second window is a single dimension histogram with the fluorescence intensity of the samples (X-axis) plotted against the number of events (Y-axis). This window allows the level of expression of the protein of interest to be analysed when compared to the negative control. The negative control is assessed by incubating cells with an isotype control, which belongs to the same class of immunoglobulin as the antibody used to detect the protein of interest. The isotype control is labelled with the same fluorophore used for the antibody of interest (figure 3.3). The negative control is fundamental to determine the background fluorescence in the sample.

Channel	Band Pass Filter	Fluorophore
FL1	530/30	FITC, Alexa-488, GFP
FL2	585/42	PE
FL3	670LP	PerCP, PE-Cy5, PE-Cy5.5, PerCP-Cy5.5, PE-Alexa647, PE-Alexa680, PE-Alexa700, PE-Cy7, PE-Alexa750

Tab. 3.1: Fluorophores compatible with the BD FACscalibur.

FACscalibur is a two laser and four colour instrument that is able to use a wide variety of fluorophores. Fluorophores are detected in different channels (FL1, FL2 and FL3) depending on the fluorophore. Each fluorophore has an excitation wavelength (laser) and an emission wavelength that will go through the band pass filter. GFP: green fluorescent protein, PerCP: Peridinin-chlorophyll-protein Complex, PE-Cy: phycoerythrin cyanine.

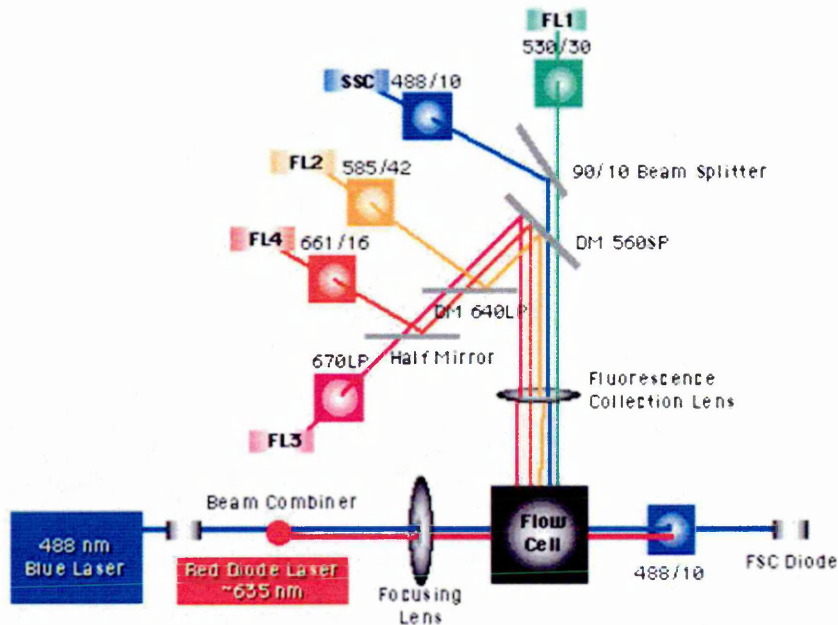


Fig. 3.1: **Optical system in a flow cytometer.**

When the sample is illuminated by the laser, the fluorophore emits fluorescence which is collected by a fluorescent collection lens. Depending on the wavelength of the signal emitted by the fluorophore, the signal will be collected in different channels (FL1: 530/30, FL2:585/42, FL3: 670LP). Information on the size and complexity of the cells is also collected in the FSC and SSC channel. This allows the differentiation of different cell populations within the sample. Image obtained from www.med.umich.edu/flowcytometry/InitialTraining/lessons/lesson4/images/caloptics.gif.

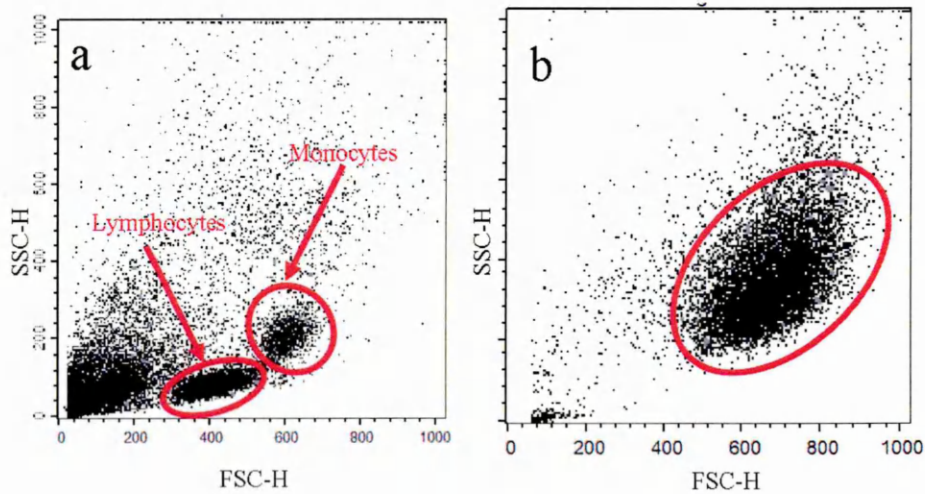


Fig. 3.2: Two dimension dot plots of PBMCs and astrocyte cells in suspension.

The 2 dimension dot plot determines the physical characteristic of a sample by analyzing the complexity of the cell (FSC) and the size of the cells (SSC). In this figure, PBMCs isolated from whole blood using HistopaqueTM (Sigma Aldrich, UK) were kindly provided by H. Denney (BMRC, Sheffield Hallam University) and were analyzed with the FCS and SSC parameters (a). The lymphocyte and monocyte subpopulations can be visualized. The second two dimension dot plot (b) corresponds to astrocyte cells with a single uniform cell population. The population of interest can be gated. This means that during the analysis, only the cells with these characteristics (FSC and SSC) will be analysed.

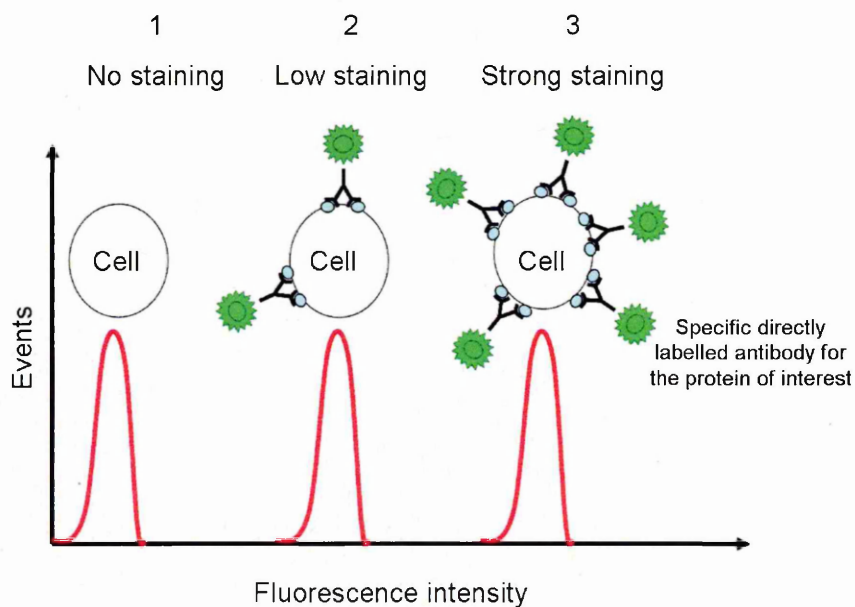


Fig. 3.3: Single dimension histogram determines the level of expression of the protein of interest.

The X-axis represents the intensity of the staining and the Y-axis represents the number of events. Three cases are presented here. Case 1, with the peak on the left of the X-axis, corresponds to the negative control with no antibody attached to protein of interest. Cases 2 and 3 correspond to positive cells with increasing amount of antibody bound, which are coupled to a fluorophore.

3.2.2.2 Detection of cell surface expression of CCR2 on unstimulated astrocytes by flow cytometry

Cells were trypsinised and incubated for 1 h at 37°C in astrocyte media for recovery. 0.25×10^6 cells/25 μ l PBS/tube were stained with antibody directed against CCR2 protein. Cells were incubated for 1.5 h with 10 μ l of PE-labelled IgG2b mouse-anti human CCR2 (R&D Systems, UK) on ice in the dark, to limit the internalisation of the receptor. Cells were stained, in parallel, with the corresponding isotype control, PE-labelled mouse IgG2b antibody, to assess the signal in the negative control. Monocytic cell line, THP-1 cells, known to express CCR2 were used as a positive control for CCR2 staining (Phillips et al. 2005). Cells were washed with 1ml of PBS and centrifuged for 5 min at 300g at 4°C. PBS was removed and cells were incubated for 1 h with 30 μ l of PE-conjugated goat anti mouse IgG whole molecule at a dilution of 1/40 in PBS (Sigma, UK) to amplify the signal. Cells were washed with PBS and run on flow cytometer where 10 000 events were counted. CCR2 expression was quantitated using FACScalibur (BD Biosciences, UK) and CellQuestTM software (BD Biosciences, UK) (n=3).

3.2.2.3 Detection of CCR2 on permeabilised unstimulated astrocytes by flow cytometry

0.5×10^6 cells/25 μ l PBS/tube were used and stained intracellularly. Cells were fixed in 1ml of 4% paraformaldehyde (Appendix) for 15 min at RT. Cells were centrifuged for 5 min at 300g in a mini spin centrifuge (Eppendorf, UK) and PFA was removed. 1ml of PBS-0.5% Triton X100 was added to the cells for 5 min at RT. Cells were centrifuged, supernatant was removed and cells were resuspended in 25 μ l of PBS. CCR2 staining was assessed as described for cell surface staining above.

Different procedures for fixation and permeabilization of astrocytes were assessed to determine the optimal staining conditions. The first condition was fixation with 4% PFA and permeabilisation with 0.5% saponin (Sigma Aldrich, UK)

followed by staining as described above. In the second condition, cells were treated following the protocol for the intracellular cytokine staining starter kit (BD Biosciences, UK). 0.25×10^6 cells were incubated in $100 \mu\text{l}$ of BD Cytofix/CytopermTM buffer, which contains 4% paraformaldehyde and saponin, for 20 min at RT. Cells were washed with 1ml of BD Perm/WashTM buffer and resuspended in $30 \mu\text{l}$ of BD Perm/WashTM buffer. This buffer contains both FBS and saponin. The staining procedure was then carried out as described above. An antigenic protection site step was also included in the staining procedure using glycine (0.1M) for 15 min at RT to assess whether there was any difference in the staining for CCR2.

3.2.2.4 Measurement of CCR2 expression at the astrocyte cell surface following pro-inflammatory stimulation.

0.25×10^6 cells/2ml/well were plated in 6 well-plates and allowed to adhere for 24 h in astrocyte cell culture media (described in section 2.2.5). Cells were stimulated with IL- 1β , TNF or IFN γ (10ng/ml) in serum-free media for 24 to 48 h. The cell surface staining procedure was described in section 3.2.2.2 following trypsinisation (n=3).

3.2.2.5 Acquisition of CCR2 PE-labelled (FL-2) astrocytes using flow cytometry.

Before running the samples, optimisation of the settings was performed on FSC, SSC and FL-2. Non labelled cells were run through the flow cytometer to optimize the settings for the FSC and SSC to have a uniform cell population in the middle of the two dimension dot plot. If the population was at the bottom of the two dimensional dot plot, the intensity of the laser for SSC was increased. If it was at the top of the two dimension dot plot, the intensity of the laser for SSC was decreased. The same principle was applied for setting the FSC.

Astrocytes stained with the isotype control (negative control) were run to opti-

mize the settings for FL-2. The peak for the negative control was located on the left side of the one dimension histogram by displacing the peak to the left or right of the X-axis by increasing or decreasing the intensity of the laser. When the peak for the negative control was correctly located, samples were analysed.

For the data acquisition of the stained samples, 10,000 events (or cells) were counted.

3.2.2.6 Analysis of CCR2 PE-labelled (FL-2) astrocytes using BDTM CellQuest Pro software.

For the analysis, the BDTM CellQuest Pro software (BD Biosciences, UK) was used. A two dimension dot plot was opened with the desired file to analyze the 10,000 events counted during the acquisition. The 10,000 events include live cells, dead cells and cellular debris. To avoid background signal due to cellular debris or dead cells, which give false positive staining, only the live cells were analysed by drawing a region or gate that includes only the live cell population (figure 3.2b). At this stage, only the cells present in the gate will be further analysed. To determine the intensity of fluorescence of the gated cells, a single dimension histogram was opened with the desired file for analysis. The gate drawn previously was selected as well as the channel for analysis (FL-2 in this case). The mean of fluorescence intensity (MFI) of the analyzed sample was obtained by using the "stats" function of the BDTM CellQuest Pro software. The same procedure was followed for all samples stained.

3.2.2.7 CCR2 expression by primary human adult astrocytes by immunocytochemistry

The same method was followed as described in section 2.2.2.2 for the characterisation of astrocytes by GFAP staining. Cells were incubated with monoclonal antibody directed against human CCR2 (R&D Systems, UK) at 1:100 dilution in

PBS-1%BSA for 1 h at RT. Three different secondary antibodies were assessed to determine the optimal signal. Cells were either incubated with PE-conjugated goat anti-mouse IgG (1:40, Sigma Aldrich, UK) or FITC-conjugated goat anti-mouse IgG(1:100, Chemicon, UK) or Rhodamine-conjugated goat anti-mouse IgG (1:100, Chemicon, UK) diluted in PBS-1%BSA for 1 h at RT in the dark.

3.2.3 Measurement of CCL2 binding to astrocytes using biotinylated CCL2 by flow cytometry

3.2.3.1 Optimisation of CCL2 binding to astrocytes: dose response

Astrocytes (B327/01) in 6 well-plates were washed with PBS, harvested with trypsin-EDTA and incubated for 1 h in a humid atmosphere at 37°C in 95% air/5% CO₂ in serum-free media to allow the cell membrane to recover after trypsinization. Cells were centrifuged at 300 g, supernatant was removed, and cells were resuspended and incubated with various concentrations of biotinylated CCL2 (0, 1, 100, 500, 800, 2000ng/ml, R&D Systems, UK) for 1 h in a humid atmosphere at 37°C in 95% air/5% CO₂. Biotinylated soybean trypsin inhibitor, supplied by the manufacturer, was used as negative control to quantitate the non-specific binding (R&D Systems, UK). 10µl of avidin-FITC was added to the cell suspension (2.2µg/ml) and incubated for a further 30 min at 4°C in the dark. Binding was quantitated using FACScalibur flow cytometry (BD Biosciences, UK) and CellQuest™ software (BD Biosciences, UK) following the same procedure as described in section 3.2.2.5. Binding was expressed as MFI. The channel used for this experiment was FL-1, corresponding to detection of FITC. Three independent experiments were performed.

3.2.3.2 Optimisation of binding of biotinylated-CCL2 to astrocytes: time course experiment

The same protocol was followed as above with 0.25 µg/ml of biotinylated-CCL2 that corresponded to previously determined half maximal effective binding

of biotinylated-CCL2. Cells were incubated for 0, 30, 60, 180 and 360 min with biotinylated-CCL2 (n=2). Then staining was performed as described above.

3.2.3.3 Specificity of CCL2 binding to astrocytes: competition assay

The specificity of CCL2 binding was assessed by incubation of astrocytes with a constant concentration of biotinylated-CCL2 in the presence of increasing concentrations of unlabelled CCL2 (Prepotech, UK). Unlabelled CCL2 (zero, 25 and 100 times more unlabelled CCL2 than biotinylated-CCL2) was pre-incubated for 30 min with the cell suspension prior to addition of biotinylated CCL2. The binding procedure was performed as previously described in section 3.2.3.2 (n=3) using biotinylated CCL2 at 0.25 μ g/ml, incubated for 1 h at 37°C in 95% air/5% CO₂ and avidin FITC (2.2 μ g/ml) for a further 30 min incubation at 4°C in the dark prior to analysis by flow cytometry.

3.2.3.4 Detection of CCL2 binding to primary human astrocytes under pro-inflammatory conditions

Astrocytes (B327/01) were plated into 6 well-plates (0.25x10⁶ cells/2ml/well) and allowed to adhere for 24 h in astrocyte cell culture media. Cells were stimulated with IL-1 β , TNF or IFN γ (10ng/ml) in serum free media for 24 and 48 h, which was the optimal concentration determined for CCL2 secretion as described in section 2.3.4. The binding procedure was carried as described in section 3.2.3.3.

3.2.4 Detection of CCL2 binding to astrocytes using confocal microscopy

CCL2 binding was also assessed on adherent cells using confocal microscopy. 1ml of 5x10⁴/ml cells in complete media was plated onto sterile glass coverslips in 24 well plates (3.8cm²) and allowed to adhere for 24 h. Cells were washed with

PBS prior to addition of 40 μ l of biotinylated CCL2 (3 μ g/ml), to completely cover the cells, for 1 h at RT. As above, biotinylated soybean trypsin inhibitor was used as a negative control at the same concentration. Excess biotinylated CCL2 was removed by tapping on filter-paper and 40 μ l of avidin-FITC (10 μ g/ml) was added to the cells and incubated for 30 min at 4°C in the dark. Cells were dipped three times in PBS, fixed with paraformaldehyde (4%) for 15 min and rinsed 3 times with PBS for 5 min. Coverslips were mounted using Vectashield mounting media with DAPI (Amersham, UK) and binding was visualized at an excitation wavelength of 488 nm and emission wavelength of 520 nm using an Axiovert 200M confocal microscopy with LSM 510 laser module (Zeiss), equipped with a krypton/argon laser. Images were captured using the DSM software provided with the Axiovert 200M confocal microscope as described in section 2.2.3.1.

3.2.5 Measurement of calcium flux following stimulation of astrocytes with CCL2

3.2.5.1 Principle of calcium flux measurement

G-protein coupled receptors use Ca²⁺ as a second messenger to activate intracellular signalling events, that will activate various downstream pathways such as Akt, resulting in gene activation [Kiselyov et al., 2003]. To assess the increase in intracellular calcium, fluorescent calcium indicators have been developed. Fluo-3 was first introduced in 1989 to observe the movement of intracellular calcium [Minta et al., 1989]. The most important properties of this dye is that it has an absorbance at 505nm, following excitation and fluorescence emission at 530nm when complexed with Ca²⁺.

Fluo-4 is an analog of fluo-3 but generates a stronger signal following the binding to intracellular Ca²⁺. Fluo-4 has a maximum absorption at 494nm and maximum emission at 516nm. The dye is coupled with a nonpolar acetoxymethyl ester(AM) which results in an uncharged molecule that can penetrate the cell

membrane. Once inside the cell, non specific esterase cleaves the AM ester resulting in a charged form of the dye that leaks out of cells, far more slowly than the original compound. To reduce the leakage of the de-esterified dye from the cells, sulfinpyrazone, an anion transport inhibitor, is added to the washing buffer (figure 3.4) [Kao, 1994, Di Virgilio et al., 1990].

To detect fluorescence, the Fluostar Optima plate reader (BMG labtech Ltd., UK) was used. The FLUOstar OPTIMA is a versatile microplate reader that allows the injection of a solution in the well to analyse and simultaneously record the level of fluorescence in a well, which corresponds to the calcium increase [Lin et al., 1999].

3.2.5.2 Procedure for calcium imaging following CCL2 treatment of astrocytes

3×10^4 astrocytes (B327/01)/200 μ l/well were plated in a black polystyrene 96 well-plate (Corning Costar, UK) and allowed to adhere for 24 h. Cells were washed three times in Krebs HEPES buffer pH7.4 (Appendix) and incubated for 30min in the dark at RT with Fluo-4AM at 5 μ M (Molecular Probes, UK) in Krebs HEPES buffer with 0.25mM sulfinpyrazone (Sigma, UK) and 1% F12 pluronic to optimize the dispersion of the dye (Sigma, UK). Cells were washed twice with Krebs HEPES buffer and 0.1%BSA to remove the dye not taken up by cells. An additional wash was carried out for 30 min to allow complete de-esterification of intracellular AM esters. Before stimulation of cells, the buffer was changed to Krebs-HEPES. The plate was placed in the FLUOstar OPTIMA (BMG labtech, UK) at 37°C. Two tubes containing 2 ml of either human recombinant CCL2 (Peprotech, UK) (0ng/ml which is later replaced by 100ng/ml) or ionomycin at 25 μ M (Sigma Aldrich, UK) in Krebs-HEPES with Ca²⁺ (1.2mM) were kept in the FLUOstar OPTIMA plate reader at 37°C.

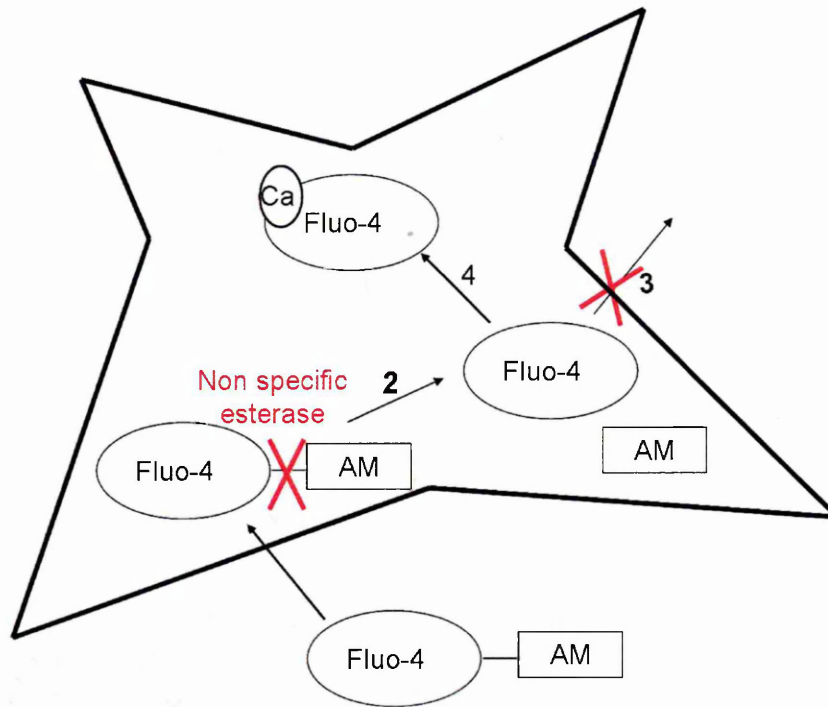


Fig. 3.4: Principle of calcium imaging in cells following activation of a receptor.

The intracellular calcium movement is monitored with a dye (Fluo-4) that is complexed to a non polar acetoxymethyl ester (AM) rendering the complex uncharged allowing the penetration into the cells (1). Inside the cell the AM ester is cleaved by non-specific esterase (2) resulting in a charged dye that leaks out far more slowly than the dye-ester (3). Fluo-4 has the property of a maximal absorption at 494nm and a maximal emission at 516nm when complexed with Ca²⁺ (4). Incubation with sulfinpyrazone, an anion transport inhibitor, prevents the leakage of Fluo-4 out of the cells.

Ionomycin, a commonly used selective Ca^{2+} ionophore, was used as a positive control at $5 \mu\text{M}$ [Brylla et al., 2005, Turner et al., 2007]. CCL2 was injected at 20 and ionomycin was injected at 150s. Measurement of the calcium signal was taken every second for 5 min, using an excitation filter of $485 \pm 12\text{nm}$ and an emission filter of 520nm . The amplitude of the response following CCL2 addition was expressed as a percentage of the maximum response (ionomycin) ($n=3$).

3.2.6 Measurement of Erk and Akt signalling using SDS PAGE and western blotting by detecting phosphorylated forms

3.2.6.1 Cell stimulation with CCL2 and fetal calf serum (FCS)

1ml of astrocyte suspension (B327/01 and Ep15) was plated into 6 well-plates (0.25×10^6 cells/ml/well) and allowed to adhere for 24 h. Media was removed and cells were cultured for 24h in SFM and then stimulated for 15 min with CCL2 at 0 to 100ng/ml (Peprotech, UK) FCS (10%) was used as a positive control [Henkler et al., 1998, Posern et al., 1998].

3.2.6.2 Sample preparation for the measurement of Erk and Akt phosphorylation following CCL2 treatment by western blotting

Cells were washed once in ice cold PBS supplemented with 1mM orthovanadate 1mM (Sigma, UK) a phosphatase inhibitor. $50\mu\text{l}$ of Laemmli buffer (Appendix) was added to the cells, which were quickly harvested using a cell scraper (Greiner Laboratories Limited, UK) and transferred into an Eppendorf tube. Samples were heated at 95°C for 10 min and sonicated for 5s at 40% amplitude (VibraCell processor 750W, Sonics) to disrupt the DNA. Samples were kept at -20°C until used.

3.2.6.3 Measurement of Erk and Akt phosphorylation following CCL2 treatment by western blotting

Since measurement of protein was not possible, due to the sample buffer, which would interfere in the assay, equivalent volumes were loaded for each conditions. Samples were run on a 10% acrylamide/0.13% bis-acrylamide gel (National Diagnostics, UK) and transferred onto a nitrocellulose membrane, HybondTM C Extra (Amersham, UK) overnight at 4°C at 0.15 A using the blotting apparatus, Power Pac 300 (Biorad, UK). Before probing the membrane with antibodies for Erk and Akt, membranes were blocked for 1 h at RT in TBS-5% powdered milk. Phosphorylated forms of Erk and Akt were visualized using rabbit polyclonal antibodies specific for Erk 1 and 2 [pTpY^{185/187}] and Akt [pS⁴⁷³] (Biosource, UK) at 1:1000 in PBS-5% powdered milk for 2h at RT. Membranes were washed five times (10 min each) with PBS-0.05% Tween 20 at RT. Secondary HRP-conjugated goat anti rabbit IgG in PBS-0.05% Tween 20 (Sigma, UK) at 1:20 000 was used for 1h at RT (Table 3.2) and membranes were then washed as before with PBS-0.05% Tween 20. An extra washing step was done with PBS for 10 min at RT.

Immunoreactivity was detected by chemiluminescence using the ECL Reagent Kit Plus, western blotting detection system (Amersham, Buckinghamshire, UK), according to the manufacturer's instructions. Briefly, 2 ml of ECL Plus substrate solution containing Tris buffer (solution A) and 50 μ l of stock acridan solution in dioxane and ethanol (solution B) were incubated on the membrane for 5 min at RT. Chemiluminescent signal was visualised using a UVP Bioimaging system (Bio-Rad, Hertfordshire, UK). Quantitative analysis was carried out by comparing the integrated optical density (IOD) using densitometric software of the UVP Bioimaging system.

To normalize the level of expression of phosphorylated forms of Erk and Akt, total Erk and Akt expression was assessed. First, each blot had to be stripped and re-probed with different primary antibodies. Blots were washed three times

for 5 min each in TBS, which acted as a neutralizing buffer. This was followed by incubating for 30 min at 50°C in stripping buffer (100mM H-mercapto-ethanol (Sigma Aldrich, UK), 2%w/v SDS, 62.5mM Tris/HCL pH 6.8). Blots were washed three times for 5 min each in TBS before starting the staining procedure with the second set of antibodies.

Total Erk was visualized using mouse monoclonal antibody specific for Erk 1 and 2 at a 1:500 dilution (Upstate, UK) and HRP-conjugated goat anti-mouse IgG antibody (1:10 000). Total Akt was visualized by probing the membrane with rabbit polyclonal antibody specific for Akt at a 1:1000 dilution (Cell Signalling, UK) and HRP-conjugated goat anti-rabbit IgG antibody (1:10 000). Visualisation of the blots was performed as described above. The antibodies used to determine the phosphorylation level of both Erk and Akt are summarised in table 3.2.

To compare the phosphorylation of Erk and Akt under pro-inflammatory conditions (section 3.2.6.1), IOD values of Erk 1 and 2 [pTpY^{185/187}] and Akt [pS⁴⁷³] were normalized to the IOD values of Erk total and Akt total respectively considering these as a value of 1. Experiments were performed twice for both SMS-12 and Ep15. Experiments were performed once with B327/01 due to limited cell availability.

3.2.7 Statistical analysis

Data are shown as mean \pm SEM. For experiments on CCR2 level expression, CCR2 expression, CCL2 binding and phosphorylation of Erk and Akt, level of significance for comparisons between samples was determined using the ANOVA parametric test with Dunnett's test. In all cases, $P \leq 0.05$ was considered significant.

	Primary antibody	Secondary antibody HRP-conjugated	Suppliers
pTpY ^{185/187}	rabbit polyclonal antibodies specific for Erk 1 and 2 [pTpY ^{185/187}] (1:1000)	goat anti rabbit IgG (1:20,000)	Biosource (UK)
Total Erk	mouse monoclonal antibody specific for Erk 1 and 2 (1:500)	goat anti mouse IgG antibody (1:10,000)	Upstate (UK)
pS ⁴⁷³	rabbit polyclonal antibodies specific for Akt [pS ⁴⁷³] (1:1000)	same as secondary antibody for pTpY ^{185/187}	Biosource (UK)
Total Akt	rabbit polyclonal antibody specific for Akt (1:1000)	same as secondary antibody for pTpY ^{185/187}	Cell signalling (UK)

Tab. 3.2: Antibodies used to assess phosphorylation of Akt and Erk by western blotting.

Antibody dilutions are given in parentheses.

3.3 Results

3.3.1 Measurement of CCR2 mRNA expression by astrocytes following cytokine stimulation using qRT-PCR

CCR2 mRNA was detected in unstimulated primary human adult astrocytes using real-time RT-PCR (figure 3.5). Following 24 and 48 h stimulation with TNF (100ng/ml), CCR2 mRNA expression was significantly increased, compared to unstimulated cells ($P \leq 0.05$) (figure 3.5 a-b). IL-1 β and IFN γ slightly increased CCR2 mRNA expression by astrocytes at 100 ng/ml, although this increase did not reach statistical significance. Stimulation of primary human adult astrocytes from three donors (SMS-12, B327/01 and EP15) with IL-1 β , TNF and IFN γ at 10ng/ml for 24 h showed no significant differences in their response to cytokines using non parametric ANOVA with Dunnett's test (figure 3.6).

3.3.2 CCR2 expression by astrocytes using flow cytometry

By contrast, CCR2 expression by astrocytes from two different donors (B327/01 and Ep15) either at the cell surface, or in Triton X-100-permeabilised cells was not detected using flow cytometry either constitutively (figure 3.7) or following 24 and 48 h stimulation with TNF at 100 ng/ml (data not shown). TNF stimulation was used as it was the only cytokine to induce a significant increase in CCR2 mRNA. The lack of detection of CCR2 on astrocytes was not due to problems related to antibody specificity, as CCR2 expression was readily detected on the monocytic cell line, THP-1 (figure 3.7c).

Various protocols were assessed to improve the detection sensitivity for CCR2 by astrocytes. Protection of the antigenic site (glycine 0.1M) as well as different fixation procedures (PBS-Triton X100, 0.5% saponin and Fix and Perm buffer from BD Bioscience (UK)) did not enhance the detection of CCR2.

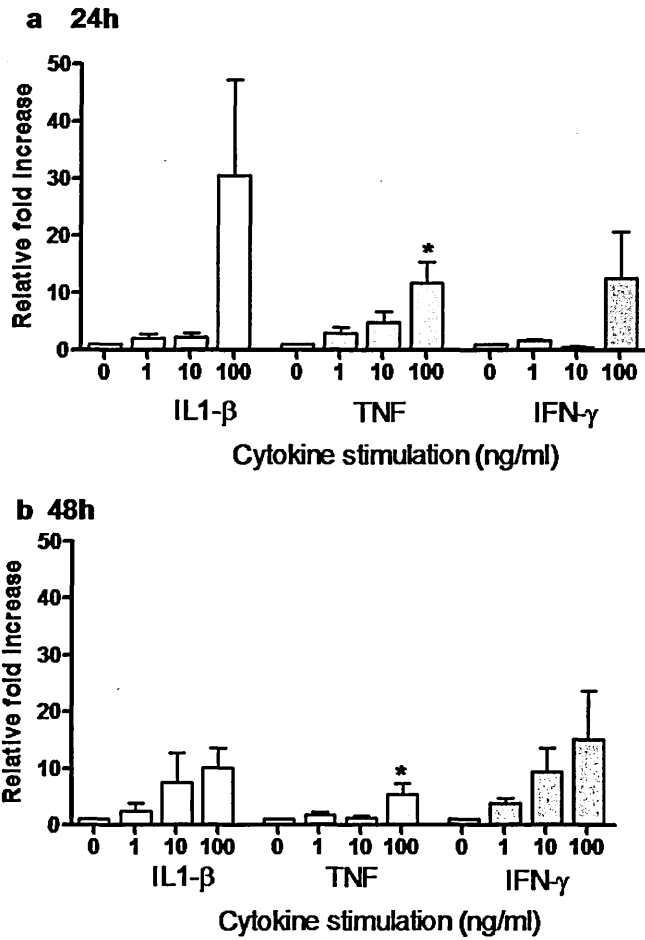


Fig. 3.5: Detection of CCR2 mRNA expression by astrocytes following pro-inflammatory cytokine stimulation using qRT-PCR. Cells (SMS-12) were stimulated with IL1- β (white), TNF (grey) and IFN γ (dark grey) at 0 to 100ng/ml for 24h (a) and 48h (b). Real time PCR was performed in triplicate on each sample (three stimulations). ANOVA followed by Dunnett's test was performed. * $p \leq 0.05$ is considered as significantly different.

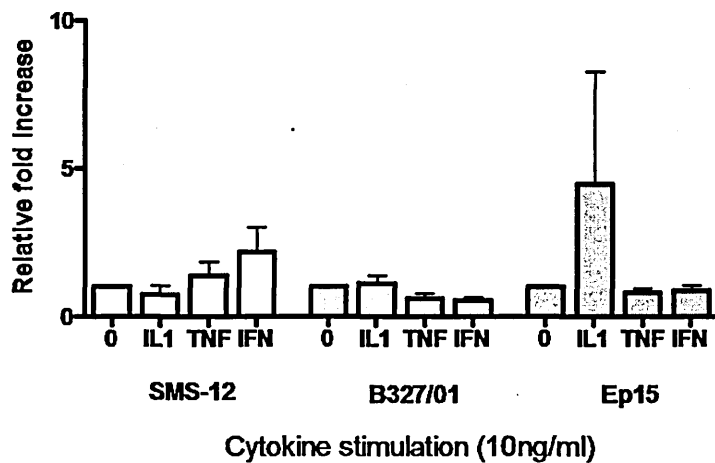


Fig. 3.6: Comparison of CCR2 mRNA expression between three astrocyte preparations

CCR2 mRNA expression by primary human adult astrocytes following pro-inflammatory stimulation using qRT-PCR with SybrGreen. SMS-12, B327/01 and Ep15 were stimulated with IL1- β (white), TNF (grey) and IFN γ (dark grey) at 0 and 10ng/ml for 24h (n=6). ANOVA followed by Dunnett's test was performed and demonstrated no significant differences in CCR2 mRNA expression following pro-inflammatory stimulation for the three astrocyte preparations.

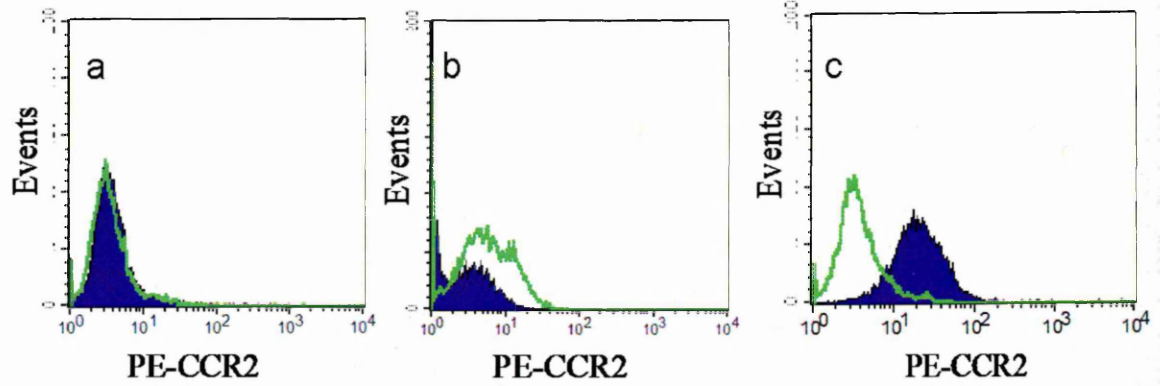


Fig. 3.7: Histogram representation of cell CCR2 expression using flow cytometry.

CCR2 expression on the cell surface (a) and intracellular staining (b) on astrocytes (B327/01) was assessed. CCR2 staining at the cell surface on the monocytic cell line THP-1 cells was performed as a positive control using the same procedure as for the astrocytes (c). Green line corresponds to the negative control (cells incubated with corresponding PE-labelled isotype control antibody).

Similarly, CCR2 was not detected by immunocytochemistry under basal conditions, using three different secondary antibodies (data not shown).

3.3.3 Binding of biotinylated CCL2 to the cell surface of human adult astrocytes detected by avidin-FITC and flow cytometry

In the absence of stimulation, biotinylated CCL2 binding to the astrocyte cell surface membrane (B327/01) was observed using biotinylated CCL2 with avidin-FITC and nuclei counterstained with DAPI (figure 3.8b). Biotinylated soybean trypsin inhibitor was used as negative control, which showed no staining (figure 3.8a). CCL2 binding was assessed on B327/01 (figure 3.8 c-d) and SMS-12 (figure 3.8 e-f). Strong localized staining for CCL2 was observed at the edge of the cells.

Binding was also assessed by flow cytometry (figure 3.9). Determination of 50% of the maximal binding, and the optimal incubation time for the biotinylated CCL2 was assessed with dose response ($n=3$) and time course experiments ($n=2$) (figure 3.10a-b). The optimal conditions for biotinylated CCL2 binding using 0.25×10^6 cells was $0.25 \mu\text{g/ml}$ biotinylated CCL2 (figure 3.10a) for 1h (figure 3.10b). The specificity of the binding was assessed by incubating biotinylated CCL2 with increasing concentrations of unlabelled CCL2 (figure 3.11). Unlabelled CCL2 reduced the binding of biotinylated CCL2 on astrocytes in a dose-dependent manner by 30.78% ($n=3$, $p \leq 0.05$) and 53.61% ($n=3$, $P \leq 0.01$) when using concentrations of unlabelled CCL2 at 25 and 100 times higher, respectively. High concentrations of cold CCL2 were required to prevent the binding of biotinylated CCL2 to astrocytes. A 50% reduction in binding of labelled CCL2 would be expected when incubating twice as much cold CCL2 than biotinylated CCL2, if both labelled and unlabelled CCL2 bind equally. Therefore biotinylated CCL2 has a higher affinity for binding to astrocytes than the unlabelled CCL2. This might be explained by non specific binding to astrocytes due to the biotin label.

However the use of biotinylated soybean trypsin inhibitor as a negative control, which showed no binding, confirmed the absence of non specific binding through the biotin label. Structural alteration of the biotinylated CCL2 may lead to this higher affinity to the binding site on astrocytes than native CCL2. However, some specificity for biotinylated CCL2 binding to astrocytes was observed in our study. Similar finding was observed in a study by Andjelkovic et al (1999) where they showed in competition experiments with human fetal astrocyte cell cultures that cold CCL2 (5 times more than biotinylated CCL2) induced a reduction of 20% in biotinylated CCL2 binding.

Following pro-inflammatory stimulation with IL-1 β , TNF and IFN γ at 10ng/ml for 24 h, no significant difference in CCL2 binding to astrocytes (B327/01) was observed (figure 3.12). However, following 48 h stimulation, IL-1 β (76.15 ± 28.85 MFI), TNF (81.56 ± 29.30 MFI) and IFN γ (72.20 ± 24.47 MFI), a non significant increase in CCL2 binding to astrocytes was observed compared to the baseline (45.10 ± 16.17 MFI) (figure 3.12). Although the absolute amount of biotinylated-CCL2 bound decreased following 48 h stimulation compared to 24 h stimulation, it did not reach statistical significance (ANOVA followed by Dunnett's test).

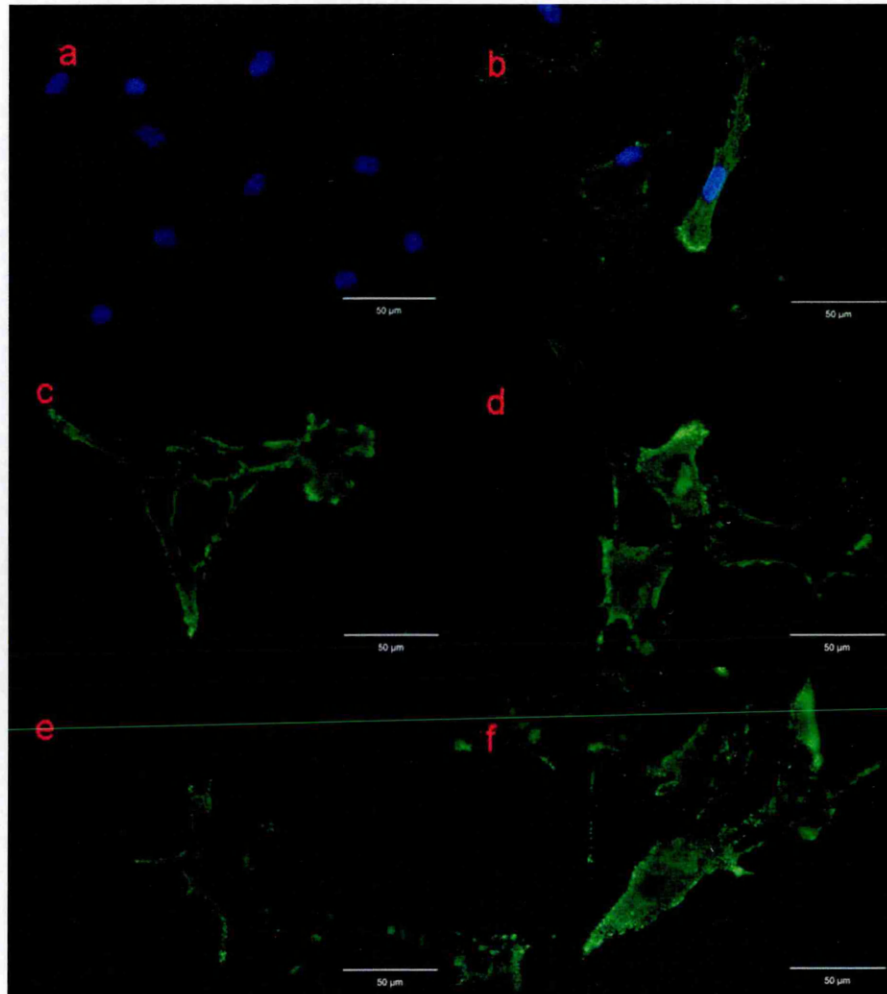


Fig. 3.8: Biotinylated CCL2 binding to primary human adult astrocytes detected by avidin-FITC.

(a) Biotinylated soybean trypsin inhibitor with avidin-FITC was used as negative control on the astrocytes (B327/01). Visualization of binding with biotinylated CCL2 ($3\mu\text{g}/\text{ml}$) on B327/01 astrocyte preparation (b, c and d) and SMS-12 astrocyte preparation (e-f).

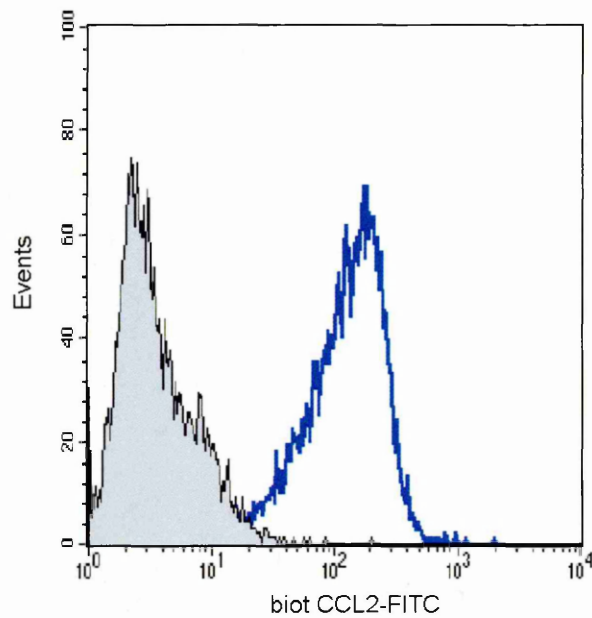


Fig. 3.9: CCL2 binding to primary human adult astrocytes (B327/01) using flow cytometry.

Representative flow cytometric histogram to demonstrate the binding of biotinylated CCL2 ($0.25\mu\text{g}/\text{ml}$) to B327/01 astrocytes, followed by detection with avidin-FITC, in PBS (blue histogram). Biotinylated soybean trypsin inhibitor was used as a negative control (filled histogram). This is representative of results obtained in three independent experiments.

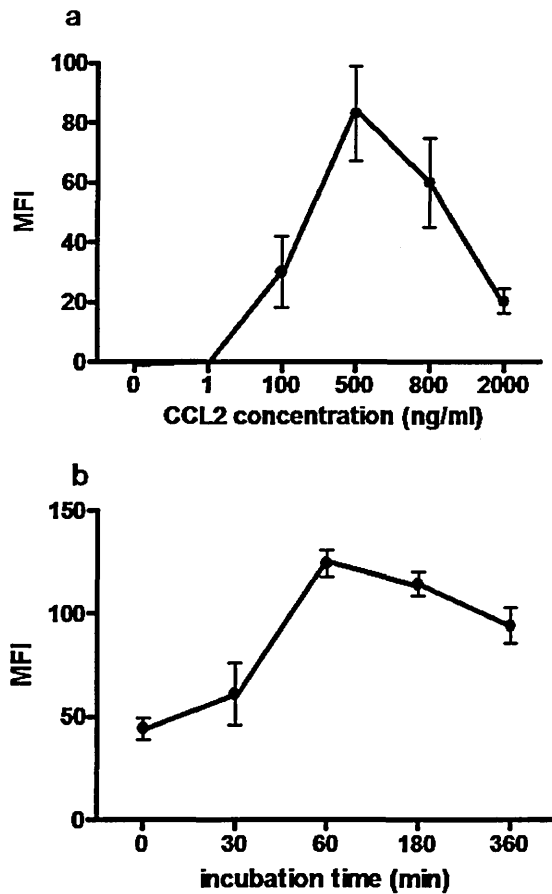


Fig. 3.10: Optimisation of CCL2 binding determined by flow cytometry: dose response and time course.

(a) Dose response experiments were done to determine the concentration of biotinylated CCL2 that produced 50% of maximal binding. Astrocytes (B327/01) were incubated with increasing concentrations of biotinylated CCL2 for 1h at 37°C (0 up to 2000ng/ml, n=3). (b) The optimal incubation time was determined by performing time course experiments (0 to 360min) using the concentration for biotinylated CCL2 that represents 50% of the maximal binding (n=2). The optimal conditions were 0.25µg/ml of biotinylated CCL2, incubated with astrocytes for 1h at 37°C. The background value with biotinylated trypsin inhibitor was subtracted for each condition.

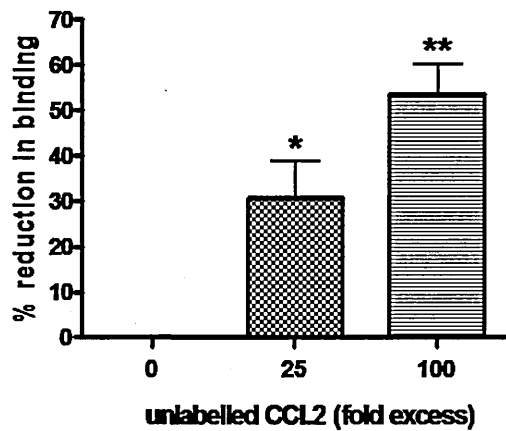


Fig. 3.11: Determination of the specificity of biotinylated CCL2 binding: competition experiments.

The specificity of CCL2 binding to astrocytes (B327/01) was assessed by performing competition experiments with pre-incubated unlabelled CCL2 (25 fold (squares) and 100 fold (horizontal lines)) CCL2 prior to the binding procedure (n=3). The background value with biotinylated trypsin inhibitor was subtracted for each condition and results were expressed as the percentage reduction in CCL2 binding to astrocytes. ANOVA followed by Dunnett's test was performed. * $p \leq 0.05$, ** $p \leq 0.01$ was considered as significantly different.

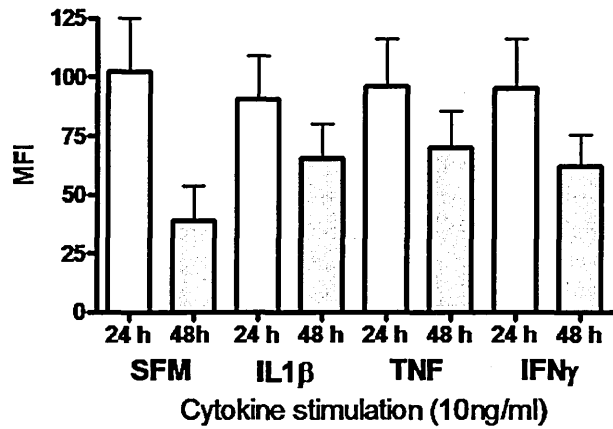


Fig. 3.12: Biotinylated CCL2 binding to astrocytes under pro-inflammatory conditions by flow cytometry.

Cells (B327/01) were stimulated with IL1- β , TNF and IFN γ at 10ng/ml for 24h (blank) and 48h (grey) in triplicate and binding experiments were performed in duplicate on each sample. ANOVA followed by Dunnett's test was performed to determine the significant difference between binding on unstimulated and stimulated cells. Differences in binding following 24 and 48 h stimulation was assessed by ANOVA followed by Dunnett's test and no significant difference was observed.

3.3.4 Measurement of calcium flux in astrocytes following CCL2 treatment

3.3.4.1 Optimisation of experimental conditions

Before stimulating the cells with recombinant human CCL2, optimisation of the technique was undertaken. As the system is extremely sensitive, turbidity resulting from injection of buffer could indicate an artefactual increase in Ca^{2+} [Miyazaki et al., 2007]. Testing the volume of solution to inject was the first optimisation step. Injection of $80\mu\text{l}$ of FCS (10%) on to the cells (in $80\mu\text{l}$ of Krebs-HEPES buffer) induced a strong increase in fluorescence due to an increase in intracellular Ca^{2+} (95% of the maximum response) (figure 3.13a). When injecting Krebs-HEPES buffer under the same conditions, a strong increase was also observed (80% of the maximum response). However, the signal obtained with FCS (figure 3.13a) was stronger than for Krebs-HEPES alone (figure 3.13b).

To reduce the background, a reduction in the injected volume of buffer was tested. One fifth of the initial volume was added to the cells ($12.5\mu\text{l}$). Figure 3.14a shows the absence of response following injection of buffer, and a strong response following ionomycin injection (from 5,865 units of fluorescence to 18,591 units of fluorescence). However, the signal for ionomycin decreased with time from 12,526 units of fluorescence (5 min) to 5,330 units of fluorescence (15 min), with 0 min corresponding to the cells just after the last wash (figure 3.14b). This provides evidence that Fluo-4 was expelled by the cells. Sulfinpyrazone, an anion inhibitor, was added to the cells to avoid any dye leakage. Stimulation of cells (B327/01) with FCS (10%, 20s) and ionomycin ($25\mu\text{M}$, 150 s) was done at 0 min (blue), 5 min (yellow) and 10 min (light blue) after the last wash. The amplitude of the fluorescence was 11194, 11473 and 10 088 respectively which showed a reduction in Fluo-4 leakage (figure 3.15).

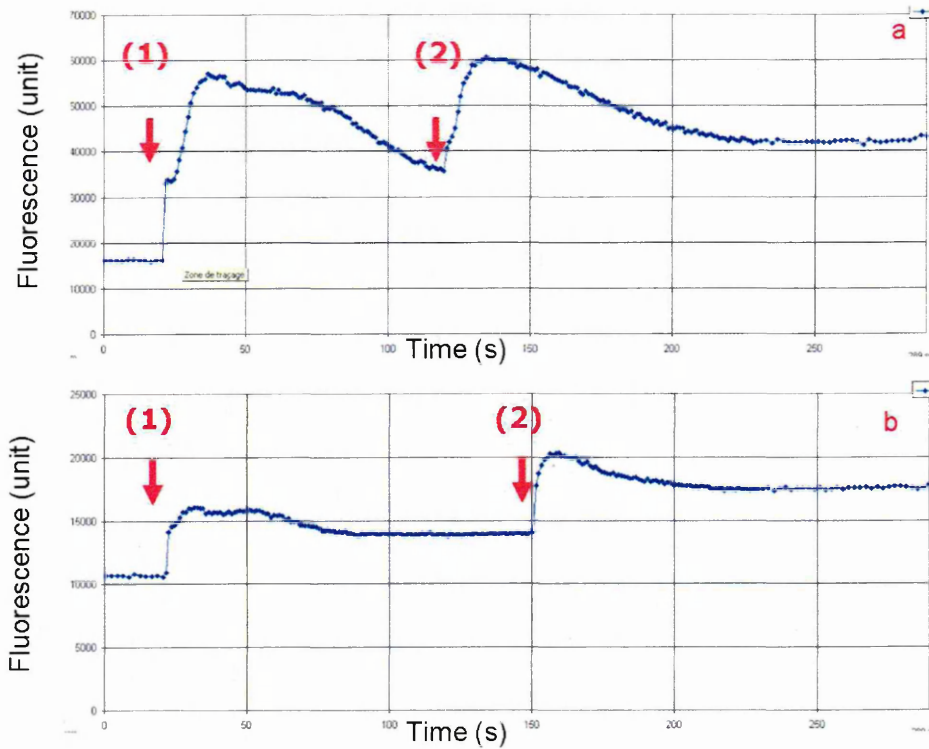


Fig. 3.13: Optimisation of the volume of solution injected for detection of calcium flux in astrocytes (1).

Cells were loaded with $5\mu\text{M}$ Fluo-4AM. Calcium imaging was assessed on B327/01 astrocytes following stimulation with FCS (1, 20s) and ionomycin (2, 150s) (a). Negative control was assessed by injecting Krebs-HEPES buffer after 20s (1) and ionomycin after 150s (2) (b). In this experiment, half of the final volume ($80\mu\text{l}$) of FCS or Krebs-HEPES was injected.

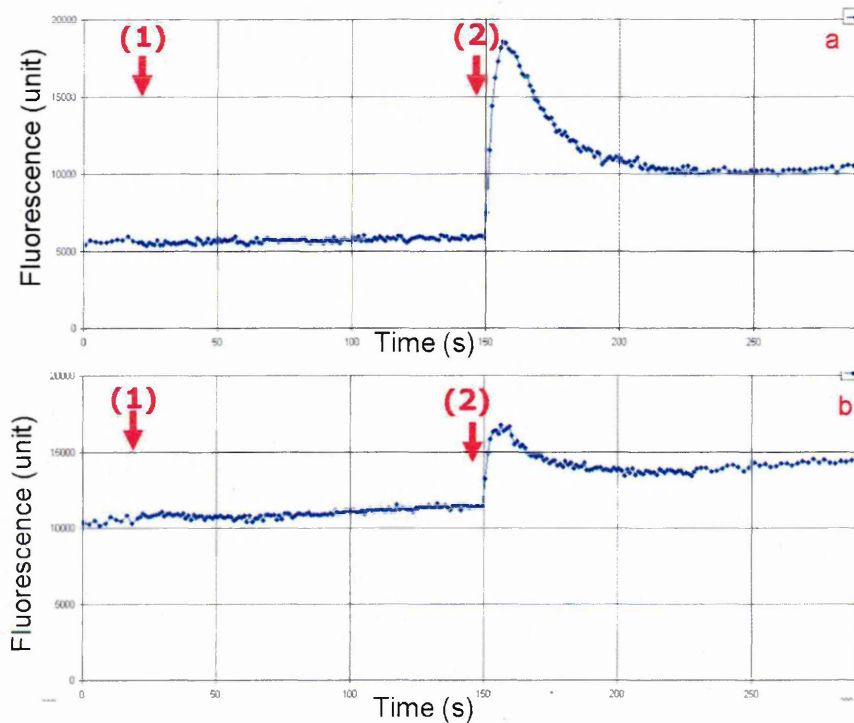


Fig. 3.14: Optimisation of the volume of solution injected for detection of calcium flux in astrocytes (2).

Cells were loaded with $5\mu\text{M}$ Fluo-4AM. Calcium imaging was assessed on B327/01 astrocytes following stimulation with Krebs-HEPES (1, 20s) and ionomycin (2, 150s) (a). In this experiment. One fifth of the initial volume ($12.5\mu\text{l}$) was injected. Injection of Krebs-HEPES (20s.) and ionomycin (150s) was assessed at 5 min (a) and 15 min (b) after the last 30 min wash. Amplitude of the response for ionomycin decreased with time.

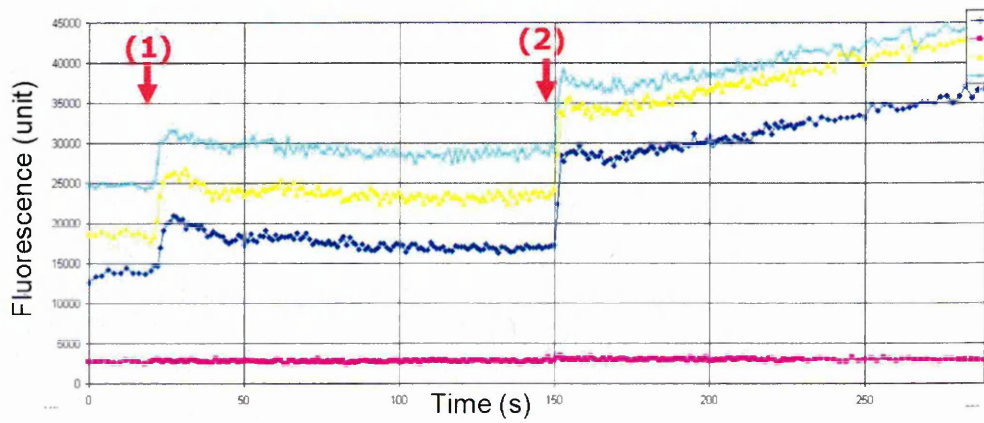


Fig. 3.15: **Incubation with sulfinpyrazone to prevent dye leakage.** Cells (B327/01) were loaded with $5\mu\text{M}$ Fluo-4AM with sulfinpyrazone to assess prevention of dye leakage. Cells were stimulated after the last wash (30 min wash) with FCS (1, 20s) and ionomycin (2, 150s) at 0 min (blue), 5 min (yellow) and 10 min (light blue). The pink line represents the baseline fluorescence.

3.3.4.2 Effect of CCL2 treatment on intracellular calcium flux in astrocytes

Stimulation of astrocytes with CCL2 (0 and 100ng/ml) was assessed to determine whether CCL2 binding had any functional effect on astrocytes. No difference in the calcium flux was observed following CCL2 stimulation (100 ng/ml) and the untreated control. Indeed, Ca^{2+} response from non stimulated astrocytes (n=3) represents $22.23 \pm 4.9\%$ of the maximal response (ionomycin) whereas Ca^{2+} response from astrocytes treated with CCL2 (100 ng/ml) represents $23.8 \pm 1\%$ (n=3) of the maximal response.

3.3.5 Effect of CCL2 treatment on Erk and Akt signalling pathways in astrocytes

To confirm the previous results, showing the absence of Ca^{2+} flux, effects of CCL2 binding to astrocytes (B327/01 and Ep15) on downstream signalling events was assessed by measurement of Erk and Akt phosphorylation. Astrocytes were stimulated with CCL2 from 0 to 100 ng/ml. No difference was observed in the level of phosphorylation of Erk in Ep15 (n=2), SMS-12 (n=2) and in B327/01 astrocyte (n=1) (figure 4.5). No difference in the band intensity was observed between CCL2 stimulation and unstimulated cells in the three astrocyte preparations assessed. Quantitative analysis, carried out by comparing the integrated optical density of each treatment (IOD) using densitometric software of the UVP Bioimaging system (n=2), showed that there was no difference in the phosphorylation between CCL2 stimulated and unstimulated cells. The absence of phosphorylation of Erk following CCL2 stimulation was not due to a technical problem as FCS, used as a positive control, induced a significant increase in expression of phosphorylated forms of Erk ($p \leq 0.01$, n=2).

Similarly to Erk, CCL2 stimulation on Ep15 (n=2) and B327/01 (n=1) did not induce any increase in phosphorylated forms of Akt compared to unstimulated cells. Again, FCS significantly increased the phosphorylation of Akt ($P \leq 0.05$,

n=2) (figure 4.6).

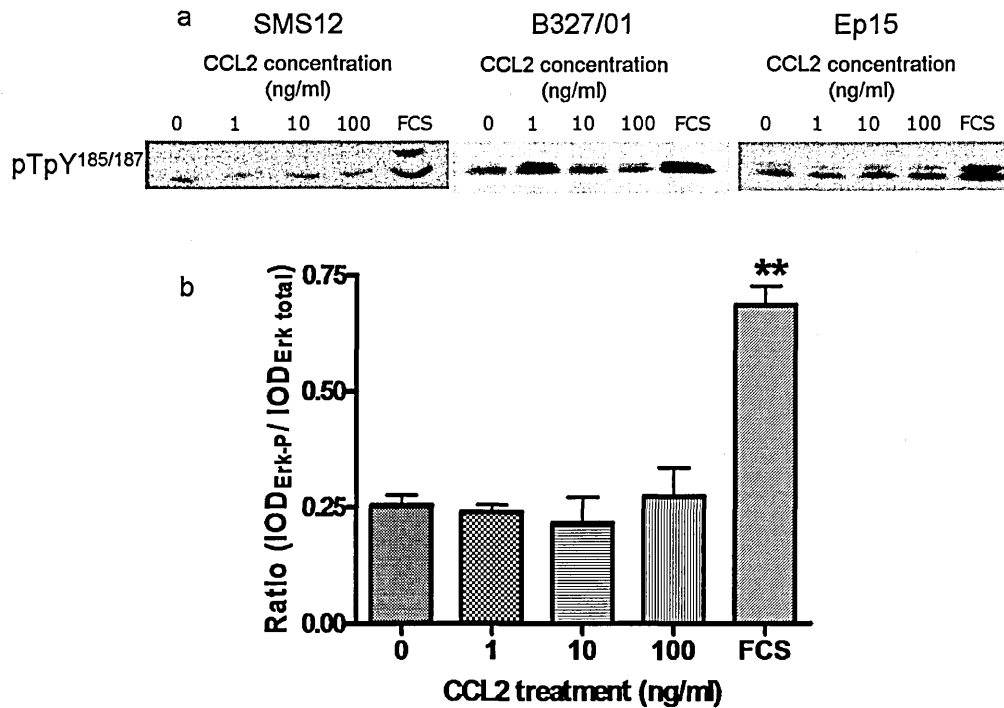


Fig. 3.16: Effect of CCL2 treatment on Erk 1 and 2 phosphorylation in primary human adult astrocytes using SDS PAGE and western blotting.

Astrocytes (SMS-12, B327/01 and Ep15) were serum starved for 24 h and stimulated with CCL2 at 0-100ng/ml or FCS, as a positive control. Erk 1 and 2 (pTpY^{185/187}) as well as the total amount of Erk were assessed by western blotting (a). Quantitative analysis was carried out by comparing the integrated optical density of each stimulation (IOD) using densitometric software of the UVP Bioimaging system (Ep15, n=2). To compare phosphorylation following pro-inflammatory stimulation, IOD values of Erk 1 and 2 (pTpY^{185/187}) were normalized to the IOD values of Erk total (b). ANOVA followed by Dunnett's test was performed and $p \leq 0.01$ was considered as significantly different.

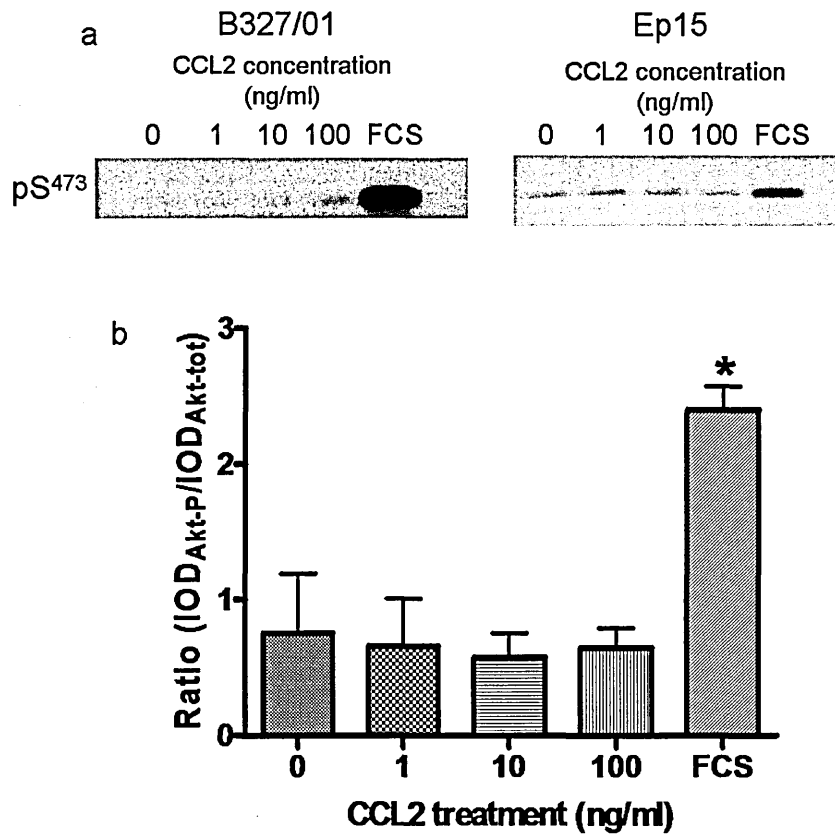


Fig. 3.17: Effect of CCL2 treatment on Akt phosphorylation in primary human adult astrocytes using SDS PAGE and western blotting.

Astrocytes (B327/01 and Ep15) were serum starved for 24 h and stimulated with CCL2 at 0-100ng/ml or FCS as a positive control. Akt (pS⁴⁷³) as well as the total amount of Akt were assessed by western blotting (a). Quantitative analysis was carried out by comparing the integrated optical density of each stimulation (IOD) using densitometric software of the UVP Bioimaging system (B327/01, n=2) (b). ANOVA followed by Dunnett's test was performed and $p \leq 0.05$ was considered as significantly different.

3.4 Discussion

Much evidence for a role for CCL2 in MS pathogenesis has been obtained in the EAE mouse model in which either CCL2 or CCR2 genes were knocked-out [Kennedy et al., 1998, Huang et al., 2001, Gaupp et al., 2003]. A significant reduction in macrophage recruitment into the CNS was observed in these animals [Huang et al., 2001]. In other reports, use of anti-CCL2 antibodies prevented the firm adhesion of leukocytes to the endothelium, but not the rolling in CNS inflammation in the EAE model induced with MOG₃₅₋₅₅ and myelin basic protein (MBP) [dos Santos et al., 2005, Youssef et al., 1999], thus leading to a reduction in the severity of the disease.

However, a role for CCL2 in MS pathogenesis is less well defined. For example, the significance of the observation that CCL2 levels decrease in the CSF of MS patients during relapse [Mahad et al., 2002a, Narikawa et al., 2004, Scarpini et al., 2002] remains to be determined. CCL2 levels in the serum have also been assessed but showed no consistency between different studies as discussed in section 1.4.9.2 [Kivisakk et al., 1998, Scarpini et al., 2002].

In the previous chapter, the rate of synthesis and secretion of CCL2 by astrocytes was assessed and no decrease in the synthesis and secretion of CCL2 was observed following pro-inflammatory treatment. Therefore the decrease in the CSF level of CCL2 might be a result of sequestration of CCL2 in the CNS by astrocytes at times of relapse in MS patients.

3.4.1 CCR2 mRNA expression by astrocytes using qRT-PCR

Firstly, the synthesis and expression of CCR2 was assessed to determine whether CCR2, expressed by astrocytes, could sequester CCL2 locally. Human adult

astrocytes express CCR2 mRNA constitutively demonstrated by qRT-PCR, confirming previous studies using human foetal and adult simian astrocytes [Andjelkovic et al. 2002, Croitoru-Lamoury et al. 2003]. However, there are previously contradicting reports of IL1- β and TNF effects on CCR2 mRNA expression. Croitoru-Lamoury et al. (2003) found by RT-PCR that IL1 β and TNF significantly induced a 3 fold increase in CCR2 mRNA using simian adult astrocytes whereas Andjelkovic et al. (2002) found the loss of CCR2 mRNA expression following 48 and 72h stimulation with IL1 β and TNF using human foetal astrocytes compared to 24 h stimulation. In this study using qRT-PCR, CCR2 mRNA was constitutively expressed and showed a significant increase following TNF stimulation with 100ng/ml for 24 and 48 hours. Although IL1- β and IFN- γ increased CCR2 mRNA expression with 100ng/ml for both 24 and 48 h, it was not significant.

3.4.2 CCR2 protein expression by astrocytes using flow cytometry

Surprisingly, human adult astrocytes did not express CCR2 protein even following TNF stimulation at 100ng/ml. This particular stimulation (TNF at 100ng/ml) was chosen as it was the only stimulation that significantly increased CCR2 mRNA expression by primary human adult astrocytes. The absence of detection of CCR2 on primary human adult astrocytes was not as a result of a technical problem as strong staining was observed on the monocytic cell line (THP-1 cells), using the same procedure. Similar findings were obtained with another chemokine receptor (CXCR3), where CXCR3 mRNA was detected but not protein in intestinal myofibroblasts possibly due to a receptor expression below the detection limit [Kouroumalis et al., 2005].

Several *in vitro* studies reported that cultured human foetal astrocytes express CCR2 [Andjelkovic et al., 2002, Rezaie et al., 2002] whereas others studies reported that human adult astrocytes or mouse astrocytes do not express CCR2

[Flynn et al., 2003, Heesen et al., 1996]. In this regard, it has to be mentioned that the astrocytes used in the different *in vitro* studies come from either different species or different developmental stages. Human foetal astrocytes aged 21 to 23 weeks and 13 to 29 weeks were used respectively by Andjelkovic et al. (2002) and Rezaie et al. (2001) which were both positive for CCR2 expression. Postnatal day 0 animals [Heesen et al. 1996] and human adult astrocytes (the present study and the Flynn study) have shown an absence of expression of CCR2. The function of astrocytes in response to inflammation thus might vary depending on the developmental stage of the cells and species origin.

The absence of detectable CCR2 protein may be due to several factors. First, qRT-PCR is the most sensitive technique currently available for the quantification of RNA samples [Klein et al., 2000] and has a high sensitivity (± 5 copies). Thus, the transcriptional activity of CCR2, and hence mRNA levels, might be so low that there is little protein expressed. However, this is unlikely to happen as the Ct values for CCR2 were similar to what found for another chemokine receptor (CXCR3) which was readily detected by flow cytometry and immunocytochemistry as shown in chapter 4. Secondly, CCR2 mRNA may be rapidly degraded or possibly repressed although studies that support this possibility are lacking. Finally, there may be a rapid turn-over of the CCR2 receptor targeting it to degradation by the proteasome rather than recycling. However, this hypothesis is unlikely as astrocytes were negative for intracellular CCR2 expression (figure 3.7).

3.4.3 Measurement of signalling pathways induced by CCL2 in astrocytes

To confirm the hypothesis that astrocytes did not express CCR2 or CCR2 was present but not detectable, measurement of the calcium flux as well as phosphorylation of the main signal transduction pathways Erk and Akt, responsible for differentiation/proliferation and chemotaxis were assessed following CCL2 treatment [Ashida et al., 2001, Thelen, 2001, Wain et al., 2002]. Despite high calcium

flux detected with ionomycin, no calcium flux was detected following CCL2 stimulation. FITC-Phalloidin staining, which stains the actin stress fibres due to chemokine stimulation, did not show any difference between unstimulated and stimulated astrocytes with CCL2 from 0 to 100ng/ml for 15 min to 60 min. (data not shown). The phosphorylation of Erk and Akt pathways was unchanged following 15 min stimulation with 0 to 100 ng/ml of CCL2 compared to the control. Again, the absence of an increase in phosphorylation was not as result of technical problems as astrocytes responded to FCS treatment, a commonly used positive control for the phosphorylation of both Akt and Erk [Posern et al., 1998, Henkler et al., 1998].

The absence of CCR2 expression by primary human adult astrocytes raises the question as to whether they are able to bind CCL2 in the absence of its cognate receptor. As discussed in sections 1.4.4.1 and 1.4.6, CCL2 has been shown to bind to various proteoglycans and the D6 decoy receptor [Kuschert et al., 1999, Johnson et al., 2005, Fra et al., 2003, Weber et al., 2004]. Therefore CCL2 binding to primary human adult astrocytes was assessed in one astrocyte preparation. Using biotinylated CCL2, astrocytes constitutively bound exogenous CCL2 on the cell surface and this was largely unaffected by pro-inflammatory cytokine treatment of the cells (24h stimulation). Since different astrocyte preparations may behave differently depending on the donor, binding of biotinylated CCL2 under pro-inflammatory conditions needs to be performed on other astrocyte preparations to confirm the statement that CCL2 binding to astrocytes was unaffected by pro-inflammatory conditions. Following 48h stimulation with pro-inflammatory cytokines, CCL2 binding to astrocytes increased compared to the baseline level at 48 h, although it was not significant. These results agree in part with a previous study [Andjelkovic et al., 1999a] where it was shown that IL1- β and TNF induced an increase in CCL2 binding following 48h stimulation using fetal human astrocytes. The amount of CCL2 binding to astrocytes slightly decreased from 24 to 48h but it was not significant. CCL2 binding to primary adult human astrocytes

is therefore, in this study, CCR2-independent. Thus, an alternative hypothesis is that CCL2 binding to astrocytes involves either chemokine decoy receptors [Fra et al., 2003] and/or proteoglycan [Johnson et al., 2005] expressed on the cell membrane, rather than CCR2.

Human adult astrocytes differ in respect to CCR2 expression compared to human foetal astrocytes. Fetal astrocytes sense and respond to gradients of CCL2 [Andjelkovic et al., 2002] that might determine the position of astrocytes at the BBB during CNS development [Dorf et al., 2000], whereas, as reported here, human adult astrocytes are not responsive to CCL2 in terms of calcium signalling. The secretion of CCL2 by primary human adult astrocytes will mainly affect other CNS resident cells including neurons, microglia and endothelial cells but also infiltrating monocytes, which express CCR2, through paracrine effects [Banisadr et al., 2005, Mahad et al., 2006, Stamatovic et al., 2003, Tanuma et al., 2006]. Banisadr et al. (2005) showed by immunohistochemistry that neurons constitutively express CCR2. *In vitro*, CCL2 activation of neurons from the cortex, the hippocampus, the hypothalamus and the mesencephalon resulted in an increase in calcium flux which demonstrated a possible neuron-glia interaction. CCL2 was shown to act on brain endothelial cells by disorganizing tight junctions resulting in an increase in the permeability of the BBB [Stamatovic et al., 2003]. This was confirmed by the absence of effect on endothelial cells from CCR2 $-/-$ mice. In the Tanuma et al. (2005) study, it was shown that *in vivo* microglia/macrophages expressed CCR2 but not CCL2. This suggests that CCL2, produced by astrocytes, will act in a paracrine way. This hypothesis was confirmed by a recent study, which showed that intrathecal injection of CCL2 induced microglial activation in WT mice but not in CCR2-deficient mice [Zhang et al., 2007]. All these findings confirm the potential paracrine effect of astrocyte derived CCL2 on CNS resident cells.

Therefore, in this *in vitro* study, human adult astrocytes have a complex role in promoting inflammation by recruiting inflammatory cells into the CNS through

the establishment of a CCL2 chemotactic gradient (figure 3.18). The constitutive binding of CCL2 in the absence of CCR2 expression by astrocytes demonstrates that CCL2 binding is CCR2-independent in primary adult human astrocytes. The absence of activation of the common signal transduction pathways for chemokine receptors demonstrates a novel function for human adult astrocytes during inflammation in MS. Astrocytes may promote inflammation by establishing a chemotactic gradient via presentation of CCL2 to infiltrating cells and may also act as a "sink" to regulate the level of CCL2 at the inflammation site possibly explaining the decrease in CCL2 in the CSF in people with MS, which correlates to time of relapse. Recently, Mahad et al. (2006) have suggested that the invading cells would consume CCL2 when entering the CNS. However, this would not fully explain the decrease in CCL2 in the CSF in MS patients at times of relapse, since other cell types are also able to bind CCL2. Endothelial cells and neurons have been shown to bind CCL2 [Banidsar et al. 2005, Stamatovic et al. 2003]. This current study gives some insight into the understanding of the mechanism resulting in the decrease of CCL2 in the CSF and the possible involvement of astrocytes.

Finally, this current study on human adult astrocytes and other studies on human foetal astrocytes [Andjelkovic et al., 2002, Rezaie et al., 2002] would suggest differences in gene regulation during development, hence caution is required when translating the data from *in vitro* studies using cells at different developmental stage to the understanding of the pathogenesis of MS.

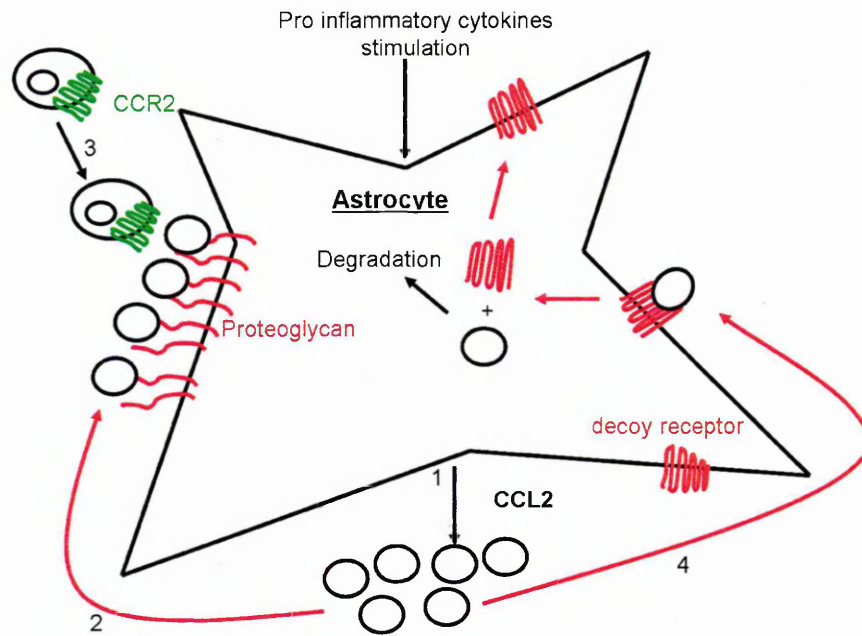


Fig. 3.18: Hypothetical mechanism for CCL2 binding to primary human adult astrocytes *in vitro*.

Primary human adult astrocytes respond to pro-inflammatory stimulation ($IL1-\beta$, TNF and $IFN\gamma$) by increasing secretion of CCL2 (1) that binds to astrocytes in a CCR2-independent way. The binding could be via proteoglycans (2) to establish a chemotactic gradient for immune cells expressing the corresponding receptor (CCR2) (3). Astrocytes might then have a role in promoting inflammation. Alternatively, CCL2 bound to the proteoglycan may be degraded by extracellular proteases [McQuibban et al., 2002]. CCL2 could also bind to decoy receptors. The absence of activation of the common signal transduction pathways for chemokine receptors suggests that CCL2 might bind to a decoy receptor, which would regulate inflammation through the internalization of CCL2 and degradation via the endosome, while the decoy receptor is recycled to the cell surface membrane (4).

CHAPTER 4

CXCR3 expression by primary human adult astrocytes

4.1 Introduction

4.1.1 CXCR3: overview

CXCL10 exerts its biological function through the interaction with the 7 transmembrane receptor, CXCR3. As previously discussed in section 1.4.3, CXCR3 can bind several chemokines belonging to the CXC chemokine family (CXCL9, CXCL10 and CXCL11). CXCR3 mRNA was first cloned from a cDNA library from CD4⁺ T cells [Loetscher et al., 1996]. The cDNA for CXCR3 has an open reading frame of 1041bp and encodes for a protein of 40KDa. A new mRNA spliced variant was discovered called CXCR3-B, which has an extended extracellular N-terminal domain of 52 amino acids [Lasagni et al., 2003]. The rest of the receptor is similar. When ligated, the two isoforms lead to distinct effects in human microvascular endothelial cell line-1 :

CXCR3-A: pro-proliferative effects, chemotactic and apoptotic

CXCR3-B: anti proliferative, no chemotactic effect and apoptotic effects

A new isoform of the receptor produced as a result of post transcriptional exon skipping was discovered. This variant, called CXCR3-alt, has a drastically altered C-terminal domain resulting in a four or five transmembrane domain structure [Ehlert et al., 2004]. It was shown that CXCR3 mediates chemotaxis and calcium mobilization via the C terminal part of the receptor [Colvin et al., 2004, Dagan-Berger et al., 2006]. Therefore it was surprising to find that, despite this major alteration of the structure of CXCR3-alt, flow cytometry experiments and migration assays showed that it is expressed at the cell surface and mediates CXCL11 activity [Ehlert et al., 2004].

4.1.2 CXCR3 expression in the CNS white matter in MS patients

Post-mortem tissue analysis by immunohistochemistry has demonstrated the accumulation of CXCR3⁺ T cells in more than 99% of perivascular leukocytes in active MS lesions [Balashov et al., 1999, Sorensen et al., 1999]. Quantitative correlation of the CXCR3⁺ cell number and demyelinating stage of MS disease has been assessed on post-mortem tissue by Sorensen et al. (2002). They found a significant increase in CXCR3⁺ T cells between early and late stages of MS lesions (early active demyelination, late active demyelination and inactive demyelinated areas). Staining for CXCR3 was occasionally found in control brain tissue samples on T cells [Sorensen et al 2002].

Expression of CXCR3 has also been observed in active and chronic MS lesions on foamy macrophages and astrocytes within the plaques [Simpson et al., 2000b, Sorensen et al., 2002]. Furthermore, in a study by Tanuma (2006) on CNS tissue from SP-MS, by dual immunostaining for CXCR3 with GFAP as well as CXCR3 with HLA-DP, DQ and DR, both astrocytes and microglia expressed CXCR3. Expression of CXCR3 was strong at the rim of the active and inactive MS plaque with ongoing demyelination, compared to the centre of the plaque where the immunoreactivity of this receptor was low. In control brain, no reactivity was detected.

4.1.3 Effect of CXCR3 agonists on Erk and Akt signalling

There are many reports on CXCR3 signalling activation pathways especially PI3K/Akt and MAPK [Bonacchi et al., 2001, Smit et al., 2003, Kukhtina et al., 2005].

Kukhtina et al. (2005) investigated intracellular pathways involved in chemokine-stimulated migration of *in vitro* activated human peripheral blood CD4⁺ T-lymphocytes. They showed that the use of specific inhibitors of PI3K, Erk1 and 2, resulted in a decrease in migration of activated lymphocytes by 35% and 40% respectively.

Phosphorylation of Akt and P44/P42 MAPK was shown to be increased in IL2 activated primary human T cells when stimulated with agonists of CXCR3 [Smit et al., 2003]. These findings were confirmed by incubating activated-T cells with Wortmannin and MEK inhibitor (U0126 and PD98059) with a total suppression of phosphorylation of both Akt and P44/P42 MAPK respectively. However, in this study, MEK inhibitor and Wortmannin (100 and 300nM respectively) failed to inhibit the transmigration of T cells in response to chemotactic gradients of CXCR3 agonist. Although the involvement of MAPK and Akt in controlling T cell chemotaxis is controversial, it is clear that CXCR3 agonists induce activation of MAPK and Akt.

Xia et al. (2000) showed in human brain that astrocytes expressed CXCL10 and neurons expressed CXCR3. Moreover, they showed *in vitro* that Erk1 and 2 were activated by CXCL10 in murine neurons. Although they did not look at the functional effect of CXCL10 on neurons, they concluded that a novel mechanism of cell-cell communication between neurons and astrocytes existed. Although two studies investigated the mechanism of CXCL10-mediated neurotoxicity [van Marle et al., 2004, Sui et al., 2004], the mechanism was not fully elucidated. Recently, Sui et al. (2006) showed in an *in vitro* study that CXCL10 induced an increase in intracellular calcium that resulted in foetal neuronal cell death due to activation of caspase 3.

Since vascular pericytes express CXCR3, Bonacchi et al. (2001) looked at signalling pathways activated by CXCR3. They showed that Erk 1 and 2 and PI3K induced migration and proliferation of pericytes which are critical biologic actions for wound healing and repair. These findings suggest that CXCR3 might be involved in tissue repair.

CXCR3 also binds other members of the CXC chemokine family, which induce signalling events when bound to CXCR3. It was shown that both CXCL9 and CXCL11 induced transient phosphorylation of Erk 1 and 2 in activated peripheral blood leukocytes [Kouroumalis et al., 2005] and p44/p42 MAPK specifically on activated T cells [Smit et al., 2003].

4.1.3.1 Aim of the study

Since astrocytes actively synthesise and secrete CXCL10, the effect of CXCL10 on astrocytes was determined *in vitro*. This aim was addressed by the following objectives:

1. the rate of synthesis and expression of CXCR3 under pro-inflammatory conditions was investigated using qRT-PCR, flow cytometry and immunocytochemistry.
2. the functional effect of CXCL10 binding to astrocytes was investigated by measuring phosphorylation of Erk1 and 2 and Akt and calcium flux following CXCL10 treatment.

4.2 Materials and methods

4.2.1 Determination of CXCR3 mRNA expression by astrocytes following pro-inflammatory stimulation using qRT-PCR

The same procedure was followed as described in section 2.2.6.5. Primers used for CXCR3 are given below:

Forward: 5'-CTTCGCCAAAGTCAGCCAAG-3' (T_m, 60.3°C)

Reverse: 5'-TGGTAGAGGAATCGGGAGGT-3' (T_m, 59.8°C)

Briefly, 2.5 μ l of cDNA was combined with 0.5 μ M of each primer, 3mM MgCl₂ and 1X absolute SybrGreen. qRT-PCR conditions were as follows: hold 95°C 15 min; 40 cycles of 95°C 15s, 60°C 15s, 72°C 30s; 1 cycle 95°C 30s; 1 cycle 50°C 30s and the melt ramp from 50°C to 95°C at 1°C/10s to determine the product specificity. All samples were run on the iCycler (Biorad). Primer efficiency was determined following the procedure described in section 2.3.2.2 with 5 dilutions (neat, 1:2, 1:4, 1:5 and 1:8). qRT-PCR was performed in duplicate on each mRNA sample from astrocytes (SMS-12) stimulated for 24 and 48 h with IL1- β , TNF and IFN γ from 0 to 100ng/ml (n=3) following the procedure described in section 2.2.6.5.

4.2.2 Detection of CXCR3 expression by primary human adult astrocytes using immunocytochemistry

CXCR3 expression by unstimulated astrocytes (B327/01) was assessed by immunocytochemistry following the procedure described in section 2.2.2.2. Incubation with monoclonal antibody IgG₁ anti human CXCR3 (R&D Systems, UK) at 1:100 dilution in PBS-1%BSA for 1.5 h at RT was followed by FITC-labelled goat anti mouse IgG (Chemicon, UK) at a dilution of 1:100 in PBS-1%BSA for

1 h at RT in the dark. CXCR3 expression was visualized with the Axiovert 200 M (Zeiss) confocal microscope and LSM 510 laser module as described in section 2.2.3.1.

4.2.3 Quantitation of CXCR3 chemokine receptor expression by primary human adult astrocytes using flow cytometry

The same procedure was followed for CXCR3 staining as described in section 3.2.2.7. Briefly, 0.25×10^6 astrocytes (B327/01) were stimulated in triplicate with 0, 10 and 100ng/ml of IL1- β , TNF and IFN γ for 24 h (n=3). Astrocytes were harvested by trypsinization and incubated with 10 μ l of PE-labelled IgG mouse anti-human CXCR3 antibody (R&D Systems) for 1.5 h in dark on ice. Astrocytes were stained in parallel with the corresponding isotype control (PE-labelled mouse IgG₁) to evaluate background staining. For intracellular staining, cells were fixed with 4% paraformaldehyde for 15 min at RT and permeabilized for 5 min in PBS-0.5% TritonX100 at RT. CXCR3 expression under pro-inflammatory stimulation was quantitated by FACScalibur flow cytometry and Cell QuestTM software (BD Biosciences, UK) as described in sections 3.2.2.5 and 3.2.2.6.

4.2.4 Analysis of CXCL10-induced calcium flux in primary human adult astrocytes

The same procedure was performed as described in section 3.2.5. Briefly, 3×10^4 astrocytes (B327/01)/200 μ l/well in a black wall 96 well plate (Nunc, UK) were incubated for 30 min in the dark at RT with 5 μ M Fluo-4AM (Molecular Probes, UK) in Krebs HEPES buffer with 0.25mM sulfinpyrazone (Sigma, UK), 1% F12 pluronic (Sigma, UK). Cells were washed twice with Krebs-HEPES buffer supplemented with sulfinpyrazone (0.25mM) and 0.1%BSA to remove the excess of dye, that was not associated with cells. CXCL10 and ionomycin were respectively injected at 20 and 150s (volume injected corresponded to one fifth of the volume of

media). Measurement of the calcium signal was taken every second for 5 min using an excitation filter of $485 \pm 12\text{nm}$ and an emission filter of 520nm . The amplitude of the response following CXCL10 addition was expressed as a percentage of the maximum response with ionomycin (Sigma Aldrich, UK), which corresponds to the internal positive control (n=3).

4.2.5 Erk and Akt phosphorylation analysis following CXCL10 stimulation of primary human adult astrocytes

The same procedure for determination of the level of phosphorylation of Erk and Akt was followed as described in section 3.2.6. Briefly, astrocytes (B327/01 and Ep15) were plated in 6 well-plates (0.25×10^6 cells/1ml/well) and allowed to adhere for 24 h. Media was removed and cells were cultured for 24h in SFM and stimulated for 15 min with CXCL10 at 0 to 100ng/ml (Peprtech, UK) and FCS (10%) used as a positive control. Western blotting was performed using the same antibodies used in section 3.2.6.3. Experiments were done in duplicate.

4.2.6 Statistical analysis

Data are shown as mean \pm SEM. For experiments on CXCR3 mRNA level expression, CXCR3 expression and phosphorylation of Erk and Akt, level of significance for comparisons between samples was determined using the ANOVA parametric test with Dunnett's test. In all cases, $P \leq 0.05$ was considered significant.

4.3 Results

4.3.1 CXCR3 expression by stimulated primary human adult astrocytes at both mRNA and protein level

4.3.1.1 CXCR3 mRNA expression by stimulated astrocytes using qRT-PCR

CXCR3 mRNA was constitutively expressed in primary human adult astrocytes (SMS-12). No increase in CXCR3 mRNA expression was observed following IL1- β or TNF stimulation. Although IFN γ induced a dose dependent increase in CXCR3 mRNA expression following 24 and 48 h stimulation, it did not reach statistical significance.

4.3.1.2 CXCR3 protein expression by primary human adult astrocytes following pro-inflammatory cytokine stimulation

CXCR3 immunostaining on unstimulated astrocytes (B327/01) was assessed by immunocytochemistry (figure 4.2a-d). Permeabilized astrocytes showed strong staining (Figure 4.2b-d) compared to the negative control (Figure 4.2a).

Similar findings were observed with flow cytometry experiments. Astrocytes (B327/01) constitutively expressed CXCR3 (figure 4.3). However, only a small fraction of CXCR3 was expressed at the cell surface (MFI value of 3, green line) compared to the total staining (MFI value of 101.2, blue line). Thus, CXCR3 surface expression represents 3% of the total cellular CXCR3. Following 24 h stimulation, the expression of cell surface CXCR3 did not show a significant difference following treatment with IL1- β (3.7 ± 0.6 MFI), TNF- α (3.3 ± 1 MFI) and IFN γ (3.4 ± 0.4 MFI) at 10ng/ml, compared to the unstimulated astrocytes (4.6 ± 1.1 MFI).

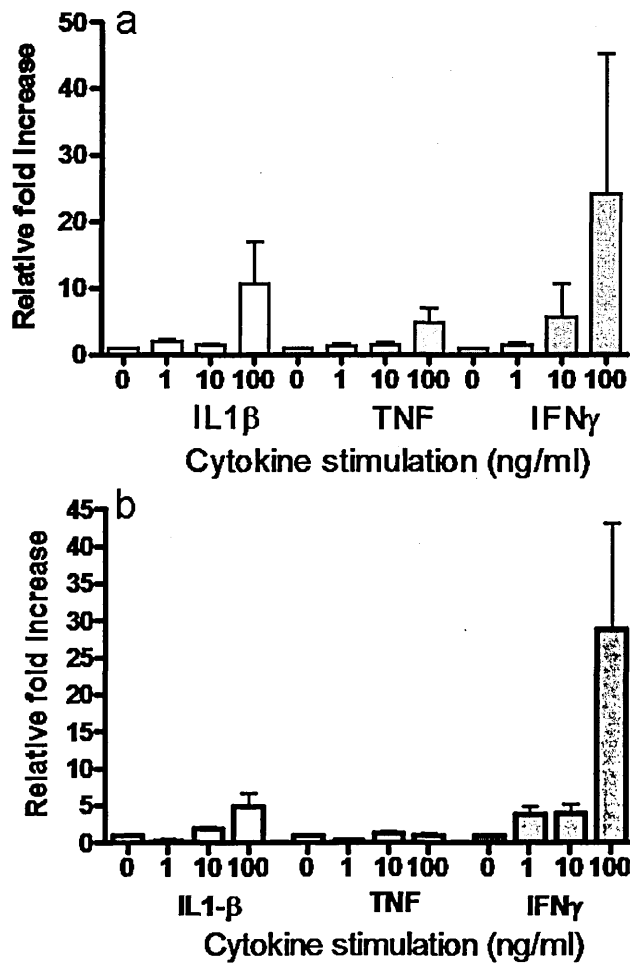


Fig. 4.1: Effect of pro-inflammatory cytokines on CXCR3 mRNA expression by primary human adult astrocytes using qRT-PCR.

Astrocytes (SMS-12) were stimulated three times with IL1- β (white), TNF (grey) and IFN γ (dark grey) at 0 to 100ng/ml for 24h (a) and 48h (b) with qRT-PCR performed in duplicate. CXCR3 was increased but did not reach the statistical significance using ANOVA followed by Dunnett's test but no significance difference was observed.

Following 48 h stimulation with IL1- β , TNF and IFN γ , no difference was observed compared to the baseline using ANOVA followed by Dunnett's test (SFM, 6.2 ± 0.2 MFI; IL1 β , 4.8 ± 0.6 MFI; TNF, 4.6 ± 0.8 ; IFN γ , 6.6 ± 0.7).

Total expression of CXCR3 on permeabilised astrocytes was assessed following 24 h stimulation with IL1- β , TNF and IFN γ at 100ng/ml. No difference was observed in total CXCR3 expression following 24 h stimulation at 100ng/ml stimulation using ANOVA followed by Dunnett's test (data not shown).

4.3.2 Effect of CXCL10 treatment on intracellular calcium increase in astrocytes

The effect of stimulation of astrocytes (B327/01) with CXCL10 at 0 and 100ng/ml (n=3) on Ca²⁺ flux was assessed using the Fluostar plate reader. No difference in the calcium flux in astrocytes was observed following CXCL10 stimulation (100 ng/ml) and the control. Indeed, Ca²⁺ response from unstimulated astrocytes (n=3) represents $22.23 \pm 4.9\%$ of the maximal response (ionomycin) whereas Ca²⁺ response from astrocytes treated with CXCL10 (100 ng/ml) represents $26.67 \pm 1\%$ (n=3) of the maximal response (data not shown).

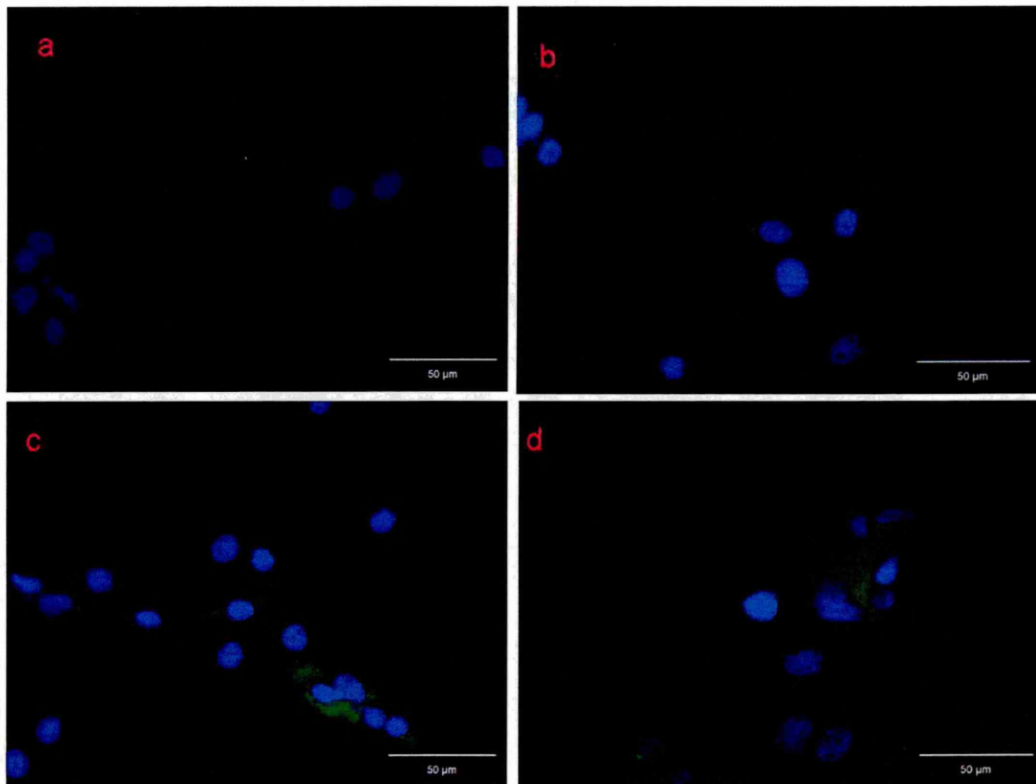


Fig. 4.2: Detection of astrocyte expression of CXCR3 using immunocytochemistry.

Astrocytes (B327/01) were permeabilized and stained with monoclonal IgG₁ antibody against human CXCR3 followed by FITC-labelled goat anti mouse (b-d). Omission of the primary antibody was used as negative control (a). Nuclei were counterstained with DAPI (blue). CXCR3 staining was visualized with the Axiovert 200M (Zeiss) confocal microscope with LSM 510 laser module as described in section 2.2.3

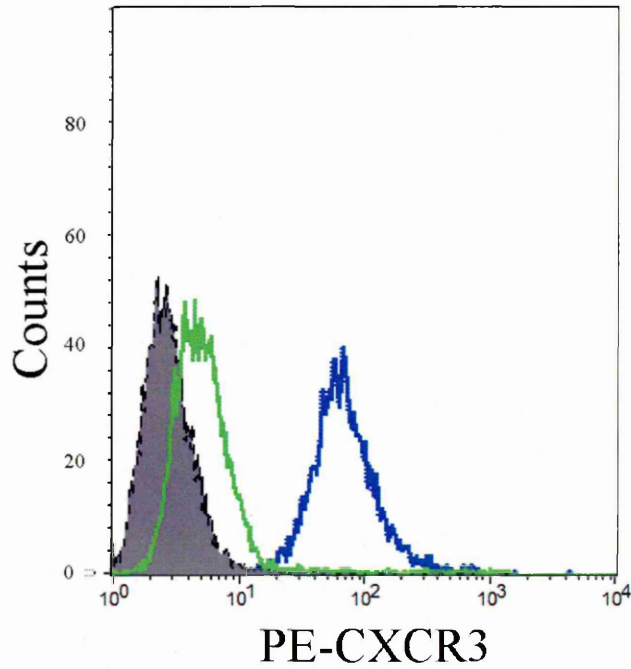


Fig. 4.3: Detection of CXCR3 expression at the cell surface and intracellularly on primary adult astrocytes using flow cytometry.

Histogram representation of CXCR3 protein expression by flow cytometry on unstimulated astrocytes (B327/01). Astrocytes were stained directly with PE-labelled IgG₁ monoclonal antibody against human CXCR3 with (blue histogram) and without fixation/permeabilization (green histogram). The negative control was run in parallel by incubating astrocytes with PE-labelled IgG1 isotype control (filled histogram). Staining was quantitated by flow cytometry and Cell QuestTM software.

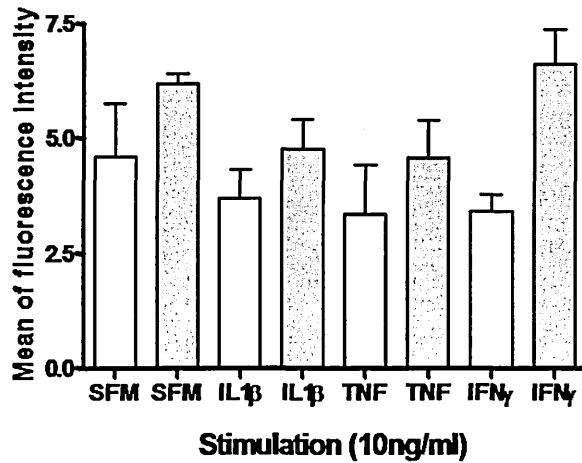


Fig. 4.4: Effect of pro-inflammatory cytokines on CXCR3 cell surface expression by primary human adult astrocytes using flow cytometry. Astrocytes (B327/01) were stimulated with IL1 β , TNF and IFN γ at 10ng/ml for 24 h (white histogram) and 48 h (grey histogram). Experiments were done in triplicate and the effect on CXCR3 expression following stimulation was analyzed by ANOVA followed by Dunnett's test. No significant difference in CXCR3 cell surface expression following cytokine stimulation at 24 and 48 h stimulation was observed compared to the baseline using ANOVA followed by Dunnett's test.

4.3.3 Measurement of phosphorylation of Erk and Akt following CXCL10 stimulation of astrocytes

To confirm the lack of Ca^{2+} flux following CXCR3 ligand binding, the effect of CXCL10 stimulation on astrocytes (SMS-12, B327/01 and Ep15) on downstream signalling pathways was assessed. No difference was observed in the level of phosphorylation of Erk in Ep15 (n=2), SMS-12 (n=2) and in B327/01 astrocytes (n=1) (figure 4.5). Quantitative analysis by densitometry of Ep15 showed that there was no difference in the phosphorylation between CXCL10 stimulated and unstimulated cells. The absence of phosphorylation of Erk following CXCL10 stimulation was not due to a technical problem as FCS, used as a positive control, induced a significant increase in expression of phosphorylated forms of Erk ($P \leq 0.01$, n=2).

Similarly to Erk, CXCL10 stimulation of Ep15 (n=2) and B327/01 (n=1) did not induce any increase in the phosphorylated form of Akt, compared to unstimulated cells. However, although FCS increased the level of phosphorylation of Akt it did not reach statistical significance (figure 4.6).

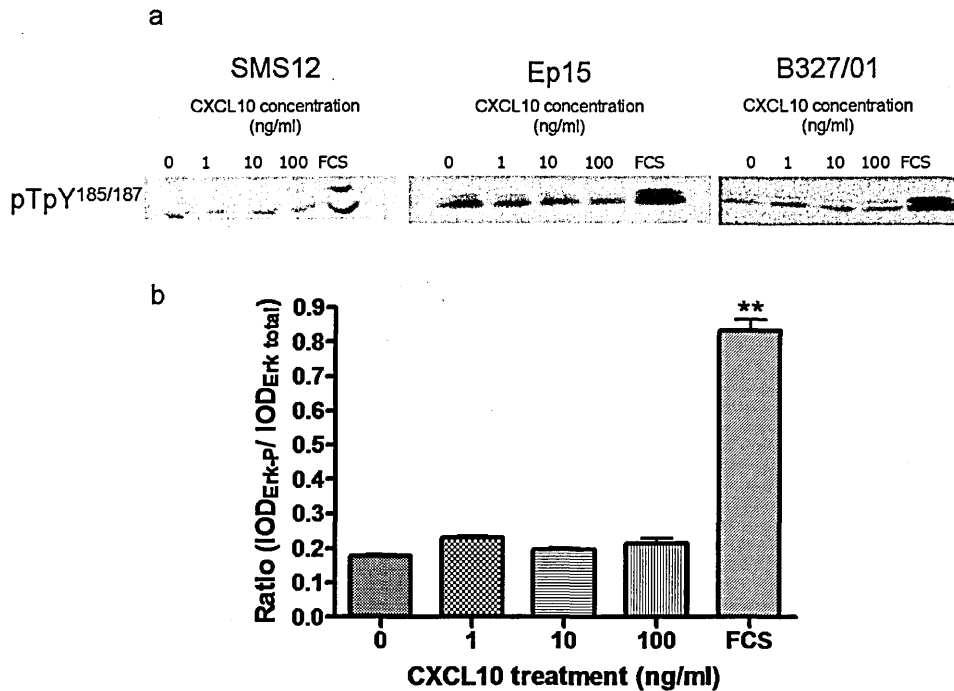


Fig. 4.5: Effect of CXCL10 treatment on Erk 1 and 2 phosphorylation by primary human adult astrocytes using SDS PAGE and western blotting.

CXCL10-induced intracellular signalling was assessed on primary human adult astrocytes (Ep15, SMS-12 and B327/01). Astrocytes were serum starved for 24 h and stimulated with CXCL10 at 0-100ng/ml or FCS (10%) as a positive control. (a) Erk 1 and 2 (pTpY^{185/187}) as well as the total amount of Erk were assessed by SDS PAGE and western blotting. (b) To compare phosphorylation following pro-inflammatory stimulation, IOD values of Erk 1 and 2 (pTpY^{185/187}) were normalized to the IOD values of Erk total (Ep15, n=2). ANOVA followed by Dunnett's test was performed and $p \leq 0.01$ was considered as significantly different.

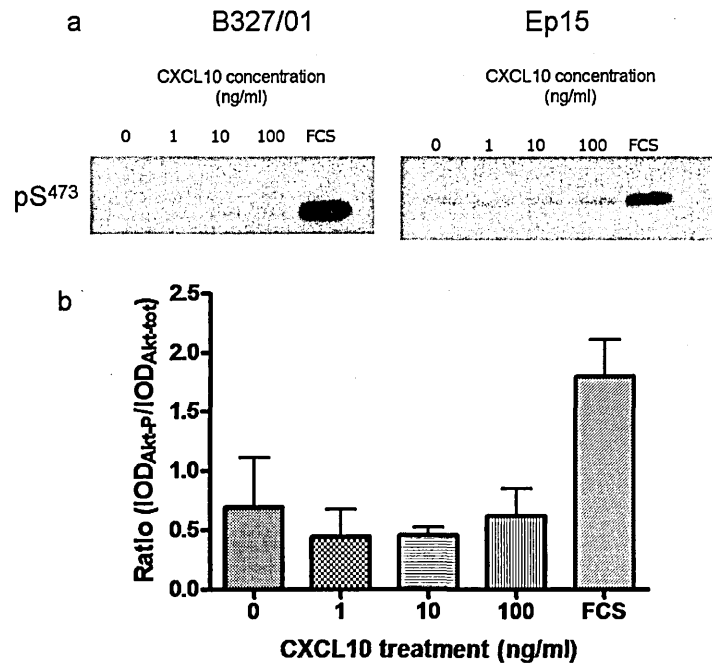


Fig. 4.6: Effect of CXCL10 treatment on Akt phosphorylation by primary human adult astrocytes using SDS PAGE and western blotting. CXCL10 induced intracellular signalling was assessed on primary human adult astrocytes (Ep15, SMS-12 and B327/01). Astrocytes were serum starved for 24 h and stimulated with CXCL10 at 0-100ng/ml or FCS (10%) as a positive control. (a) Akt (pS⁴⁷³) as well as the total amount of Akt were assessed by western blotting. (b) To compare phosphorylation following pro-inflammatory stimulation, IOD values of Akt (pS⁴⁷³) were normalized to the IOD values of Akt total (Ep15, n=2). Although there is an apparent increase for FCS, ANOVA followed by Dunnett's test was performed and no significant difference in the phosphorylation of Akt was obtained.

4.4 Discussion

Post-mortem tissue analysis using immunohistochemistry has demonstrated the accumulation of CXCR3⁺ T cells in active MS lesions [Balashov et al., 1999, Sorensen et al., 1999]. The Expression of CXCR3 on CD3⁺ T cells correlates with the evolution of the severity of MS determined by quantitative immunohistochemistry on MS brain tissue sections [Sorensen et al., 2002]. Expression of CXCR3 was also found on microglia and astrocytes within the plaques in active MS lesions [Simpson et al., 2000b, Sorensen et al., 2002].

Astrocytes have been previously shown to express CXCL10 under IFN γ stimulation (section 2.3.5). To assess whether CXCL10 had any functional effects on astrocytes, CXCR3 expression as well as CXCL10 effects on downstream signalling were assessed on primary human adult astrocytes.

4.4.1 CXCR3 mRNA expression by astrocytes following pro-inflammatory cytokine treatment

CXCR3 mRNA expression was assessed by qRT-PCR following stimulation of cells for 24 and 48 h with IL1 β , TNF or IFN γ from 0 to 100 ng/ml. Astrocytes constitutively expressed CXCR3 mRNA, which confirmed previous *in vitro* studies on simian adult and human foetal astrocytes [Croitoru-Lamoury et al., 2003] or mouse and human adult astrocytes [Biber et al., 2002] using semi quantitative PCR. In this study, CXCR3 mRNA expression was unaffected by stimulation with IL1 β , TNF and IFN γ (0 to 100ng/ml) by primary human adult astrocytes. Again Croitoru-Lamoury et al. (2003) also reported that CXCR3 was unchanged in adult simian and foetal human astrocytes following stimulation with IL1 β , TNF and IFN γ (100IU/ml). These results are contradictory to those of Flynn et al. (2003) where primary human adult astrocytes stimulated with TNF (25ng/ml) increased expression of CXCR3 mRNA using non quantitative RT-PCR.

4.4.2 CXCR3 protein expression by astrocytes following pro-inflammatory cytokine treatment

CXCR3 protein was constitutively detected in astrocytes using flow cytometry and immunocytochemistry. This finding is in agreement with previous studies where it was reported that astrocytes expressed CXCR3 *in vivo* by immunohistochemistry [Goldberg et al., 2001, Simpson et al., 2000b]. However, CXCR3 cell surface expression was largely unaffected following 24 and 48 h stimulation with IL1- β , TNF and IFN γ (10 and 100 ng/ml). Similarly, cytoplasmic CXCR3 expression level on astrocytes did not show any difference following stimulation with the three pro-inflammatory cytokines. Cytoplasmic CXCR3 level of expression was similar to that reported by Flynn et al. (2003) who reported a level of expression of CXCR3 around 100 MFI. However, the level of expression of CXCR3 following stimulation is in contradiction with their study using the same antibody against CXCR3 where they found that TNF (25ng/ml) and IFN γ (200UI/ml) significantly increased the expression of CXCR3 in permeabilized astrocytes by 6 fold and 2 fold respectively. Although primary human adult astrocytes used in both studies were isolated using the same procedure, discrepancies could be explained by different donors of astrocytes.

In this study the proportion of CXCR3 expressed at the cell surface was low compared to the total amount of CXCR3 and represented only 3% of the total expression (permeabilized astrocytes) for unstimulated astrocytes.

Similar findings were observed with the IFN γ R2, one chain of the IFN γ receptor. Rigamonti et al. (2000) showed that the expression of IFN γ R2 was low at the cell surface but highly expressed and stored in the cytoplasm of resting and activated T cells. The low expression of IFN γ -R2 makes Th1 cells resistant to IFN γ reducing their apoptosis [Rigamonti et al., 2000]. Thus, low expression of CXCR3 at the astrocyte cell surface (3% of the total CXCR3) might be a regulatory mecha-

nism that makes astrocytes non responsive to CXCL10.

4.4.3 Measurement of signalling pathways induced by CXCL10 in astrocytes

To validate this hypothesis, CXCL10 effects on intracellular calcium levels in primary human adult astrocytes was assessed. No increase in calcium was detected following CXCL10 stimulation at 100ng/ml. To confirm this finding, phosphorylation of Erk and Akt was assessed. No increase in the phosphorylation of either Erk or Akt was observed. This was not due to technical issues as FCS significantly increased the phosphorylation of Erk. Akt phosphorylation was also increased with CXCL10 but it did not reach statistical significance. These findings are in contradiction with Flynn et al. (2003) who reported that CXCL10 induced Erk phosphorylation in astrocytes. The fact that in our study no calcium flux or phosphorylation of Erk or Akt was detected could be explained by a low expression of CXCR3 at the cell surface (less than 3% of total CXCR3), which would not be sufficient to induce any functional activity. Although Flynn et al. (2003) only assessed CXCR3 expression on permeabilised astrocytes but not at the cell surface, the difference in signalling between this study and the Flynn study might result from a differential expression of CXCR3 at the cell surface between different astrocyte preparations.

Indeed, the level of expression of the cell surface receptor is an important factor for measurement of successful signalling. It was shown that in a dendritic cell line (D1 cells) treated with LPS (10 μ g/ml) for 2-3 h a decrease in CCR1 expression was seen. The expression of CCR1 was dramatically decreased following 24 h stimulation [Foti et al., 1999]. Interestingly, the levels of calcium increase followed the pattern of CCR1 expression with a decrease after 2-3 hours and total loss of calcium flux after 24 h stimulation with LPS. Similar findings were obtained from Salentin et al. (2003) where it was shown that CCR2 was markedly down-regulated in monocytes following incubation with Influenza A virus strain

A/PR/8 (H1N1). The calcium flux correlated with the level of expression of CCR2 with an absence of calcium flux with A/PR/8 [Salentin et al., 2003].

Thus, although astrocytes express CXCR3, CXCL10 did not have any effect on Ca^{2+} flux, Erk and Akt phosphorylation in the astrocyte preparations used in this study. Therefore, CXCL10 secreted by astrocytes *in vitro* would appear not to have autocrine effects. However, CXCL10 might bind to cell surface proteoglycan to establish a chemotactic gradient for immune cells. Further experiments on CXCL10 binding to astrocytes are required to validate this hypothesis as discussed in the chapter 6. However, no CXCL10 biotinylated is yet available. Binding of CXCL10 can be performed only with radiolabelled ^{125}I -CXCL10. Therefore the direct comparison with CCL2 binding to astrocytes using another methodology would be difficult.

4.4.4 Effect of CXCL10 on other CNS resident cells

CXCL10 acts on other CNS cell types including microglia and neurons. For example, CXCL10 acts on microglia to recruit these cells to the axonal injury site in the entorhinal cortex mouse model. In CXCR3^{-/-} mice, a marked reduction in the recruitment of microglia compared to the WT mice was seen especially in the outer molecular layer in the brain of the KO animal, with only a few microglia cells recruited compared to the WT, which presented a full layer of microglia [Rappert et al., 2004]. A similar finding was also reported by Biber et al. (2002) where they showed that *in vitro* microglia expressed CXCR3 and responded to CXCL10 by increasing intracellular calcium transients and chemotaxis. Studies have shown that neurons express CXCR3 in brain tissue in CNS disease [Goldberg et al., 2001, Xia et al., 2000]. Isolation of primary mouse cortical neurons and *in vitro* stimulation with rodent CXCL10 (25nM) for 15 min induced a strong phosphorylation of Erk 1 and 2 compared to unstimulated neurons. This finding suggests a possible mechanism of neuronal-glia cell interaction through CXCL10 derived from astrocytes.

Taken together, this *in vitro* data and published data, suggests that astrocyte derived CXCL10 acts in a paracrine way on CXCR3⁺ cells, including microglia and neurons rather than in an autocrine way on astrocytes within the CNS.

CHAPTER 5

Expression of decoy chemokine receptor D6

5.1 Introduction

Since chemokines play an important role in recruitment of immune cells to sites of inflammation, mechanisms exist to control their expression level in tissues. Decoy receptors are well characterized in mammalian cells as regulators of chemokine levels in tissues [Mantovani et al., 2001]. IL1 type II receptor was the first cytokine decoy receptor to be reported [Colotta et al., 1993]. There are three different types of chemokine decoy receptor that have been described to date, namely Duffy antigen receptor chemokine (DARC) [Neote et al., 1994], CCX CKR [Gosling et al., 2000] and D6 receptor [Nibbs et al., 1997]. Since D6 exhibits specificity for the CC family and is expressed by astrocytes [Neil et al., 2005], the work in this chapter examined the expression of D6 receptor *in vitro* in primary human adult astrocytes and *in vivo* in human brain tissue sections.

5.1.1 D6 decoy receptor: characteristics

The D6 decoy receptor is a typical 7 transmembrane chemokine receptor [Nibbs et al., 1997]. However, it lacks the cytoplasmic sequence motif that is required for the induction of chemokine signalling i.e. the DRY (Asp-Arg-Tyr) motif in the second intracellular loop and the TXP (Thr-X_{aa}-Pro) in the second transmembrane domain [Mantovani et al., 2001, Nibbs et al., 1997, Borroni et al., 2006]. It binds a wide range of CC chemokines including CCL2 [Mantovani et al., 2006, Locati et al., 2005, Fra et al., 2003]. However, D6 exhibits some specificity and does not bind homeostatic chemokines or other chemokine families such as CXC [Nibbs et al., 1997].

Because D6 binds chemokines but does not induce any signalling, studies were performed to assess the function of D6. Fra et al. (2003) investigated the internalization rate for ¹²⁵I labelled CCL2 bound to L1.2 lymphoma cell line transfected with D6. After 2-4 min at 37°C, 70% of the bound ligand was internalized, 5% was still attached to the membrane and 25% was released into the supernatant. These findings demonstrate the ability of D6 to internalize chemokines. This finding was confirmed in a study by Weber et al. (2004) where they showed that D6 internalized CCL3, which trafficked from the cell surface to the cytoplasm through the endosome. When bound to the D6 receptor, ligands are recycled into the cytoplasm and degraded by an NH₄Cl sensitive pathway suggesting lysosomes are involved [Weber et al., 2004]. Indeed, NH₄Cl is a specific inactivator of the proton pump vacuolar ATPase that inhibits acidification of early endosomes and impairs the transport between early and late endosomes [Bowman et al., 1988].

In another study, D6 was shown to be phosphorylated in the absence of ligand, and this was unaffected when adding the ligand [Blackburn et al., 2004]. Since phosphorylation is required for receptor internalisation [Ferguson, 2001], it is not surprising that D6 was shown to be constitutively internalized through clathrin-coat pits and was rapidly recycled to the cell surface [Galliera et al., 2004].

D6 has the characteristic of a scavenger receptor for CC chemokine family members, which could thus serve an important role in the regulation of inflammation in the CNS in MS.

5.1.2 Role of D6 receptor in inflammation

Evidence for an effect of D6 in the regulation of inflammation was obtained by Jamieson et al. (2005) using the well characterized model of cutaneous inflammation, induced by administration of the phorbol ester 12-O-tetradecanoylphorbol-13-acetate (TPA) to dorsal skin. Injection of TPA in D6 deficient mice resulted in a rapid increase in mRNA expression for CCL2, CCL3, CCL4, CCL5 and CCL11 similar to the control [Jamieson et al., 2005]. However, 24 h after TPA injection, D6 deficient mice had an elevated level of CC chemokines compared to the WT suggesting that D6 deficient mice failed to clear the CC chemokine. Similar findings showed that in the TPA model, mice lacking D6 expression resulted in an increase in leukocyte invasion, necrosis and angiogenesis [Martinez de la Torre et al., 2005].

5.1.3 D6 in EAE

There is a single report on the role of D6 in EAE. In EAE, induced in mice deficient for D6, an unexpected reduction in the severity of EAE was observed due to impaired encephalitogenic responses, compared to the WT littermate [Liu et al., 2006a]. These findings were confirmed by examination of the inflammation and demyelination level in the spinal cord of D6 deficient mice and WT mice using anti-CD45 and anti-MBP antibodies. It was shown that inflammation and demyelination were more extensive in WT mice compared to D6 deficient mice. Therefore, D6 was not involved in the clearance of CC chemokines in the CNS in this model [Liu et al., 2006a]. In adoptive transfer studies, no difference in the EAE disease course in D6^{-/-} and WT was seen when T cells injected from EAE

D6+/- animals [Liu et al., 2006a]. They further showed that transfer of T cells from EAE mice deficient for D6 into D6+/- animals resulted in a weak induction of EAE compared to T cells from WT. This suggests that D6 could be involved in the priming of T cells but not clearance of CC chemokine in this model. This finding was confirmed by a lower IFN γ production in D6 deficient mice compared to the WT mice and a lower proliferative effect of T cells in response to MOG restimulation. Further studies on EAE are needed to fully assess D6 involvement.

5.1.4 D6 in MS

No study has yet investigated the expression and distribution of D6 within the human CNS.

5.2 Aim of the study

The aim of this chapter was to determine whether astrocytes have the ability to regulate CC chemokine levels in the CNS, through the expression of D6 receptors. It was addressed by the following objectives:

1. Determine D6 expression on astrocytes *in vitro* at the mRNA (qRT-PCR) and protein level (flow cytometry and western blot).
2. Measure D6 expression *in vivo* in normal and MS CNS tissue at the mRNA (qRT-PCR), and protein level (immunohistochemistry and western blot) and determine the cell type expressing D6 receptor.
3. Determine the ability of D6 to bind biotinylated CCL2 *in vivo*.

5.3 Materials and methods

5.3.1 Measurement of D6 mRNA expression by astrocytes following pro-inflammatory cytokine stimulation using qRT-PCR

The set of primers used for the amplification of D6 were designed with Primer3 software, and are presented below:

Forward- 5'-AACCAGCTCAATTGGGTGTC-3' (T_m, 57.3°C)

Reverse- 5'-GAAAGCGTGGTATCCTGGAA-3' (T_m, 57.3°C)

cDNA was amplified as follows: hold 95°C 15 min; 40 cycles of 95°C 15s, 60°C 15s, 72°C 30s; 1 cycle 95°C 30s; 1 cycle 50°C 30s and the melt ramp from 50°C to 95°C at 1°C/10s to determine the product specificity. All samples were run on the iCycler (Biorad). The relative expression of D6 against the HK gene UBC, was performed using the Pfaffl equation, described in section 2.2.6.1.

5.3.2 Detection of D6 receptor expression by primary human adult astrocytes using western blotting

5.3.2.1 Protein extraction

Protein was extracted using the Tri-Reagent method. Confluent astrocytes (Ep15) from a 75cm² flask were resuspended in 1ml of Tri-reagent, transferred into an eppendorf tube and 0.2ml of chloroform (Sigma,UK) added to samples, mixed and incubated for 10 min at RT. Samples were centrifuged for 15 min at 12,000 g at 4°C (mini spin plus, Eppendorf, UK) and the protein, in the pink phase, was precipitated by adding 1.5ml isopropanol. Samples were mixed, incubated for 10 min at RT and centrifuged at 12,000 g for 10 min at 4°C. Supernatants were removed and pellets were washed 3 x 20 min in 1 ml of 0.3M guanidine hydrochloride/95% ethanol solution. A centrifugation step was performed for 5 min at 7,500 g at 4°C between washes. Pellets were further washed in 1 ml

of 100% ethanol for 20 min at RT. Samples were centrifuged, supernatants were discarded and pellets were air-dried for 5 min and resuspended in 200 μ l PBS-1% SDS. Proteins were stored at -20°C until used.

5.3.2.2 Protein estimation: bicinchoninic acid (BCA) assay

Protein estimation was performed using the bicinchoninic acid (BCA) assay. 20 μ l of bovine serum albumin (BSA) proteins standards in PBS-1% SDS (ranging from 0 to 2mg/ml) as well as 20 μ l of extracted protein sample in duplicate were loaded in a 96 well plate. 200 μ l of copper II BCA solution (24.5ml BCA (Sigma Aldrich, UK) plus 500 μ l of copper (II) sulfate pentahydrate 4% (W/V) solution (Sigma Aldrich, UK)) was added to the samples. The plate was incubated for 30 min at RT and the absorbance was read with a Victor Wallac² plate reader at 570nm. A standard curve was drawn and protein concentration was determined using the trend line of the equation of the standard curve :

$Y=aX+b$ where Y corresponds to absorbance, a corresponds to the trend line, X corresponds to the concentration of protein in the sample and b corresponds to the intercept point with curve and the X-axis.

5.3.2.3 Sample preparation for western blotting analysis

100 μ l of protein extract sample was mixed with 50 μ l of NuPAGE LDS sample buffer (Invitrogen, UK), 20 μ l of reducing agent (InVitrogen, UK) and 30 μ l of water. Samples were heated at 60°C for 30 min or 3 min at 95°C and stored at -20°C until analysis.

5.3.2.4 SDS-PAGE and western blotting for D6 expression in primary human adult astrocytes

Optimal dilution for the primary antibody directed against human D6 (1:250, 1:500 and 1:1000) was determined by dot plot (10 μ g of protein, 10 μ l loaded). Staining was performed as described previously described in section 3.2.6.3 using rabbit polyclonal antibody directed against human D6 (Abcam, UK) for 90 min

at RT and HRP-goat antibody directed against rabbit IgG (1:2000, Dako, UK) for 1 h at RT. Omission of the primary antibody allowed determination of the background level.

Protein (8, 16 and 32 μg) from Ep15 and 5.5 μl of marker Seeblue plus 2 (Invitrogen, UK), to determine the molecular weight of the protein of interest, were loaded and run on pre-cast NuPAGE 10% Bis-Tris gel (Invitrogen, UK) in MOPS SDS running buffer-0.05% antioxidant (Invitrogen, UK) as described in section 3.2.6.3, for 1 h at 120V and 300mA. To improve the separation of the protein, migration was performed for 2 h at 100V in some experiments. Western blotting was performed as described in section 3.2.6.3 for 1h at 100V and 300mA. The detection of D6 on the blot was performed as described in section 3.2.6.3 using rabbit polyclonal antibody directed against human D6 (1:250, Abcam, UK) for 90 min at RT and HRP-goat antibody directed against rabbit IgG (1:2000, Dako, UK) for 1 h at RT. Three washes of 10 min each were performed after each antibody incubation. Immunoreactivity was detected as described in section 3.2.6.3.

5.3.2.5 Detection of D6 receptor by primary human adult astrocytes using flow cytometry

D6 staining was assessed on primary human adult astrocytes (SMS-12 and B327/01) at the cell surface and intracellularly as described in section 3.2.2. Antibody used was PE conjugated rat IgG_{2a} directed against human D6 (R&D Systems, UK). Non specific binding was assessed by incubating astrocytes with PE-labelled rat IgG_{2a} isotype control antibody (R&D Systems, UK). D6 cell surface expression was also assessed under pro-inflammatory conditions. Briefly, 0.25×10^6 astrocytes/2ml/well were plated in 6 well-plates and allowed to adhere for 24 h in astrocyte cell culture media. Astrocytes were stimulated with IL1 β , TNF and IFN γ stimulation (100ng/ml) for 24 h in SFM. Staining was performed as described in section 3.2.2.

5.3.3 Analysis of D6 expression on human brain tissue

Six different MS cases were obtained from the UK MS Tissue Bank London and used for the determination of the cell type expressing D6. Case details for the different donors are summarised in Table 5.1. Eight blocks were obtained including: four MS lesions (L1 to L4), two normal appearing white matter (NAWM) (N1 and N2) and two normal control white matter (C1 and C2). Another case (MS122 A4E5) was used for optimisation of D6 staining and CCL2 binding as well as colocalisation with D6 and CCL2. MS122 A4E5 brain tissue sample (provided by the UK MS Tissue Bank London) was obtained from a 59 year old male diagnosed with MS who died from bronchial pneumoniae.

5.3.3.1 Tissue characterisation: Oil red O (ORO) staining

All MS and control blocks were provided snap-frozen and stored at -80°C until used. Blocks were sectioned ($10\mu\text{m}$) using a cryostat and placed onto polylysine slides (BDH Laboratories, UK). ORO staining, that is routinely used to detect areas of myelin breakdown and demyelination, was performed on these sections [Van Der Voorn et al., 1999]. ORO solution was prepared by adding 1 g of ORO (Acros Organics, UK) to 60% solution of triethyl phosphate (TEP, BDH Laboratories, UK) in distilled water. The solution was heated at 100°C for 5 min with constant stirring. The solution was filtered when hot and again prior to the staining procedure. Tissue for ORO staining was fixed for 1 h in 4%-PFA at 4°C and incubated in 60% TEP solution for 2 min. Sections were stained with filtered ORO solution for 20 min at RT and washed in 60% TEP solution until all the excess stain was removed. Sections were further washed in distilled water for 5 min. Cell nuclei were counter stained with 20% Harris's haematoxylin (Sigma Aldrich, UK) for 1 min. Sections were washed in distilled water and mounted in glycerin jelly (kept in water bath at 37°C , Fisher Scientific, UK). Sections were visualized using an Olympus BX60 microscope. Sections were classified as (++) for strong demyelination, (+) for low level of demyelination and (-) for no demyelination. Similar classification was performed for the level of inflammation.

Case No	Sex	Age	Block	Characteristic	DTPI (h)	Cause of death
C11	male	77	Co11 A1B5	control	26	Carcinoma of the lung metastasis
C14	female	64	Co14 P2C3	control	18	Cardiac failure
MS74	female	64	MS74 A1E77 MS74 A1C6	NAWM Lesion	7	Gastrointestinal bleed/obstruction, aspiration pneumonia
MS90	male	62	MS90 P2E3	Lesion	17	MS (secondary progressive)
MS130	female	57	MS130 P2F4 MS130 P2E3	NAWM Lesion	22	MS (secondary progressive)
MS100	male	46	MS100 A2D2	Lesion	7	Pneumonia

Tab. 5.1: Case details of donors used to study D6 expression in the CNS.

DTPI (h) = Death to tissue preservation interval (hours)

NAWM = Normal appearing white matter

5.3.3.2 Measurement of D6 mRNA expression in human brain tissue using qRT-PCR

Five sections of 30 μm from each block were collected in an eppendorf tube. 1 ml of Tri-reagent (Sigma Aldrich, UK) was added to each tube and sections were homogenized using a loosely fitting homogenizer (Sigma Aldrich, UK). Since the brain has a high content of lipid, an extra spin was performed at 12 000 g for 10 min at 4°C prior to mRNA extraction and cDNA synthesis procedure as described in sections 2.2.6.2 and 2.2.6.3. mRNA extraction was performed twice for each block and each of these samples run twice on the iCycler as described in section 5.3.1.

5.3.3.3 Detection of D6 in human brain tissue using SDS-PAGE and western blotting

Proteins were extracted using Tri-Reagent (Sigma Aldrich, UK) and quantified as described in section 5.3.2. D6 expression was assessed on six different donors (N1 to N4, NAWM 1 and 2, C 1 and 2) as described in section 5.3.2. To compare the level of expression of D6 in the different blocks, membranes were stripped as described in section 3.2.6.3 and reprobed with polyclonal goat antibody directed against actin (Sigma Aldrich, UK) at 1:1000 for 90 min at RT followed by HRP rabbit anti-goat IgG (whole molecule) 1:80 000 (Sigma Aldrich, UK) for 1 h at RT. IOD values of D6 were normalized to the IOD values of actin, considered as 1. Each protein extraction (n=2) was analysed in duplicate by western blotting.

5.3.3.4 Detection of D6 on human brain sections by immunohistochemistry: optimisation

Optimal dilution for the primary antibody directed against human D6 was initially determined (1:50, 1:75, 1:100 and 1:250). 10 μm sections (MS122 A4E5) were air-dried for 30 min at RT and blocked in PBS-5% BSA (blocking buffer) for 1h at RT. Sections were stained overnight at 4°C with a polyclonal rabbit antibody directed against the D6 receptor (Genetex, USA) diluted at 1:50, 1:75,

1:100 and 1:250 in the blocking buffer. Sections were washed 3 x 5 min with PBS and stained with Alexa-568 goat anti rabbit antibody (1:500, Molecular Probes, UK). Sections were washed and incubated in 0.15% Sudan Black B (SBB) in 70% ethanol (Appendix) to quench lipofuscin autofluorescence in the brain [Romijn et al., 1999]. Sections were washed in PBS until excess SSB dye was removed, mounted with DAPI medium (Vector laboratories, UK) and sealed with nail varnish to avoid drying out. D6 expression was visualized with the Axiovert 200 M (Zeiss) confocal microscope and LSM 510 laser module as described in section 2.2.3.1.

5.3.3.5 Determination of the cell type expressing D6 by double indirect immunofluorescence staining

To determine the cell type expressing D6, sections were double stained for D6 and cellular markers including Neuronal Nuclei (Neu-N), GFAP (Chemicon, UK), HLA-DR (Novastra, UK), for the detection of neurons, astrocytes and macrophages respectively (table 5.2), following the same procedure as described in section 5.3.3.4. First, sections were stained overnight at 4°C with the polyclonal rabbit antibody directed against D6 (Genetex, USA) diluted at 1:75 in blocking buffer. Sections were washed 3 x 5 min with PBS and stained with Alexa 488 goat anti rabbit antibody (1:500, Molecular Probes, UK). Sections were washed and primary antibody directed against the appropriate cellular marker (GFAP, Neu-N or HLA-DR) was applied for 3 h at RT in the dark (table 5.2). Sections were washed 3 x 5 min and Alexa 568 goat anti mouse (1:500) was applied for 1 h at RT in the dark for GFAP and HLA-DR staining. For the Neu-N staining, primary antibody was directly conjugated with Alexa-488. Background level was assessed by incubating primary antibody with the secondary antibody that should not bind to it. Cross reactivity between the two secondary antibodies was also assessed by incubating sections with the two secondary antibody. Sections were washed 3 x 5 min and fluorescent background signal was quenched with 0.15% SBB in 70% ethanol for 10 min at RT. Sections were washed in PBS, mounted

with DAPI media (Vector laboratories, UK) and sealed with nail varnish.

Colocalisation with D6 and the cell markers was assessed using the Zeiss 510 CSLM software. This software analysed each individual pixel of each fluorescent channel used and produces a composite picture with white pixels when colocalisation occurs.

5.3.4 CCL2 binding to human brain tissue sections by immunofluorescence: optimisation of concentration of biotinylated CCL2 and avidin-FITC

Human brain tissue sections (10 μm) were air-dried for 30 min at RT and blocked with PBS-5%BSA (blocking buffer) for 1 h at RT. Different dilutions of biotinylated CCL2 (1:4, 1:10 and 1:20) in blocking buffer were performed overnight at 4°C. A negative control was included by omitting biotinylated CCL2. Sections were washed 3 x 5 min and avidin-FITC (neat), provided by the manufacturer, was added to the cells and incubated 1 h at RT in the dark. Sections were washed as described previously and fluorescent signal was quenched as described in section 5.3.3.4. CCL2 binding was visualized with the Axiovert 200 M (Zeiss) confocal microscope and LSM 510 laser module as described in section 2.2.3.1.

To reduce the background level of bound biotinylated CCL2 to human brain tissue sections, the optimal dilution of avidin-FITC was determined. The same procedure was followed as described above. Biotinylated CCL2 was diluted at 1:4 in blocking buffer and avidin-FITC was used at either 1:2, 1:4 or 1:10 in PBS.

Primary antibody	working dilution	Secondary antibody (Molecular Probes, UK)	Supplier
Polyclonal rabbit anti D6	1:75	Alexa 488 or Alexa 588 goat anti rabbit antibody (1:500)	Genetex, USA
Monoclonal mouse anti GFAP	1:1000	Alexa 568 goat anti mouse (1:500)	Chemicon, UK
Monoclonal mouse anti Alexa fluor 488 Neu-N	1:1000	-	Chemicon, UK
Monoclonal mouse anti HLA-DR	1:500	Alexa 568 goat anti mouse (1:500)	Novastra, UK

Tab. 5.2: Summary table of primary and secondary antibodies used for the detection of the cellular origin of D6 by immunohistochemistry on human brain sections.

5.3.5 Determination of the cell type binding biotinylated CCL2 in human brain sections: dual staining with D6

CCL2 binding was first performed as described in section 5.3.4. Sections were washed 3 x 5 min and D6 staining was performed as described in section 5.3.3.4. Colocalisation was assessed as described in section 5.3.3.5.

5.3.6 Statistical analysis

Data are shown as mean \pm SEM. For experiments on D6 mRNA level expression and D6 expression, level of significance for comparison between samples was determined using the ANOVA parametric test with Dunnett's test. In all cases, $P \leq 0.05$ was considered significant.

5.4 Results

5.4.1 D6 expression on primary human adult astrocytes

5.4.1.1 Measurement of D6 mRNA expression by astrocytes using qRT-PCR

Astrocytes (SMS-12) constitutively expressed D6 mRNA (figure 5.1). The expression was increased following pro-inflammatory stimulation (24 h) with IL1 β , TNF and IFN γ at 100 ng/ml reaching 33.5 ± 7.6 fold increase, 12 ± 5.2 fold increase and 28.1 ± 13.9 fold increase respectively. However, only the effect of IL1 β and IFN γ reached statistical significance ($p \leq 0.01$). Lower dilutions of the three cytokines were assessed (1 and 10 ng/ml) but did not affect the level of expression of D6 mRNA (figure 5.1).

5.4.1.2 Measurement of D6 protein expression by astrocytes using SDS-PAGE and western blotting

Optimisation of the dilution of the antibody directed against D6 (1:250, 1:500 and 1:1000) was performed by dot plot. 1:250 showed the optimal immunoreactivity compared to 1:500 and 1:1000. The negative control showed no immunoreactivity (data not shown). Western blotting experiments were performed on protein from non-stimulated astrocytes (Ep15) using different protein amounts (8, 16 and 32 μ g). Two bands at 53KDa and 60 KDa were observed.

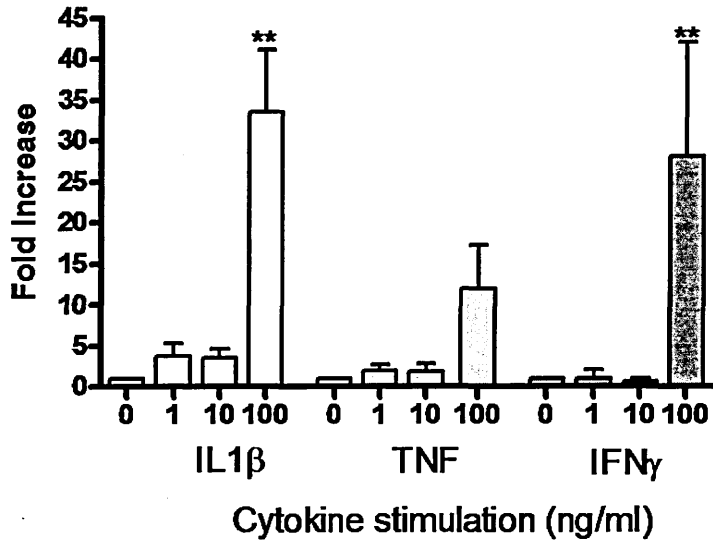


Fig. 5.1: Measurement of D6 mRNA expression in astrocytes by qRT-PCR following pro-inflammatory cytokine stimulation. Cells (SMS-12) were stimulated with IL1- β (white), TNF (grey) and IFN γ (dark grey) at 0 to 100ng/ml for 24h (n=4). ANOVA followed by Dunnett's test was performed. ** $p \leq 0.01$ was considered as significant.

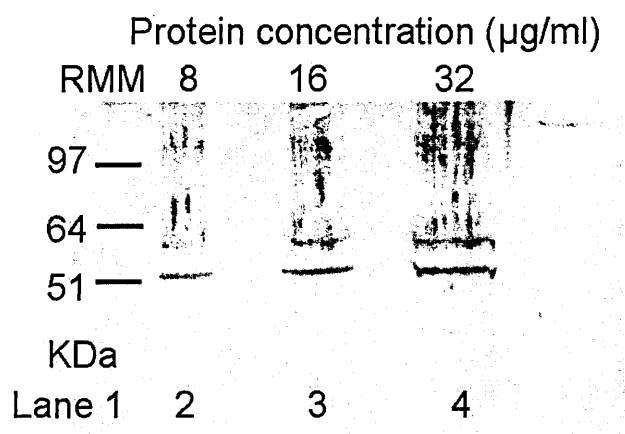


Fig. 5.2: Detection of D6 receptor on astrocytes using SDS-PAGE and western blotting: optimisation of protein concentration.

Different amounts of protein extracted from astrocytes (Ep15) were loaded on to a NuPAGE 10% bis tris acrylamide gel (8, 16 and $32\mu\text{g}$) in lanes 2, 3 and 4. Proteins were transferred on to a nitrocellulose membrane and incubated sequentially with a rabbit polyclonal antibody directed against human D6 (Abcam, UK) and HRP-goat anti rabbit IgG. Molecular weight markers (RMM) lane 1, Seeblue plus 2 (Invitrogen, UK), was used to determine the molecular weight of the bands (KDa). Immunoreactivity was detected by chemiluminescence using the ECL Reagent Kit Plus and UVP imager.

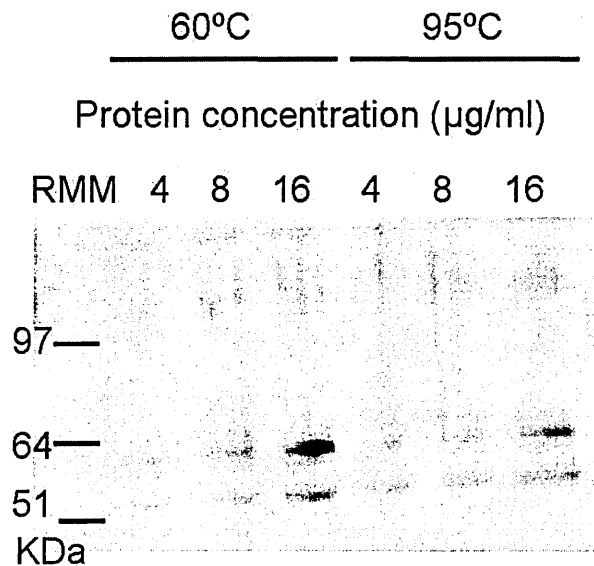


Fig. 5.3: Detection of D6 receptor on astrocytes using western blotting: optimisation of the sample preparation.

Sample preparation times, temperature and range of protein loading concentrations were compared. Protein extracts from astrocytes (Ep15) were loaded onto a NuPAGE 10% bis tris acrylamide gel (4, 8 and 12µg). The gel was run for 2 h at 110 V. Proteins were transferred onto a nitrocellulose membrane and incubated sequentially with a polyclonal antibody directed against human D6 and HRP-goat anti rabbit IgG. (RMM) Relative molecular mass marker, see blue plus 2 (Invitrogen, UK), was used to determine the molecular weight of the bands of interest (KDa). Immunoreactivity was detected by chemiluminescence using ECL Reagent Kit Plus and UVP imager.

Proteins were smeared at the top of the gel which could interfere with the band analysis which was due to over loading of protein (figure 5.2). Thus a lower amount of protein was loaded onto the gel (ranging from 4 up to 16 μg of protein) and a longer time for migration with a lower voltage was performed to improve the separation of the proteins. Two different sample preparations (either heated for 30 min at 60°C or heated for 3 min at 95°C) were compared. No difference in the resolution of the band was observed between the two different sample preparations. Although the smear was still present at the top of the blot, it did not interfere with the two specific bands (figure 5.3).

5.4.1.3 Measurement of D6 protein expression by astrocytes using flow cytometry

D6 was constitutively expressed by astrocytes (B327/01). Histogram representation of D6 expression by flow cytometry showed that D6 was expressed both at the cell surface (green line) and in the cytoplasmic compartment (blue line) (figure 5.4). The filled histogram corresponds to the negative control (PE labelled IgG isotype control). Quantitation of D6 expression was determined both at the cell surface and in the cytoplasmic compartment in two astrocyte preparations (B327/01 and SMS-12) (figure 5.5). Both astrocyte preparations mainly expressed D6 in the cytoplasmic compartment (SMS-12, 12.25 ± 1.1 MFI and B327/01, 12.7 ± 0.6 MFI) compared to the cell surface (SMS-12, 2 ± 0.4 MFI and B327/01, 1.4 ± 0.1 MFI). D6 cell surface expression represented only 11 and 16 % of the total D6 expression in B327/01 and SMS-12 astrocyte preparation respectively.

Following 24 h stimulation with pro-inflammatory cytokines, the expression of D6 at the astrocyte cell surface was unaffected with IL1- β (2.4 ± 0.2 MFI) , TNF (3.1 ± 0.8 MFI) and IFN γ (2.6 ± 0.4 MFI) at 100 ng/ml compared to the control (2.9 ± 0.4 MFI).

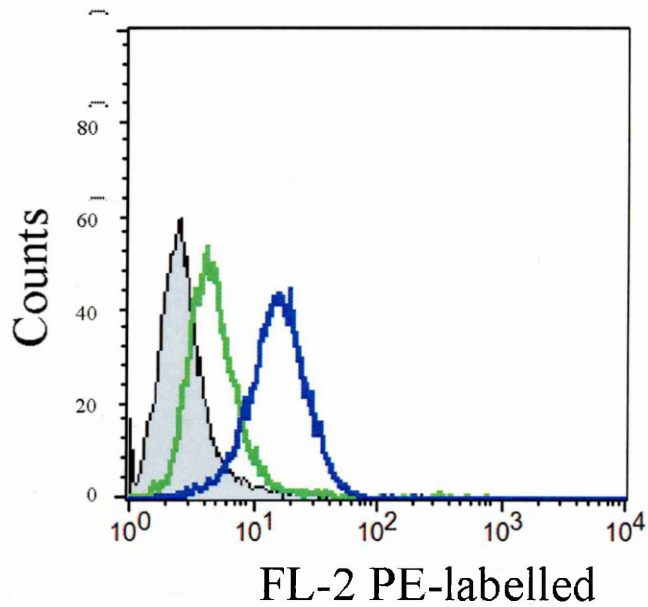


Fig. 5.4: Histogram representation of D6 expression at the cell surface and intracellularly in primary human adult astrocytes using flow cytometry.

Astrocytes (B32/01) were stained directly with PE-labelled rat IgG_{2a} antibody against human D6 (R&D Systems) with (blue histogram) and without fixation/permeabilization (green histogram). A negative control was run in parallel by incubating astrocytes with PE-labelled rat IgG_{2a} isotype control (filled histogram). Staining was quantitated by flow cytometry.

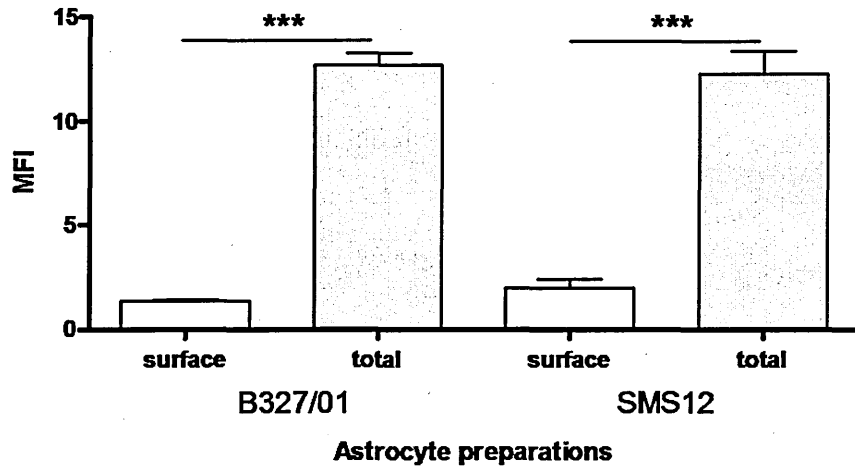


Fig. 5.5: Measurement of D6 expression level at the cell surface and intracellularly on primary human adult astrocytes using flow cytometry. D6 expression level was assessed at the cell surface (white) and in the cytoplasmic compartment (grey) of two astrocyte preparations using directly labelled D6 antibody (R&D Systems, UK)(n=3). A negative control was run in parallel by incubating astrocytes with PE-labelled rat IgG_{2a} isotype control and the background was subtracted from each value. ANOVA followed by Dunnett's test was performed to determine significant differences between the cell surface and the cytoplasmic D6 expression. *** p ≤ 0.01 was considered significant.

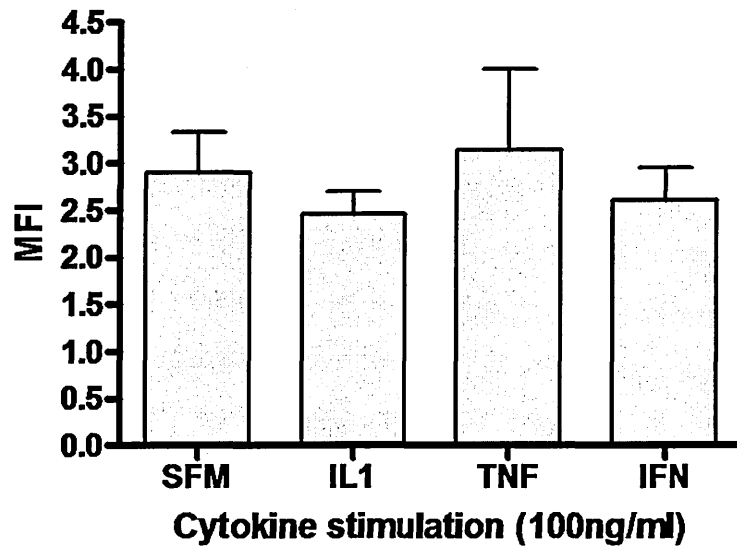


Fig. 5.6: Effect of pro-inflammatory cytokine stimulation on cell surface D6 expression by primary human adult astrocytes using flow cytometry. Astrocytes (B327/01) were stimulated with IL1- β , TNF and IFN γ at 100 ng/ml for 24 h. D6 expression was assessed at the astrocyte cell surface using directly labelled D6 antibody (R&D Systems, UK). Stimulations were done in triplicate and the effect on D6 expression following stimulation was analyzed by ANOVA followed by Dunnett's test. No significant difference was seen.

5.4.2 Analysis of D6 expression on human brain tissue sections

5.4.2.1 Characterisation of brain tissue sections using ORO staining

Eight blocks were stained for ORO to measure the extent of demyelination (figure 5.7). MS90 P2E3 showed strong demyelination ORO (++) compared to MS74 A1C6 and MS100 A2D2 ORO (+) and the remainder of blocks were ORO (-) (no demyelination). Harris's haematoxylin staining, which is commonly used to detect the cellular infiltration, was able to detect perivascular inflammatory cells synonymous with inflammation (MS90 P2E3 and MS130 P2F4). Levels of demyelination and inflammation for the eight blocks are summarised in table 5.3.

5.4.2.2 Measurement of D6 mRNA expression in brain tissue using qRT-PCR.

D6 mRNA expression was assessed in the eight different blocks (figure 5.8). Ct values for the two controls were averaged and the mRNA expression for the control was normalized to 1. The level of expression of D6 mRNA was slightly decreased in the N1 and 2 compared to the control (0.8 ± 0.1 fold increase and 0.3 ± 0.1 fold increase) but it did not reach statistical significance. D6 mRNA was increased for L2 (1.6 ± 0.4 fold increase) and L4 (3.3 ± 0.5 fold increase). However only L4 was statistical significant ($p \leq 0.01$). For L1 and L3, a slight but non significant decrease was observed (0.2 ± 0.04 fold increase and 0.3 ± 0.1 fold increase) compared to the control.

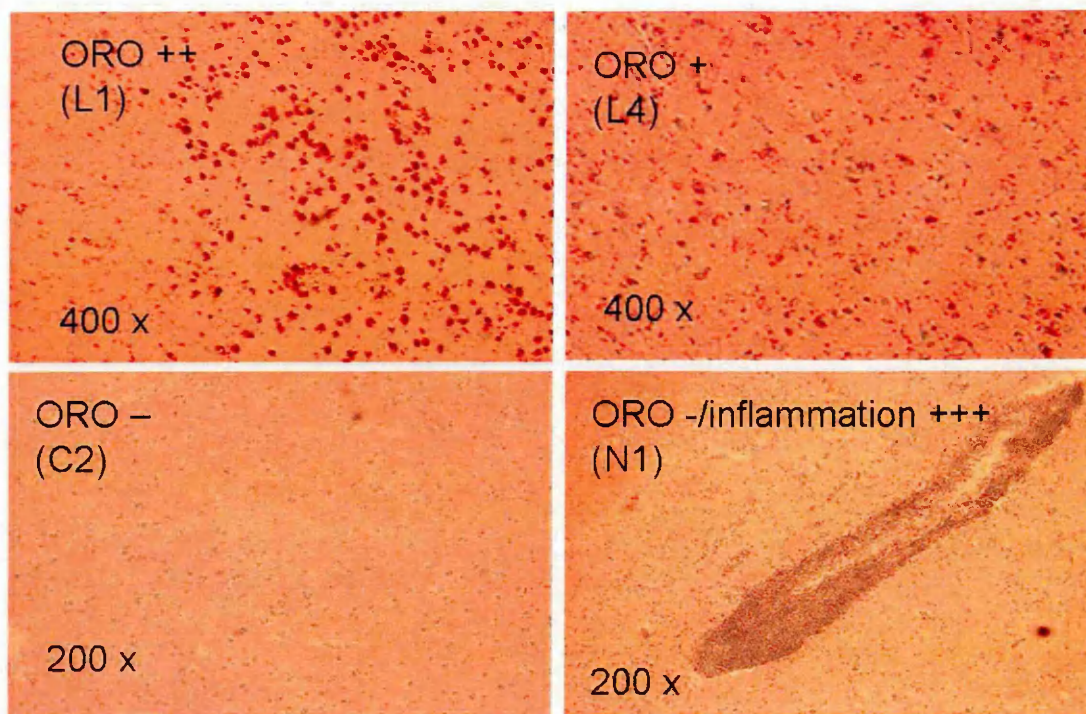


Fig. 5.7: Assessment of demyelination and inflammation in human brain tissue sections: Oil Red O (ORO) staining.

Sections were stained with ORO and haematoxylin. Different grades were given to the sections depending on the extent of demyelination, characterized by red staining due to the accumulation of myelin. MS90 P2E3 (L1) had strong demyelination (ORO++) , compared to MS100 A2D2 (L4) which had low demyelination level (ORO+) and C14 P2C3 (C2) which had no demyelination (ORO-). Inflammation was also assessed and MS130 P2F4 (N1) was shown to have strong perivascular cell infiltration (inflammation). Sections were visualized with the an Olympus BX60 microscope.

Tissue block	type	Code	ORO	inflammation
MS90 P2E3	lesion	L1	++	+
MS130 P2E3	lesion	L2	-	-
MS74 A1C6	lesion	L3	+	-
MS100 A2D2	lesion	L4	+	-
MS130 P2F4	NAWM	N1	-	++
MS74 A1E7	NAWM	N2	-	-
Co11 A1B5	Control	C1	-	-
Co14 P2C3	Control	C2	-	-

Tab. 5.3: Characterisation of eight tissue blocks used in this study by ORO and haematoxylin staining.

Grading of demyelination was assessed by ORO staining corresponding to strong demyelination (+++), low level of demyelination (+) and absence of demyelination (-) respectively. Inflammation corresponds to the presence of perivascular cuffs visualized with haematoxylin staining. Different grades in inflammation were observed (++ strong, + low and - absent).

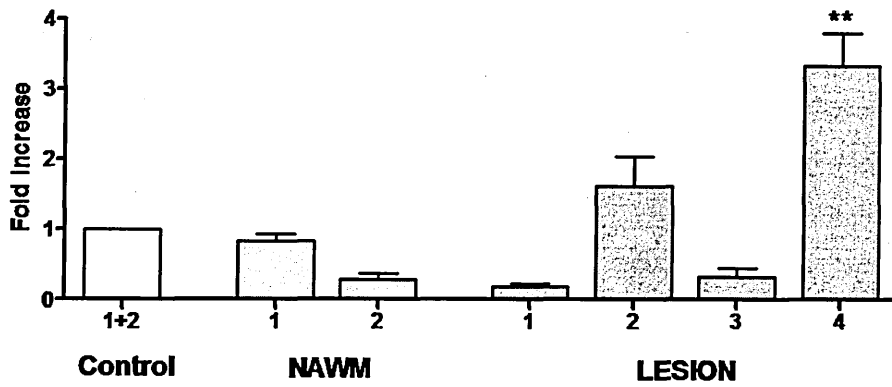


Fig. 5.8: D6 mRNA expression in MS, NAWM and control brain tissue by qRT-PCR.

Extraction of brain tissue mRNA was done in duplicate and cDNA amplification was performed twice per sample (n=4). The HK gene UBC was used as an internal control. Expression of D6 mRNA was normalised to 1 for the control. ANOVA followed by Dunnett's test was performed. ** $p \leq 0.01$ is considered significantly different.

5.4.2.3 Detection of D6 protein expression in brain tissue using SDS-PAGE and western blotting

Two bands of 49KDa and 58 KDa were observed for D6. D6 was expressed in all the samples (figure 5.9). To determine the level of expression in the eight different blocks, IOD values of D6 were normalized to the IOD values of actin, considered as 1. D6 was shown to be expressed in all the lesions but no significant difference in D6 expression level was observed (figure 5.10).

5.4.2.4 Optimisation of D6 staining on human brain sections by immunohistochemistry

Optimisation of the D6 antibody concentration was performed by incubating brain sections (MS122 A4E5) with four different dilutions (1:50, 1:75, 1:100 and 1:250) (figure 5.11). The negative control showed absence of immunoreactivity. 1:50 and 1:75 gave a good signal for detection of D6 compared to 1:100 and 1:250 dilutions, which gave a weak or total absence of staining respectively. 1:75 dilution was selected for further use to determine the cellular origin of D6 in brain tissue sections. D6 staining was associated with the cell body, as indicated by the white arrows. Pictures taken at higher magnification confirmed this finding and further showed that the D6 staining pattern was vesicular (figure 5.11).

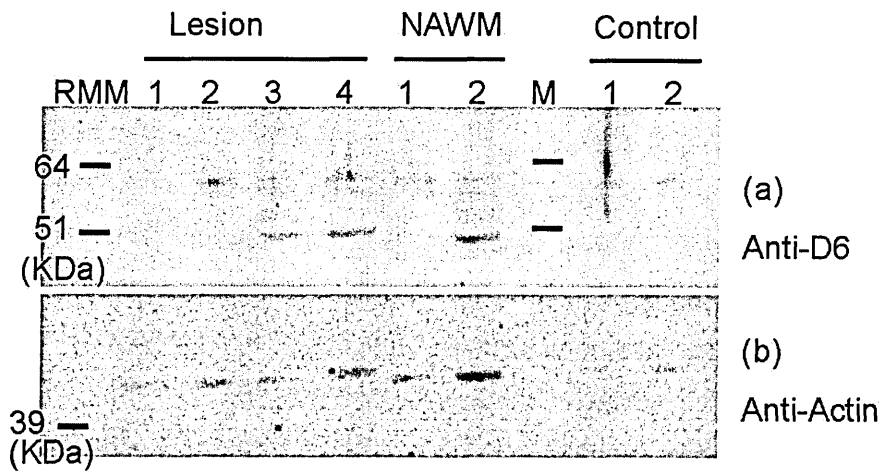


Fig. 5.9: Detection of D6 receptor in MS, NAWM and control human brain tissue using SDS-PAGE and western blotting.

Proteins extracted from brain were loaded onto a NuPAGE 10% bis tris acrylamide gel and run for 2 h at 110 V. Proteins were transferred onto a nitrocellulose membrane and incubated sequentially with a rabbit polyclonal antibody directed against human D6 (Abcam, UK) and HRP-goat anti rabbit IgG (a). (RMM) Marker, Seeblue plus 2 (Invitrogen, UK), was used to determine the molecular weight of the bands of interest (kDa). To assess protein loading for the different samples, membranes were stripped and reprobed with polyclonal goat antibody directed against actin followed by HRP rabbit anti-goat IgG (b). Immunoreactivity was detected by chemiluminescence using ECL Reagent Kit Plus and UVP imager.

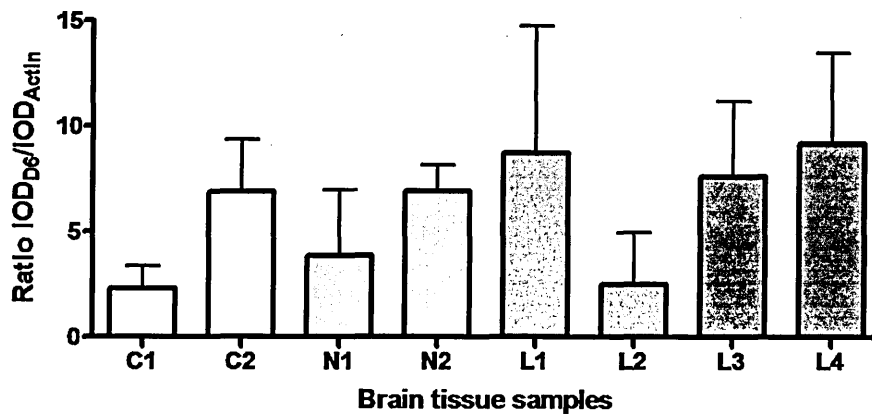


Fig. 5.10: Quantitative comparison of D6 expression between MS, NAWM and control human brain tissue.

To compare D6 expression in the eight different blocks, a normalization step was performed. Western blots were analysed with UVP bioimaging software. IOD values of D6 were normalized with the IOD values of actin. D6 was expressed in all the different sections. However, no significant difference was observed between the different samples (ANOVA followed by Dunnett's test, n=4).

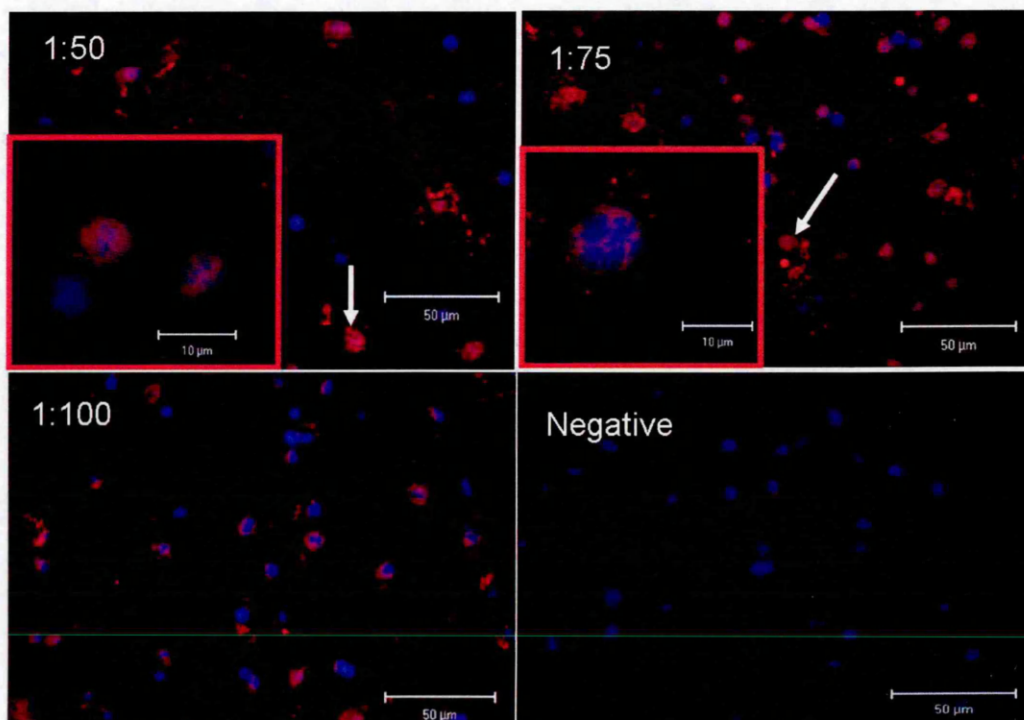


Fig. 5.11: Detection of D6 receptor in human brain tissue sections using immunofluorescence.

Sections (MS122 A4E5) were stained with polyclonal goat antibody directed against D6 at different dilutions (1:50, 1:75 and 1:100) and PE-labelled rabbit anti goat antibody IgG. Negative control was performed by omitting the primary antibody. Autofluorescence was quenched with 0.15% SBB-70% ethanol solution. Nuclei were counter stained with DAPI (blue). Immunofluorescence was visualized with the CSLM following the procedure described in section 2.2.3.1. Fluorescence was associated with the cell body as shown by the white arrows. Higher magnification images are shown in the red frame.

5.4.2.5 Cell phenotype expressing D6 in brain using immunohistochemistry

Dual labelling for D6 and cellular markers, including GFAP (astrocytes), Neu-N (neurons) and HLA-DR (activated microglia/macrophages), was used to determine the cell type expressing D6 in human brain tissue sections. Utilisation of the Zeiss 510 software enabled pixels to be scanned in the different channels and were designated as a white colour when colocalisation was observed. Strong colocalisation was observed with D6 and the neuronal marker (Neu-N) as shown in lesion tissue sections L1 (figure 5.12) indicated with the white arrows. The staining for D6 appeared to be mainly on the grey matter compared to the absence of reactivity for D6 in the white matter. Some Neu-N⁻ cells (green) were positive for D6 (red). A low level of colocalisation was observed with D6 (green) and HLA-DR (red) in L1 lesion (figure 5.13). No staining for HLA-DR was observed in control tissue sections. Complete absence of colocalisation for D6 (green) and GFAP (red) was observed as shown in lesion tissue sections L4 (figure 5.14). Therefore, colocalisation experiments provided evidence for strong D6 neuronal expression, low level expression on microglia/macrophages and no expression by astrocytes.

5.4.3 CCL2 binding to human brain tissue sections

5.4.3.1 Optimisation of the binding of biotinylated CCL2 to brain tissue sections

Three different dilutions of biotinylated CCL2 were tested (1:4, 1:10 and 1:20). Figure 5.15a shows the absence of fluorescence background when biotinylated CCL2 was omitted. The strongest fluorescent signal was observed for the 1:4 dilution (b) compared to 1:10 (c) and 1:20 (d). CCL2 binding was associated with cell nuclei (white arrows). To reduce the fluorescent background, different dilutions of avidin-FITC were tested (1:2, 1:4 and 1:10) with biotinylated CCL2 at 1:4. Figure 5.16 shows that the background level decreased with the lower concentration of avidin-FITC. The three dilutions gave a good signal for detection

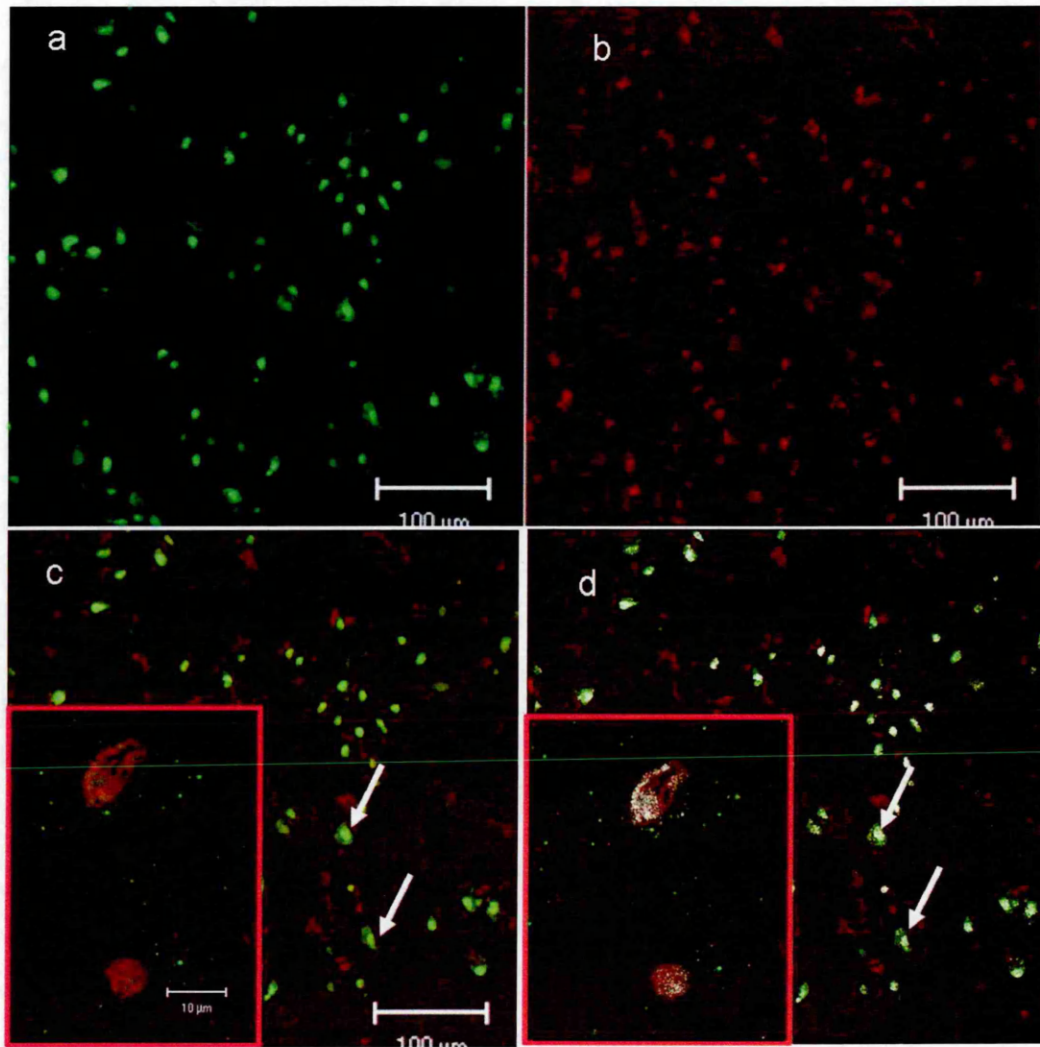


Fig. 5.12: Determination of the neuronal expression of D6 in human brain tissue.

Brain tissue sections (L1) were sequentially stained with antibody directed against D6 (a, red) and Neu-N (b, green). Immunofluorescence was visualized with the CSLM following the procedure described in section 2.2.3.1. The two channels were overlaid (c) and colocalisation (white colour pixels) was observed using the Zeiss 510 software (d).

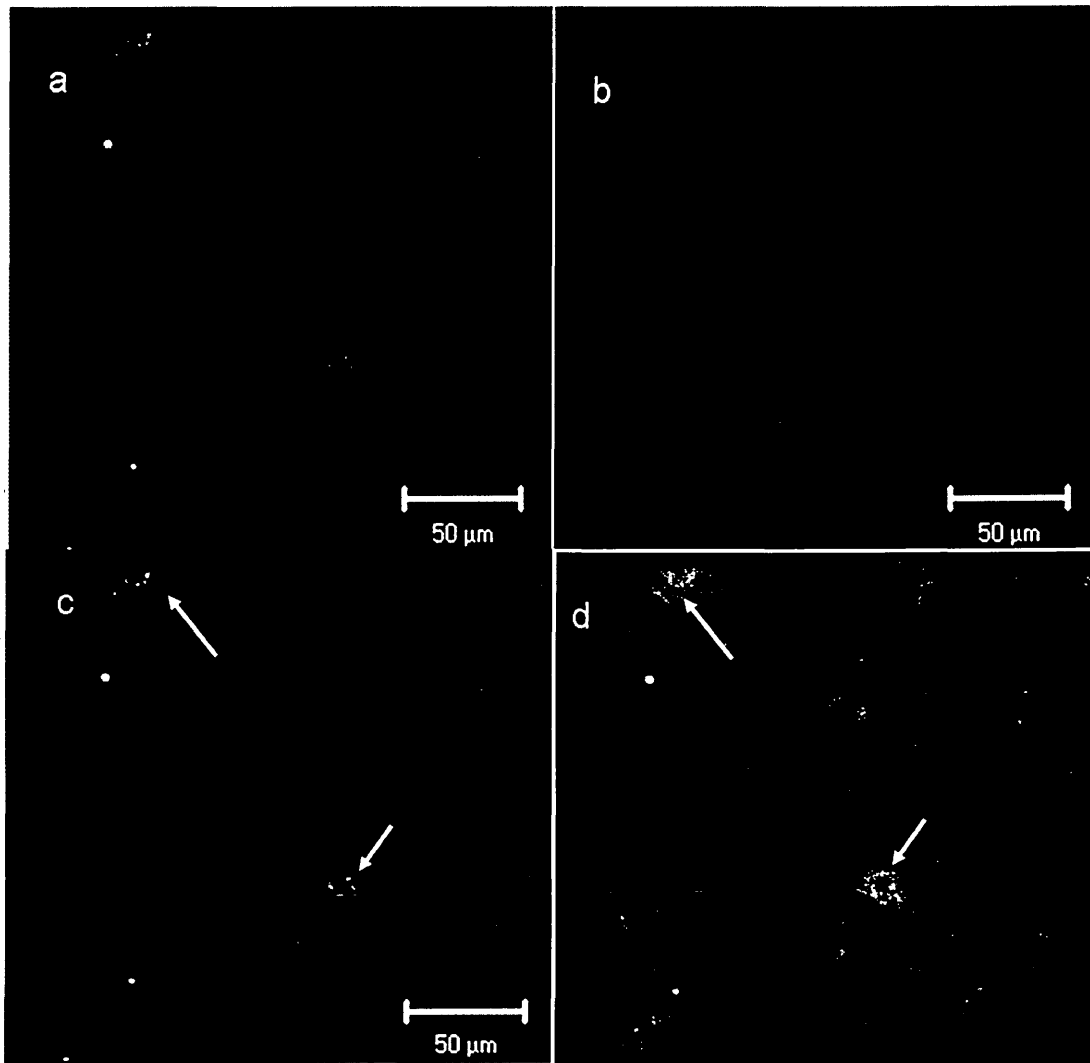


Fig. 5.13: Determination of the microglia expression of D6 in human brain tissue.

Brain tissue sections (L1) were sequentially stained with antibody directed against D6 (a, green) and HLA-DR (b, red). Immunofluorescence was visualized with the CSLM following the procedure described in section 2.2.3.1. The two channels were overlaid (c) and colocalisation (white colour pixels shown by the white arrows) was observed using the Zeiss 510 software (d).

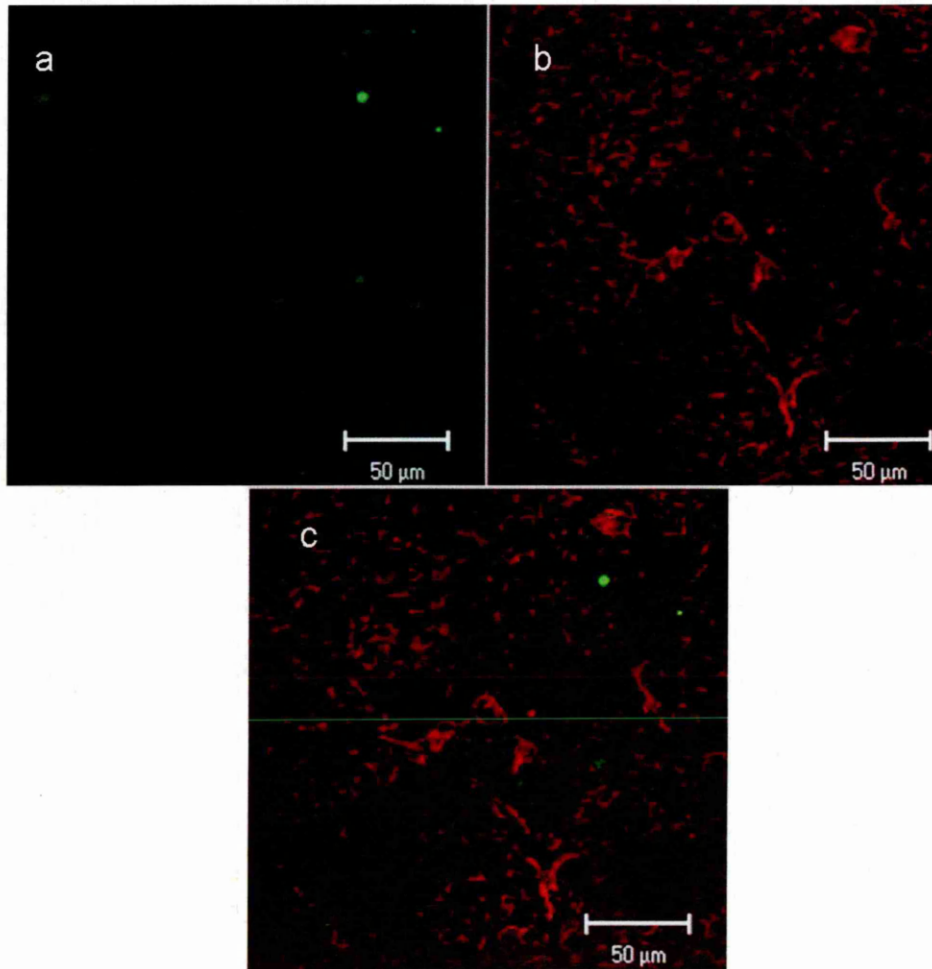


Fig. 5.14: Determination of the astrocytic expression of D6 in human brain tissue.

Brain tissue sections (L4) were sequentially stained with antibody directed against D6 (a, green) and GFAP (b, red). Immunofluorescence was visualized with the CSLM following the procedure described in section 2.2.3.1. The two channels (red and green) were overlaid (c). No colocalisation between D6 and GFAP was observed using the Zeiss 510 software.

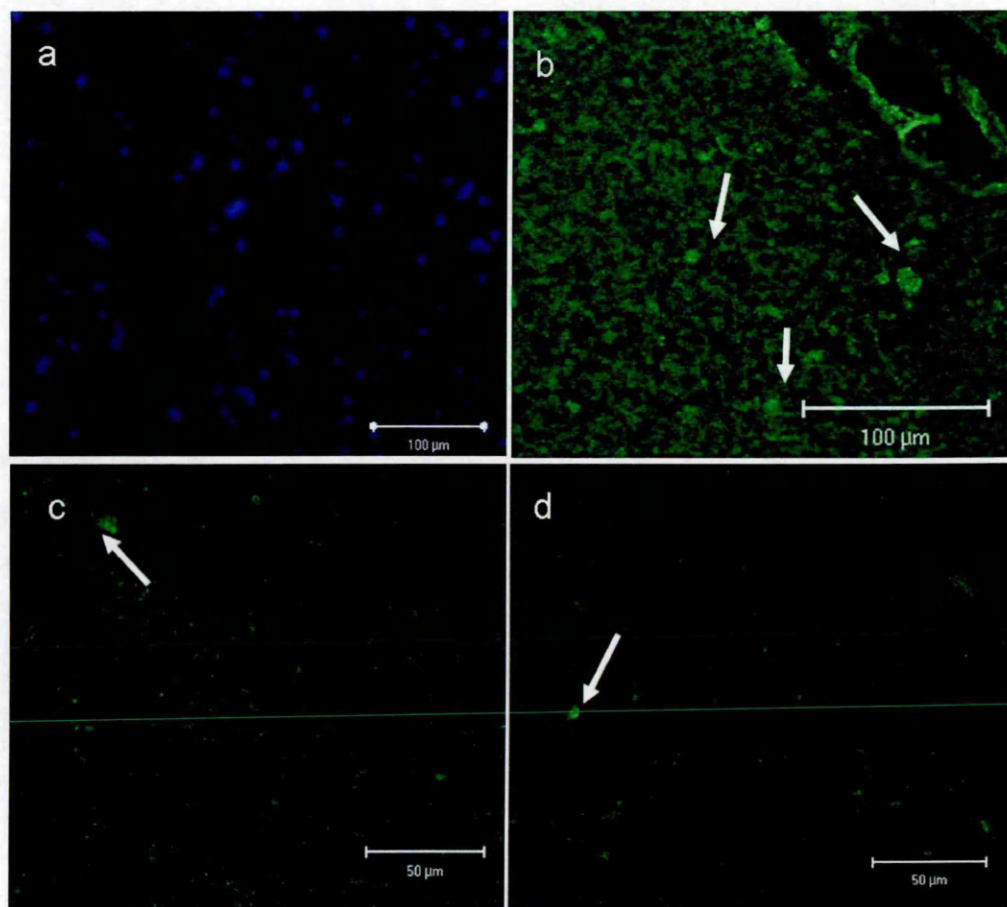


Fig. 5.15: Optimisation of binding of biotinylated CCL2 to human brain tissue sections: determination of optimal concentration for biotinylated CCL2

Brain tissue sections (MS122 A4E5) were incubated with increasing dilution of biotinylated CCL2 (b, 1:4 c, 1:10 d, 1:20) followed by incubation with avidin-FITC. (a) The background level was observed by omitting biotinylated CCL2 (a). Immunofluorescence was visualized with the CSLM following the procedure described in section 2.2.3.1.

of binding of biotinylated CCL2. However, the background level was lowest with avidin FITC diluted at 1:10. This dilution was used for the further experiments. CCL2 binding was shown to be associated with cell nuclei. Higher magnification showed that biotinylated binding was associated with vesicles (figure 5.16c).

5.4.3.2 Determination of the ability of D6 to bind CCL2 in brain tissue sections

Dual labelling on MS lesion sections (MS122 A4E5) showed that D6 (red) and CCL2 (green) showed a strong colocalization represented by the white pixels (figures (5.17)). However, some cells were positive for CCL2 and negative for D6.

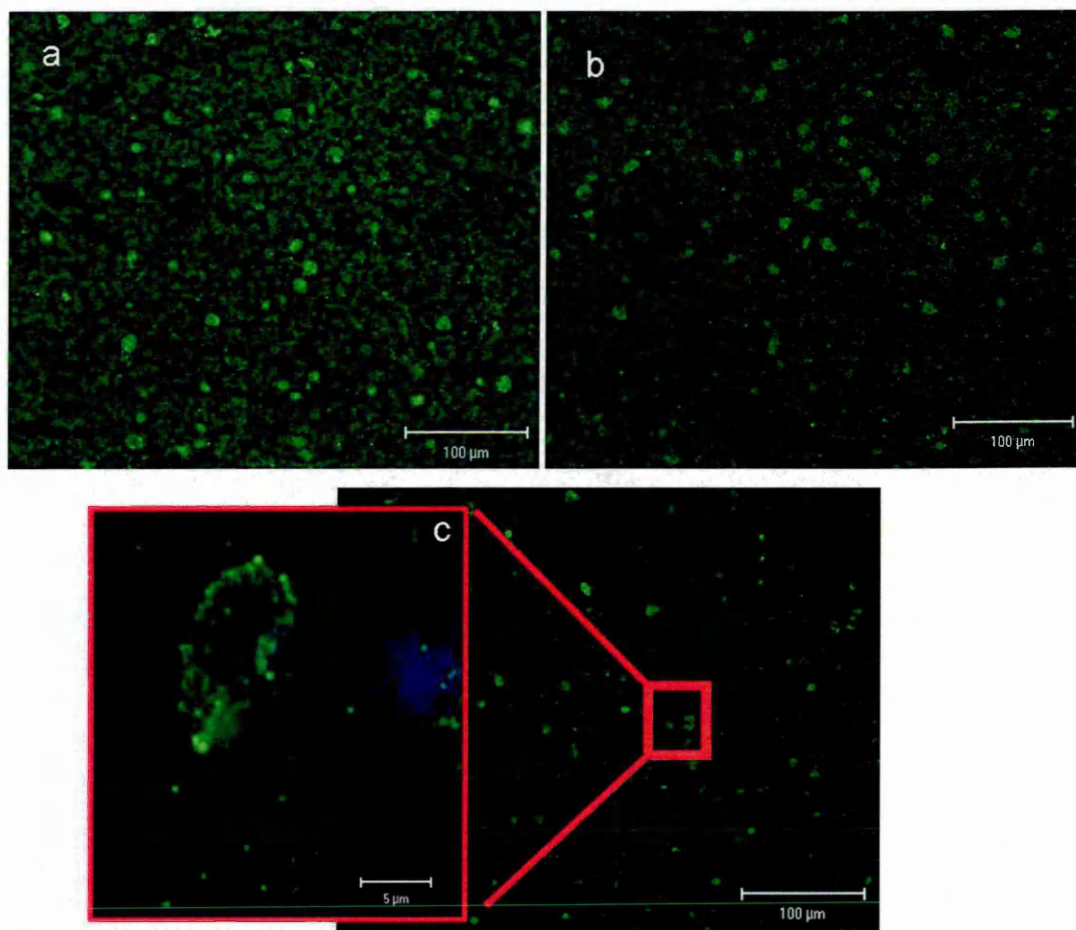


Fig. 5.16: Optimisation of binding of biotinylated CCL2 to human brain tissue sections: determination of the optimal concentration for avidin FITC.

Brain tissue sections (MS122 A4E5) were incubated with biotinylated CCL2 (1:4) followed by incubation with increasing dilution of avidin-FITC (a, 1:2 b, 1:4 c, 1:10). (c) Picture at higher magnification shows the vesicular staining for CCL2 binding. Immunofluorescence was visualized with the CSLM following the procedure described in section 2.2.3.1.

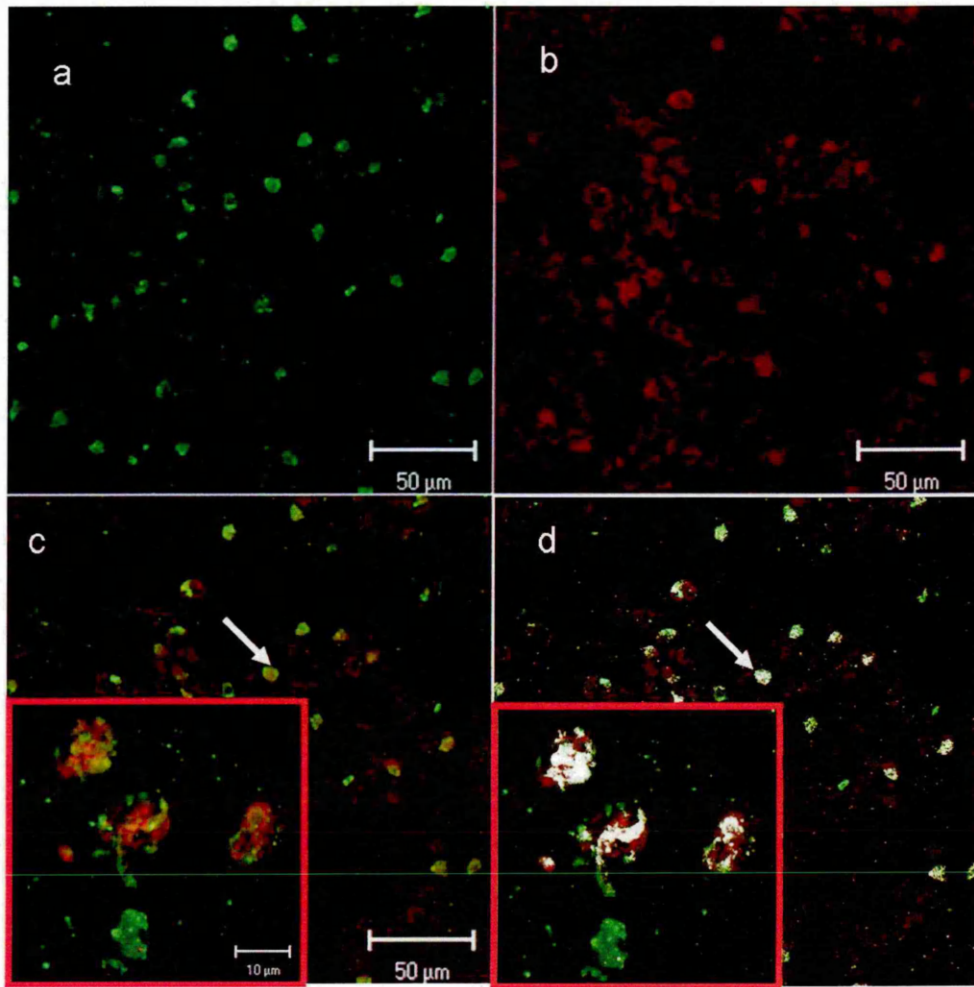


Fig. 5.17: Determination of the ability of D6 to bind CCL2 in human brain tissue.

10 μ m brain tissue section (MS122 A4E5) was incubated with biotinylated CCL2 and avidin FITC (a, green) followed by D6 antibody (b, red). Immunofluorescence was visualized with the CSLM following the procedure described in section 2.2.3.1. The two channels (red and green) were overlaid (c) with high magnification in the frame. Colocalisation (white colour pixels) was observed using the Zeiss 510 software (d) at low and high magnification (frame). Arrow indicates cell with colocalised biotinylated CCL2 and D6 which appears to be of neuronal morphology.

5.5 Discussion

The decoy receptor D6 shares some similarities with conventional chemokine receptors. It is a 7 transmembrane receptor that can bind chemokines [Fra et al., 2003, Locati et al., 2005, Mantovani et al., 2006]. The D6 decoy receptor has some specificity in ligand binding, it binds only pro-inflammatory CC chemokines but not homeostatic CC chemokines or other chemokine families such as CXC chemokines [Fra et al., 2003, Locati et al., 2005, Mantovani et al., 2006]. However, the D6 decoy receptor lacks motifs in the second intracellular loop that transduce signalling events [Borroni et al., 2006, Mantovani et al., 2001, Nibbs et al., 1997]. It has been shown to be constitutively internalized to the cytoplasm independently of CC chemokine binding [Blackburn et al. 2004]. It was further demonstrated that the decoy receptor internalized CC chemokines and lead to their degradation in lysosomes [Galliera et al., 2004, Weber et al., 2004].

Evidence in mice has shown a role for D6 in regulating inflammation. A model of cutaneous inflammation in mice deficient for the D6 gene, suffered from aggravated inflammation due to increased leukocyte invasion, necrosis and angiogenesis [Jamieson et al., 2005, Martinez de la Torre et al., 2007]. However, an unexpected resistance to EAE in D6 KO mice was observed due to an impaired encephalitogenic response [Liu et al., 2006a].

The D6 decoy receptor serves a regulatory function for CC chemokine expression at sites of inflammation. D6 was shown to be strongly expressed by endothelial cells in the lymphatic afferent vessels in the skin, gut and placenta as well as on circulating leukocytes at low levels [McKimmie and Graham, 2006, Nibbs et al., 2001]. No studies to date have examined the expression of D6 in human brain. To determine if D6 was expressed in the CNS, it was assessed on astrocytes *in vitro* as well as on human brain tissue sections.

5.5.1 D6 mRNA expression by unstimulated astrocytes using qRT-PCR

In this study, astrocytes have been shown to constitutively express D6 mRNA. Two reports on constitutive D6 mRNA expression by astrocytes were previously published [Zuurman et al., 2003, Neil et al., 2005]. Zuurman et al. (2003) showed that murine astrocytes did not express D6 mRNA using RT-PCR experiments whereas Neil et al. (2005) showed that primary human astrocytes constitutively expressed D6 mRNA using qRT-PCR. The discrepancy might be explained by the difference in the species of astrocytes. Indeed, Zuurman et al. (2003) isolated astrocytes from cortex of mouse pups (\leq day 1) whereas in this study and in the study by Neil et al. (2005), astrocytes were isolated from human brain.

5.5.2 D6 mRNA expression by astrocytes following pro-inflammatory cytokine treatment using qRT-PCR

In this study, under pro-inflammatory conditions, astrocyte D6 mRNA was significantly increased following IL1 β (33.5 ± 7.6 fold increase) and IFN γ (28.1 ± 13.9 fold increase) at 100ng/ml compared to unstimulated cells. Although TNF induced a 12 ± 5.2 fold increase in D6 mRNA expression it did not reach statistical significance. No modulation of D6 mRNA was observed at lower cytokine concentration. Since D6 has been shown to be involved in the clearance of CC chemokines, it is not surprising to observe an increase in D6 mRNA expression following cytokine stimulation, which also increased CCL2 mRNA expression as described in chapter 2. However, there was a large difference in D6 mRNA expression between cytokine stimulation at 10 ng/ml and 100 ng/ml . This difference might be due to the fact that the characteristic dose response might be between these two concentrations. Thus further cytokine treatments (20 ng/ml, 40 ng/ml, 60 ng/ml and 80 ng/ml) should be performed to determine if D6 mRNA expression has a gradual increase in expression with increasing concentration of cytokines.

5.5.3 D6 protein expression by astrocytes using western blotting and flow cytometry

To confirm the previous finding that astrocytes express D6 and to check if protein expression mirrored mRNA expression, western blotting as well as flow cytometry experiments were performed on astrocytes. We report in this study that astrocytes expressed D6 using both methods. In western blot experiments for D6 receptor on proteins extracted from astrocytes, two bands of 53KDa and 60KDa with similar intensity were obtained. The expected size for D6 receptor was 50 KDa [Blackburn et al., 2004] which supports the finding here of astrocyte expression of D6. Since N-terminal sulphation of chemokine receptors has been reported and this post-translational modification is believed to be important for chemokine binding [Farzan et al., 1999, 2002], D6 receptor might be modified *in vivo* which would yield a band at higher molecular weight (possibly 60KDa). Further experiments to sequence proteins in these bands are required.

D6 expression by astrocytes was quantitated by flow cytometry. Astrocytes expressed D6 receptor at both the cell surface and in the cytoplasmic compartment. However, only a small fraction of the total D6 was expressed at the cell surface (10 and 16% for B327/01 and SMS-12 astrocyte preparations). This finding was also observed in other published studies. Blackburn et al. (2004) showed in transfected L1.2 pre B cells and human embryonic kidney (HEK) cells that only between 10 to 20 % of D6 was expressed at the cell surface. Similarly, Weber et al. (2004), investigating trafficking of D6 from the cell surface to the cytoplasm in HEK cells, found that only 5% of the total D6 was expressed at the cell surface.

Astrocytes stimulated with pro-inflammatory cytokines (100ng/ml) showed no modulation of the level of expression (IL1 β , 2.4 \pm 0.2 MFI, TNF, 3.1 \pm 0.9 MFI and IFN γ : 2.6 \pm 0.3 MFI) compared to unstimulated astrocytes (2.9 \pm 0.4 MFI). We previously demonstrated in Chapter 2 that pro-inflammatory cytokine stimulation (100ng/ml) induced an increase in CCL2 secretion, therefore D6 cell surface expression is unaffected by increasing concentrations of CCL2. These findings agreed with the study by Weber et al. (2004) where they showed that D6 cell

surface expression was unaffected following incubation with recombinant CCL3 compared to CCR5 which showed strong internalization. The ability of decoy receptors to actively remove CC chemokines from the extracellular milieu is due to a faster rate of internalisation and recycling to the cell surface compared to functional receptors [Weber et al., 2004]. These findings suggest that the internalisation rate is an important factor in the regulation of the level of CC chemokines rather than the actual cell surface expression which is unaffected following pro-inflammatory treatment.

The data reported here are consistent with the fact that *in vitro* astrocytes express D6 (mRNA and protein level). Moreover, for the detection of D6 protein, two different antibodies and two different staining procedures were used. The antibody used for flow cytometry (R&D Systems) was a monoclonal antibody raised against human D6 transfected RBL-1 cells whereas the antibody for the western blot was obtained by injecting a synthetic peptide (C-LATEDADSENSSFYYYDYLDDEVAFML), corresponding to N terminal amino acids 10-35 of human D6 in goat.

To relate these *in vitro* findings to *in vivo*, expression of D6 was assessed in human brain tissue. Real time PCR as well as western blotting showed the presence of D6 at the mRNA and protein level in the brain of control, NAWM and MS lesions.

5.5.4 D6 mRNA expression *in vivo* using qRT-PCR

At the mRNA level, only L2 and L4 showed an increase in D6 expression compared to control with a 1.6 ± 0.4 fold increase and 3.3 ± 0.5 fold increase. L4 block was shown to have limited demyelination and no apparent inflammation. Surprisingly, L3 which showed a similar level of demyelination and no inflammation did not show any difference in D6 mRNA expression compared to the control. At the protein level, the band pattern for western blotting was similar to that found for the astrocytes *in vitro*. Two bands of 49 and 58 KDa were detected, which

suggested post-translational modification of D6. The quantitative analysis of the blots, using actin to normalize D6 expression, did not show any difference between control, MS and NAWM brain.

5.5.5 D6 protein expression *in vivo* using western blotting

In this study, D6 was shown to be strongly expressed by neurons, present in the grey matter (GM). Absence of staining was observed in the white matter. It is therefore difficult to relate D6 expression with the level of inflammation in the white matter (WM). It was traditionally considered that MS is a demyelinating disease characterized by demyelinated plaques in the WM. However, pathology can be found in the deep cerebral nuclei and cerebral cortex [Cifelli et al., 2002, Kidd et al., 1999, Kutzelnigg et al., 2007]. Cortical lesions differ from the WM lesions by having demyelination without an increase in lymphocyte count or altered distributions of subsets of lymphocytes compared to control. The authors concluded that inflammation in the cortex is independent of lymphocytes [Bo et al., 2003].

In this study, no assumption can be made on the comparison of the level of expression of D6 in the WM between control, NAWM and lesion since the proportion of WM/GM was not assessed. We can only conclude that D6 was detected at the mRNA and protein level within the brain and that D6 was mainly detected in the GM. To be able to accurately compare the level of expression of D6 in control, lesions and NAWM, the composition of WM/GM should be determined as well as including a greater number of brains for each category (control, NAWM and lesion).

5.5.6 Determination of cell types expressing D6 *in vivo* using immunohistochemistry

The fact that neurons express D6 might be a protective mechanism against CCL2 actions. It was shown in an *in vitro* study that hippocampal neurons incubated with CCL2 were subjected to apoptosis, which was inhibited by prior treatment with caspase 1 inhibitor [Kalehua et al., 2004]. This finding was confirmed *in vivo* by intrahippocampal injection of CCL2 that induced neuronal death. Therefore D6 expression would render neurons less sensitive to CCL2 by removing CCL2 in their close environment.

Images obtained by immunohistochemistry showed that D6 labelling was mainly associated with the cell body which seemed to be, at higher magnification, a vesicular pattern, which may mean that it is mainly endoplasmic reticulum or an endosomal compartment. Similar staining was observed in studies by Blackburn et al. (2003) and Weber et al. (2003) where they found that both the L1.2 cell line and HEK cells that expressed GFP-D6 presented a granular distribution in the cells. Weber et al. (2003) further showed that the fusion protein, GFP-D6, colocalised with rab 5 and the transferrin receptor, which are markers for early and recycling endosomes.

We report here that D6 expression was also associated with HLA-DR⁺ activated microglia/macrophages. Microglia have been shown to play a central role in MS pathogenesis. They are able to sense danger signals through the ligation of conserved innate receptors such as Toll-like receptors (TLRs), which result in increased expression of pro-inflammatory mediators such as chemokines [Jack et al., 2005]. Microglia activate immune cells through their expression of MHC class II and co-stimulatory molecules [Rezaie and Male, 1999, Bechmann et al., 2001] resulting in an amplification of the inflammatory response in the CNS. Microglia cells have been shown to clear apoptotic cells and downregulate their APC ability, representing an active mechanism to limit the inflammatory response that is characteristic of acute MS lesions [Magnus et al., 2001, Chan et al., 2003]. The fact that microglia express D6 would further support the finding that microglia

cells act in controlling inflammation by regulating the level of pro-inflammatory CC chemokines.

Surprisingly, D6 expression was not associated with astrocytes. Although our *in vitro* data are consistent with the fact that astrocytes express D6 at the mRNA level and protein level (using two different procedures), it did not correlate with the *in vivo* findings. The discrepancy might be due to an *in vitro* artefact. Indeed, evidence has been published on the discrepancy between *in vitro* and *in vivo* findings. Tian et al. (2004) compared gene expression of retinal pigment epithelial cells grown in different conditions and native RPE using laser microdissection, using microarray analysis, which was further confirmed by qRT-PCR. They showed that cells grown *in vitro* had a significantly different overall gene expression compared to native cells [Tian et al., 2004]. To confirm the fact that astrocytes express D6 *in vivo*, laser microdissection with qRT-PCR would be the ideal procedure.

5.5.7 Determination of D6 ability to bind CCL2 *in vivo* using immunohistochemistry

Many reports have shown that D6 binds various CC chemokines. We report in this study that CCL2 binding on human brain tissue sections showed a strong colocalisation with D6 expression (white pixels). However, some D6⁻ cells also had bound CCL2. Further investigation is needed to identify these cells by doing dual labelling with cellular markers such as GFAP, HLA-DR, CD3 (T-cells).

In Chapter 3, CCL2 binding was shown to be CCR2-independent in primary adult human astrocytes. The absence of activation of the common signal transduction pathways for chemokine receptors and the expression of the D6 receptor *in vitro* might suggest a new regulatory function for human adult astrocytes during inflammation in MS by sequestration of chemokines released during inflammatory cell recruitment. *In vivo*, microglia and neurons expressed D6, which could contribute to the removal of CCL2 from the extracellular space, providing some

explanation for the decrease in CCL2 in the CSF at the time of relapse in MS patients [Mahad et al., 2002b, Narikawa et al., 2004, Scarpini et al., 2002]. D6 expression on astrocytes has to be further investigated *in vivo* due to the failure to detect it on astrocytes in the current preliminary study.

CHAPTER 6

General discussion

6.1 General discussion

The research question addressed in this thesis was the possible contribution of astrocytes to the differential expression of CCL2 and CXCL10 in the CSF in MS patients [Mahad et al., 2002b, Narikawa et al., 2004, Scarpini et al., 2002]. Since both chemokines are highly expressed in the CNS in active lesions, it was surprising that CCL2 was decreased whereas CXCL10 was increased in MS patients. Thus the differences in relation to synthesis of the 2 chemokines in response to inflammatory cytokines was investigated.

In this study, astrocytes were found to respond to pro-inflammatory cytokine treatment by increasing synthesis and secretion of both CCL2 and CXCL10. CCL2 was more highly expressed than CXCL10 both at the mRNA and protein level. Thus, the reduced levels of CCL2 in the CSF during relapse in MS patients cannot be explained by an differential expression of CCL2 and CXCL10 by astrocytes. A second possible explanation may relate to the sequestration of CCL2 within the brain parenchyma. Thus CCR2 expression and CCL2 binding to astrocytes *in vitro* was assessed. Although CCR2 mRNA was expressed by astrocytes, no protein was detected either at the cell surface nor in the cytoplasmic compartment. Since astrocytes showed the ability to bind CCL2, which was unaffected

following cytokine treatment, and showed a complete absence of activation of both calcium flux and phosphorylation of Erk and Akt, it would appear that the binding of CCL2 was CCR2-independent. Therefore, CCL2 could bind either to decoy chemokine receptors or to proteoglycans known ligand for CCL2 [Proudfoot et al., 2003]. Astrocytes were shown to constitutively express D6 receptor at the mRNA (qRT-PCR) and protein (flow cytometry and western blot) level. The expression at the cell surface was not modulated by pro-inflammatory cytokine treatment. Therefore *in vitro* data might suggest that astrocytes regulate the level of CC chemokines through binding to the decoy chemokine receptor. Although mRNA and protein were not affected by cytokines, it remains to be investigated whether the rate of recycling of D6 to the surface is modulated.

Levels of chemokines can also be regulated by storage in intracellular stores that can be released rapidly following cell activation. It was shown that CD8⁺ T cells were able to release CCL5 from small vesicles following activation through the T cell receptor [Catalfamo et al., 2004]. Similar findings were obtained with peripheral blood eosinophils [Lacy et al., 1999] who found that CCL5 released by eosinophils under IFN γ stimulation was quicker than expected reaching its maximal effect following 60 to 120 min treatment. Subcellular fractionation demonstrated that CCL5 was associated with small secretory vesicles, suggesting the presence of intracellular stores of CCL5.

Not only T cells and eosinophils, ECs have also been shown to store several chemokines such as CXCL8, CXCL1 and CCL2 to allow them to respond quickly to stimulation [Oynebraten et al., 2005]. It was proposed that CXCL8 storage in EC corresponds to a memory mechanism of preceding inflammatory conditions [Wolff et al., 1998]. Therefore, EC can respond to the next inflammatory insult without the delay of *de novo* synthesis. These findings illustrate the existence of mechanisms that rapidly regulate the level of chemokines in the extracellular milieu.

When chemokines are secreted, their diffusion is limited by GAGs. As previously said in section 1.4.6, GAGs are composed of long linear polysaccharides and a protein core [Johnson et al., 2005]. Since chemokines are primarily basic and proteoglycans are highly negatively charged, it is not surprising to observe interaction between chemokines and proteoglycans. The interaction of chemokines and proteoglycans have been under investigation to understand their role in chemokine regulation. It was hypothesised that this interaction provides a mechanism that concentrates chemokine in a close environment, from the site of synthesis, to recruit immune cells to the site of inflammation [Rot, 1992]. It was further demonstrated that this interaction is fundamental for chemokine function. Mutations in the binding site for CCL2, CCL4 and CCL5 have been assessed *in vitro* and *in vivo* to determine the effect of proteoglycan on chemokine function. The chemotactic activity of the mutated chemokines was retained only *in vitro* and were unable to recruit any cells when injected intraperitoneally [Proudfoot et al., 2003]. The fact that chemokines can induce chemotactic effects on immune cells *in vitro* but not *in vivo* is not surprising as *in vitro* tests solely examine the effect on chemokines on recruitment of immune cells without consideration of flow conditions. Therefore, this study demonstrates the importance of proteoglycans for the establishment and maintenance of chemokine gradient.

As discussed in section 1.4.6, proteoglycans possess some specificity for chemokines [Kuschert et al., 1999]. Therefore, cells that are producing proteoglycan might favour the formation of a specific gradient of a particular chemokine that will recruit a certain type of immune cells [Witt and Lander, 1994]. This specificity in binding of chemokines to proteoglycans controls the localisation of chemokines in tissues.

Existence of soluble GAGs which bind chemokines might modulate the activity of chemokines although the data to support this is controversial. It was demonstrated that heparin and heparan sulphate decreased the chemotactic effect of CXCL12 *in vitro* on acute lymphoblastic leukemia cell line [Murphy et al., 2007].

This finding was confirmed by studies where co-incubation of soluble GAGs (heparin) with chemokines resulted in a reduction in binding and a resultant effect on their functional effect on neutrophils and chinese hamster ovary K1 (CHO-K1) cells (CCL5, CCL3 and CXCL8) [Kuschert et al., 1999, Martin et al., 2001]. Contradictory results were obtained with heparan sulphate [Netelenbos et al., 2002]. Incubation of myeloblastic CD34⁺ KG-1 cell line with increasing amounts of heparan sulphate resulted in a significant increase in migration. Although there are obvious discrepancies in the effect of soluble GAGs on chemokine effects, it would appear that the chemokine activity can be modulated by soluble GAGs.

Since chemokines exert their biological effect through GPCRs, it is not surprising that chemokine actions can be regulated by the regulation of their receptors. GPCRs can be desensitized, following binding of a chemokine receptor agonist and activation of signalling inactivation pathways. This mechanism is extremely rapid and is followed by endocytosis of the receptor, in less than 1 hour [Steele et al., 2002]. This mechanism is important as it provides a tight mechanism of regulation that could be necessary during the chemotaxis of immune cells toward the inflammation site to avoid over-stimulation of the receptor [Ferguson, 2001]. It was shown, for example, that the mono Mac 1 cell line strongly responded to CCL2 stimulation by increasing calcium mobilization. However, a second stimulation with CCL2 induced a decreased in calcium mobilization, suggesting desensitization [Aragay et al., 1998]. This mechanism is regulated by the GPCR kinases (GRKs) and arrestins. The GRK family is composed of seven family members with four of them ubiquitously expressed (2, 3, 5 and 6) whereas the arrestin family is composed of two members with one ubiquitously expressed (Arrestin β 2). The desensitization occurs following phosphorylation of the C terminal domain of the receptor by GRKs, inducing an increased affinity for arrestin. This interaction results in the steric inhibition for further coupling of the receptor with the G protein rendering the receptor unresponsive to its ligand [Vroon et al., 2006, Pierce and Lefkowitz, 2001]. The GRK-arrestin complex promotes internalisation

through clathrin pathways to the endosome to degrade or resensitize the receptor [Pierce and Lefkowitz, 2001]. Thus desensitization is a rapid and effective mechanism for regulating chemokine activity. Binding of chemokines to a decoy receptor is another mechanism that can quickly regulate the level of chemokines at the site of inflammation as discussed in the sections 5.1.1 and 1.4.4.1.

Finally, proteolysis of chemokines is another mechanism, which may regulate of chemokine activity. The NH₂ part of the chemokine is important for the binding, hence why proteolytic cleavage can change the activity of chemokines [Proost et al., 2001]. It was shown that the dipeptide peptidase IV (CD26) which cleaved CXCL8, CXCL9 and CXCL10 induced a reduction in both the migration effect and calcium mobilization on CXCR3 transfected CHO-K1 cells. Many other reports have shown modulation of chemokine effects following protease processing. It was shown that CCL2 was cleaved by MMP1, 3 and 8, CCL7 was cleaved by MMP3 and CCL13 was cleaved by MMP1 and 3 [McQuibban et al., 2002]. These authors further showed that the proteolytic cleavage took place on the N terminal part of the chemokine which resulted in the strong reduction of migration effect for CCL2 CCL8 and CCL13 on THP1 cells. Whether proteolytic cleavage of CCL2 in the CNS might explain reduced CSF levels in MS remains to be determined.

All these findings reported in this thesis demonstrate the complexity of regulation of chemokine actions. This current study has indicated a number of mechanisms which are potentially involved *in vivo* in MS CNS in controlling chemokine expression levels. However, further work is required to fully understand the *in vivo* processes.

6.2 Future work

Further work should include further characterization of D6 expression *in vivo*. The preliminary work performed in this thesis on human brain tissue sections

was only to determine whether D6 was expressed *in vivo* and to determine the cellular localization. To compare the level of D6 expression in lesions, NAWM and control brain, the ratio of white matter/grey matter has to be characterised using a greater number of brain samples from MS lesion, NAWM and control, to quantitate differences in expression level.

The effect of proteases (MMP2, 9 and CD26), which are known to be up regulated in the CNS lesions in MS, on CCL2 and CXCL10 should be determined. It would then be interesting to determine whether the affinity of cleaved CCL2 for D6 is affected. It would also be interesting to determine whether cleaved CCL2 has a more potent effect on astrocytes by investigating the calcium mobilization and the phosphorylation of Erk1 and 2 and Akt.

Study of the binding of CXCL10, as well as the cleaved CXCL10, would also give us greater insight into the differential regulation of chemokines by primary human astrocytes.

Binding of CXCL10 to tissue sections as well as potential binding to decoy receptors such as DARC would also give greater understanding of the regulation of CXC chemokines in relation to MS. It would then be possible to compare findings for both CCL2 and CXCL10 to enhance understanding of any differential control mechanisms.

Appendix

Paraformaldehyde (4 %):

solution A: dissolve 11.36 g Na_2HPO_4 in 400 ml deionized water

solution B: dissolve 3.2 g $\text{NaH}_2\text{PO}_4 \cdot 2\text{H}_2\text{O}$ in 200 ml deionized water

Mix solution A and B and pH was adjusted to 7.2 (0.2M phosphate buffer).

4 g of PFA (Sigma Aldrich, UK) were resuspended in 25 ml of deionized water.

The solution was heated at 60°C and NaOH (2M) was added to the solution until it was clear. Deionized water was added to have a final volume of 50 ml. Solution was filtered and 50 ml of 0.2M phosphate buffer was added to the filtered solution and the pH was adjusted at 7.2.

RNA loading buffer (6X):

60% Glycerol

0.03% Bromophenol blue

0.03% Xylene cyanole FF

10mM Tris/HCl pH 7.6

Krebs HEPES:

Solution was composed of 134 mM NaCl, 4.7 mM KCl, 1.2 mM KH_2PO_4 , 1.2 mM MgCl_2 , 2.5 mM CaCl_2 , 0.56 mM ascorbic acid, and 11 mM glucose.

Laemmli buffer

62.5mM Tris/HCL pH 6.8, 2%w/v SDS (BDH Chemicals, UK), 10% glycerol, 50nM DTT, 0.01% w/v bromophenol blue (Sigma, Aldrich, UK). Working solution used 2 x SDS sample buffer diluted in distilled water containing 1nM ortho-vanadate (phosphate inhibitor).

Sudan black B

100ml of 70% ethanol was added to 0.15 g of Sudan black B (Sigma Aldrich, UK) and mixed for 1 h at RT. Solution was incubated overnight at 4°C and filtered prior to use. The solution was stored at 4°C for up to 2 months.

Conferences attended

May 2005: MS Frontiers held in Edinburgh. Poster presented entitled: Cytokine regulation of CCL2 and CXCL10 expression by primary adult human astrocytes in vitro.

Dec 2005: British Society for Immunology held in Harrogate. Oral presentation was presented in the Neuroimmunology workshop entitled: Cytokine regulation of CCL2 and CXCL10 expression by primary human adult astrocytes in vitro.

Sept 2006: EFIS conference held in Paris. Poster presented entitled: In vitro characterization of chemokine receptor CCR2 and CXCR3 expression and ligand binding by primary human adult astrocytes.

May 07: National MS conference held in Sheffield. An award oral presentation was presented entitled: Chemokine CCL2 to primary adult human astrocytes is CCR2-independent: a new role for astrocytes in the regulation of inflammation.

June 07: MS Frontiers conference held in London. Poster was presented entitled: CCL2 binding to primary adult human astrocytes is CCR2-independent: a new role for astrocytes in the regulation of inflammation.

Sept 07: 8th European Meeting on Glial Cell Function in Health and Disease held in London. Poster presented entitled: Astrocytes regulate CCL2 level in CCR2-independent way.

Publications

Fouillet, A, Romero, IA, Woodroffe, N. CCL2 binding to primary adult human astrocytes is CCR2-independent: A new role for astrocytes in the regulation of inflammation. *Neuron Glia Biology* vol. 2, Pages: S113-S113. Published: 2007.

A.Fouillet, I.Romero, MN Woodroffe. Astrocytes regulate CCL2 level in CCR2-independent way (2007). *Proceedings of the 8th European Meeting on Glial Cell Function in Health and Disease*; Pages: 79-82. Published: 2007.

Suliman O, Fouillet A, Romero I, Keynes M, Sharrack B, Woodroffe MN. Expression of CCL2, CXCL10 and their receptors CCR2 and CXCR3 by primary adult human astrocytes in vitro: Effect of pro-inflammatory cytokines *Neurology* 66 (5): A371-A371 Suppl. 2 MAR 14 2006.

Fouillet A, Suliman O, Sharrack B, Romero I, Woodroffe N. Cytokine regulation of CXCL10 and CCL2 expression by primary adult human astrocytes in vitro. *Immunology* 116: 41-42 Suppl. 1 DEC 2005.

5.5 Discussion

The decoy receptor D6 shares some similarities with conventional chemokine receptors. It is a 7 transmembrane receptor that can bind chemokines [Fra et al., 2003, Locati et al., 2005, Mantovani et al., 2006]. The D6 decoy receptor has some specificity in ligand binding, it binds only pro-inflammatory CC chemokines but not homeostatic CC chemokines or other chemokine families such as CXC chemokines [Fra et al., 2003, Locati et al., 2005, Mantovani et al., 2006]. However, the D6 decoy receptor lacks motifs in the second intracellular loop that transduce signalling events [Borroni et al., 2006, Mantovani et al., 2001, Nibbs et al., 1997]. It has been shown to be constitutively internalized to the cytoplasm independently of CC chemokine binding [Blackburn et al. 2004]. It was further demonstrated that the decoy receptor internalized CC chemokines and lead to their degradation in lysosomes [Galliera et al., 2004, Weber et al., 2004].

Evidence in mice has shown a role for D6 in regulating inflammation. A model of cutaneous inflammation in mice deficient for the D6 gene, suffered from aggravated inflammation due to increased leukocyte invasion, necrosis and angiogenesis [Jamieson et al., 2005, Martinez de la Torre et al., 2007]. However, an unexpected resistance to EAE in D6 KO mice was observed due to an impaired encephalitogenic response [Liu et al., 2006a].

The D6 decoy receptor serves a regulatory function for CC chemokine expression at sites of inflammation. D6 was shown to be strongly expressed by endothelial cells in the lymphatic afferent vessels in the skin, gut and placenta as well as on circulating leukocytes at low levels [McKimmie and Graham, 2006, Nibbs et al., 2001]. No studies to date have examined the expression of D6 in human brain. To determine if D6 was expressed in the CNS, it was assessed on astrocytes *in vitro* as well as on human brain tissue sections.

5.5.1 D6 mRNA expression by unstimulated astrocytes using qRT-PCR

In this study, astrocytes have been shown to constitutively express D6 mRNA. Two reports on constitutive D6 mRNA expression by astrocytes were previously published [Zuurman et al., 2003, Neil et al., 2005]. Zuurman et al. (2003) showed that murine astrocytes did not express D6 mRNA using RT-PCR experiments whereas Neil et al. (2005) showed that primary human astrocytes constitutively expressed D6 mRNA using qRT-PCR. The discrepancy might be explained by the difference in the species of astrocytes. Indeed, Zuurman et al. (2003) isolated astrocytes from cortex of mouse pups (\leq day 1) whereas in this study and in the study by Neil et al. (2005), astrocytes were isolated from human brain.

5.5.2 D6 mRNA expression by astrocytes following pro-inflammatory cytokine treatment using qRT-PCR

In this study, under pro-inflammatory conditions, astrocyte D6 mRNA was significantly increased following IL1 β (33.5 ± 7.6 fold increase) and IFN γ (28.1 ± 13.9 fold increase) at 100ng/ml compared to unstimulated cells. Although TNF induced a 12 ± 5.2 fold increase in D6 mRNA expression it did not reach statistical significance. No modulation of D6 mRNA was observed at lower cytokine concentration. Since D6 has been shown to be involved in the clearance of CC chemokines, it is not surprising to observe an increase in D6 mRNA expression following cytokine stimulation, which also increased CCL2 mRNA expression as described in chapter 2. However, there was a large difference in D6 mRNA expression between cytokine stimulation at 10 ng/ml and 100 ng/ml . This difference might be due to the fact that the characteristic dose response might be between these two concentrations. Thus further cytokine treatments (20 ng/ml, 40 ng/ml, 60 ng/ml and 80 ng/ml) should be performed to determine if D6 mRNA expression has a gradual increase in expression with increasing concentration of cytokines.

5.5.3 D6 protein expression by astrocytes using western blotting and flow cytometry

To confirm the previous finding that astrocytes express D6 and to check if protein expression mirrored mRNA expression, western blotting as well as flow cytometry experiments were performed on astrocytes. We report in this study that astrocytes expressed D6 using both methods. In western blot experiments for D6 receptor on proteins extracted from astrocytes, two bands of 53KDa and 60KDa with similar intensity were obtained. The expected size for D6 receptor was 50 KDa [Blackburn et al., 2004] which supports the finding here of astrocyte expression of D6. Since N-terminal sulphation of chemokine receptors has been reported and this post-translational modification is believed to be important for chemokine binding [Farzan et al., 1999, 2002], D6 receptor might be modified *in vivo* which would yield a band at higher molecular weight (possibly 60KDa). Further experiments to sequence proteins in these bands are required.

D6 expression by astrocytes was quantitated by flow cytometry. Astrocytes expressed D6 receptor at both the cell surface and in the cytoplasmic compartment. However, only a small fraction of the total D6 was expressed at the cell surface (10 and 16% for B327/01 and SMS-12 astrocyte preparations). This finding was also observed in other published studies. Blackburn et al. (2004) showed in transfected L1.2 pre B cells and human embryonic kidney (HEK) cells that only between 10 to 20 % of D6 was expressed at the cell surface. Similarly, Weber et al. (2004), investigating trafficking of D6 from the cell surface to the cytoplasm in HEK cells, found that only 5% of the total D6 was expressed at the cell surface.

Astrocytes stimulated with pro-inflammatory cytokines (100ng/ml) showed no modulation of the level of expression (IL1 β , 2.4 \pm 0.2 MFI, TNF, 3.1 \pm 0.9 MFI and IFN γ : 2.6 \pm 0.3 MFI) compared to unstimulated astrocytes (2.9 \pm 0.4 MFI). We previously demonstrated in Chapter 2 that pro-inflammatory cytokine stimulation (100ng/ml) induced an increase in CCL2 secretion, therefore D6 cell surface expression is unaffected by increasing concentrations of CCL2. These findings agreed with the study by Weber et al. (2004) where they showed that D6 cell

surface expression was unaffected following incubation with recombinant CCL3 compared to CCR5 which showed strong internalization. The ability of decoy receptors to actively remove CC chemokines from the extracellular milieu is due to a faster rate of internalisation and recycling to the cell surface compared to functional receptors [Weber et al., 2004]. These findings suggest that the internalisation rate is an important factor in the regulation of the level of CC chemokines rather than the actual cell surface expression which is unaffected following pro-inflammatory treatment.

The data reported here are consistent with the fact that *in vitro* astrocytes express D6 (mRNA and protein level). Moreover, for the detection of D6 protein, two different antibodies and two different staining procedures were used. The antibody used for flow cytometry (R&D Systems) was a monoclonal antibody raised against human D6 transfected RBL-1 cells whereas the antibody for the western blot was obtained by injecting a synthetic peptide (C-LATEDADSENSSFYYYDYLDDEVAFML), corresponding to N terminal amino acids 10-35 of human D6 in goat.

To relate these *in vitro* findings to *in vivo*, expression of D6 was assessed in human brain tissue. Real time PCR as well as western blotting showed the presence of D6 at the mRNA and protein level in the brain of control, NAWM and MS lesions.

5.5.4 D6 mRNA expression *in vivo* using qRT-PCR

At the mRNA level, only L2 and L4 showed an increase in D6 expression compared to control with a 1.6 ± 0.4 fold increase and 3.3 ± 0.5 fold increase. L4 block was shown to have limited demyelination and no apparent inflammation. Surprisingly, L3 which showed a similar level of demyelination and no inflammation did not show any difference in D6 mRNA expression compared to the control. At the protein level, the band pattern for western blotting was similar to that found for the astrocytes *in vitro*. Two bands of 49 and 58 KDa were detected, which

suggested post-translational modification of D6. The quantitative analysis of the blots, using actin to normalize D6 expression, did not show any difference between control, MS and NAWM brain.

5.5.5 D6 protein expression *in vivo* using western blotting

In this study, D6 was shown to be strongly expressed by neurons, present in the grey matter (GM). Absence of staining was observed in the white matter. It is therefore difficult to relate D6 expression with the level of inflammation in the white matter (WM). It was traditionally considered that MS is a demyelinating disease characterized by demyelinated plaques in the WM. However, pathology can be found in the deep cerebral nuclei and cerebral cortex [Cifelli et al., 2002, Kidd et al., 1999, Kutzelnigg et al., 2007]. Cortical lesions differ from the WM lesions by having demyelination without an increase in lymphocyte count or altered distributions of subsets of lymphocytes compared to control. The authors concluded that inflammation in the cortex is independent of lymphocytes [Bo et al., 2003].

In this study, no assumption can be made on the comparison of the level of expression of D6 in the WM between control, NAWM and lesion since the proportion of WM/GM was not assessed. We can only conclude that D6 was detected at the mRNA and protein level within the brain and that D6 was mainly detected in the GM. To be able to accurately compare the level of expression of D6 in control, lesions and NAWM, the composition of WM/GM should be determined as well as including a greater number of brains for each category (control, NAWM and lesion).

5.5.6 Determination of cell types expressing D6 *in vivo* using immunohistochemistry

The fact that neurons express D6 might be a protective mechanism against CCL2 actions. It was shown in an *in vitro* study that hippocampal neurons incubated with CCL2 were subjected to apoptosis, which was inhibited by prior treatment with caspase 1 inhibitor [Kalehua et al., 2004]. This finding was confirmed *in vivo* by intrahippocampal injection of CCL2 that induced neuronal death. Therefore D6 expression would render neurons less sensitive to CCL2 by removing CCL2 in their close environment.

Images obtained by immunohistochemistry showed that D6 labelling was mainly associated with the cell body which seemed to be, at higher magnification, a vesicular pattern, which may mean that it is mainly endoplasmic reticulum or an endosomal compartment. Similar staining was observed in studies by Blackburn et al. (2003) and Weber et al. (2003) where they found that both the L1.2 cell line and HEK cells that expressed GFP-D6 presented a granular distribution in the cells. Weber et al. (2003) further showed that the fusion protein, GFP-D6, colocalised with rab 5 and the transferrin receptor, which are markers for early and recycling endosomes.

We report here that D6 expression was also associated with HLA-DR⁺ activated microglia/macrophages. Microglia have been shown to play a central role in MS pathogenesis. They are able to sense danger signals through the ligation of conserved innate receptors such as Toll-like receptors (TLRs), which result in increased expression of pro-inflammatory mediators such as chemokines [Jack et al., 2005]. Microglia activate immune cells through their expression of MHC class II and co-stimulatory molecules [Rezaie and Male, 1999, Bechmann et al., 2001] resulting in an amplification of the inflammatory response in the CNS. Microglia cells have been shown to clear apoptotic cells and downregulate their APC ability, representing an active mechanism to limit the inflammatory response that is characteristic of acute MS lesions [Magnus et al., 2001, Chan et al., 2003]. The fact that microglia express D6 would further support the finding that microglia

cells act in controlling inflammation by regulating the level of pro-inflammatory CC chemokines.

Surprisingly, D6 expression was not associated with astrocytes. Although our *in vitro* data are consistent with the fact that astrocytes express D6 at the mRNA level and protein level (using two different procedures), it did not correlate with the *in vivo* findings. The discrepancy might be due to an *in vitro* artefact. Indeed, evidence has been published on the discrepancy between *in vitro* and *in vivo* findings. Tian et al. (2004) compared gene expression of retinal pigment epithelial cells grown in different conditions and native RPE using laser microdissection, using microarray analysis, which was further confirmed by qRT-PCR. They showed that cells grown *in vitro* had a significantly different overall gene expression compared to native cells [Tian et al., 2004]. To confirm the fact that astrocytes express D6 *in vivo*, laser microdissection with qRT-PCR would be the ideal procedure.

5.5.7 Determination of D6 ability to bind CCL2 *in vivo* using immunohistochemistry

Many reports have shown that D6 binds various CC chemokines. We report in this study that CCL2 binding on human brain tissue sections showed a strong colocalisation with D6 expression (white pixels). However, some D6⁻ cells also had bound CCL2. Further investigation is needed to identify these cells by doing dual labelling with cellular markers such as GFAP, HLA-DR, CD3 (T-cells).

In Chapter 3, CCL2 binding was shown to be CCR2-independent in primary adult human astrocytes. The absence of activation of the common signal transduction pathways for chemokine receptors and the expression of the D6 receptor *in vitro* might suggest a new regulatory function for human adult astrocytes during inflammation in MS by sequestration of chemokines released during inflammatory cell recruitment. *In vivo*, microglia and neurons expressed D6, which could contribute to the removal of CCL2 from the extracellular space, providing some

explanation for the decrease in CCL2 in the CSF at the time of relapse in MS patients [Mahad et al., 2002b, Narikawa et al., 2004, Scarpini et al., 2002]. D6 expression on astrocytes has to be further investigated *in vivo* due to the failure to detect it on astrocytes in the current preliminary study.

CHAPTER 6

General discussion

6.1 General discussion

The research question addressed in this thesis was the possible contribution of astrocytes to the differential expression of CCL2 and CXCL10 in the CSF in MS patients [Mahad et al., 2002b, Narikawa et al., 2004, Scarpini et al., 2002]. Since both chemokines are highly expressed in the CNS in active lesions, it was surprising that CCL2 was decreased whereas CXCL10 was increased in MS patients. Thus the differences in relation to synthesis of the 2 chemokines in response to inflammatory cytokines was investigated.

In this study, astrocytes were found to respond to pro-inflammatory cytokine treatment by increasing synthesis and secretion of both CCL2 and CXCL10. CCL2 was more highly expressed than CXCL10 both at the mRNA and protein level. Thus, the reduced levels of CCL2 in the CSF during relapse in MS patients cannot be explained by an differential expression of CCL2 and CXCL10 by astrocytes. A second possible explanation may relate to the sequestration of CCL2 within the brain parenchyma. Thus CCR2 expression and CCL2 binding to astrocytes *in vitro* was assessed. Although CCR2 mRNA was expressed by astrocytes, no protein was detected either at the cell surface nor in the cytoplasmic compartment. Since astrocytes showed the ability to bind CCL2, which was unaffected

following cytokine treatment, and showed a complete absence of activation of both calcium flux and phosphorylation of Erk and Akt, it would appear that the binding of CCL2 was CCR2-independent. Therefore, CCL2 could bind either to decoy chemokine receptors or to proteoglycans known ligand for CCL2 [Proudfoot et al., 2003]. Astrocytes were shown to constitutively express D6 receptor at the mRNA (qRT-PCR) and protein (flow cytometry and western blot) level. The expression at the cell surface was not modulated by pro-inflammatory cytokine treatment. Therefore *in vitro* data might suggest that astrocytes regulate the level of CC chemokines through binding to the decoy chemokine receptor. Although mRNA and protein were not affected by cytokines, it remains to be investigated whether the rate of recycling of D6 to the surface is modulated.

Levels of chemokines can also be regulated by storage in intracellular stores that can be released rapidly following cell activation. It was shown that CD8⁺ T cells were able to release CCL5 from small vesicles following activation through the T cell receptor [Catalfamo et al., 2004]. Similar findings were obtained with peripheral blood eosinophils [Lacy et al., 1999] who found that CCL5 released by eosinophils under IFN γ stimulation was quicker than expected reaching its maximal effect following 60 to 120 min treatment. Subcellular fractionation demonstrated that CCL5 was associated with small secretory vesicles, suggesting the presence of intracellular stores of CCL5.

Not only T cells and eosinophils, ECs have also been shown to store several chemokines such as CXCL8, CXCL1 and CCL2 to allow them to respond quickly to stimulation [Oynebraten et al., 2005]. It was proposed that CXCL8 storage in EC corresponds to a memory mechanism of preceding inflammatory conditions [Wolff et al., 1998]. Therefore, EC can respond to the next inflammatory insult without the delay of *de novo* synthesis. These findings illustrate the existence of mechanisms that rapidly regulate the level of chemokines in the extracellular milieu.

When chemokines are secreted, their diffusion is limited by GAGs. As previously said in section 1.4.6, GAGs are composed of long linear polysaccharides and a protein core [Johnson et al., 2005]. Since chemokines are primarily basic and proteoglycans are highly negatively charged, it is not surprising to observe interaction between chemokines and proteoglycans. The interaction of chemokines and proteoglycans have been under investigation to understand their role in chemokine regulation. It was hypothesised that this interaction provides a mechanism that concentrates chemokine in a close environment, from the site of synthesis, to recruit immune cells to the site of inflammation [Rot, 1992]. It was further demonstrated that this interaction is fundamental for chemokine function. Mutations in the binding site for CCL2, CCL4 and CCL5 have been assessed *in vitro* and *in vivo* to determine the effect of proteoglycan on chemokine function. The chemotactic activity of the mutated chemokines was retained only *in vitro* and were unable to recruit any cells when injected intraperitoneally [Proudfoot et al., 2003]. The fact that chemokines can induce chemotactic effects on immune cells *in vitro* but not *in vivo* is not surprising as *in vitro* tests solely examine the effect on chemokines on recruitment of immune cells without consideration of flow conditions. Therefore, this study demonstrates the importance of proteoglycans for the establishment and maintenance of chemokine gradient.

As discussed in section 1.4.6, proteoglycans possess some specificity for chemokines [Kuschert et al., 1999]. Therefore, cells that are producing proteoglycan might favour the formation of a specific gradient of a particular chemokine that will recruit a certain type of immune cells [Witt and Lander, 1994]. This specificity in binding of chemokines to proteoglycans controls the localisation of chemokines in tissues.

Existence of soluble GAGs which bind chemokines might modulate the activity of chemokines although the data to support this is controversial. It was demonstrated that heparin and heparan sulphate decreased the chemotactic effect of CXCL12 *in vitro* on acute lymphoblastic leukemia cell line [Murphy et al., 2007].

This finding was confirmed by studies where co-incubation of soluble GAGs (heparin) with chemokines resulted in a reduction in binding and a resultant effect on their functional effect on neutrophils and chinese hamster ovary K1 (CHO-K1) cells (CCL5, CCL3 and CXCL8) [Kuschert et al., 1999, Martin et al., 2001]. Contradictory results were obtained with heparan sulphate [Netelenbos et al., 2002]. Incubation of myeloblastic CD34⁺ KG-1 cell line with increasing amounts of heparan sulphate resulted in a significant increase in migration. Although there are obvious discrepancies in the effect of soluble GAGs on chemokine effects, it would appear that the chemokine activity can be modulated by soluble GAGs.

Since chemokines exert their biological effect through GPCRs, it is not surprising that chemokine actions can be regulated by the regulation of their receptors. GPCRs can be desensitized, following binding of a chemokine receptor agonist and activation of signalling inactivation pathways. This mechanism is extremely rapid and is followed by endocytosis of the receptor, in less than 1 hour [Steele et al., 2002]. This mechanism is important as it provides a tight mechanism of regulation that could be necessary during the chemotaxis of immune cells toward the inflammation site to avoid over-stimulation of the receptor [Ferguson, 2001]. It was shown, for example, that the mono Mac 1 cell line strongly responded to CCL2 stimulation by increasing calcium mobilization. However, a second stimulation with CCL2 induced a decreased in calcium mobilization, suggesting desensitization [Aragay et al., 1998]. This mechanism is regulated by the GPCR kinases (GRKs) and arrestins. The GRK family is composed of seven family members with four of them ubiquitously expressed (2, 3, 5 and 6) whereas the arrestin family is composed of two members with one ubiquitously expressed (Arrestin β 2). The desensitization occurs following phosphorylation of the C terminal domain of the receptor by GRKs, inducing an increased affinity for arrestin. This interaction results in the steric inhibition for further coupling of the receptor with the G protein rendering the receptor unresponsive to its ligand [Vroon et al., 2006, Pierce and Lefkowitz, 2001]. The GRK-arrestin complex promotes internalisation

through clathrin pathways to the endosome to degrade or resensitise the receptor [Pierce and Lefkowitz, 2001]. Thus desensitization is a rapid and effective mechanism for regulating chemokine activity. Binding of chemokines to a decoy receptor is another mechanism that can quickly regulate the level of chemokines at the site of inflammation as discussed in the sections 5.1.1 and 1.4.4.1.

Finally, proteolysis of chemokines is another mechanism, which may regulate of chemokine activity. The NH₂ part of the chemokine is important for the binding, hence why proteolytic cleavage can change the activity of chemokines [Proost et al., 2001]. It was shown that the dipeptide peptidase IV (CD26) which cleaved CXCL8, CXCL9 and CXCL10 induced a reduction in both the migration effect and calcium mobilization on CXCR3 transfected CHO-K1 cells. Many other reports have shown modulation of chemokine effects following protease processing. It was shown that CCL2 was cleaved by MMP1, 3 and 8, CCL7 was cleaved by MMP3 and CCL13 was cleaved by MMP1 and 3 [McQuibban et al., 2002]. These authors further showed that the proteolytic cleavage took place on the N terminal part of the chemokine which resulted in the strong reduction of migration effect for CCL2 CCL8 and CCL13 on THP1 cells. Whether proteolytic cleavage of CCL2 in the CNS might explain reduced CSF levels in MS remains to be determined.

All these findings reported in this thesis demonstrate the complexity of regulation of chemokine actions. This current study has indicated a number of mechanisms which are potentially involved *in vivo* in MS CNS in controlling chemokine expression levels. However, further work is required to fully understand the *in vivo* processes.

6.2 Future work

Further work should include further characterization of D6 expression *in vivo*. The preliminary work performed in this thesis on human brain tissue sections

was only to determine whether D6 was expressed *in vivo* and to determine the cellular localization. To compare the level of D6 expression in lesions, NAWM and control brain, the ratio of white matter/grey matter has to be characterised using a greater number of brain samples from MS lesion, NAWM and control, to quantitate differences in expression level.

The effect of proteases (MMP2, 9 and CD26), which are known to be up regulated in the CNS lesions in MS, on CCL2 and CXCL10 should be determined. It would then be interesting to determine whether the affinity of cleaved CCL2 for D6 is affected. It would also be interesting to determine whether cleaved CCL2 has a more potent effect on astrocytes by investigating the calcium mobilization and the phosphorylation of Erk1 and 2 and Akt.

Study of the binding of CXCL10, as well as the cleaved CXCL10, would also give us greater insight into the differential regulation of chemokines by primary human astrocytes.

Binding of CXCL10 to tissue sections as well as potential binding to decoy receptors such as DARC would also give greater understanding of the regulation of CXC chemokines in relation to MS. It would then be possible to compare findings for both CCL2 and CXCL10 to enhance understanding of any differential control mechanisms.

Appendix

Paraformaldehyde (4 %):

solution A: dissolve 11.36 g Na_2HPO_4 in 400 ml deionized water

solution B: dissolve 3.2 g $\text{NaH}_2\text{PO}_4 \cdot 2\text{H}_2\text{O}$ in 200 ml deionized water

Mix solution A and B and pH was adjusted to 7.2 (0.2M phosphate buffer).

4 g of PFA (Sigma Aldrich, UK) were resuspended in 25 ml of deionized water.

The solution was heated at 60°C and NaOH (2M) was added to the solution until it was clear. Deionized water was added to have a final volume of 50 ml. Solution was filtered and 50 ml of 0.2M phosphate buffer was added to the filtered solution and the pH was adjusted at 7.2.

RNA loading buffer (6X):

60% Glycerol

0.03% Bromophenol blue

0.03% Xylene cyanole FF

10mM Tris/HCl pH 7.6

Krebs HEPES:

Solution was composed of 134 mM NaCl, 4.7 mM KCl, 1.2 mM KH_2PO_4 , 1.2 mM MgCl_2 , 2.5 mM CaCl_2 , 0.56 mM ascorbic acid, and 11 mM glucose.

Laemmli buffer

62.5mM Tris/HCL pH 6.8, 2%w/v SDS (BDH Chemicals, UK), 10% glycerol, 50nM DTT, 0.01% w/v bromophenol blue (Sigma, Aldrich, UK). Working solution used 2 x SDS sample buffer diluted in distilled water containing 1nM ortho-vanadate (phosphate inhibitor).

Sudan black B

100ml of 70% ethanol was added to 0.15 g of Sudan black B (Sigma Aldrich, UK) and mixed for 1 h at RT. Solution was incubated overnight at 4°C and filtered prior to use. The solution was stored at 4°C for up to 2 months.

Conferences attended

May 2005: MS Frontiers held in Edinburgh. Poster presented entitled: Cytokine regulation of CCL2 and CXCL10 expression by primary adult human astrocytes in vitro.

Dec 2005: British Society for Immunology held in Harrogate. Oral presentation was presented in the Neuroimmunology workshop entitled: Cytokine regulation of CCL2 and CXCL10 expression by primary human adult astrocytes in vitro.

Sept 2006: EFIS conference held in Paris. Poster presented entitled: In vitro characterization of chemokine receptor CCR2 and CXCR3 expression and ligand binding by primary human adult astrocytes.

May 07: National MS conference held in Sheffield. An award oral presentation was presented entitled: Chemokine CCL2 to primary adult human astrocytes is CCR2-independent: a new role for astrocytes in the regulation of inflammation.

June 07: MS Frontiers conference held in London. Poster was presented entitled: CCL2 binding to primary adult human astrocytes is CCR2-independent: a new role for astrocytes in the regulation of inflammation.

Sept 07: 8th European Meeting on Glial Cell Function in Health and Disease held in London. Poster presented entitled: Astrocytes regulate CCL2 level in CCR2-independent way.

Publications

Fouillet, A, Romero, IA, Woodroffe, N. CCL2 binding to primary adult human astrocytes is CCR2-independent: A new role for astrocytes in the regulation of inflammation. *Neuron Glia Biology* vol. 2, Pages: S113-S113. Published: 2007.

A.Fouillet, I.Romero, MN Woodroffe. Astrocytes regulate CCL2 level in CCR2-independent way (2007). *Proceedings of the 8th European Meeting on Glial Cell Function in Health and Disease*; Pages: 79-82. Published: 2007.

Suliman O, Fouillet A, Romero I, Keynes M, Sharrack B, Woodroffe MN. Expression of CCL2, CXCL10 and their receptors CCR2 and CXCR3 by primary adult human astrocytes in vitro: Effect of pro-inflammatory cytokines *Neurology* 66 (5): A371-A371 Suppl. 2 MAR 14 2006.

Fouillet A, Suliman O, Sharrack B, Romero I, Woodroffe N. Cytokine regulation of CXCL10 and CCL2 expression by primary adult human astrocytes in vitro. *Immunology* 116: 41-42 Suppl. 1 DEC 2005.

References

Abbott NJ. 2002. Astrocyte-endothelial interactions and blood-brain barrier permeability. *J. Anat.* 200(6):629-38.

Adams DH, Lloyd AR. 1997. Chemokines: leucocyte recruitment and activation cytokines. *Lancet* 349(9050):490-5.

Agresti C, Bernardo A, Del Russo N, Marziali G, Battistini A, Aloisi F, Levi G, Coccia EM. 1998. Synergistic stimulation of MHC class I and IRF-1 gene expression by IFN-gamma and TNF-alpha in oligodendrocytes. *Eur. J. Neurosci.* 10(9):2975-83.

Aktas O, Smorodchenko A, Brocke S, Infante-Duarte C, Topphoff US, Vogt J, Prozorovski T, Meier S, Osmanova V, Pohl E and others. 2005. Neuronal damage in autoimmune neuroinflammation mediated by the death ligand TRAIL. *Neuron* 46(3):421-32.

Albright AV, Shieh JT, Itoh T, Lee B, Pleasure D, O'Connor MJ, Doms RW, Gonzalez-Scarano F. 1999. Microglia express CCR5, CXCR4, and CCR3, but of these, CCR5 is the principal coreceptor for human immunodeficiency virus type 1 dementia isolates. *J. Virol.* 73(1):205-13.

Alessi DR, Andjelkovic M, Caudwell B, Cron P, Morrice N, Cohen P, Hemmings BA. 1996. Mechanism of activation of protein kinase B by insulin and IGF-1. *Embo J.* 15(23):6541-51.

- Amor S, O'Neill JK, Morris MM, Smith RM, Wraith DC, Groome N, Travers PJ, Baker D. 1996. Encephalitogenic epitopes of myelin basic protein, proteolipid protein, myelin oligodendrocyte glycoprotein for experimental allergic encephalomyelitis induction in Biozzi ABH (H-2Ag7) mice share an amino acid motif. *J. Immunol.* 156(8):3000-8.
- Anderson CM, Swanson RA. 2000. Astrocyte glutamate transport: review of properties, regulation, and physiological functions. *Glia* 32(1):1-14.
- Andjelkovic AV, Kerkovich D, Pachter JS. 2000. Monocyte:astrocyte interactions regulate MCP-1 expression in both cell types. *J. Leukoc. Biol.* 68(4):545-52.
- Andjelkovic AV, Kerkovich D, Shanley J, Pulliam L, Pachter JS. 1999a. Expression of binding sites for beta chemokines on human astrocytes. *Glia* 28(3):225-35.
- Andjelkovic AV, Pachter JS. 2000. Characterization of binding sites for chemokines MCP-1 and MIP-1alpha on human brain microvessels. *J. Neurochem.* 75(5):1898-906. Andjelkovic AV, Song L, Dzenko KA, Cong H, Pachter JS. 2002. Functional expression of CCR2 by human foetal astrocytes. *J. Neurosci. Res.* 70(2):219-31.
- Andjelkovic AV, Spencer DD, Pachter JS. 1999b. Visualization of chemokine binding sites on human brain microvessels. *J. Cell. Biol.* 145(2):403-12.
- Arnett HA, Mason J, Marino M, Suzuki K, Matsushima GK, Ting JP. 2001. TNF alpha promotes proliferation of oligodendrocyte progenitors and remyelination. *Nat. Neurosci.* 4(11):1116-22.
- Ashida N, Arai H, Yamasaki M, Kita T. 2001. Distinct signaling pathways for MCP-1-dependent integrin activation and chemotaxis. *J. Biol. Chem.* 276(19):16555-60.

Babbe H, Roers A, Waisman A, Lassmann H, Goebels N, Hohlfeld R, Friese M, Schroder R, Deckert M, Schmidt S and others. 2000. Clonal expansions of CD8(+) T cells dominate the T cell infiltrate in active multiple sclerosis lesions as shown by micromanipulation and single cell polymerase chain reaction. *J. Exp. Med.* 192(3):393-404.

Baecher-Allan C, Hafler DA. 2004. Suppressor T cells in human diseases. *J. Exp. Med.* 200(3):273-6.

Bagaeva LV, Rao P, Powers JM, Segal BM. 2006. CXC chemokine ligand 13 plays a role in experimental autoimmune encephalomyelitis. *J. Immunol.* 176(12):7676-85.

Baggiolini M. 1998. Chemokines and leukocyte traffic. *Nature* 392(6676):565-8.

Baker D, O'Neill JK, Gschmeissner SE, Wilcox CE, Butter C, Turk JL. 1990. Induction of chronic relapsing experimental allergic encephalomyelitis in Biozzi mice. *J. Neuroimmunol.* 28(3):261-70.

Baker MS, Chen X, Rotramel AR, Nelson JJ, Lu B, Gerard C, Kanwar Y, Kaufman DB. 2003. Genetic deletion of chemokine receptor CXCR3 or antibody blockade of its ligand IP-10 modulates posttransplantation graft-site lymphocytic infiltrates and prolongs functional graft survival in pancreatic islet allograft recipients. *Surgery* 134(2):126-33.

Balabanov R, Dore-Duffy P. 1998. Role of the CNS microvascular pericyte in the blood-brain barrier. *J. Neurosci. Res.* 53(6):637-44.

Balabanov R, Strand K, Kemper A, Lee JY, Popko B. 2006. Suppressor of cytokine signaling 1 expression protects oligodendrocytes from the deleterious effects of interferon-gamma. *J. Neurosci.* 26(19):5143-52.

Balashov KE, Rottman JB, Weiner HL, Hancock WW. 1999. CCR5(+) and CXCR3(+) T cells are increased in multiple sclerosis and their ligands MIP-1alpha and IP-10 are expressed in demyelinating brain lesions. *Proc. Natl. Acad. Sci. USA* 96(12):6873-8.

Ballabh P, Braun A, Nedergaard M. 2004. The blood-brain barrier: an overview: structure, regulation, and clinical implications. *Neurobiol. Dis.* 16(1):1-13.

Bandopadhyay R, Orte C, Lawrenson JG, Reid AR, De Silva S, Allt G. 2001. Contractile proteins in pericytes at the blood-brain and blood-retinal barriers. *J. Neurocytol.* 30(1):35-44.

Banisadr G, Gosselin RD, Mechighel P, Rostene W, Kitabgi P, Melik Parsadaniantz S. 2005. Constitutive neuronal expression of CCR2 chemokine receptor and its colocalization with neurotransmitters in normal rat brain: functional effect of MCP-1/CCL2 on calcium mobilization in primary cultured neurons. *J. Comp. Neurol.* 492(2):178-92.

Banisor I, Leist TP, Kalman B. 2005. Involvement of beta-chemokines in the development of inflammatory demyelination. *J. Neuroinflammation* 2(1):7.

Bar-Or A, Oliveira EM, Anderson DE, Hafler DA. 1999. Molecular pathogenesis of multiple sclerosis. *J. Neuroimmunol.* 100(1-2):252-9.

Baron JL, Madri JA, Ruddle NH, Hashim G, Janeway CA, Jr. 1993. Surface expression of alpha 4 integrin by CD4 T cells is required for their entry into brain

parenchyma. *J. Exp. Med.* 177(1):57-68.

Bazan JF, Bacon KB, Hardiman G, Wang W, Soo K, Rossi D, Greaves DR, Zlotnik A, Schall TJ. 1997. A new class of membrane-bound chemokine with a CX3C motif. *Nature* 385(6617):640-4. Bechmann I, Peter S, Beyer M, Gimsa U, Nitsch R. 2001. Presence of B7-2 (CD86) and lack of B7-1 (CD80) on myelin phagocytosing MHC-II-positive rat microglia is associated with nondestructive immunity in vivo. *FASEB J.* 15(6):1086-8.

Begolka WS, Vanderlugt CL, Rahbe SM, Miller SD. 1998. Differential expression of inflammatory cytokines parallels progression of central nervous system pathology in two clinically distinct models of multiple sclerosis. *J. Immunol.* 161(8):4437-46.

Bellamy WT. 1996. P-glycoproteins and multidrug resistance. *Annu. Rev. Pharmacol. Toxicol.* 36:161-83.

Biber K, Dijkstra I, Trebst C, De Groot CJ, Ransohoff RM, Boddeke HW. 2002. Functional expression of CXCR3 in cultured mouse and human astrocytes and microglia. *Neuroscience* 112(3):487-97.

Bielekova B, Goodwin B, Richert N, Cortese I, Kondo T, Afshar G, Gran B, Eaton J, Antel J, Frank JA and others. 2000. Encephalitogenic potential of the myelin basic protein peptide (amino acids 83-99) in multiple sclerosis: results of a phase II clinical trial with an altered peptide ligand. *Nat. Med.* 6(10):1167-75.

Bitsch A, Schuchardt J, Bunkowski S, Kuhlmann T, Bruck W. 2000. Acute axonal injury in multiple sclerosis. Correlation with demyelination and inflammation. *Brain* 123(6):1174-83.

Bjartmar C, Wujek JR, Trapp BD. 2003. Axonal loss in the pathology of MS: consequences for understanding the progressive phase of the disease. *J. Neurol. Sci.* 206(2):165-71.

Blackburn PE, Simpson CV, Nibbs RJ, O'Hara M, Booth R, Poulos J, Isaacs NW, Graham GJ. 2004. Purification and biochemical characterization of the D6 chemokine receptor. *Biochem. J.* 379(2):263-72.

Blasi F, Riccio M, Brogi A, Strazza M, Taddei ML, Romagnoli S, Luddi A, D'Angelo R, Santi S, Costantino-Ceccarini E and others. 1999. Constitutive expression of interleukin-1beta (IL-1beta) in rat oligodendrocytes. *Biol. Chem.* 380(2):259-64.

Bo L, Vedeler CA, Nyland H, Trapp BD, Mork SJ. 2003. Intracortical multiple sclerosis lesions are not associated with increased lymphocyte infiltration. *Mult. Scler.* 9(4):323-31.

Bohatschek M, Kloss CU, Kalla R, Raivich G. 2001. In vitro model of microglial deramification: ramified microglia transform into amoeboid phagocytes following addition of brain cell membranes to microglia-astrocyte cocultures. *J. Neurosci. Res.* 64(5):508-22.

Bonacchi A, Romagnani P, Romanelli RG, Efsen E, Annunziato F, Lasagni L, Francalanci M, Serio M, Laffi G, Pinzani M and others. 2001. Signal transduction by the chemokine receptor CXCR3: activation of Ras/Erk, Src, and phosphatidylinositol 3-kinase/Akt controls cell migration and proliferation in human vascular pericytes. *J. Biol. Chem.* 276(13):9945-54.

Borroni EM, Buracchi C, de la Torre YM, Galliera E, Vecchi A, Bonecchi R, Mantovani A, Locati M. 2006. The chemoattractant decoy receptor D6 as a neg-

ative regulator of inflammatory responses. *Biochem. Soc. Trans.* 34(6):1014-7.

Bouzier-Sore AK, Voisin P, Bouchaud V, Bezancon E, Franconi JM, Pellerin L. 2006. Competition between glucose and lactate as oxidative energy substrates in both neurons and astrocytes: a comparative NMR study. *Eur. J. Neurosci.* 24(6):1687-94.

Bowman EJ, Siebers A, Altendorf K. 1988. Bafilomycins: a class of inhibitors of membrane ATPases from microorganisms, animal cells, and plant cells. *Proc. Natl. Acad. Sci. USA* 85(21):7972-6.

Brown PD, Davies SL, Speake T, Millar ID. 2004. Molecular mechanisms of cerebrospinal fluid production. *Neuroscience* 129(4):957-70.

Brown SJ. 2006. The role of vitamin D in multiple sclerosis. *Ann. Pharmacother.* 40(6):1158-61.

Brown Z, Gerritsen ME, Carley WW, Strieter RM, Kunkel SL, Westwick J. 1994. Chemokine gene expression and secretion by cytokine-activated human microvascular endothelial cells. Differential regulation of monocyte chemoattractant protein-1 and interleukin-8 in response to interferon-gamma. *Am. J. Pathol.* 145(4):913-21.

Bruck W, Stadelmann C. 2003. Inflammation and degeneration in multiple sclerosis. *Neurol. Sci.* 24(Suppl 5):S265-7.

Brueckmann M, Borggrefe M. 2007. Therapeutic potential of fractalkine: a novel approach to metastatic colon cancer. *Gut* 56(3):314-6.

Brylla E, Aust G, Geyer M, Uckermann O, Loffler S, Spanel-Borowski K. 2005.

Coexpression of preprotachykinin A and B transcripts in the bovine corpus luteum and evidence for functional neurokinin receptor activity in luteal endothelial cells and ovarian macrophages. *Regul. Pept.* 125(1-3):125-33.

Buntinx M, Moreels M, Vandenabeele F, Lambrechts I, Raus J, Steels P, Stinissen P, Ameloot M. 2004. Cytokine-induced cell death in human oligodendroglial cell lines: I. Synergistic effects of IFN-gamma and TNF-alpha on apoptosis. *J. Neurosci. Res.* 76(6):834-45.

Bustin. 2004. *A-Z for Quantitative PCR*. San Diego: IUL Press.

Bustin SA. 2000. Absolute quantification of mRNA using real-time reverse transcription polymerase chain reaction assays. *J. Mol. Endocrinol.* 25(2):169-93.

Bustin SA. 2002. Quantification of mRNA using real-time reverse transcription PCR (RT-PCR): trends and problems. *J. Mol. Endocrinol.* 29(1):23-39.

Callahan MK, Williams KA, Kivisakk P, Pearce D, Stins MF, Ransohoff RM. 2004. CXCR3 marks CD4+ memory T lymphocytes that are competent to migrate across a human brain microvascular endothelial cell layer. *J. Neuroimmunol.* 153(1-2):150-7.

Calvo CF, Yoshimura T, Gelman M, Mallat M. 1996. Production of monocyte chemotactic protein-1 by rat brain macrophages. *Eur. J. Neurosci.* 8(8):1725-34.

Cancilla BJ, Berliner J. 1993. *Astrocyte endothelial cells interactions*. New York: Academic Press. p.383-397.

Caravan P. 2006. Strategies for increasing the sensitivity of gadolinium based MRI contrast agents. *Chem. Soc. Rev.* 35(6):512-23.

Carlson NG, Wieggl WA, Chen J, Bacchi A, Rogers SW, Gahring LC. 1999. Inflammatory cytokines IL-1 alpha, IL-1 beta, IL-6, and TNF-alpha impart neuroprotection to an excitotoxin through distinct pathways. *J. Immunol.* 163(7):3963-8.

Carpentier PA, Begolka WS, Olson JK, Elhofy A, Karpus WJ, Miller SD. 2005. Differential activation of astrocytes by innate and adaptive immune stimuli. *Glia* 49(3):360-74.

Carson MJ. 2002. Microglia as liaisons between the immune and central nervous systems: functional implications for multiple sclerosis. *Glia* 40(2):218-31.

Carson MJ, Reilly CR, Sutcliffe JG, Lo D. 1998. Mature microglia resemble immature antigen-presenting cells. *Glia* 22(1):72-85.

Cartier L, Hartley O, Dubois-Dauphin M, Krause KH. 2005. Chemokine receptors in the central nervous system: role in brain inflammation and neurodegenerative diseases. *Brain Res. Rev.* 48(1):16-42.

Catalfamo M, Karpova T, McNally J, Costes SV, Lockett SJ, Bos E, Peters PJ, Henkart PA. 2004. Human CD8+ T cells store RANTES in a unique secretory compartment and release it rapidly after TcR stimulation. *Immunity* 20(2):219-30.

Cermelli C, Berti R, Soldan SS, Mayne M, D'Ambrosia J M, Ludwin SK, Jacobson S. 2003. High frequency of human herpesvirus 6 DNA in multiple sclerosis plaques isolated by laser microdissection. *J. Infect. Dis.* 187(9):1377-87.

Chan A, Seguin R, Magnus T, Papadimitriou C, Toyka KV, Antel JP, Gold R. 2003. Phagocytosis of apoptotic inflammatory cells by microglia and its therapeutic

tic implications: termination of CNS autoimmune inflammation and modulation by interferon-beta. *Glia* 43(3):231-42.

Chang A, Tourtellotte WW, Rudick R, Trapp BD. 2002. Premyelinating oligodendrocytes in chronic lesions of multiple sclerosis. *N. Engl. J. Med.* 346(3):165-73.

Chang L, Karin M. 2001. Mammalian MAP kinase signalling cascades. *Nature* 410(6824):37-40. Chatzipanagiotou S, Tsakanikas C, Anagnostouli M, Rentzos M, Ioannidis A, Nicolaou C. 2003. Detection of *Chlamydia pneumoniae* in the cerebrospinal fluid of patients with multiple sclerosis by combination of cell culture and PCR: no evidence for possible association. *Mol. Diagn.* 7(1):41-3.

Chavarria A, Alcocer-Varela J. 2004. Is damage in central nervous system due to inflammation? *Autoimmun. Rev.* 3(4):251-60.

Chitnis T. 2007. The role of CD4 T cells in the pathogenesis of multiple sclerosis. *Int. Rev. Neurobiol.* 79:43-72.

Choi C, Xu X, Oh JW, Lee SJ, Gillespie GY, Park H, Jo H, Benveniste EN. 2001. Fas-induced expression of chemokines in human glioma cells: involvement of extracellular signal-regulated kinase 1/2 and p38 mitogen-activated protein kinase. *Cancer Res.* 61(7):3084-91.

Chu CQ, Wittmer S, Dalton DK. 2000. Failure to suppress the expansion of the activated CD4 T cell population in interferon gamma-deficient mice leads to exacerbation of experimental autoimmune encephalomyelitis. *J. Exp. Med.* 192(1):123-8.

Cifelli A, Arridge M, Jezzard P, Esiri MM, Palace J, Matthews PM. 2002. Thalamic neurodegeneration in multiple sclerosis. *Ann. Neurol.* 52(5):650-3.

Coelho AL, Schaller MA, Benjamim CF, Orlofsky AZ, Hogaboam CM, Kunkel SL. 2007. The chemokine CCL6 promotes innate immunity via immune cell activation and recruitment. *J. Immunol.* 179(8):5474-82.

Colotta F, Re F, Muzio M, Bertini R, Polentarutti N, Sironi M, Giri JG, Dower SK, Sims JE, Mantovani A. 1993. Interleukin-1 type II receptor: a decoy target for IL-1 that is regulated by IL-4. *Science* 261(5120):472-5.

Colvin RA, Campanella GS, Sun J, Luster AD. 2004. Intracellular domains of CXCR3 that mediate CXCL9, CXCL10, and CXCL11 function. *J. Biol. Chem.* 279(29):30219-27.

Compston A, Coles A. 2002. Multiple sclerosis. *Lancet* 359(9313):1221-31.

Coons CH, Jones RN. 1941. Immunological properties of an antibody containing a fluorescent group. *Proc. Soc. Exp. Biol. Med.* 47:200-202.

Correale J, Villa A. 2007. The blood-brain-barrier in multiple sclerosis: functional roles and therapeutic targeting. *Autoimmunity* 40(2):148-60.

Cossins JA, Clements JM, Ford J, Miller KM, Pigott R, Vos W, Van der Valk P, De Groot CJ. 1997. Enhanced expression of MMP-7 and MMP-9 in demyelinating multiple sclerosis lesions. *Acta Neuropathol.* 94(6):590-8.

Coughlan CM, McManus CM, Sharron M, Gao Z, Murphy D, Jaffer S, Choe W, Chen W, Hesselgesser J, Gaylord H and others. 2000. Expression of multiple functional chemokine receptors and monocyte chemoattractant protein-1 in human neurons. *Neuroscience* 97(3):591-600.

Cournu-Rebeix I, Lesca G, Tubridy N, Azoulay-Cayla A, Lyon-Caen O, Fontaine B. 2001. Genetic factors in multiple sclerosis. *Presse Med.* 30(37):1844-7.

Croitoru-Lamoury J, Guillemin GJ, Boussin FD, Mognetti B, Gigout LI, Cheret A, Vaslin B, Le Grand R, Brew BJ, Dormont D. 2003. Expression of chemokines and their receptors in human and simian astrocytes: evidence for a central role of TNF alpha and IFN gamma in CXCR4 and CCR5 modulation. *Glia* 41(4):354-70.

Dagan-Berger M, Feniger-Barish R, Avniel S, Wald H, Galun E, Grabovsky V, Alon R, Nagler A, Ben-Baruch A, Peled A. 2006. Role of CXCR3 carboxyl terminus and third intracellular loop in receptor-mediated migration, adhesion and internalization in response to CXCL11. *Blood* 107(10):3821-31.

Datta A, David R, Glennie S, Scott D, Cernuda-Morollon E, Lechler RI, Ridley AJ, Marelli-Berg FM. 2006. Differential effects of immunosuppressive drugs on T-cell motility. *Am. J. Transplant.* 6(12):2871-83.

Davies CA, Loddick SA, Toulmond S, Stroemer RP, Hunt J, Rothwell NJ. 1999. The progression and topographic distribution of interleukin-1beta expression after permanent middle cerebral artery occlusion in the rat. *J. Cereb. Blood Flow Metab.* 19(1):87-98.

De Simone R, Giampaolo A, Giometto B, Gallo P, Levi G, Peschle C, Aloisi F. 1995. The costimulatory molecule B7 is expressed on human microglia in culture and in multiple sclerosis acute lesions. *J. Neuropathol. Exp. Neurol.* 54(2):175-87.

De Stefano N, Narayanan S, Mortilla M, Guidi L, Bartolozzi ML, Federico A, Arnold DL. 2000. Imaging axonal damage in multiple sclerosis by means of MR spectroscopy. *Neurol. Sci.* 21(4, Suppl 2):S883-7.

Dey R, Majumder N, Bhattacharyya Majumdar S, Bhattacharjee S, Banerjee S, Roy S, Majumdar S. 2007. Induction of host protective Th1 immune response by chemokines in *Leishmania donovani*-infected BALB/c mice. *Scand. J. Immunol.* 66(6):671-83.

Di Virgilio F, Steinberg TH, Silverstein SC. 1990. Inhibition of Fura-2 sequestration and secretion with organic anion transport blockers. *Cell Calcium* 11(2-3):57-62. Diestel A, Aktas O, Hackel D, Hake I, Meier S, Raine CS, Nitsch R, Zipp F, Ullrich O. 2003. Activation of microglial poly(ADP-ribose)-polymerase-1 by cholesterol breakdown products during neuroinflammation: a link between demyelination and neuronal damage. *J. Exp. Med.* 198(11):1729-40.

Dogan RN, Karpus WJ. 2004. Chemokines and chemokine receptors in autoimmune encephalomyelitis as a model for central nervous system inflammatory disease regulation. *Front. Biosci.* 9:1500-5.

Dong Y, Benveniste EN. 2001. Immune function of astrocytes. *Glia* 36(2):180-90. Dore-Duffy P, Washington R, Dragovic L. 1993. Expression of endothelial cell activation antigens in microvessels from patients with multiple sclerosis. *Adv. Exp. Med. Biol.* 331:243-8.

Dorf ME, Berman MA, Tanabe S, Heesen M, Luo Y. 2000. Astrocytes express functional chemokine receptors. *J. Neuroimmunol.* 111(1-2):109-21.

Dos Santos AC, Barsante MM, Estêves Arantes RM, Bernard CC, Teixeira MM, Carvalho-Tavares J. 2005. CCL2 and CCL5 mediate leukocyte adhesion in experimental autoimmune encephalomyelitis—an intravital microscopy study. *J. Neuroimmunol.* 162(1-2):122-9.

Dyment DA, Ebers GC, Sadovnick AD. 2004. Genetics of multiple sclerosis.

Lancet Neurol. 3(2):104-10.

Ehlert JE, Addison CA, Burdick MD, Kunkel SL, Strieter RM. 2004. Identification and partial characterization of a variant of human CXCR3 generated by posttranscriptional exon skipping. *J. Immunol.* 173(10):6234-40.

Elhofy A, Kennedy KJ, Fife BT, Karpus WJ. 2002. Regulation of experimental autoimmune encephalomyelitis by chemokines and chemokine receptors. *Immunol. Res.* 25(2):167-75.

Elian M, Nightingale S, Dean G. 1990. Multiple sclerosis among United Kingdom-born children of immigrants from the Indian subcontinent, Africa and the West Indies. *J. Neurol. Neurosurg. Psychiatry* 53(10):906-11.

Elices MJ, Osborn L, Takada Y, Crouse C, Luhowskyj S, Hemler ME, Lobb RR. 1990. VCAM-1 on activated endothelium interacts with the leukocyte integrin VLA-4 at a site distinct from the VLA-4/fibronectin binding site. *Cell* 60(4):577-84.

Elovaara I, Lalla M, Spare E, Lehtimäki T, Dastidar P. 1998. Methylprednisolone reduces adhesion molecules in blood and cerebrospinal fluid in patients with MS. *Neurology* 51(6):1703-8.

Eng LF. 1985. Glial fibrillary acidic protein (GFAP): the major protein of glial intermediate filaments in differentiated astrocytes. *J. Neuroimmunol.* 8(4-6):203-14.

Engelhardt B, Ransohoff RM. 2005. The ins and outs of T-lymphocyte trafficking to the CNS: anatomical sites and molecular mechanisms. *Trends Immunol.* 26(9):485-95.

Eugenin EA, D'Aversa TG, Lopez L, Calderon TM, Berman JW. 2003. MCP-1 (CCL2) protects human neurons and astrocytes from NMDA or HIV-tat-induced apoptosis. *J. Neurochem.* 85(5):1299-311.

Farber K, Kettenmann H. 2005. Physiology of microglial cells. *Brain Res. Rev.* 48(2):133-43.

Farzan M, Chung S, Li W, Vasilieva N, Wright PL, Schnitzler CE, Marchione RJ, Gerard C, Gerard NP, Sodroski J and others. 2002. Tyrosine-sulfated peptides functionally reconstitute a CCR5 variant lacking a critical amino-terminal region. *J. Biol. Chem.* 277(43):40397-402.

Farzan M, Mirzabekov T, Kolchinsky P, Wyatt R, Cayabyab M, Gerard NP, Gerard C, Sodroski J, Choe H. 1999. Tyrosine sulfation of the amino terminus of CCR5 facilitates HIV-1 entry. *Cell* 96(5):667-76.

Fawcett JW, Asher RA. 1999. The glial scar and central nervous system repair. *Brain. Res. Bull.* 49(6):377-91.

Ferber IA, Brocke S, Taylor-Edwards C, Ridgway W, Dinisco C, Steinman L, Dalton D, Fathman CG. 1996. Mice with a disrupted IFN-gamma gene are susceptible to the induction of experimental autoimmune encephalomyelitis (EAE). *J. Immunol.* 156(1):5-7.

Ferguson SS. 2001. Evolving concepts in G protein-coupled receptor endocytosis: the role in receptor desensitization and signaling. *Pharmacol. Rev.* 53(1):1-24.

Fife BT, Huffnagle GB, Kuziel WA, Karpus WJ. 2000. CC chemokine receptor 2 is critical for induction of experimental autoimmune encephalomyelitis. *J. Exp. Med.* 192(6):899-905.

Fife BT, Kennedy KJ, Paniagua MC, Lukacs NW, Kunkel SL, Luster AD, Karpus WJ. 2001. CXCL10 (IFN-gamma-inducible protein-10) control of encephalitogenic CD4+ T cell accumulation in the central nervous system during experimental autoimmune encephalomyelitis. *J. Immunol.* 166(12):7617-24.

Flugel A, Matsumuro K, Neumann H, Klinkert WE, Birnbacher R, Lassmann H, Otten U, Wekerle H. 2001. Anti-inflammatory activity of nerve growth factor in experimental autoimmune encephalomyelitis: inhibition of monocyte transendothelial migration. *Eur. J. Immunol.* 31(1):11-22.

Flynn G, Maru S, Loughlin J, Romero IA, Male D. 2003. Regulation of chemokine receptor expression in human microglia and astrocytes. *J. Neuroimmunol.* 136(1-2):84-93.

Fontenot JD, Gavin MA, Rudensky AY. 2003. Foxp3 programs the development and function of CD4+CD25+ regulatory T cells. *Nat. Immunol.* 4(4):330-6.

Foti M, Granucci F, Aggujaro D, Liboi E, Luini W, Minardi S, Mantovani A, Sozzani S, Ricciardi-Castagnoli P. 1999. Upon dendritic cell (DC) activation chemokines and chemokine receptor expression are rapidly regulated for recruitment and maintenance of DC at the inflammatory site. *Int. Immunol.* 11(6):979-86.

Fra AM, Locati M, Otero K, Sironi M, Signorelli P, Massardi ML, Gobbi M, Vecchi A, Sozzani S, Mantovani A. 2003. Cutting edge: scavenging of inflammatory CC chemokines by the promiscuous putatively silent chemokine receptor D6. *J. Immunol.* 170(5):2279-82.

Galliera E, Jala VR, Trent JO, Bonecchi R, Signorelli P, Lefkowitz RJ, Mantovani

- A, Locati M, Haribabu B. 2004. beta-Arrestin-dependent constitutive internalization of the human chemokine decoy receptor D6. *J. Biol. Chem.* 279(24):25590-7.
- Gao X, Gillig TA, Ye P, D'Ercole AJ, Matsushima GK, Popko B. 2000. Interferon-gamma protects against cuprizone-induced demyelination. *Mol. Cell. Neurosci.* 16(4):338-49.
- Garton KJ, Gough PJ, Blobel CP, Murphy G, Greaves DR, Dempsey PJ, Raines EW. 2001. Tumor necrosis factor-alpha-converting enzyme (ADAM17) mediates the cleavage and shedding of fractalkine (CX₃CL1). *J. Biol. Chem.* 276(41):37993-8001.
- Gaupp S, Pitt D, Kuziel WA, Cannella B, Raine CS. 2003. Experimental autoimmune encephalomyelitis (EAE) in CCR2(-/-) mice: susceptibility in multiple strains. *Am. J. Pathol.* 162(1):139-50.
- Gether U. 2000. Uncovering molecular mechanisms involved in activation of G protein-coupled receptors. *Endocr. Rev.* 21(1):90-113.
- Giuliani F, Goodyer CG, Antel JP, Yong VW. 2003. Vulnerability of human neurons to T cell-mediated cytotoxicity. *J. Immunol.* 171(1):368-79.
- Givan L. 2001. *Flow Cytometry: First Principles (Second Edition)*: Wiley-Liss, Inc.
- Glabinski AR, Bielecki B, Kawczak JA, Tuohy VK, Selmaj K, Ransohoff RM. 2004. Treatment with soluble tumor necrosis factor receptor (sTNFR):Fc/p80 fusion protein ameliorates relapsing-remitting experimental autoimmune encephalomyelitis and decreases chemokine expression. *Autoimmunity* 37(6-7):465-71.

Glabinski AR, Bielecki B, O'Bryant S, Selmaj K, Ransohoff RM. 2002. Experimental autoimmune encephalomyelitis: CC chemokine receptor expression by trafficking cells. *J. Autoimmun.* 19(4):175-81.

Glabinski AR, Tani M, Strieter RM, Tuohy VK, Ransohoff RM. 1997. Synchronous synthesis of alpha- and beta-chemokines by cells of diverse lineage in the central nervous system of mice with relapses of chronic experimental autoimmune encephalomyelitis. *Am. J. Pathol.* 150(2):617-30.

Glabinski AR, Tani M, Tuohy VK, Tuthill RJ, Ransohoff RM. 1995. Central nervous system chemokine mRNA accumulation follows initial leukocyte entry at the onset of acute murine experimental autoimmune encephalomyelitis. *Brain Behav. Immun.* 9(4):315-30.

Godiska R, Chantry D, Dietsch GN, Gray PW. 1995. Chemokine expression in murine experimental allergic encephalomyelitis. *J. Neuroimmunol.* 58(2):167-76.

Goldberg SH, van der Meer P, Hesselgesser J, Jaffer S, Kolson DL, Albright AV, Gonzalez-Scarano F, Lavi E. 2001. CXCR3 expression in human central nervous system diseases. *Neuropathol. Appl. Neurobiol.* 27(2):127-38.

Gosling J, Dairaghi DJ, Wang Y, Hanley M, Talbot D, Miao Z, Schall TJ. 2000. Cutting edge: identification of a novel chemokine receptor that binds dendritic cell- and T cell-active chemokines including ELC, SLC, and TECK. *J. Immunol.* 164(6):2851-6.

Goverman J, Woods A, Larson L, Weiner LP, Hood L, Zaller DM. 1993. Transgenic mice that express a myelin basic protein-specific T cell receptor develop spontaneous autoimmunity. *Cell* 72(4):551-60.

Grassi F, Piacentini A, Cristino S, Toneguzzi S, Cavallo C, Facchini A, Lisignoli G. 2003. Human osteoclasts express different CXC chemokines depending on cell culture substrate: molecular and immunocytochemical evidence of high levels of CXCL10 and CXCL12. *Histochem. Cell. Biol.* 120(5):391-400.

Halonen SK, Woods T, McInnerney K, Weiss LM. 2006. Microarray analysis of IFN-gamma response genes in astrocytes. *J. Neuroimmunol.* 175(1-2):19-30.

Hammond SR, English DR, McLeod JG. 2000. The age-range of risk of developing multiple sclerosis: evidence from a migrant population in Australia. *Brain* 123:968-74.

Han KH, Green SR, Tangirala RK, Tanaka S, Quehenberger O. 1999. Role of the first extracellular loop in the functional activation of CCR2. The first extracellular loop contains distinct domains necessary for both agonist binding and transmembrane signaling. *J. Biol. Chem.* 274(45):32055-62.

Haraldsen G, Rot A. 2006. Coy decoy with a new ploy: interceptor controls the levels of homeostatic chemokines. *Eur J. Immunol.* 36(7):1659-61.

Harkness KA, Sussman JD, Davies-Jones GA, Greenwood J, Woodroffe MN. 2003. Cytokine regulation of MCP-1 expression in brain and retinal microvascular endothelial cells. *J. Neuroimmunol.* 142(1-2):1-9.

Hartline DK, Colman DR. 2007. Rapid conduction and the evolution of giant axons and myelinated fibers. *Curr. Biol.* 17(1):R29-35.

Hayashi M, Luo Y, Laning J, Strieter RM, Dorf ME. 1995. Production and function of monocyte chemoattractant protein-1 and other beta-chemokines in murine glial cells. *J. Neuroimmunol.* 60(1-2):143-50.

Hayashi Y, Nomura M, Yamagishi S, Harada S, Yamashita J, Yamamoto H. 1997. Induction of various blood-brain barrier properties in non-neural endothelial cells by close apposition to co-cultured astrocytes. *Glia* 19(1):13-26.

Heesen M, Tanabe S, Berman MA, Yoshizawa I, Luo Y, Kim RJ, Post TW, Gerard C, Dorf ME. 1996. Mouse astrocytes respond to the chemokines MCP-1 and KC, but reverse transcriptase-polymerase chain reaction does not detect mRNA for the KC or new MCP-1 receptor. *J. Neurosci. Res.* 45(4):382-91.

Heid CA, Stevens J, Livak KJ, Williams PM. 1996. Real time quantitative PCR. *Genome Res.* 6(10):986-94.

Hellings N, Baree M, Verhoeven C, D'Hooghe M B, Medaer R, Bernard CC, Raus J, Stinissen P. 2001. T-cell reactivity to multiple myelin antigens in multiple sclerosis patients and healthy controls. *J. Neurosci. Res.* 63(3):290-302.

Henkler F, Lopes AR, Jones M, Koshy R. 1998. Erk-independent partial activation of AP-1 sites by the hepatitis B virus HBx protein. *J. Gen. Virol.* 79:2737-42.

Higashi K, Fujita A, Inanobe A, Tanemoto M, Doi K, Kubo T, Kurachi Y. 2001. An inwardly rectifying K(+) channel, Kir4.1, expressed in astrocytes surrounds synapses and blood vessels in brain. *Am. J. Physiol. Cell. Physiol.* 281(3):C922-31.

Hinks GL, Chari DM, O'Leary MT, Zhao C, Keirstead HS, Blakemore WF, Franklin RJ. 2001. Depletion of endogenous oligodendrocyte progenitors rather than increased availability of survival factors is a likely explanation for enhanced survival of transplanted oligodendrocyte progenitors in X-irradiated compared to normal CNS. *Neuropathol. Appl. Neurobiol.* 27(1):59-67.

Hirsch E, Costa C, Ciruolo E. 2007. Phosphoinositide 3-kinases as a common platform for multi-hormone signaling. *J. Endocrinol.* 194(2):243-56.

Hohlfeld R. 2004. Immunologic factors in primary progressive multiple sclerosis. *Mult. Scler.* 10(Suppl 1):S16-21; S21-2.

Hohol MJ, Orav EJ, Weiner HL. 1995. Disease steps in multiple sclerosis: a simple approach to evaluate disease progression. *Neurology* 45(2):251-5.

Holley JE, Gveric D, Newcombe J, Cuzner ML, Gutowski NJ. 2003. Astrocyte characterization in the multiple sclerosis glial scar. *Neuropathol. Appl. Neurobiol.* 29(5):434-44.

Hollsberg P, Kusk M, Bech E, Hansen HJ, Jakobsen J, Haahr S. 2005. Presence of Epstein-Barr virus and human herpesvirus 6B DNA in multiple sclerosis patients: associations with disease activity. *Acta Neurol. Scand.* 112(6):395-402.

Horwitz MS, Evans CF, McGavern DB, Rodriguez M, Oldstone MB. 1997. Primary demyelination in transgenic mice expressing interferon-gamma. *Nat. Med.* 3(9):1037-41.

Hu S, Sheng WS, Ehrlich LC, Peterson PK, Chao CC. 2000. Cytokine effects on glutamate uptake by human astrocytes. *Neuroimmunomodulation* 7(3):153-9.

Hua LL, Lee SC. 2000. Distinct patterns of stimulus-inducible chemokine mRNA accumulation in human foetal astrocytes and microglia. *Glia* 30(1):74-81.

Huang D, Shi FD, Jung S, Pien GC, Wang J, Salazar-Mather TP, He TT, Weaver JT, Ljunggren HG, Biron CA and others. 2006. The neuronal chemokine CX₃CL1/fractalkine

selectively recruits NK cells that modify experimental autoimmune encephalomyelitis within the central nervous system. *FASEB J.* 20(7):896-905.

Huang DR, Wang J, Kivisakk P, Rollins BJ, Ransohoff RM. 2001. Absence of monocyte chemoattractant protein 1 in mice leads to decreased local macrophage recruitment and antigen-specific T helper cell type 1 immune response in experimental autoimmune encephalomyelitis. *J. Exp. Med.* 193(6):713-26.

Hurwitz AA, Berman JW, Rashbaum WK, Lyman WD. 1993. Human foetal astrocytes induce the expression of blood-brain barrier specific proteins by autologous endothelial cells. *Brain Res.* 625(2):238-43.

Imitola J, Chitnis T, Khoury SJ. 2005. Cytokines in multiple sclerosis: from bench to bedside. *Pharmacol. Ther.* 106(2):163-77.

Innis MA GD, Sninsky JJ, White TJ. 1990. PCR protocol: A guide to methods and application, Academic Press Limited, 24-28 Oval road, London NW1 7DX 512.

Izikson L, Klein RS, Charo IF, Weiner HL, Luster AD. 2000. Resistance to experimental autoimmune encephalomyelitis in mice lacking the CC chemokine receptor (CCR)2. *J. Exp. Med.* 192(7):1075-80.

Jack C, Ruffini F, Bar-Or A, Antel JP. 2005. Microglia and multiple sclerosis. *J. Neurosci. Res.* 81(3):363-73.

Jamieson T, Cook DN, Nibbs RJ, Rot A, Nixon C, McLean P, Alcamì A, Lira SA, Wiekowski M, Graham GJ. 2005. The chemokine receptor D6 limits the inflammatory response in vivo. *Nat. Immunol.* 6(4):403-11.

Johnson Z, Proudfoot AE, Handel TM. 2005. Interaction of chemokines and glycosaminoglycans: a new twist in the regulation of chemokine function with opportunities for therapeutic intervention. *Cytokine Growth Factor Rev.* 16(6):625-36.

Kalehua AN, Nagel JE, Whelchel LM, Gides JJ, Pyle RS, Smith RJ, Kusiak JW, Taub DD. 2004. Monocyte chemoattractant protein-1 and macrophage inflammatory protein-2 are involved in both excitotoxin-induced neurodegeneration and regeneration. *Exp. Cell. Res.* 297(1):197-211.

Kandel SJ, Jessel TM. 1991. Nerve cell and behavior. In: Kandel ER SJ, editor. *Principles of Neural Science*. New York: Elsevier Science Publishing. p 5-17.

Kao JP. 1994. Practical aspects of measuring $[Ca^{2+}]$ with fluorescent indicators. *Methods Cell. Biol.* 40:155-81.

Karasek M, Swiltoslawski J, Zieliniska A. 2004. Ultrastructure of the central nervous system: the basics. *Folia Neuropathol.* 42(Suppl B):1-9.

Karl E, Warner K, Zeitlin B, Kaneko T, Wurtzel L, Jin T, Chang J, Wang S, Wang CY, Strieter RM and others. 2005. Bcl-2 acts in a proangiogenic signaling pathway through nuclear factor-kappaB and CXC chemokines. *Cancer Res.* 65(12):5063-9.

Keirstead HS, Blakemore WF. 1997. Identification of post-mitotic oligodendrocytes incapable of remyelination within the demyelinated adult spinal cord. *J. Neuropathol. Exp. Neurol.* 56(11):1191-201.

Kennedy KJ, Strieter RM, Kunkel SL, Lukacs NW, Karpus WJ. 1998. Acute and relapsing experimental autoimmune encephalomyelitis are regulated by differen-

tial expression of the CC chemokines macrophage inflammatory protein-1 α and monocyte chemoattractant protein-1. *J. Neuroimmunol.* 92(1-2):98-108.

Kent SJ, Karlik SJ, Cannon C, Hines DK, Yednock TA, Fritz LC, Horner HC. 1995. A monoclonal antibody to α 4 integrin suppresses and reverses active experimental allergic encephalomyelitis. *J. Neuroimmunol.* 58(1):1-10.

Kerschensteiner M, Gallmeier E, Behrens L, Leal VV, Misgeld T, Klinkert WE, Kolbeck R, Hoppe E, Oropeza-Wekerle RL, Bartke I and others. 1999. Activated human T cells, B cells, and monocytes produce brain-derived neurotrophic factor *in vitro* and in inflammatory brain lesions: a neuroprotective role of inflammation? *J. Exp. Med.* 189(5):865-70.

Kidd D, Barkhof F, McConnell R, Algra PR, Allen IV, Revesz T. 1999. Cortical lesions in multiple sclerosis. *Brain* 122:17-26.

Kieseier BC, Tani M, Mahad D, Oka N, Ho T, Woodroffe N, Griffin JW, Toyka KV, Ransohoff RM, Hartung HP. 2002. Chemokines and chemokine receptors in inflammatory demyelinating neuropathies: a central role for IP-10. *Brain* 125:823-34.

Kim MO, Suh HS, Brosnan CF, Lee SC. 2004. Regulation of RANTES/CCL5 expression in human astrocytes by interleukin-1 and interferon-beta. *J. Neurochem.* 90(2):297-308.

Kiselyov K, Shin DM, Muallem S. 2003. Signalling specificity in GPCR-dependent Ca²⁺ signalling. *Cell Signal.* 15(3):243-53.

Kivisakk P, Teleshova N, Ozenci V, Huang Y, Matusevicius D, Fredrikson S, Soderstrom M, Link H. 1998. No evidence for elevated numbers of mononuclear

cells expressing MCP-1 and RANTES mRNA in blood and CSF in multiple sclerosis. *J. Neuroimmunol.* 91(1-2):108-12.

Klein L, Klugmann M, Nave KA, Tuohy VK, Kyewski B. 2000. Shaping of the autoreactive T-cell repertoire by a splice variant of self protein expressed in thymic epithelial cells. *Nat. Med.* 6(1):56-61.

Kobayashi Y, Kawai K, Honda H, Tomida S, Niimi N, Tamatani T, Miyasaka M, Yoshikai Y. 1995. Antibodies against leukocyte function-associated antigen-1 and against intercellular adhesion molecule-1 together suppress the progression of experimental allergic encephalomyelitis. *Cell. Immunol.* 164(2):295-305.

Korner H, Lemckert FA, Chaudhri G, Etteldorf S, Sedgwick JD. 1997. Tumor necrosis factor blockade in actively induced experimental autoimmune encephalomyelitis prevents clinical disease despite activated T cell infiltration to the central nervous system. *Eur. J. Immunol.* 27(8):1973-81.

Kouroumalis A, Nibbs RJ, Aptel H, Wright KL, Kolios G, Ward SG. 2005. The chemokines CXCL9, CXCL10, and CXCL11 differentially stimulate G alpha i-independent signaling and actin responses in human intestinal myofibroblasts. *J. Immunol.* 175(8):5403-11.

Kremenichutzky M. 2003. Primary progressive MS. *Int. MS. J.* 10(3):89-95.

Kreutzberg GW. 1995. Microglia, the first line of defence in brain pathologies. *Arzneimittelforschung* 45(3A):357-60.

Kreutzberg GW. 1996. Microglia: a sensor for pathological events in the CNS. *Trends Neurosci.* 19(8):312-8.

Kristiansen K. 2004. Molecular mechanisms of ligand binding, signaling, and regulation within the superfamily of G-protein-coupled receptors: molecular modeling and mutagenesis approaches to receptor structure and function. *Pharmacol. Ther.* 103(1):21-80.

Krumbholz M, Theil D, Cepok S, Hemmer B, Kivisakk P, Ransohoff RM, Hofbauer M, Farina C, Derfuss T, Hartle C and others. 2006. Chemokines in multiple sclerosis: CXCL12 and CXCL13 up-regulation is differentially linked to CNS immune cell recruitment. *Brain* 129:200-11.

Krzan M, Stenovec M, Kreft M, Pangrsic T, Grilc S, Haydon PG, Zorec R. 2003. Calcium-dependent exocytosis of atrial natriuretic peptide from astrocytes. *J. Neurosci.* 23(5):1580-3.

Kuchler-Bopp S, Delaunoy JP, Artault JC, Zaepfel M, Dietrich JB. 1999. Astrocytes induce several blood-brain barrier properties in non-neural endothelial cells. *Neuroreport* 10(6):1347-53.

Kuhlmann T, Lingfeld G, Bitsch A, Schuchardt J, Bruck W. 2002. Acute axonal damage in multiple sclerosis is most extensive in early disease stages and decreases over time. *Brain* 125:2202-12.

Kukhtina NB, Arefieva TI, Krasnikova TL. 2005. Intracellular signal cascade in CD4+ T-lymphocyte migration stimulated by interferon-gamma-inducible protein-10. *Biochemistry (Mosc.)* 70(6):652-6.

Kuno R, Yoshida Y, Nitta A, Nabeshima T, Wang J, Sonobe Y, Kawanokuchi J, Takeuchi H, Mizuno T, Suzumura A. 2006. The role of TNF-alpha and its receptors in the production of NGF and GDNF by astrocytes. *Brain Res.* 1116(1):12-8.

- Kurtzke JF. 1977. Geography in multiple sclerosis. *J. Neurol.* 215(1):1-26.
- Kuschert GS, Coulin F, Power CA, Proudfoot AE, Hubbard RE, Hoogewerf AJ, Wells TN. 1999. Glycosaminoglycans interact selectively with chemokines and modulate receptor binding and cellular responses. *Biochemistry* 38(39):12959-68.
- Kutzelnigg A, Faber-Rod JC, Bauer J, Lucchinetti CF, Sorensen PS, Laursen H, Stadelmann C, Bruck W, Rauschka H, Schmidbauer M and others. 2007. Widespread demyelination in the cerebellar cortex in multiple sclerosis. *Brain Pathol.* 17(1):38-44.
- Lacy P, Mahmudi-Azer S, Bablitz B, Hagen SC, Velazquez JR, Man SF, Moqbel R. 1999. Rapid mobilization of intracellularly stored RANTES in response to interferon-gamma in human eosinophils. *Blood* 94(1):23-32.
- Lai CH, Kuo KH. 2005. The critical component to establish in vitro BBB model: Pericyte. *Brain Res. Rev.* 50(2):258-65.
- Laing KJ, Secombes CJ. 2004. Chemokines. *Dev. Comp. Immunol.* 28(5):443-60.
- Lasagni L, Francalanci M, Annunziato F, Lazzeri E, Giannini S, Cosmi L, Sagninati C, Mazzinghi B, Orlando C, Maggi E and others. 2003. An alternatively spliced variant of CXCR3 mediates the inhibition of endothelial cell growth induced by IP-10, Mig, and I-TAC, and acts as functional receptor for platelet factor 4. *J. Exp. Med.* 197(11):1537-49.
- Lassmann H. 1998. Neuropathology in multiple sclerosis: new concepts. *Mult. Scler.* 4(3):93-8.
- Lassmann H. 2003. Hypoxia-like tissue injury as a component of multiple sclerosis

lesions. *J. Neurol. Sci.* 206(2):187-91.

Lazarini F, Tham TN, Casanova P, Arenzana-Seisdedos F, Dubois-Dalcq M. 2003. Role of the alpha-chemokine stromal cell-derived factor (SDF-1) in the developing and mature central nervous system. *Glia* 42(2):139-48.

Lee SJ, Benveniste EN. 1999. Adhesion molecule expression and regulation on cells of the central nervous system. *J. Neuroimmunol.* 98(2):77-88.

Ley K, Allietta M, Bullard DC, Morgan S. 1998. Importance of E-selectin for firm leukocyte adhesion *in vivo*. *Circ. Res.* 83(3):287-94.

Limatola C, Di Bartolomeo S, Catalano M, Trettel F, Fucile S, Castellani L, Eusebi F. 2005. Cysteine residues are critical for chemokine receptor CXCR2 functional properties. *Exp. Cell. Res.* 307(1):65-75.

Lin K, Sadee W, Quillan JM. 1999. Rapid measurements of intracellular calcium using a fluorescence plate reader. *Biotechniques* 26(2):318-22, 324-6.

Lin W, Kemper A, Dupree JL, Harding HP, Ron D, Popko B. 2006. Interferon-gamma inhibits central nervous system remyelination through a process modulated by endoplasmic reticulum stress. *Brain* 129:1306-18.

Lincoln MR, Montpetit A, Cader MZ, Saarela J, Dyment DA, Tiislar M, Ferretti V, Tienari PJ, Sadovnick AD, Peltonen L and others. 2005. A predominant role for the HLA class II region in the association of the MHC region with multiple sclerosis Complex interactions among MHC haplotypes in multiple sclerosis: susceptibility and resistance. *Nat. Genet.* 37(10):1108-12.

Lindahl P, Johansson BR, Leveen P, Betsholtz C. 1997. Pericyte loss and mi-

croaneurysm formation in PDGF-B-deficient mice. *Science* 277(5323):242-5.

Link H. 1998. The cytokine storm in multiple sclerosis. *Mult. Scler.* 4(1):12-5.

Linker RA, Rott E, Hofstetter HH, Hanke T, Toyka KV, Gold R. 2005. EAE in beta-2 microglobulin-deficient mice: axonal damage is not dependent on MHC-I restricted immune responses. *Neurobiol. Dis.* 19(1-2):218-28.

Lipton HL. 1975. Theiler's virus infection in mice: an unusual biphasic disease process leading to demyelination. *Infect. Immun.* 11(5):1147-55.

Liu L, Graham GJ, Damodaran A, Hu T, Lira SA, Sasse M, Canasto-Chibuque C, Cook DN, Ransohoff RM. 2006a. Cutting edge: the silent chemokine receptor D6 is required for generating T cell responses that mediate experimental autoimmune encephalomyelitis. *J. Immunol.* 177(1):17-21.

Liu L, Huang D, Matsui M, He TT, Hu T, Demartino J, Lu B, Gerard C, Ransohoff RM. 2006b. Severe disease, unaltered leukocyte migration, and reduced IFN-gamma production in CXCR3^{-/-} mice with experimental autoimmune encephalomyelitis. *J. Immunol.* 176(7):4399-409.

Liu MT, Keirstead HS, Lane TE. 2001. Neutralization of the chemokine CXCL10 reduces inflammatory cell invasion and demyelination and improves neurological function in a viral model of multiple sclerosis. *J. Immunol.* 167(7):4091-7.

Livak KJ, Schmittgen TD. 2001. Analysis of relative gene expression data using real-time quantitative PCR and the 2^{(-Delta Delta C(T))} Method. *Methods* 25(4):402-8.

Lo D, Feng L, Li L, Carson MJ, Crowley M, Pauza M, Nguyen A, Reilly CR. 1999. Integrating innate and adaptive immunity in the whole animal. *Immunol. Rev.* 169:225-39.

Locati M, Torre YM, Galliera E, Bonecchi R, Bodduluri H, Vago G, Vecchi A, Mantovani A. 2005. Silent chemoattractant receptors: D6 as a decoy and scavenger receptor for inflammatory CC chemokines. *Cytokine Growth Factor Rev.* 16(6):679-86.

Lock C, Hermans G, Pedotti R, Brendolan A, Schadt E, Garren H, Langer-Gould A, Strober S, Cannella B, Allard J and others. 2002. Gene-microarray analysis of multiple sclerosis lesions yields new targets validated in autoimmune encephalomyelitis. *Nat. Med.* 8(5):500-8.

Loetscher M, Gerber B, Loetscher P, Jones SA, Piali L, Clark-Lewis I, Baggiolini M, Moser B. 1996. Chemokine receptor specific for IP10 and mig: structure, function, and expression in activated T-lymphocytes. *J. Exp. Med.* 184(3):963-9.

Lovett-Racke AE, Trotter JL, Lauber J, Perrin PJ, June CH, Racke MK. 1998. Decreased dependence of myelin basic protein-reactive T cells on CD28-mediated costimulation in multiple sclerosis patients. A marker of activated/memory T cells. *J. Clin. Invest.* 101(4):725-30.

Lu B, Pang PT, Woo NH. 2005. The yin and yang of neurotrophin action. *Nat. Rev. Neurosci.* 6(8):603-14.

Lu M, Grove EA, Miller RJ. 2002. Abnormal development of the hippocampal dentate gyrus in mice lacking the CXCR4 chemokine receptor. *Proc. Natl. Acad. Sci. USA* 99(10):7090-5.

Lucchinetti CF, Brueck W, Rodriguez M, Lassmann H. 1998. Multiple sclerosis: lessons from neuropathology. *Semin. Neurol.* 18(3):337-49.

Lucitti JL, Dickinson ME. 2006. Moving toward the light: using new technology to answer old questions. *Pediatr. Res.* 60(1):1-5.

Lukacs NW, Chensue SW, Karpus WJ, Lincoln P, Keefer C, Strieter RM, Kunkel SL. 1997. C-C chemokines differentially alter interleukin-4 production from lymphocytes. *Am. J. Pathol.* 150(5):1861-8.

Luster AD. 1998. Chemokines-chemotactic cytokines that mediate inflammation. *N. Engl. J. Med.* 338(7):436-45.

Luther SA, Cyster JG. 2001. Chemokines as regulators of T cell differentiation. *Nat. Immunol.* 2(2):102-7.

Ma Q, Jones D, Borghesani PR, Segal RA, Nagasawa T, Kishimoto T, Bronson RT, Springer TA. 1998. Impaired B-lymphopoiesis, myelopoiesis, and derailed cerebellar neuron migration in CXCR4- and SDF-1-deficient mice. *Proc. Natl. Acad. Sci. USA* 95(16):9448-53.

MacAulay N, Gether U, Klaeke DA, Zeuthen T. 2002. Passive water and urea permeability of a human Na(+)-glutamate cotransporter expressed in *Xenopus* oocytes. *J. Physiol.* 542:817-28.

Magnus T, Chan A, Grauer O, Toyka KV, Gold R. 2001. Microglial phagocytosis of apoptotic inflammatory T cells leads to down-regulation of microglial immune activation. *J. Immunol.* 167(9):5004-10.

Mahad D, Callahan MK, Williams KA, Ubogu EE, Kivisakk P, Tucky B, Kidd

G, Kingsbury GA, Chang A, Fox RJ and others. 2006. Modulating CCR2 and CCL2 at the blood-brain barrier: relevance for multiple sclerosis pathogenesis. *Brain* 129:212-23.

Mahad DJ, Howell SJ, Woodroffe MN. 2002a. Expression of chemokines in cerebrospinal fluid and serum of patients with chronic inflammatory demyelinating polyneuropathy. *J. Neurol. Neurosurg. Psychiatry* 73(3):320-3.

Mahad DJ, Howell SJ, Woodroffe MN. 2002b. Expression of chemokines in the CSF and correlation with clinical disease activity in patients with multiple sclerosis. *J. Neurol. Neurosurg. Psychiatry* 72(4):498-502.

Mahad DJ, Lawry J, Howell SJ, Woodroffe MN. 2003. Longitudinal study of chemokine receptor expression on peripheral lymphocytes in multiple sclerosis: CXCR3 upregulation is associated with relapse. *Mult. Scler.* 9(2):189-98.

Mantovani A, Bonecchi R, Locati M. 2006. Tuning inflammation and immunity by chemokine sequestration: decoys and more. *Nat. Rev. Immunol.* 6(12):907-18.

Mantovani A, Locati M, Vecchi A, Sozzani S, Allavena P. 2001. Decoy receptors: a strategy to regulate inflammatory cytokines and chemokines. *Trends Immunol.* 22(6):328-36.

Markovic-Plese S, Pinilla C, Martin R. 2004. The initiation of the autoimmune response in multiple sclerosis. *Clin. Neurol. Neurosurg.* 106(3):218-22.

Marsland BJ, Battig P, Bauer M, Ruedl C, Lassing U, Beerli RR, Dietmeier K, Ivanova L, Pfister T, Vogt L and others. 2005. CCL19 and CCL21 induce a potent proinflammatory differentiation program in licensed dendritic cells. *Immunity* 22(4):493-505.

Martin L, Blanpain C, Garnier P, Wittamer V, Parmentier M, Vita C. 2001. Structural and functional analysis of the RANTES-glycosaminoglycans interactions. *Biochemistry* 40(21):6303-18.

Martinez de la Torre Y, Buracchi C, Borroni EM, Dupor J, Bonecchi R, Nebuloni M, Pasqualini F, Doni A, Lauri E, Agostinis C and others. 2007. Protection against inflammation- and autoantibody-caused foetal loss by the chemokine decoy receptor D6. *Proc. Natl. Acad. Sci. USA* 104(7):2319-24.

Martinez de la Torre Y, Locati M, Buracchi C, Dupor J, Cook DN, Bonecchi R, Nebuloni M, Rukavina D, Vago L, Vecchi A and others. 2005. Increased inflammation in mice deficient for the chemokine decoy receptor D6. *Eur J. Immunol.* 35(5):1342-6.

Marx N, Mach F, Sauty A, Leung JH, Sarafi MN, Ransohoff RM, Libby P, Plutzky J, Luster AD. 2000. Peroxisome proliferator-activated receptor-gamma activators inhibit IFN-gamma-induced expression of the T cell-active CXC chemokines IP-10, Mig, and I-TAC in human endothelial cells. *J. Immunol.* 164(12):6503-8.

Mason JL, Suzuki K, Chaplin DD, Matsushima GK. 2001. Interleukin-1beta promotes repair of the CNS. *J. Neurosci.* 21(18):7046-52.

Matsui M, Weaver J, Proudfoot AE, Wujek JR, Wei T, Richer E, Trapp BD, Rao A, Ransohoff RM. 2002. Treatment of experimental autoimmune encephalomyelitis with the chemokine receptor antagonist Met-RANTES. *J. Neuroimmunol.* 128(1-2):16-22.

May AE, Neumann FJ, Schomig A, Preissner KT. 2000. VLA-4 (alpha(4)beta(1)) engagement defines a novel activation pathway for beta(2) integrin-dependent

leukocyte adhesion involving the urokinase receptor. *Blood* 96(2):506-13.

McKenna MC. 2007. The glutamate-glutamine cycle is not stoichiometric: Fates of glutamate in brain. *J. Neurosci. Res.* 85(15):3347-58.

McKimmie CS, Graham GJ. 2006. Leucocyte expression of the chemokine scavenger D6. *Biochem. Soc. Trans.* 34:1002-4.

McMahon EJ, Bailey SL, Castenada CV, Waldner H, Miller SD. 2005. Epitope spreading initiates in the CNS in two mouse models of multiple sclerosis. *Nat. Med.* 11(3):335-9.

McManus C, Berman JW, Brett FM, Staunton H, Farrell M, Brosnan CF. 1998. MCP-1, MCP-2 and MCP-3 expression in multiple sclerosis lesions: an immunohistochemical and *in situ* hybridization study. *J. Neuroimmunol.* 86(1):20-9.

McQuibban GA, Gong JH, Wong JP, Wallace JL, Clark-Lewis I, Overall CM. 2002. Matrix metalloproteinase processing of monocyte chemoattractant proteins generates CC chemokine receptor antagonists with anti-inflammatory properties *in vivo*. *Blood* 100(4):1160-7.

Mead RJ, Singhrao SK, Neal JW, Lassmann H, Morgan BP. 2002. The membrane attack complex of complement causes severe demyelination associated with acute axonal injury. *J. Immunol.* 168(1):458-65.

Medana IM, Gallimore A, Oxenius A, Martinic MM, Wekerle H, Neumann H. 2000. MHC class I-restricted killing of neurons by virus-specific CD8+ T lymphocytes is effected through the Fas/FasL, but not the perforin pathway. *Eur J. Immunol.* 30(12):3623-33.

- Meeuwsen S, Persoon-Deen C, Bsibsi M, Ravid R, van Noort JM. 2003. Cytokine, chemokine and growth factor gene profiling of cultured human astrocytes after exposure to proinflammatory stimuli. *Glia* 43(3):243-53.
- Meng SZ, Oka A, Takashima S. 1999. Developmental expression of monocyte chemoattractant protein-1 in the human cerebellum and brainstem. *Brain. Dev.* 21(1):30-5.
- Mi H, Barres BA. 1999. Purification and characterization of astrocyte precursor cells in the developing rat optic nerve. *J. Neurosci.* 19(3):1049-61.
- Miller RH, Bai L. 2007. Cellular approaches for stimulating CNS remyelination. *Regen. Med.* 2(5):817-29.
- Minagar A, Shapshak P, Fujimura R, Ownby R, Heyes M, Eisdorfer C. 2002. The role of macrophage/microglia and astrocytes in the pathogenesis of three neurologic disorders: HIV-associated dementia, Alzheimer disease, and multiple sclerosis. *J. Neurol. Sci.* 202(1-2):13-23.
- Minagar A, Toledo EG, Alexander JS, Kelley RE. 2004. Pathogenesis of brain and spinal cord atrophy in multiple sclerosis. *J. Neuroimaging* 14(3 Suppl):5S-10S.
- Minta A, Kao JP, Tsien RY. 1989. Fluorescent indicators for cytosolic calcium based on rhodamine and fluorescein chromophores. *J. Biol. Chem.* 264(14):8171-8.
- Misu T, Onodera H, Fujihara K, Matsushima K, Yoshie O, Okita N, Takase S, Itoyama Y. 2001. Chemokine receptor expression on T cells in blood and cerebrospinal fluid at relapse and remission of multiple sclerosis: imbalance of Th1/Th2-associated chemokine signaling. *J. Neuroimmunol.* 114(1-2):207-12.

Miyazaki T, Honda K, Ohata H. 2007. Modulation of Ca²⁺ transients in cultured endothelial cells in response to fluid flow through α 5 β 1 integrin. *Life Sci.* 81(19-20):1421-30.

Mokhtarian F, McFarlin DE, Raine CS. 1984. Adoptive transfer of myelin basic protein-sensitized T cells produces chronic relapsing demyelinating disease in mice. *Nature* 309(5966):356-8.

Muller DM, Pender MP, Greer JM. 2004. Chemokines and chemokine receptors: potential therapeutic targets in multiple sclerosis. *Curr. Drug. Targets Inflamm. Allergy* 3(3):279-90.

Murao K, Ohyama T, Imachi H, Ishida T, Cao WM, Namihira H, Sato M, Wong NC, Takahara J. 2000. TNF- α stimulation of MCP-1 expression is mediated by the Akt/PKB signal transduction pathway in vascular endothelial cells. *Biochem. Biophys. Res. Commun.* 276(2):791-6.

Murdoch C, Finn A. 2000. Chemokine receptors and their role in inflammation and infectious diseases. *Blood* 95(10):3032-43.

Murphy JW, Cho Y, Sachpatzidis A, Fan C, Hodsdon ME, Lolis E. 2007. Structural and functional basis of CXCL12 (stromal cell-derived factor-1 α) binding to heparin. *J. Biol. Chem.* 282(13):10018-27.

Murphy PM. 2002. International Union of Pharmacology XXX. Update on chemokine receptor nomenclature. *Pharmacol. Rev.* 54(2):227-9.

Murray J. 2002. Infection as a cause of multiple sclerosis. *BMJ* 325(7373):1128.

- Muzio L, Martino G, Furlan R. 2007. Multifaceted aspects of inflammation in multiple sclerosis: the role of microglia. *J. Neuroimmunol.* 191(1-2):39-44.
- Mycko MP, Papoian R, Boschert U, Raine CS, Selmaj KW. 2004. Microarray gene expression profiling of chronic active and inactive lesions in multiple sclerosis. *Clin. Neurol. Neurosurg.* 106(3):223-9.
- Myers JD. 1989. Development and application of immunocytochemical staining techniques: a review. *Diagn. Cytopathol.* 5(3):318-30.
- Nagler K, Mauch DH, Pfrieder FW. 2001. Glia-derived signals induce synapse formation in neurones of the rat central nervous system. *J. Physiol.* 533:665-79.
- Nakajima H, Fukuda K, Doi Y, Sugino M, Kimura F, Hanafusa T, Ikemoto T, Shimizu A. 2004. Expression of TH1/TH2-related chemokine receptors on peripheral T cells and correlation with clinical disease activity in patients with multiple sclerosis. *Eur. Neurol.* 52(3):162-8.
- Namura S, Maeno H, Takami S, Jiang XF, Kamichi S, Wada K, Nagata I. 2002. Inhibition of glial glutamate transporter GLT-1 augments brain edema after transient focal cerebral ischemia in mice. *Neurosci. Lett.* 324(2):117-20.
- Narikawa K, Misu T, Fujihara K, Nakashima I, Sato S, Itoyama Y. 2004. CSF chemokine levels in relapsing neuromyelitis optica and multiple sclerosis. *J. Neuroimmunol.* 149(1-2):182-6.
- Neil SJ, Aasa-Chapman MM, Clapham PR, Nibbs RJ, McKnight A, Weiss RA. 2005. The promiscuous CC chemokine receptor D6 is a functional coreceptor for primary isolates of human immunodeficiency virus type 1 (HIV-1) and HIV-2 on astrocytes. *J. Virol.* 79(15):9618-24.

Neote K, Mak JY, Kolakowski LF, Jr., Schall TJ. 1994. Functional and biochemical analysis of the cloned Duffy antigen: identity with the red blood cell chemokine receptor. *Blood* 84(1):44-52.

Netelenbos T, Zuijderduijn S, Van Den Born J, Kessler FL, Zweegman S, Huijgens PC, Drager AM. 2002. Proteoglycans guide SDF-1-induced migration of hematopoietic progenitor cells. *J. Leukoc. Biol.* 72(2):353-62.

Newman TA, Woolley ST, Hughes PM, Sibson NR, Anthony DC, Perry VH. 2001. T-cell- and macrophage-mediated axon damage in the absence of a CNS-specific immune response: involvement of metalloproteinases. *Brain* 124:2203-14.

Nibbs R, Graham G, Rot A. 2003. Chemokines on the move: control by the chemokine "interceptors" Duffy blood group antigen and D6. *Semin. Immunol.* 15(5):287-94.

Nibbs RJ, Kriehuber E, Ponath PD, Parent D, Qin S, Campbell JD, Henderson A, Kerjaschki D, Maurer D, Graham GJ and others. 2001. The beta-chemokine receptor D6 is expressed by lymphatic endothelium and a subset of vascular tumors. *Am. J. Pathol.* 158(3):867-77.

Nibbs RJ, Wylie SM, Yang J, Landau NR, Graham GJ. 1997. Cloning and characterization of a novel promiscuous human beta-chemokine receptor D6. *J. Biol. Chem.* 272(51):32078-83. Nitsch R, Pohl EE, Smorodchenko A, Infante-Duarte C, Aktas O, Zipp F. 2004. Direct impact of T cells on neurons revealed by two-photon microscopy in living brain tissue. *J. Neurosci.* 24(10):2458-64.

O'Garra A, Arai N. 2000. The molecular basis of T helper 1 and T helper 2 cell differentiation. *Trends Cell. Biol.* 10(12):542-50.

Odemis V, Lamp E, Pezeshki G, Moepps B, Schilling K, Gierschik P, Littman DR, Engele J. 2005. Mice deficient in the chemokine receptor CXCR4 exhibit impaired limb innervation and myogenesis. *Mol. Cell. Neurosci.* 30(4):494-505.

Oh JW, Schwiebert LM, Benveniste EN. 1999. Cytokine regulation of CC and CXC chemokine expression by human astrocytes. *J. Neurovirol.* 5(1):82-94.

Oksenberg JR, Barcellos LF. 2005. Multiple sclerosis genetics: leaving no stone unturned. *Genes Immun.* 6(5):375-87.

Oleszak EL, Chang JR, Friedman H, Katsetos CD, Platsoucas CD. 2004. Theiler's virus infection: a model for multiple sclerosis. *Clin. Microbiol. Rev.* 17(1):174-207.

Omari KM, John G, Lango R, Raine CS. 2006. Role for CXCR2 and CXCL1 on glia in multiple sclerosis. *Glia* 53(1):24-31.

Opsahl ML, Kennedy PG. 2005. Early and late HHV-6 gene transcripts in multiple sclerosis lesions and normal appearing white matter. *Brain* 128:516-27.

Ota K, Matsui M, Milford EL, Mackin GA, Weiner HL, Hafler DA. 1990. T-cell recognition of an immunodominant myelin basic protein epitope in multiple sclerosis. *Nature* 346(6280):183-7.

Owens T. 2002. Identification of new therapeutic targets for prevention of CNS inflammation. *Expert Opin. Ther. Targets* 6(2):203-15.

Øynebraten I, Barois N, Hagelsteen K, Johansen FE, Bakke O, Haraldsen G. 2005. Characterization of a novel chemokine-containing storage granule in en-

endothelial cells: evidence for preferential exocytosis mediated by protein kinase A and diacylglycerol. *J. Immunol.* 175(8):5358-69.

Ozenci V, Kouwenhoven M, Huang YM, Kivisakk P, Link H. 2000. Multiple sclerosis is associated with an imbalance between tumour necrosis factor-alpha (TNF-alpha)- and IL-10-secreting blood cells that is corrected by interferon-beta (IFN-beta) treatment. *Clin. Exp. Immunol.* 120(1):147-53.

Paddock SW. 2000. Principles and practices of laser scanning confocal microscopy. *Mol. Biotechnol.* 16(2):127-49.

Pan W, Zadina JE, Harlan RE, Weber JT, Banks WA, Kastin AJ. 1997. Tumor necrosis factor-alpha: a neuromodulator in the CNS. *Neurosci. Biobehav. Rev.* 21(5):603-13.

Patani R, Balaratnam M, Vora A, Reynolds R. 2007. Remyelination can be extensive in multiple sclerosis despite a long disease course. *Neuropathol. Appl. Neurobiol.* 33(3):277-87.

Patrikios P, Stadelmann C, Kutzelnigg A, Rauschka H, Schmidbauer M, Laursen H, Sorensen PS, Bruck W, Lucchinetti C, Lassmann H. 2006. Remyelination is extensive in a subset of multiple sclerosis patients. *Brain* 129:3165-72.

Pender MP. 2005. CSF testing for multiple sclerosis. *Lancet Neurol.* 4(9):522-3.

Perea G, Araque A. 2005. Glial calcium signaling and neuron-glia communication. *Cell. Calcium* 38(3-4):375-82.

Peters W, Dupuis M, Charo IF. 2000. A mechanism for the impaired IFN-gamma production in C-C chemokine receptor 2 (CCR2) knockout mice: role of CCR2

- in linking the innate and adaptive immune responses. *J. Immunol.* 165(12):7072-7.
- Pfaffl MW. 2001. A new mathematical model for relative quantification in real-time RT-PCR. *Nucleic Acids Res.* 29(9):e45.
- Pfriegeer FW, Barres BA. 1997. Synaptic efficacy enhanced by glial cells in vitro. *Science* 277(5332):1684-7.
- Pierce KL, Lefkowitz RJ. 2001. Classical and new roles of beta-arrestins in the regulation of G-protein-coupled receptors. *Nat. Rev. Neurosci.* 2(10):727-33.
- Pitt D, Werner P, Raine CS. 2000. Glutamate excitotoxicity in a model of multiple sclerosis. *Nat. Med.* 6(1):67-70.
- Poser CM, Brinar VV. 2004. Diagnostic criteria for multiple sclerosis: an historical review. *Clin. Neurol. Neurosurg.* 106(3):147-58.
- Posern G, Weber CK, Rapp UR, Feller SM. 1998. Activity of Rap1 is regulated by bombesin, cell adhesion, and cell density in NIH3T3 fibroblasts. *J. Biol. Chem.* 273(38):24297-300.
- Pouly S, Becher B, Blain M, Antel JP. 2000. Interferon-gamma modulates human oligodendrocyte susceptibility to Fas-mediated apoptosis. *J. Neuropathol. Exp. Neurol.* 59(4):280-6.
- Preobrazhensky AA, Dragan S, Kawano T, Gavrilin MA, Gulina IV, Chakravarty L, Kolattukudy PE. 2000. Monocyte chemoattractant protein-1 receptor CCR2B is a glycoprotein that has tyrosine sulfation in a conserved extracellular N-terminal region. *J. Immunol.* 165(9):5295-303.

Price DL, Ludwig JW, Mi H, Schwarz TL, Ellisman MH. 2002. Distribution of rSlo Ca²⁺-activated K⁺ channels in rat astrocyte perivascular endfeet. *Brain Res.* 956(2):183-93.

Proost P, Schutyser E, Menten P, Struyf S, Wuyts A, Opdenakker G, Detheux M, Parmentier M, Durinx C, Lambeir AM and others. 2001. Amino-terminal truncation of CXCR3 agonists impairs receptor signaling and lymphocyte chemotaxis, while preserving antiangiogenic properties. *Blood* 98(13):3554-61.

Proudfoot AE, Handel TM, Johnson Z, Lau EK, LiWang P, Clark-Lewis I, Borlat F, Wells TN, Kosco-Vilbois MH. 2003. Glycosaminoglycan binding and oligomerization are essential for the in vivo activity of certain chemokines. *Proc. Natl. Acad. Sci. USA* 100(4):1885-90.

Purves D, Augustine GJ, Fitzpatrick D, Katz LC, LaMantia A-S, McNamara JO, Williams SM. 2001. *Neuroscience*, 2nd edition: Sinauer Associates, Inc.

Racke MK, Ratts RB, Arredondo L, Perrin PJ, Lovett-Racke A. 2000. The role of costimulation in autoimmune demyelination. *J. Neuroimmunol.* 107(2):205-15.

Radeff-Huang J, Seasholtz TM, Matteo RG, Brown JH. 2004. G protein mediated signaling pathways in lysophospholipid induced cell proliferation and survival. *J. Cell. Biochem.* 92(5):949-66.

Raivich G, Banati R. 2004. Brain microglia and blood-derived macrophages: molecular profiles and functional roles in multiple sclerosis and animal models of autoimmune demyelinating disease. *Brain Res. Rev.* 46(3):261-81.

Raivich G, Bohatschek M, Kloss CU, Werner A, Jones LL, Kreutzberg GW. 1999. Neuroglial activation repertoire in the injured brain: graded response, molecular

mechanisms and cues to physiological function. *Brain Res. Rev.* 30(1):77-105.

Raju R, Malloy A, Shah T, Smith R, Oaks M, Hosenpud JD. 2003. Alloimmune induction of endothelial cell-derived interferon-gamma-inducible chemokines. *Transplantation* 75(7):1072-4.

Ramsauer M, Krause D, Dermietzel R. 2002. Angiogenesis of the blood-brain barrier in vitro and the function of cerebral pericytes. *Faseb J* 16(10):1274-6. Epub 2002 Jun 21. Ransohoff RM, Hamilton TA, Tani M, Stoler MH, Shick HE, Major JA, Estes ML, Thomas DM, Tuohy VK. 1993. Astrocyte expression of mRNA encoding cytokines IP-10 and JE/MCP-1 in experimental autoimmune encephalomyelitis. *FASEB J.* 7(6):592-600.

Rappert A, Bechmann I, Pivneva T, Mahlo J, Biber K, Nolte C, Kovac AD, Gerard C, Boddeke HW, Nitsch R and others. 2004. CXCR3-dependent microglial recruitment is essential for dendrite loss after brain lesion. *J. Neurosci.* 24(39):8500-9.

Rauen T, Taylor WR, Kuhlbrodt K, Wiessner M. 1998. High-affinity glutamate transporters in the rat retina: a major role of the glial glutamate transporter GLAST-1 in transmitter clearance. *Cell Tissue Res.* 291(1):19-31.

Renno T, Taupin V, Bourbonniere L, Verge G, Tran E, De Simone R, Krakowski M, Rodriguez M, Peterson A, Owens T. 1998. Interferon-gamma in progression to chronic demyelination and neurological deficit following acute EAE. *Mol. Cell. Neurosci.* 12(6):376-89.

Rezaie P, Male D. 1999. Colonisation of the developing human brain and spinal cord by microglia: a review. *Microsc. Res. Tech.* 45(6):359-82.

- Rezaie P, Trillo-Pazos G, Everall IP, Male DK. 2002. Expression of beta-chemokines and chemokine receptors in human foetal astrocyte and microglial co-cultures: potential role of chemokines in the developing CNS. *Glia* 37(1):64-75.
- Ridet JL, Malhotra SK, Privat A, Gage FH. 1997. Reactive astrocytes: cellular and molecular cues to biological function. *Trends Neurosci.* 20(12):570-7.
- Rieckmann P, Altenhofen B, Riegel A, Baudewig J, Felgenhauer K. 1997. Soluble adhesion molecules (sVCAM-1 and sICAM-1) in cerebrospinal fluid and serum correlate with MRI activity in multiple sclerosis. *Ann. Neurol.* 41(3):326-33.
- Rigamonti L, Ariotti S, Losana G, Gradini R, Russo MA, Jouanguy E, Casanova JL, Forni G, Novelli F. 2000. Surface expression of the IFN-gamma R2 chain is regulated by intracellular trafficking in human T lymphocytes. *J. Immunol.* 164(1):201-7.
- Robinson SC, Scott KA, Balkwill FR. 2002. Chemokine stimulation of monocyte matrix metalloproteinase-9 requires endogenous TNF-alpha. *Eur. J. Immunol.* 32(2):404-12.
- Romijn HJ, van Uum JF, Breedijk I, Emmering J, Radu I, Pool CW. 1999. Double immunolabeling of neuropeptides in the human hypothalamus as analyzed by confocal laser scanning fluorescence microscopy. *J. Histochem. Cytochem.* 47(2):229-36.
- Rosenberg GA. 2002. Matrix metalloproteinases and neuroinflammation in multiple sclerosis. *Neuroscientist* 8(6):586-95.
- Rossi D, Zlotnik A. 2000. The biology of chemokines and their receptors. *Annu. Rev. Immunol.* 18:217-42.

Rot A. 1992. Endothelial cell binding of NAP-1/IL-8: role in neutrophil emigration. *Immunol. Today* 13(8):291-4.

Rothstein JD, Dykes-Hoberg M, Pardo CA, Bristol LA, Jin L, Kuncl RW, Kanai Y, Hediger MA, Wang Y, Schielke JP and others. 1996. Knockout of glutamate transporters reveals a major role for astroglial transport in excitotoxicity and clearance of glutamate. *Neuron* 16(3):675-86.

Rothwell NJ, Luheshi GN. 2000. Interleukin 1 in the brain: biology, pathology and therapeutic target. *Trends Neurosci.* 23(12):618-25.

Rottem S, Barile MF. 1993. Beware of mycoplasma. *Trends Biotechnol.* 11(4):143-51

Rottman JB, Slavin AJ, Silva R, Weiner HL, Gerard CG, Hancock WW. 2000. Leukocyte recruitment during onset of experimental allergic encephalomyelitis is CCR1 dependent. *Eur. J. Immunol.* 30(8):2372-7.

Roy ML, Saal D, Perney T, Sontheimer H, Waxman SG, Kaczmarek LK. 1996. Manipulation of the delayed rectifier Kv1.5 potassium channel in glial cells by antisense oligodeoxynucleotides. *Glia* 18(3):177-84.

Rozen S, Skaletsky H. 2000. Primer3 on the WWW for general users and for biologist programmers. *Methods Mol. Biol.* 132:365-86.

Rucker HK, Wynder HJ, Thomas WE. 2000. Cellular mechanisms of CNS pericytes. *Brain Res. Bull.* 51(5):363-9.

Sakaguchi S, Ono M, Setoguchi R, Yagi H, Hori S, Fehervari Z, Shimizu J, Taka-

hashi T, Nomura T. 2006. Foxp3+ CD25+ CD4+ natural regulatory T cells in dominant self-tolerance and autoimmune disease. *Immunol. Rev.* 212:8-27.

Salentin R, Gemsa D, Sprenger H, Kaufmann A. 2003. Chemokine receptor expression and chemotactic responsiveness of human monocytes after influenza A virus infection. *J. Leukoc. Biol.* 74(2):252-9.

Savarin-Vuailat C, Ransohoff RM. 2007. Chemokines and chemokine receptors in neurological disease: raise, retain, or reduce? *Neurotherapeutics* 4(4):590-601.

Sawada M, Kondo N, Suzumura A, Marunouchi T. 1989. Production of tumor necrosis factor-alpha by microglia and astrocytes in culture. *Brain Res.* 491(2):394-7.

Scarpini E, Galimberti D, Baron P, Clerici R, Ronzoni M, Conti G, Scarlato G. 2002. IP-10 and MCP-1 levels in CSF and serum from multiple sclerosis patients with different clinical subtypes of the disease. *J. Neurol. Sci.* 195(1):41-6.

Scheiffele P. 2003. Cell-cell signaling during synapse formation in the CNS. *Ann. Rev. Neurosci.* 26:485-508.

Schrijver HM, van As J, Crusius JB, Dijkstra CD, Uitdehaag BM. 2003. Interleukin (IL)-1 gene polymorphisms: relevance of disease severity associated alleles with IL-1beta and IL-1ra production in multiple sclerosis. *Mediators Inflamm.* 12(2):89-94.

Segal MB. 1993. Extracellular and cerebrospinal fluids. *J. Inher. Metab. Dis.* 16(4):617-38.

Seguin R, Biernacki K, Prat A, Wosik K, Kim HJ, Blain M, McCrea E, Bar-Or

A, Antel JP. 2003. Differential effects of Th1 and Th2 lymphocyte supernatants on human microglia. *Glia* 42(1):36-45.

Sellebjerg F, Sorensen TL. 2003. Chemokines and matrix metalloproteinase-9 in leukocyte recruitment to the central nervous system. *Brain. Res. Bull.* 61(3):347-55.

Shelton MK, McCarthy KD. 2000. Hippocampal astrocytes exhibit Ca²⁺-elevating muscarinic cholinergic and histaminergic receptors in situ. *J. Neurochem.* 74(2):555-63.

Sheremata WA, Minagar A, Alexander JS, Vollmer T. 2005. The role of alpha-4 integrin in the aetiology of multiple sclerosis: current knowledge and therapeutic implications. *CNS Drugs* 19(11):909-22.

Shimaoka T, Nakayama T, Fukumoto N, Kume N, Takahashi S, Yamaguchi J, Minami M, Hayashida K, Kita T, Ohsumi J and others. 2004. Cell surface-anchored SR-PSOX/CXC chemokine ligand 16 mediates firm adhesion of CXC chemokine receptor 6-expressing cells. *J. Leukoc. Biol.* 75(2):267-74.

Shyu AB, Wilkinson MF, van Hoof A. 2008. Messenger RNA regulation: to translate or to degrade. *Embo J.* 27(3):471-81.

Silver J, Miller JH. 2004. Regeneration beyond the glial scar. *Nat. Rev. Neurosci.* 5(2):146-56.

Simard M, Nedergaard M. 2004. The neurobiology of glia in the context of water and ion homeostasis. *Neuroscience* 129(4):877-96.

Simons M, Trotter J. 2007. Wrapping it up: the cell biology of myelination.

Curr. Opin. Neurobiol. 6:553-40.

Simpson J, Rezaie P, Newcombe J, Cuzner ML, Male D, Woodroffe MN. 2000a. Expression of the beta-chemokine receptors CCR2, CCR3 and CCR5 in multiple sclerosis central nervous system tissue. *J. Neuroimmunol.* 108(1-2):192-200.

Simpson JE, Newcombe J, Cuzner ML, Woodroffe MN. 1998. Expression of monocyte chemoattractant protein-1 and other beta-chemokines by resident glia and inflammatory cells in multiple sclerosis lesions. *J. Neuroimmunol.* 84(2):238-49.

Simpson JE, Newcombe J, Cuzner ML, Woodroffe MN. 2000b. Expression of the interferon-gamma-inducible chemokines IP-10 and Mig and their receptor, CXCR3, in multiple sclerosis lesions. *Neuropathol. Appl. Neurobiol.* 26(2):133-42.

Skulina C, Schmidt S, Dornmair K, Babbe H, Roers A, Rajewsky K, Wekerle H, Hohlfeld R, Goebels N. 2004. Multiple sclerosis: brain-infiltrating CD8+ T cells persist as clonal expansions in the cerebrospinal fluid and blood. *Proc. Natl. Acad. Sci. USA* 101(8):2428-33.

Smit MJ, Verdijk P, van der Raaij-Helmer EM, Navis M, Hensbergen PJ, Leurs R, Tensen CP. 2003. CXCR3-mediated chemotaxis of human T cells is regulated by a Gi- and phospholipase C-dependent pathway and not via activation of MEK/p44/p42 MAPK nor Akt/PI-3 kinase. *Blood* 102(6):1959-65.

Song H, Stevens CF, Gage FH. 2002. Astroglia induce neurogenesis from adult neural stem cells. *Nature* 417(6884):39-44.

Sorensen TL, Tani M, Jensen J, Pierce V, Lucchinetti C, Folcik VA, Qin S,

Rottman J, Sellebjerg F, Strieter RM and others. 1999. Expression of specific chemokines and chemokine receptors in the central nervous system of multiple sclerosis patients. *J. Clin. Invest.* 103(6):807-15.

Sorensen TL, Trebst C, Kivisakk P, Klaege KL, Majmudar A, Ravid R, Lassmann H, Olsen DB, Strieter RM, Ransohoff RM and others. 2002. Multiple sclerosis: a study of CXCL10 and CXCR3 co-localization in the inflamed central nervous system. *J. Neuroimmunol.* 127(1-2):59-68.

Sospedra M, Martin R. 2005. Immunology of multiple sclerosis. *Annu. Rev. Immunol.* 23:683-747.

Sozzani S, Introna M, Bernasconi S, Polentarutti N, Cinque P, Poli G, Sica A, Mantovani A. 1997. MCP-1 and CCR2 in HIV infection: regulation of agonist and receptor expression. *J. Leukoc. Biol.* 62(1):30-3.

Sriram S, Steiner I. 2005. Experimental allergic encephalomyelitis: a misleading model of multiple sclerosis. *Ann. Neurol.* 58(6):939-45.

Sriram S, Yao SY, Stratton C, Calabresi P, Mitchell W, Ikejima H, Yamamoto Y. 2002. Comparative study of the presence of *Chlamydia pneumoniae* in cerebrospinal fluid of Patients with clinically definite and monosymptomatic multiple sclerosis. *Clin. Diagn. Lab. Immunol.* 9(6):1332-7.

Stamatovic SM, Keep RF, Kunkel SL, Andjelkovic AV. 2003. Potential role of MCP-1 in endothelial cell tight junction 'opening': signaling via Rho and Rho kinase. *J. Cell. Sci.* 116:4615-28.

Staunton DE, Marlin SD, Stratowa C, Dustin ML, Springer TA. 1988. Primary structure of ICAM-1 demonstrates interaction between members of the im-

munoglobulin and integrin supergene families. *Cell* 52(6):925-33.

Steele AD, Szabo I, Bednar F, Rogers TJ. 2002. Interactions between opioid and chemokine receptors: heterologous desensitization. *Cytokine Growth Factor Rev.* 13(3):209-22.

Steinman L, Zamvil SS. 2006. How to successfully apply animal studies in experimental allergic encephalomyelitis to research on multiple sclerosis. *Ann. Neurol.* 60(1):12-21.

Stratmann T, Martin-Orozco N, Mallet-Designe V, Poirot L, McGavern D, Losyev G, Dobbs CM, Oldstone MB, Yoshida K, Kikutani H and others. 2003. Susceptible MHC alleles, not background genes, select an autoimmune T cell reactivity. *J. Clin. Invest.* 112(6):902-14.

Strieter RM, Burdick MD, Gomperts BN, Belperio JA, Keane MP. 2005. CXC chemokines in angiogenesis. *Cytokine Growth Factor Rev.* 16(6):593-609.

Sui Y, Potula R, Dhillon N, Pinson D, Li S, Nath A, Anderson C, Turchan J, Kolson D, Narayan O and others. 2004. Neuronal apoptosis is mediated by CXCL10 overexpression in simian human immunodeficiency virus encephalitis. *Am. J. Pathol.* 164(5):1557-66.

Tachibana K, Hirota S, Iizasa H, Yoshida H, Kawabata K, Kataoka Y, Kitamura Y, Matsushima K, Yoshida N, Nishikawa S and others. 1998. The chemokine receptor CXCR4 is essential for vascularization of the gastrointestinal tract. *Nature* 393(6685):591-4.

Takahashi JL, Giuliani F, Power C, Imai Y, Yong VW. 2003. Interleukin-1beta promotes oligodendrocyte death through glutamate excitotoxicity. *Ann. Neurol.*

53(5):588-95.

Takeuchi H, Jin S, Wang J, Zhang G, Kawanokuchi J, Kuno R, Sonobe Y, Mizuno T, Suzumura A. 2006. Tumor necrosis factor-alpha induces neurotoxicity via glutamate release from hemichannels of activated microglia in an autocrine manner. *J. Biol. Chem.* 281(30):21362-8.

Tanaka M, Sotomatsu A, Yoshida T, Hirai S, Nishida A. 1994. Detection of superoxide production by activated microglia using a sensitive and specific chemiluminescence assay and microglia-mediated PC12h cell death. *J. Neurochem.* 63(1):266-70.

Tanuma M, Shin T, Kogure K, Matsamoto Y. 1999. Differential role of TNF-alpha and IFN-gamma in the brain of rats with chronic relapsing remitting autoimmune encephalomyelitis. *J. Neuroimmunol.* 93(1):73-9.

Tanuma N, Sakuma H, Sasaki A, Matsumoto Y. 2006. Chemokine expression by astrocytes plays a role in microglia/macrophage activation and subsequent neurodegeneration in secondary progressive multiple sclerosis. *Acta Neuropathol. (Berl.)* 112(2):195-204.

Thelen M. 2001. Dancing to the tune of chemokines. *Nat. Immunol.* 2(2):129-34.

Thellin O, Zorzi W, Lakaye B, De Borman B, Coumans B, Hennen G, Grisar T, Igout A, Heinen E. 1999. Housekeeping genes as internal standards: use and limits. *J. Biotechnol.* 75(2-3):291-5.

Thompson AJ, Kermode AG, Wicks D, MacManus DG, Kendall BE, Kingsley DP, McDonald WI. 1991. Major differences in the dynamics of primary and secondary progressive multiple sclerosis. *Ann. Neurol.* 29(1):53-62.

Tian J, Ishibashi K, Handa JT. 2004. The expression of native and cultured RPE grown on different matrices. *Physiol. Genomics* 17(2):170-82.

Tran PB, Banisadr G, Ren D, Chenn A, Miller RJ. 2007. Chemokine receptor expression by neural progenitor cells in neurogenic regions of mouse brain. *J. Comp. Neurol.* 500(6):1007-33.

Trapp BD, Bo L, Mork S, Chang A. 1999. Pathogenesis of tissue injury in MS lesions. *J. Neuroimmunol.* 98(1):49-56.

Trebst C, Ransohoff RM. 2001. Investigating chemokines and chemokine receptors in patients with multiple sclerosis: opportunities and challenges. *Arch. Neurol.* 58(12):1975-80.

Trebst C, Staugaitis SM, Kivisakk P, Mahad D, Cathcart MK, Tucky B, Wei T, Rani MR, Horuk R, Aldape KD and others. 2003. CC chemokine receptor 8 in the central nervous system is associated with phagocytic macrophages. *Am. J. Pathol.* 162(2):427-38.

Tsai HH, Frost E, To V, Robinson S, Ffrench-Constant C, Geertman R, Ransohoff RM, Miller RH. 2002. The chemokine receptor CXCR2 controls positioning of oligodendrocyte precursors in developing spinal cord by arresting their migration. *Cell* 110(3):373-83.

Tsunoda I, Fujinami RS. 1996. Two models for multiple sclerosis: experimental allergic encephalomyelitis and Theiler's murine encephalomyelitis virus. *J. Neuropathol. Exp. Neurol.* 55(6):673-86.

Tuohy VK, Sobel RA, Lu Z, Laursen RA, Lees MB. 1992. Myelin proteolipid

protein: minimum sequence requirements for active induction of autoimmune encephalomyelitis in SWR/J and SJL/J mice. *J. Neuroimmunol.* 39(1-2):67-74.

Turner DJ, Martin PC, Rao JN, Greenspon J, Zou T, Bass BL, Wang JY, Strauch ED. 2007. Substance P regulates migration in rat intestinal epithelial cells. *Ann. Surg.* 245(3):408-14.

Ullian EM, Sapperstein SK, Christopherson KS, Barres BA. 2001. Control of synapse number by glia. *Science* 291(5504):657-61.

Van Der Voorn P, Tekstra J, Beelen RH, Tensen CP, Van Der Valk P, De Groot CJ. 1999. Expression of MCP-1 by reactive astrocytes in demyelinating multiple sclerosis lesions. *Am. J. Pathol.* 154(1):45-51.

van Marle G, Henry S, Todoruk T, Sullivan A, Silva C, Rourke SB, Holden J, McArthur JC, Gill MJ, Power C. 2004. Human immunodeficiency virus type 1 Nef protein mediates neural cell death: a neurotoxic role for IP-10. *Virology* 329(2):302-18.

VanAmerongen BM, Dijkstra CD, Lips P, Polman CH. 2004. Multiple sclerosis and vitamin D: an update. *Eur. J. Clin. Nutr.* 58(8):1095-109.

Vandesompele J, De Preter K, Pattyn F, Poppe B, Van Roy N, De Paepe A, Speleman F. 2002. Accurate normalization of real-time quantitative RT-PCR data by geometric averaging of multiple internal control genes. *Genome Biol* 3(7):1-11.

Vanhaesebroeck B, Alessi DR. 2000. The PI3K-PDK1 connection: more than just a road to PKB. *Biochem. J.* 346:561-76.

Viglietta V, Baecher-Allan C, Weiner HL, Hafler DA. 2004. Loss of functional

suppression by CD4+CD25+ regulatory T cells in patients with multiple sclerosis. *J. Exp. Med.* 199(7):971-9.

Villoslada P, Hauser SL, Bartke I, Unger J, Heald N, Rosenberg D, Cheung SW, Mobley WC, Fisher S, Genain CP. 2000. Human nerve growth factor protects common marmosets against autoimmune encephalomyelitis by switching the balance of T helper cell type 1 and 2 cytokines within the central nervous system. *J. Exp. Med.* 191(10):1799-806.

Vitkovic L, Bockaert J, Jacque C. 2000. "Inflammatory" cytokines: neuromodulators in normal brain? *J. Neurochem.* 74(2):457-71.

von Budingen HC, Tanuma N, Villoslada P, Ouallet JC, Hauser SL, Genain CP. 2001. Immune responses against the myelin/oligodendrocyte glycoprotein in experimental autoimmune demyelination. *J. Clin. Immunol.* 21(3):155-70.

Vroon A, Heijnen CJ, Kavelaars A. 2006. GRKs and arrestins: regulators of migration and inflammation. *J. Leukoc. Biol.* 80(6):1214-21.

Wain JH, Kirby JA, Ali S. 2002. Leucocyte chemotaxis: Examination of mitogen-activated protein kinase and phosphoinositide 3-kinase activation by Monocyte Chemoattractant Proteins-1, -2, -3 and -4. *Clin. Exp. Immunol.* 127(3):436-44.

Walker KS, Deak M, Paterson A, Hudson K, Cohen P, Alessi DR. 1998. Activation of protein kinase B beta and gamma isoforms by insulin *in vivo* and by 3-phosphoinositide-dependent protein kinase-1 *in vitro*: comparison with protein kinase B alpha. *Biochem. J.* 331:299-308.

Wan MX, Wang Y, Liu Q, Schramm R, Thorlacius H. 2003. CC chemokines induce P-selectin-dependent neutrophil rolling and recruitment *in vivo*: interme-

diary role of mast cells. *Br. J. Pharmacol.* 138(4):698-706.

Wandinger K, Jabs W, Siekhaus A, Bubel S, Trillenber P, Wagner H, Wessel K, Kirchner H, Hennig H. 2000. Association between clinical disease activity and Epstein-Barr virus reactivation in MS. *Neurology* 55(2):178-84.

Washington R, Burton J, Todd RF, 3rd, Newman W, Dragovic L, Dore-Duffy P. 1994. Expression of immunologically relevant endothelial cell activation antigens on isolated central nervous system microvessels from patients with multiple sclerosis. *Ann. Neurol.* 35(1):89-97.

Weber M, Blair E, Simpson CV, O'Hara M, Blackburn PE, Rot A, Graham GJ, Nibbs RJ. 2004. The chemokine receptor D6 constitutively traffics to and from the cell surface to internalize and degrade chemokines. *Mol. Biol. Cell.* 15(5):2492-508.

Weinshenker BG. 1994. Natural history of multiple sclerosis. *Ann. Neurol.* 36(Suppl):S6-11.

Weinstock-Guttman B, Baier M, Stockton R, Weinstock A, Justinger T, Munschauer F, Brownschidle C, Williams J, Fisher E, Miller D and others. 2003. Pattern reversal visual evoked potentials as a measure of visual pathway pathology in multiple sclerosis. *Mult. Scler.* 9(5):529-34.

Wekerle H, Bradl M, Linington C, Kaab G, Kojima K. 1996. The shaping of the brain-specific T lymphocyte repertoire in the thymus. *Immunol Rev* 149:231-43. Wilhelm J, Pingoud A. 2003. Real-time polymerase chain reaction. *Chem. biochem.* 4(11):1120-8.

Williams A, Piaton G, Lubetzki C. 2007. Astrocytes—friends or foes in multi-

ple sclerosis? *Glia* 55(13):1300-12.

Willis CL, Taylor GL, Ray DE. 2007. Microvascular P-glycoprotein expression at the blood-brain barrier following focal astrocyte loss and at the fenestrated vasculature of the area postrema. *Brain Res.* 1173:126-36.

Witt DP, Lander AD. 1994. Differential binding of chemokines to glycosaminoglycan subpopulations. *Curr. Biol.* 4(5):394-400.

Wolff B, Burns AR, Middleton J, Rot A. 1998. Endothelial cell "memory" of inflammatory stimulation: human venular endothelial cells store interleukin 8 in Weibel-Palade bodies. *J. Exp. Med.* 188(9):1757-62.

Wu GF, Laufer TM. 2007. The role of dendritic cells in multiple sclerosis. *Curr. Neurol. Neurosci. Rep.* 7(3):245-52.

Wu M, Chen Q, Li D, Li X, Li X, Huang C, Tang Y, Zhou Y, Wang D, Tang K and others. 2007. LRRC4 inhibits human glioblastoma cells proliferation, invasion, and proMMP-2 activation by reducing SDF-1alpha/CXCR4-mediated Erk1/2 and Akt signaling pathways. *J. Cell. Biochem.* 4:735-41.

Wucherpfennig KW. 2001. Structural basis of molecular mimicry. *J. Autoimmun.* 16(3):293-302.

Wucherpfennig KW. 2005. The structural interactions between T cell receptors and MHC-peptide complexes place physical limits on self-nonsel discrimination. *Curr. Top. Microbiol. Immunol.* 296:19-37.

Xia MQ, Bacskai BJ, Knowles RB, Qin SX, Hyman BT. 2000. Expression of the chemokine receptor CXCR3 on neurons and the elevated expression of its lig-

and IP-10 in reactive astrocytes: in vitro Erk1/2 activation and role in Alzheimer's disease. *J. Neuroimmunol.* 108(1-2):227-35.

Yang Y, Estrada EY, Thompson JF, Liu W, Rosenberg GA. 2007. Matrix metalloproteinase-mediated disruption of tight junction proteins in cerebral vessels is reversed by synthetic matrix metalloproteinase inhibitor in focal ischemia in rat. *J. Cereb. Blood. Flow Metab.* 27(4):697-709.

Ye P, D'Ercole AJ. 1999. Insulin-like growth factor I protects oligodendrocytes from tumor necrosis factor-alpha-induced injury. *Endocrinology* 140(7):3063-72.

Yednock TA, Cannon C, Fritz LC, Sanchez-Madrid F, Steinman L, Karin N. 1992. Prevention of experimental autoimmune encephalomyelitis by antibodies against alpha 4 beta 1 integrin. *Nature* 356(6364):63-6.

Youssef S, Wildbaum G, Karin N. 1999. Prevention of experimental autoimmune encephalomyelitis by MIP-1alpha and MCP-1 naked DNA vaccines. *J. Autoimmun.* 13(1):21-9.

Zeinstra E, Wilczak N, Streefland C, De Keyser J. 2000. Astrocytes in chronic active multiple sclerosis plaques express MHC class II molecules. *Neuroreport* 11(1):89-91.

Zhang J, Markovic-Plese S, Lacet B, Raus J, Weiner HL, Hafler DA. 1994. Increased frequency of interleukin 2-responsive T cells specific for myelin basic protein and proteolipid protein in peripheral blood and cerebrospinal fluid of patients with multiple sclerosis. *J. Exp. Med.* 179(3):973-84.

Zhang J, Shi XQ, Echeverry S, Mogil JS, De Koninck Y, Rivest S. 2007. Expression of CCR2 in both resident and bone marrow-derived microglia plays a

critical role in neuropathic pain. *J. Neurosci.* 27(45):12396-406.

Zozulya A, Weidenfeller C, Galla HJ. 2007. Pericyte-endothelial cell interaction increases MMP-9 secretion at the blood-brain barrier in vitro. *Brain Res.* 12:1-11.

Zuurman MW, Heeroma J, Brouwer N, Boddeke HW, Biber K. 2003. LPS-induced expression of a novel chemokine receptor (L-CCR) in mouse glial cells in vitro and in vivo. *Glia* 41(4):327-36.